

1-1-1980

# Constitutive equations for polymers undergoing changes in microstructure with deformation.

Rosanna, Falabella

*University of Massachusetts Amherst*

Follow this and additional works at: [https://scholarworks.umass.edu/dissertations\\_1](https://scholarworks.umass.edu/dissertations_1)

---

## Recommended Citation

Falabella, Rosanna,, "Constitutive equations for polymers undergoing changes in microstructure with deformation." (1980). *Doctoral Dissertations 1896 - February 2014*. 650.

[https://scholarworks.umass.edu/dissertations\\_1/650](https://scholarworks.umass.edu/dissertations_1/650)

This Open Access Dissertation is brought to you for free and open access by ScholarWorks@UMass Amherst. It has been accepted for inclusion in Doctoral Dissertations 1896 - February 2014 by an authorized administrator of ScholarWorks@UMass Amherst. For more information, please contact [scholarworks@library.umass.edu](mailto:scholarworks@library.umass.edu).

UMASS/AMHERST



312066 0015 5896 9



CONSTITUTIVE EQUATIONS FOR POLYMERS UNDERGOING CHANGES  
IN MICROSTRUCTURE WITH DEFORMATION

A Dissertation Presented

By

ROSANNA FALABELLA

Submitted to the Graduate School of the  
University of Massachusetts in partial fulfillment  
of the requirements for the degree of

DOCTOR OF PHILOSOPHY

February 1980

Polymer Science and Engineering

© Rosanna Falabella 1980  
All Rights Reserved




CONSTITUTIVE EQUATIONS FOR POLYMERS UNDERGOING  
CHANGES IN MICROSTRUCTURE WITH DEFORMATION

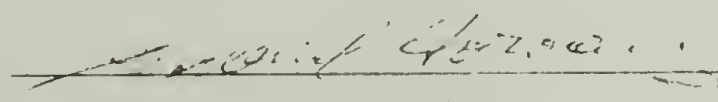
A Dissertation Presented

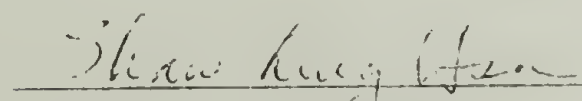
By


ROSANNA FALABELLA

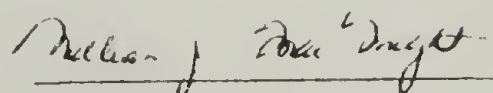
Approved as to style and content by:

  
Richard J. Farris, Chairperson of Committee

  
Gabriel Horvay, Member

  
Shaw-Ling Hsu, Member

  
Richard S. Stein, Member

  
William J. MacKnight, Head  
Polymer Science and Engineering



To my sisters

Digitized by the Internet Archive  
in 2014

## ACKNOWLEDGMENTS

I would like to first acknowledge the help, guidance, friendship, and inspiration I received from my thesis advisor, Dr. Richard Farris, throughout my graduate education, and especially during the final months of writing my dissertation.

I would also like to thank Dr. Richard Stein for introducing me to the field of polymer science, for encouraging me to attend graduate school, and for serving on my thesis committee. Drs. Gabriel Horvay, Shaw-Ling Hsu, and Robert Laurence also have my thanks and appreciation for serving on my committee and for many enjoyable, helpful hours of discussion, both in the classroom and out.

My sincere appreciation is extended also to: Drs. Jeffery Koberstein, John Van Bogart, Stuart L. Cooper, and Larry Hewitt for providing data and samples for my work; the University Computer Center and the Materials Research Laboratory for their financial support; Gladys and the Physical Sciences Library staff for their cheerful and competent service; the faculty, students and staff of the Polymer Science and Engineering Department, the Chemical Engineering Department, and the Chemistry Department, for their personal and professional encouragement.

I must add a special mention to those people who by their friendship and camaraderie, filled my years at UMass with warmth, humor and happiness. My heartfelt thanks to: Mike Mallone, Matt



Tirrell, Andrei Filippov, Mr. Tom Juska, Kay Weischedel, Ed and Kathy Reiff, and Chuck and Nancy Ryan, for all the good times we shared; Sensei Dan Partridge, for teaching me to be strong, and the members of the Uechi-ryu Karate Club, for letting me take out my frustrations on them; Carolyn Merriam, Marguerite "Terry" Atkinson, Claudia Poser, Paul Gilmore, and Joy Kempton, for their love, strength, and loyalty; my family, for everything they have done for me; and lastly, James Young, for putting everything into perspective at the end.

## ABSTRACT

### Constitutive Equations for Polymers Undergoing Changes In Microstructure with Deformation

(February 1980)

Rosanna Falabella, B.S., University of Massachusetts

M.S., University of Massachusetts

Ph.D., University of Massachusetts

Directed by: Professor Richard J. Farris

Constitutive equations for stress for solid polymers such as segmented polyurethane elastomers that undergo microstructural change with deformation are developed. Viscoelastic constitutive relations based on the fading memory assumption are shown to be inappropriate for materials that suffer a microstructural weakening that depends on maximums in the strain history, regardless of when in the history the maximums occur. This type of history dependence is termed permanent memory and may be described by  $p^{\text{th}}$  order Lebesgue norms of the strain history.

For the specific case of polyurethanes, a constitutive equation for stress is developed by defining the stress functional in terms of the history of the strain and the history of the orientation function of the hard chain segments of the polymers. The orientation functions of the hard and soft chain segments of the polyurethane, as determined by infrared dichroism, are shown to be simply related to each other and the tensile strain by assuming that the hard and soft chain segments

act in series under load.

A model for the irreversible change in orientation of the hard segments with strain is constructed based on a distribution of hard elements, all with the same orientation strain behavior but with different yield strains at which orientation may begin. The strain history dependence of the orientation function is of the permanent memory type and is contained by Lebesgue norms of the strain. The model is developed for both time independent and time dependent orientation and successfully predicts the observed hysteresis and time dependence in stress relaxation of the orientation function of the hard chain segments. The soft chain segment orientation may then be predicted using the series model.

Using the hard segment orientation function as a measure of the change in microstructure with deformation in polyurethanes, a constitutive equation for stress is developed which is a simple function of the strain and orientation. The results show that all of the time and history dependence seen in the mechanical response of polyurethanes may be attributed to the changing microstructure as measured by the orientation, which itself is a functional of the strain. This approach suggests that by introduction of a new internal parameter which describes the changing state of the material as it is deformed, the development of constitutive equations is greatly simplified and also allows the effect of chemical and structural parameters of the polymer on the stress-strain response to be quantitatively determined.



## TABLE OF CONTENTS

	Page
ACKNOWLEDGMENTS . . . . .	v
ABSTRACT . . . . .	vii
LIST OF TABLES . . . . .	xi
LIST OF FIGURES . . . . .	xii
 Chapter	
I. INTRODUCTION . . . . .	1
II. CONSTITUTIVE EQUATIONS AND MATERIAL BEHAVIOR . . . . .	6
II.1. Definitions . . . . .	6
II.2. Green-Rivlin Fading Memory Viscoelastic Theory . . . . .	7
II.2.1. Applications of Green-Rivlin theory . . . . .	13
II.3. Other Classes of Materials with Memory . . . . .	18
II.3.1. Aging materials . . . . .	19
II.3.2. Mechanical aging . . . . .	20
II.3.3. Constitutive equations for materials with permanent memory . . . . .	25
II.4. Mechanical Behavior of Polyurethanes . . . . .	37
II.5. Conclusions and Recommendations . . . . .	47
III. POLYURETHANE MICROSTRUCTURAL MODELS . . . . .	52
III.1. Microstructure of Polyurethane Elastomers . . . . .	53
III.2. Orientation Function as a Measure of Microstructural Change . . . . .	70
III.3. Series Model for Polyurethane Domains . . . . .	74
III.4. Microstructural Models for Orientation in Polyurethanes . . . . .	97
III.4.1. Time independent orientation of hard segment domains . . . . .	97
III.4.2. Time dependent orientation of hard segment domains . . . . .	108
III.5. Conclusions and Recommendations . . . . .	123

Chapter	Page
IV. CONSTITUTIVE EQUATIONS FOR STRESS . . . . .	127
IV.1. Stress as a Function of Strain and Orientation . . . . .	128
IV.2. Material Characterization . . . . .	137
IV.3. Conclusions and Recommendations . . . . .	146
REFERENCES . . . . .	149
Appendices	
A. DESCRIPTION OF POLYURETHANE CHEMISTRY . . . . .	157
B. EXPERIMENTAL PROCEDURE FOR STRESS-STRAIN TESTING . . . . .	160
C. STRAIN MEASURES IN THE DEFORMED COORDINATE SYSTEM . . . . .	163
D. EQUIVALENCE OF LINE, AREA, AND VOLUME FRACTIONS . . . . .	166
E. NONLINEAR REGRESSION ANALYSIS . . . . .	168
F. INTEGRATION OF ORIENTATION FUNCTION INTEGRAL . . . . .	206
G. EXACT ANALYTICAL EXPRESSIONS FOR $L_p$ NORM FOR CONSTANT STRAIN RATE HYSTERESIS TESTS . . . . .	208
H. EXACT ANALYTICAL EXPRESSIONS FOR $L_p$ NORM FOR STRESS RELAXATION EXPERIMENT . . . . .	211
I. EXACT ANALYTICAL EXPRESSIONS FOR FADING MEMORY VISCOELASTIC INTEGRAL FOR CONSTANT STRAIN RATE HYSTERESIS TESTS . . . . .	212

## LIST OF TABLES

Table		Page
1.	Observed and Calculated Values of Orientation Functions and Strain . . . . .	85
2.	Observed and Calculated Values of Orientation Functions and Strain . . . . .	91
3.	Polyurethane Compositions . . . . .	159



## LIST OF FIGURES

	Page
1. Stress Output of ES5701 after Indicated Strain Histories and 22 hr Rest Period at Zero Stress . . .	17
2. Stress Softening in Black-filled Rubber upon Repeated Deformation to Increasing Strain Levels . . . . .	22
3. Hysteresis of Solid Rocket Propellant (after Farris, 1970) . . . . .	27
4. Calculated Stress Response (Equation 21) to Indicated Strain History (after Farris, 1970) . . .	30
5. Time Dependence of $p^{th}$ Order Lebesgue Norms of the Indicated Strain History, $e(t)$ . . . . .	32
6. Stress Relaxation Predicted by Equation 21 for the Indicated Strain History (after Farris, 1970) . . .	33
7. Stress-strain Response of ES5701 in Simple Tension . . . . .	38
8. Hysteresis of ES5701 in Simple Tension . . . . .	40
9. Stress Softening of ES5701 . . . . .	41
10. Stress Relaxation of ES5701 . . . . .	42
11. Stress Relaxation Function Defined by Equation 30 of Text, for Indicated Strain Levels . . . . .	43
12. Stress Relaxation Response of ES5701 to Indicated Strain History . . . . .	44
13. Effect of Strain Rate on ES5701 in Simple Tension . . . . .	45
14. Permanent Set in ES5701, as Measured by the Plastic Strain . . . . .	46
15. Recovery of Hysteresis after Straining to 200% and Resting for the Indicated Times . . . . .	48
16. Schematic of Polyurethane Microstructure Showing Hydrogen Bonding in the Hard Chain Segments and Between the Hard and Soft Chain Segments . . . . .	55
17. Schematic of Polyurethane Microstructure Undergoing Deformation . . . . .	57
18. Orientation Function of Hard Segments (FH) vs. Strain for Virgin Samples and Samples with Prestrain of 2.0 . . . . .	61
19. Orientation Function of Soft Segments (FS) vs. Strain for Virgin Samples and Samples with Prestrain of 2.0 . . . . .	62

20.	Hard (NH) and Soft (CH) Segment of Orientation Functions as a Function of Time after Straining Quickly to 150% Strain . . . . .	63
21.	Constant Strain Rate History . . . . .	65
22.	Hard Segment Orientation as Indicated by NH Stretching (FH) vs. Extension Ratio for ET-38 (data of Cooper) . . . . .	66
23.	Hard Segment Orientation as Indicated by CO Stretching (FCO) vs. Extension Ratio for ET-38 (data of Cooper) . . . . .	67
24.	Soft Segment Orientation as Indicated by CH Stretching Vibration (FS) vs. Extension Ratio for ET-38 (data of Cooper) . . . . .	68
25.	Example Test Configurations with Indicated Stresses, $S_i$ , and IR Absorbances, $A_i$ , in the Principle Directions . . . . .	71
26.	Principle Directions of IR Absorbances, $A_i$ , for the Case of Simple Tension . . . . .	72
27.	Hard Segment Orientation Function Multiplied by Extension Ratio $\lambda$ vs. Nominal Strain . . . . .	75
28.	Series Model of Soft and Hard Domains in Polyurethanes . . . . .	76
29.	Calculated (Equation 47) vs. Observed Values of Soft Segment Orientation (FS) . . . . .	82
30.	Calculated (Equation 47) vs. Observed Values of Hard Segment Orientation (FH) . . . . .	83
31.	Calculated (Equation 47) vs. Observed Values of Total Strain . . . . .	84
32.	Calculated (Equation 47) vs. Observed Values of Soft Segment Orientation (FS) . . . . .	88
33.	Calculated (Equation 47) vs. Observed Values of Hard Segment Orientation (FCO) . . . . .	89
34.	Calculated (Equation 47) vs. Observed Values of Total Strain (ET) . . . . .	90
35.	Residual Orientation in Hard (FH) and soft (FS) Segments after Indicated Prestrain and 5 Minutes at Zero Stress . . . . .	96
36.	Orientation Function of the $i^{\text{th}}$ Hard Element, $f_i$ , vs. Strain for the Indicated Strain History, Given by Equation (49) of Text . . . . .	101
37.	Orientation Function of Hard Segment (FH) vs. Strain for the Monotonic Portion of the Strain History Given in Figure 21 . . . . .	104
38.	Schematic Representation of Dilatation, $V$ , vs. Strain Relationship and its First and Second Derivatives (after Farris, 1968) . . . . .	105

	Page
39. Distribution Function of Yield Strains, $N(\epsilon_y)$ , Determined from Data of Figure 22 . . . . .	107
40. Hard Segment Orientation Function vs. Strain . . . . .	109
41. Soft Segment Orientation Function Predicted by Equations 55 and 47 of Text . . . . .	110
42. Soft Segment Orientation Data (points) and Prediction (curve) of Equations 55 and 47 of Text . . . . .	111
43. Hard Segment Orientation Function vs. Strain . . . . .	113
44. Soft Segment Orientation Function vs. Strain . . . . .	114
45. Hard Segment Orientation Function . . . . .	116
46. Soft Segment Orientation Function vs. Strain . . . . .	117
47. Soft and Hard Segment Orientation Functions for the Indicated Strain History, Predicted by Equation 56 of Text, with $p=10$ . . . . .	118
48. Hard Segment Orientation Function vs. Time in Stress Relaxation Test at 150% Strain, for Indicated Values of $p$ (Equation 56) . . . . .	119
49. Soft Segment Orientation Function vs. Time in Stress Relaxation at 150% Strain, for Indicated Values of $p$ (Equation 56) . . . . .	120
50. Hard Segment Orientation Function vs. Time in Stress Relaxation at Indicated Strain Levels; Prediction of Equation 56 with $p=10$ . . . . .	121
51. Soft Segment Orientation Function vs. Time in Stress Relaxation at Indicated Strain Levels; Prediction of Equation 56 with $p=10$ . . . . .	122
52. Stress-strain Response of ET-38 Corresponding to the Strain History in Figure 21 and the Orienta- tion Functions in Figures 22, 23, and 24 . . . . .	132
53. Stress Predicted by Equation (63) of Text (points) Compared to Data of Figure 52 (curves) . . . . .	134
54. Stress Response Predicted by Equations (55) and (63) of Text (curve) . . . . .	136
55. Stress-strain Response of Lycra 2240 in Simple Tension . . . . .	138
56. Stress Relaxation of Lycra 2240 at Extension Ratio of 3.5 . . . . .	141
57. Stress Response of Lycra 2240 for Strain History Similar to Figure 21. . . . .	142
58. Stress-strain Response of ES5701 in Simple Tension . . . . .	143
59. Stress Response of ES5701 to Strain History Similar to Figure 21 . . . . .	145



	Page
60. Polyurethane Chemistry . . . . .	158
61. Experimental Configuration for Tensile Testing of ES5701 . . . . .	161
62. Strain Histories Used in Appendices G and I (A.) and Appendix H (B.) . . . . .	210

## C H A P T E R    I

### INTRODUCTION

Polymeric solids exhibit many complexities in their response to deformation. A few types of mechanical behavior of polymers have been observed, studied intensively, and represented by simple mathematical idealizations, for example the nonlinear reversible elastic behavior of rubbers and linear viscoelastic behavior. Considering the intricate microstructural processes accompanying deformation in most polymers, it is surprising that any simple descriptions of their mechanical response have been successful. It is apparent that any model of polymer mechanical response that includes the wide range of observed rate, temperature, and deformation history dependent effects, especially at large strains, must be based on sophisticated nonlinear theories.

A number of broad classes of nonlinear constitutive equations that are applicable to the description of polymer behavior have been defined in the literature of modern continuum mechanics. Examples of these classes of equations are finite elasticity and nonlinear viscoelasticity. Developments in the latter category have been based almost exclusively on the classic results of Green and Rivlin (1957) and Noll (1958), who described the class of "simple materials," i.e., materials for which the stress depends in an arbitrary way on the history of the first spatial gradients of the displacements in the

body. The history dependence of the simple material also has, with limited exceptions, been treated as a fading memory type dependence. The assumption of fading memory has been a natural one based on the physical observation that some materials forget their sufficiently long past deformations and behave as if they were new materials with no prior history of deformation.

The fading memory viscoelastic body is then, by definition, one in which no permanent changes in the nature of the material are produced by the deformation theory. However, it is commonly observed that with deformation some polymeric materials suffer irreversible microstructural weakening via the mechanisms of bond rupture, accelerated chemical reaction, filler-matrix delamination, cavitation, breaking of crystalline lamella, etc. A well-known manifestation of this weakening is the stress-softening, or Mullins' effect, seen in materials like filled rubbers when they are strained repeatedly. And like true fading memory materials, polymers that undergo changes in their microstructure with deformation very often display stress relaxation when suddenly strained to a new equilibrium length, a fact that has mistakenly led many experimentalists to analyze the mechanical response of all polymers that exhibit stress relaxation with fading memory viscoelastic equations.

The deformation of some polymers therefore essentially produces a new material at each point in its history, a phenomenon which requires that any description of the stress in the body must be in terms of not only the displacement gradients, but also the state of

weakening of the microstructure caused by the deformation history. The constitutive relations developed for such classes of materials cannot be restricted by the fading memory assumption; rather they must be allowed a possible strong dependency on events in the distant past, a property henceforth referred to as permanent memory.

It is the goal of this study to develop constitutive equations for stress for a two phase polymer system--solid polyurethane elastomers. Polyurethanes undergo a continuous, permanent change in their microstructure during deformation, as evidenced by the measurement of the change in the orientation of the two different types of chain segments in the polymer. The development of the overall constitutive equation for stress therefore first demands development of a microstructural constitutive equation for the orientation of the chain segments. The final result will thus be a constitutive equation within a constitutive equation. The theoretical framework necessary for the description of the mechanical behavior of polyurethanes has been provided by Farris (1970, 1973), who presented constitutive equations based on Lebesgue norms of the strain for materials with permanent memory of past strain states. Also important are the results of Quinlan and Fitzgerald (1973), who generalized the results of Farris by showing that the constitutive equation for stress may be written in terms of both the history of the deformation gradients and a tensor-valued measure of microstructural damage, which itself depends on the history of the deformation gradients.

The purpose of this investigation is two-fold. First, the use



of constitutive equations for polymers in engineering stress analyses is becoming increasingly widespread, especially in the aerospace and automotive industries, so it is important to have available accurate constitutive relations for materials whose mechanical response has permanent memory character. Farris' (1969) initial work on the description of permanent memory effects was motivated by the incorrect usage of fading memory viscoelastic equations for the stress analysis of solid rocket propellant structures that suffered permanent damage with deformation.

Second, the specific problem outlined here for polyurethane elastomers demonstrates that it is possible to quantitatively determine the nature of the stress response from a consideration of the reaction of the microstructure to deformation. A connection is thus made between the macroscopic properties and the microstructure by introduction of the orientation of the polymer chain segments as the measure of microstructural change. Since it is easy to change the chemical composition of polyurethanes, and thereby change structural parameters such as the compliances of the two domains, in principle it becomes possible to meet an essential goal of polymer science, namely to design polymers with specific desired mechanical properties.

A general background to constitutive equations for fading memory and permanent memory materials, details of the results of Farris, and a description of the mechanical behavior of polyurethanes is given in Chapter II. A detailed review of information on the microstructure of polyurethanes, and a definition of the orientation func-



tion as a measure of the state of microstructural weakening is given in Chapter III. The dependence of the orientation on the deformation history is developed by analysis of simple stochastic models of the polyurethane microstructure, and the predictions of the model compared to recent data provided by Dr. S.L. Cooper.

The final chapter shows the development of a constitutive equation for stress for polyurethanes which is based on the permanent memory equations developed in Chapter III. The stress-strain data of solid polyurethanes is characterized with the developed relation. The results show that the permanent memory features of the mechanical behavior of polyurethanes may be successfully predicted with a constitutive equation for stress that contains the measure of microstructural change occurring with deformation in the polymer.

## C H A P T E R   I I

### CONSTITUTIVE EQUATIONS AND MATERIAL BEHAVIOR

In this chapter a general background to constitutive equations for materials with fading memory and permanent memory will be given, along with a description of the mechanical behavior of polyurethanes.

Several definitions will be given here to facilitate the ensuing discussion of constitutive relations.

#### II.1. Definitions

1. Reversible and Irreversible. A reversible process is one which is conservative in the thermodynamic sense. Therefore, an ideal elastic body displays reversible mechanical response with deformation, while a viscoelastic body, even if it returns to its original dimensions after removal of tractions, undergoes an irreversible process since energy is dissipated.

2. Linear and Nonlinear. Mathematically, the linearity requirement is

$$(1) \quad F(x_1+x_2) = F(x_1) + F(x_2)$$

where  $F$  is any operator, function, or functional, and  $x_1, x_2$  are the arguments of  $F$ . An example of a linear constitutive equation is the one-dimensional viscoelastic equation for an incompressible material:

$$(2) \quad S(t) = \int_0^t G(t-\xi) \frac{d e(\xi)}{dt} dt$$

where  $S$  is the stress,  $e$  is the strain,  $G(t)$  is the relaxation modulus function, and  $t$  is the time. Obviously,  $S(e_1+e_2) = S(e_1) + S(e_2)$  since the integral is a linear operator. The strain measure  $e$  may be any strain measure. However, if the strain measure used is a finite strain measure, such as the Lagrangian strain  $E$ , defined for the one-dimensional case here as  $E = \frac{1}{2} (\lambda^2 - 1)$  where  $\lambda$  is the extension ratio, then Equation (2) will not be linear in the strain measure  $\lambda$ , the measure commonly determined by experiment.

## II.2. Green-Rivlin Fading Memory Viscoelastic Theory

Since the late 1950s, the field of polymer science has expanded tremendously, and seen the introduction of a myriad of new materials that often display extremely complex mechanical behavior. Concurrently, the field of continuum mechanics saw a period of growth which roughly reflected the need for the increased mathematical sophistication necessary to categorize and analyze the mechanical response of polymeric solids and liquids. A large body of the work in mechanics has dealt with the formulation of nonlinear constitutive equations, also called rheological equations of state, for materials that have some memory of their past deformation states. That most polymers fall into the class of materials is well known; also, the interest in nonlinear mechanics of dissipative materials stems from the fact that many

commonly used polymers are capable of experiencing finite deformations, and in the range of such deformations, linear constitutive relations are usually not satisfied.

In the field of continuum mechanics, two main approaches are used to derive constitutive laws: the method of Cauchy and the method of Green (see Eringen, 1962). Briefly, Cauchy's method was to simply consider that for an elastic body the stress is a function of the displacement gradients in the body, while Green derived a constitutive equation by considering the internal energy produced by elastic deformation. The two approaches yield the identical result for the perfectly elastic body. While many researchers have worked along the lines of Green by defining internal energy functions for dissipative materials, this approach suffers from the difficulties involved in defining these functions uniquely (see Farris, 1978). Some examples of the energy method are the BKZ elastic fluid theory (Bernstein et al., 1963; Zapas and Craft, 1965), linear viscoelastic results by Herrmann (1965) and Christensen and Naghdi (1966), and a nonlinear viscoelastic theory by Peng et al. (1977).

For the purposes of this dissertation, constitutive equations will be discussed from the point of view of the Cauchy approach. Cauchy's method was generalized by Volterra (1959), who suggested that all history dependent phenomena in the mechanics of materials could be taken into account if the stress was expressed as a general functional of the history of the displacement gradients. Materials that fit into the above class, with the additional restriction that only the first

spatial gradients of the displacements are allowed in the constitutive formulation, have been termed "simple materials" by Eringen (1962).

The most important results in the nonlinear theory of the mechanical behavior of simple materials with memory were given by Green and Rivlin (1957) and equivalently by Noll (1958). Since a large body of subsequent theoretical developments in the area of continuum mechanics were based on their work, the results of Green and Rivlin will be discussed in detail.

The formalism of Green and Rivlin begins with the definition of motion of a body as a mapping of all points in the body from a reference configuration  $X_i$  to a deformed configuration  $x_i$ . The first spatial displacement gradients,  $F_{ij}$ , are defined as

$$(3) \quad F_{ij} = \frac{\partial x_i}{\partial X_j} \quad i, j = 1, 2, 3$$

The components of stress at time  $t$ ,  $S_{ij}(t)$ , are assumed to be polynomial functions of the displacement gradients  $\partial x_r(\tau_\alpha)/\partial X_s$  at  $N+1$  distinct instants of past time  $\tau_\alpha$  ( $\alpha=0, 1, 2, \dots, N$ ) between  $\tau=0$  and  $\tau=t$ , i.e.,

$$(4) \quad S_{ij}(t) = S_{ij} \left[ \frac{\partial x_r(\tau_\alpha)}{\partial X_s} \right] = S_{ij} \left[ F_{rs}(\tau_\alpha) \right]$$

In order to recast (4) in terms of strain, any one of a number of definitions for strain may be used; all may be written in terms of the displacement gradient  $F_{rs}$ . The finite strain tensor  $E_{ij}$ , known as the Green strain tensor and defined by



$$(5) \quad E_{ij} = 1/2 [F_{ij}F_{ij}^T - \delta_{ij}]$$

where  $F_{ij}^T$  is the transpose of  $F_{ij}$  and  $\delta_{ij}$  is the Kroneker delta, will be used in the following treatment. Since both the Green tensor and the stress tensor are symmetric, and  $F_{ij}$  is not, the mathematics is simplified by the choice of the Green tensor. Thus the stress may be equivalently written in terms of  $E_{ij}$ ;

$$(6) \quad S_{ij}(t) = S_{ij} [E_{pq}(\tau_\alpha)]; \quad \alpha = 0, 1, 2, \dots, N$$

Using the ideas of Volterra (1959), Green and Rivlin passed from the polynomial expression for stress in (6) to a tensor valued functional,  $G_{ij}$ , defined over a continuous variable  $\tau$  of past time;

$$(7) \quad S_{ij}(t) = G_{ij} \int_{\tau=0}^{\tau=t} [E_{pq}(\tau)]$$

The notation in Equation (7) means that the stress is dependent on the values of  $E_{pq}$  over all past times  $\tau$ , in the interval  $0 \leq \tau \leq t$ . In order to develop a workable approximation to the functional in (7), the ideas of Frechét (1910) are used. Frechét generalized the polynomial expansion of a continuous function (Weirstrauss theorem) to produce an equivalent integral series approximation to a continuous functional. One method of assuring the continuity of the functional  $G_{ij}$ , and thus assuring the applicability of the Frechét integral expansion, is to invoke a mathematical formulation of the fading memory assumption. The fading memory assumption embodies the physical notion

that the memory of the body for its past deformations fades in the sense that the deformations which occurred in the distant past contribute less to the present stress state than do more recent deformations. A rigorous mathematical expression of fading memory was given by Coleman and Noll (1960, 1961) and Coleman and Mizel (1966, 1968).

The Frechét expansion given by Green and Rivlin (1957) as an approximation to (7), under the assumption of fading memory, is

$$\begin{aligned}
 (8) \quad S_{ij}(t) &= G_{ij} [E_{pq}(\tau)] \\
 &= K(t) + \int_0^t K_{pq}(t, \tau) E_{pq}(\tau) d\tau \\
 &\quad + \int_0^t \int_0^t K_{p_1 q_1 p_2 q_2}(t, \tau_1, \tau_2) E_{p_1 q_1}(\tau_1) E_{p_2 q_2}(\tau_2) d\tau_1 d\tau_2 \\
 &\quad + \dots + \int_0^t \int_0^t \dots \int_0^t K_{p_1 q_1 p_2 q_2 \dots p_R q_R}(t, \tau_1, \tau_2 \dots \tau_R) \times \\
 &\quad E_{p_1 q_1}(\tau_1) E_{p_2 q_2}(\tau_2) \dots E_{p_R q_R}(\tau_R) d\tau_1 d\tau_2 \dots d\tau_R
 \end{aligned}$$

Equation (8) is a constitutive relation for an anisotropic material with memory.

Aside from the application of certain general invariance requirements, Equation (8) was specialized in two ways. First, the assumption of a non-aging material, i.e., a material whose properties do not change with absolute time, is incorporated into (8) by making the kernel functions,  $K_R$ , dependent on relative time  $(t - \tau_n)$ ,  $n = 1, 2 \dots R$ , so that (Green-Rivlin, 1957)

$$(9) \quad K_{p_1 q_1 p_2 q_2 \dots p_R q_R}(t, \tau_1, \tau_2, \dots, \tau_R) = \\ K_{p_1 q_1 p_2 q_2 \dots p_R q_R}(t - \tau_1, t - \tau_2, \dots, t - \tau_R)$$

If equation (9) is satisfied, the functional in (8) is said to be hereditary.

Second, (8) was specialized for the case of an isotropic material in the following manner (see Farris, 1970). The functional  $G_{ij}$  was rewritten in the form (Pipkin, 1964; Rivlin, 1965)

$$(10) \quad G_{ij} = k_0 \delta_{ij} + \int_0^t K_1(t-\tau_1) \dot{E}_{pq}(\tau_1) d\tau_1 + \\ \int_0^t \int_0^t K_2(t-\tau_1, t-\tau_2) \dot{E}_{pq}(\tau_1) \dot{E}_{pq}(\tau_2) d\tau_1 d\tau_2 + \dots$$

where the  $K_n$  are now scalar polynomials dependent on the history of the invariants,  $I_i$ ,  $i = 1, 2, 3$ , of  $E_{pq}$  as well as the variables  $t-\tau_i$ :

$$(11) \quad K_n = K_n \left[ \begin{matrix} \xi=t \\ t-\tau_1, \dots, t-\tau_n, I_i(\xi) \end{matrix} \right]; \quad i = 1, 2, 3 \\ \xi=0$$

and

$$\dot{E}_{pq}(\tau_i) = \frac{\partial}{\partial \tau_i} E_{pq}(\tau_i)$$

Now the kernels,  $K_n$ , are functionally dependent on the invariants  $I_i$ , and this functional dependence is approximated in the same manner as  $G_{ij}$  above so that the history of  $I_i(\xi)$  is expressed in an integral series in terms of the traces of the strain tensor,  $\text{tr } \underline{E}$ ,  $\text{tr } \underline{E}^2$ ,

$\text{tr } \underline{E}^3$ .<sup>\*</sup> The traces of  $\underline{E}$  were used as they form an integrity basis for the three scalar invariants (Rivlin, 1965 and Pipkin, 1964). This second integral expansion was then inserted into (10) and after gathering of like terms, the general isotropic constitutive equation remaining was of the form

$$\begin{aligned}
 (12) \quad \underline{S}(t) = & \int_0^t [\underline{I}k_1 \text{tr } \dot{\underline{E}}(\tau_1) + k_2 \dot{\underline{E}}(\tau_1)] d\tau_1 \\
 & + \int_0^t \int_0^t \{ \underline{I}k_3 \text{tr } \dot{\underline{E}}(\tau_1) \text{tr } \dot{\underline{E}}(\tau_2) + \underline{I}k_4 \text{tr}[\dot{\underline{E}}(\tau_1)\dot{\underline{E}}(\tau_2)] \\
 & + k_4 \dot{\underline{E}}(\tau_1) \text{tr } \dot{\underline{E}}(\tau_2) + k_6 \dot{\underline{E}}(\tau_1) \dot{\underline{E}}(\tau_2) \} d\tau_1 d\tau_2 + \dots
 \end{aligned}$$

In (12), the kernels  $k_n$  are now scalar functions of the arguments  $(t-\tau_i)$  such that  $k_1, k_2$  are functions of  $(t-\tau_1)$ ;  $k_3, k_4, k_5, k_6$  are functions of  $(t-\tau_1, t-\tau_2)$ , etc.

The first term of (12) is the familiar linear viscoelastic expression:

$$(13) \quad \underline{S} = \int_0^t \underline{I}k_1(t-\tau) \text{tr } \dot{\underline{E}}(\tau) d\tau + \int_0^t k_2(t-\tau) \dot{\underline{E}}(\tau) d\tau$$

11.2.1. Applications of Green-Rivlin theory. Applications of the Green-Rivlin equation (12), or modifications thereof, to actual materials have been numerous. The review presented here in no way pretends to be rigorous, especially in light of the fact that this field

---

<sup>\*</sup>Throughout this dissertation, the notation  $\underline{E}$  will be used to denote the matrix with components  $E_{ij}$ .

is still growing at a rapid pace. An excellent review of the entire field of nonlinear viscoelastic theory has been given by Hadley and Ward (1975). Here, the two main approaches to the application of Green-Rivlin theory that have been used by researchers in nonlinear viscoelasticity will be discussed.

The first approach has been to modify the linear integral term (Equation 13) by incorporating a general or nonlinear strain measure into the integral to make the constitutive equation nonlinear. Examples of this line of reasoning may be seen in the results of Smith (1962), Leaderman (1962) and Chang et al. (1976). The single integral method simplifies material characterization, but in general cannot describe very strong nonlinearities.

A second set of developments have focused on taking several terms in the expansion (12) to produce an equation for the description of nonlinear mechanical behavior. Theoretical discussions on the forms that the multiple integral terms should take for different strain histories have been given by Pipkin (1964), Lockett (1965), Pipkin and Rogers (1967), Lockett and Stafford (1969), and Stafford (1969). Applications of the multiple integral constitutive equation to specific materials have been made by Goldberg and Lianis (1968) and McGuirt and Lianis (1969) for SBS rubber, Yannas and Lunn (1970) for polycarbonates, Foot and Ward (1972) for poly(ethylene terephthalate), Smart and Williams (1972) for polyethylene, and Davis and Macosko (1978) for polycarbonate and poly(methyl methacrylate).

The application of the Green-Rivlin multiple integral expansion



has been motivated by the assumption that the expansion is completely general, and therefore taking an increasing number of nonlinear terms will allow increasingly accurate description of nonlinear behavior. Pipkin (1964) has pointed out, however, that the accuracy of the approximation to the functional  $G_{ij}$  is not improved by merely adding terms to the expansion, unless the kernels of the lower order terms are adjusted at the same time. Thus in the usual applications to viscoelasticity, it is assumed that the kernels represent fixed properties of the material, and that the very smallest strain histories require the fewest terms while venturing into finite strain regions requires the adding on of more terms. Since the integral expansion is already an approximation, it is not necessarily the case that the smaller the strains, the lower the error of approximation. In particular, although at certain points in the development of (12) Green and Rivlin (1957) required the deformations to be small, the integral expansion may be made without recourse to this assumption (Pipkin, 1964). There appears, therefore, no justification for assuming that in the limit of small deformations, the linear equation (13) represents the behavior of the most general material with memory. Indeed, there are several examples in the literature of polymers that obey nonlinear constitutive laws even at the smallest strains (Farris, 1970; Brereton et al., 1974).

An implicit feature of the above cited works is that, since the Green-Rivlin theory is used, the materials characterized are assumed to be of the fading memory viscoelastic type. Usually the polymers under discussion exhibit creep and stress relaxation, but the observation of

these time dependent properties, which are certainly characteristic of a fading memory material, is not sufficient to prove that the polymer belongs to this class of materials. As discussed in the Introduction, the fading memory assumption can be an unnecessarily restrictive one if a material undergoes any permanent microstructural changes with deformation. Despite this fact, the fading memory quality in itself has been seen as so intrinsic to the discussion of materials with memory, that Eringen (1967), for example, contends that the fading memory assumption should be a feature of all constitutive functionals.

Firm proof for fading memory mechanical behavior is discussed by Quinlan and Fitzgerald (1973). They outline a simple experiment in which two tensile test specimens are subjected to strain histories,  $E_1$  and  $E_2$ , which differ in their maximum, but not in their present value, i.e.,

$$(14) \quad (a) \quad E_1(t) = E_2(t)$$

$$(b) \quad \max_{\xi=0}^{\xi=t} [E_1(\xi)] > \max_{\xi=0}^{\xi=t} [E_2(\xi)]$$

An example plot of such strain histories is given in Figure 1. The fading memory hypothesis would contend that after waiting some reasonable time after the first portion of the strain history, the stress in both samples will be the same, i.e.,  $S_1(t) = S_2(t)$ , where  $t$  is the current value of time. Experimentally it is observed (Figure 1) that for Estane polyurethane,  $S_1(t) < S_2(t)$ , therefore it is not a simple fading

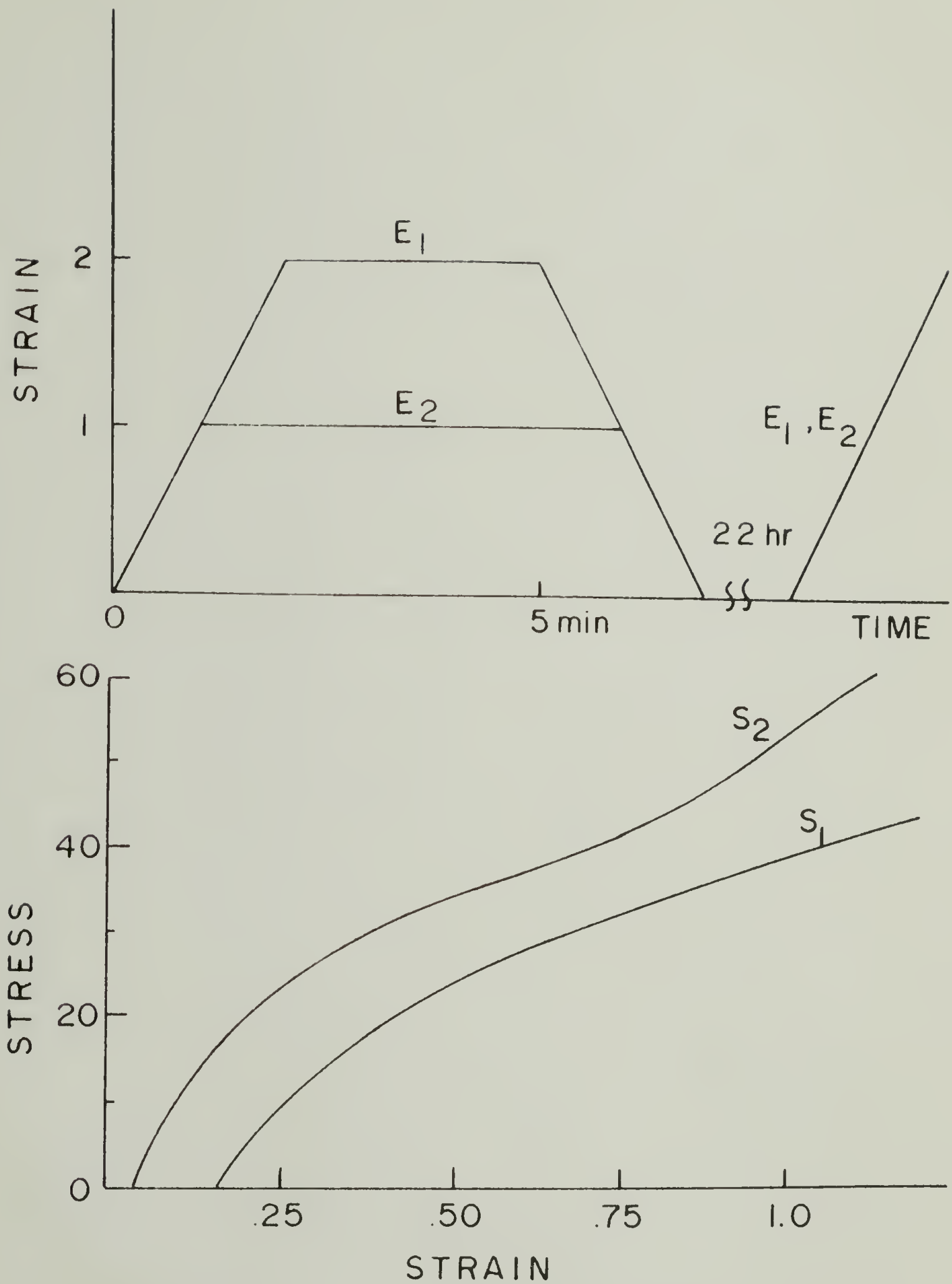


Figure 1. Stress output of ES5701 after indicated strain histories and 22 hr rest period at zero stress.

memory material.

Constitutive equations for materials that have memory of their past deformation states that is not a fading memory only, but rather is a perfect or permanent memory, or some combination of permanent and fading memory, have been the subject of some theoretical treatments. Constitutive theories in this category which consider aging and mechanical breakdown of the polymer material will be discussed in the following sections.

### II.3. Other Classes of Materials with Memory

Classes of material behavior other than the Green-Rivlin simple material with fading memory behavior have been considered in some detail in the literature of continuum mechanics. The two main divisions of materials with memory other than fading memory will be classified as follows: (1) materials that change their properties with absolute time, known as aging materials. The mechanism of aging may be some kind of degradation process or a continuing polymerization reaction such as post-curing of rubbers. (2) Materials whose properties change with deformation, sometimes referred to as mechanically aging or mechanically degrading materials. In this category fall all materials that undergo deformation-induced irreversible changes in their microstructure that are not of a viscous nature. Polyurethane elastomers fall into this latter category of material behavior by virtue of the observed irreversible orientation induced by deformation which takes place in the polymer's two different chain segments.



Mathematical idealizations for these two classes of materials will be discussed in the following sections. Special emphasis will be given to the results of Farris (1970, 1973) who described the stress-strain response of highly filled rubbers by considering that deformation caused irreversible damage in the material. The damage model led to a constitutive equation that successfully described the permanent memory character of the stress-strain behavior of these polymers.

II.3.1. Aging materials. The theoretical treatments of aging materials are important to this discussion since they represent attempts to expand the results of linear and nonlinear viscoelasticity by including description of history dependent phenomena other than those of a fading memory type. Aging materials, then, are viewed as having a perfect memory of their birth date. Aging effects have been seen in such varied materials as concrete (Predeleanu, 1973), wool (Rigby et al., 1974), and solid rocket propellant (Fitzgerald, 1973).

Predeleanu (1973) observed that the consideration that rheological properties are time-invariant brings certain simplifications to the mathematical treatment of constitutive equations, but one cannot ignore the fact that some materials exhibit a response to stress that changes with absolute time, i.e., the material ages. As noted above, the non-aging hypothesis was included in the Green-Rivlin work at an early stage, via the conditions on the kernel functions given in Equation (9). One consequence of the non-aging assumption in viscoelastic theory is that the linear term, Equation (13), is a convolution integral lending itself to easy inversion through use of Laplace



transforms.

The usual approach to developing constitutive equations that include the aging effect has been to preserve the dependence on absolute time in the Green-Rivlin viscoelastic theory (see Equation 8). For example, Predeleanu's (1973) linear integral form for an aging, viscoelastic body is:

$$(15) \quad S_{ij}(t) = \int_0^t G_{ijkl}(t, \tau) dE_{kl}(\tau)$$

II.3.2. Mechanical aging. The observation that significant changes occur in the mechanical properties of polymers upon their being subjected to deformations is well known. Polymers undergo irreversible changes in their microstructure when they are deformed and most of these changes cannot be idealized as elastic or viscous processes. Also, a large percentage of the microstructural changes that occur serve to weaken the material for further use; these changes with deformation have been collectively termed mechanical aging.

Documented evidence for microstructural changes induced by deformation in polymers abounds in the literature. Examples are chain rupture in polymers (Park et al., 1978; Huang and Aklonis, 1978); the breakdown of coulombic interactions in wool (Feughelman, 1973); stress induced crystallization in rubbers, and cavitation in filled elastomers (Farris, 1968).

One of the physical manifestations of mechanical breakdown or weakening of a polymeric material is the stress softening, or Mullins'

effect, which occurs on repeated straining of materials such as filled rubbers (Figure 2). The Mullins effect, first described by Mullins (1948) for filled natural rubber, is generally irreversible and time independent for such highly crosslinked systems (Mullins, 1947). Bueche (1960, 1961) proposed a molecular model to describe this mechanical breakdown of rubbers in which the mode of degradation of the polymer was stress activated chain rupture. His theory successfully predicted the stress softening of SBR (styrene-butadiene rubber) and represents one of the earliest attempts to predict mechanical response from a model of the microstructural breakdown. Farris (1970) developed models of time independent and time dependent chain failure in a manner similar to Bueche's to describe the stress softening and permanent memory effects in highly filled, lightly crosslinked rubbers. His theoretical work will be discussed in detail below.

Other researchers have attempted to describe mechanical aging effects with mechanical or molecular models or general continuum mechanics approaches. Examples in the former category are the works of Askan and Zurek (1975), who proposed a model containing an inertial-frictional element to describe the plasticity and hysteresis in viscose rayon; Moacanin et al. (1975), who predicted creep behavior by considering a network which simultaneously undergoes physical relaxation and chain scission; and Wu and Brown (1970), who presented a theory of stress relaxation based on microstructural parameters of craze formation, size, and growth. The results of these workers are valuable in that they demonstrate the inappropriateness of fading memory arguments

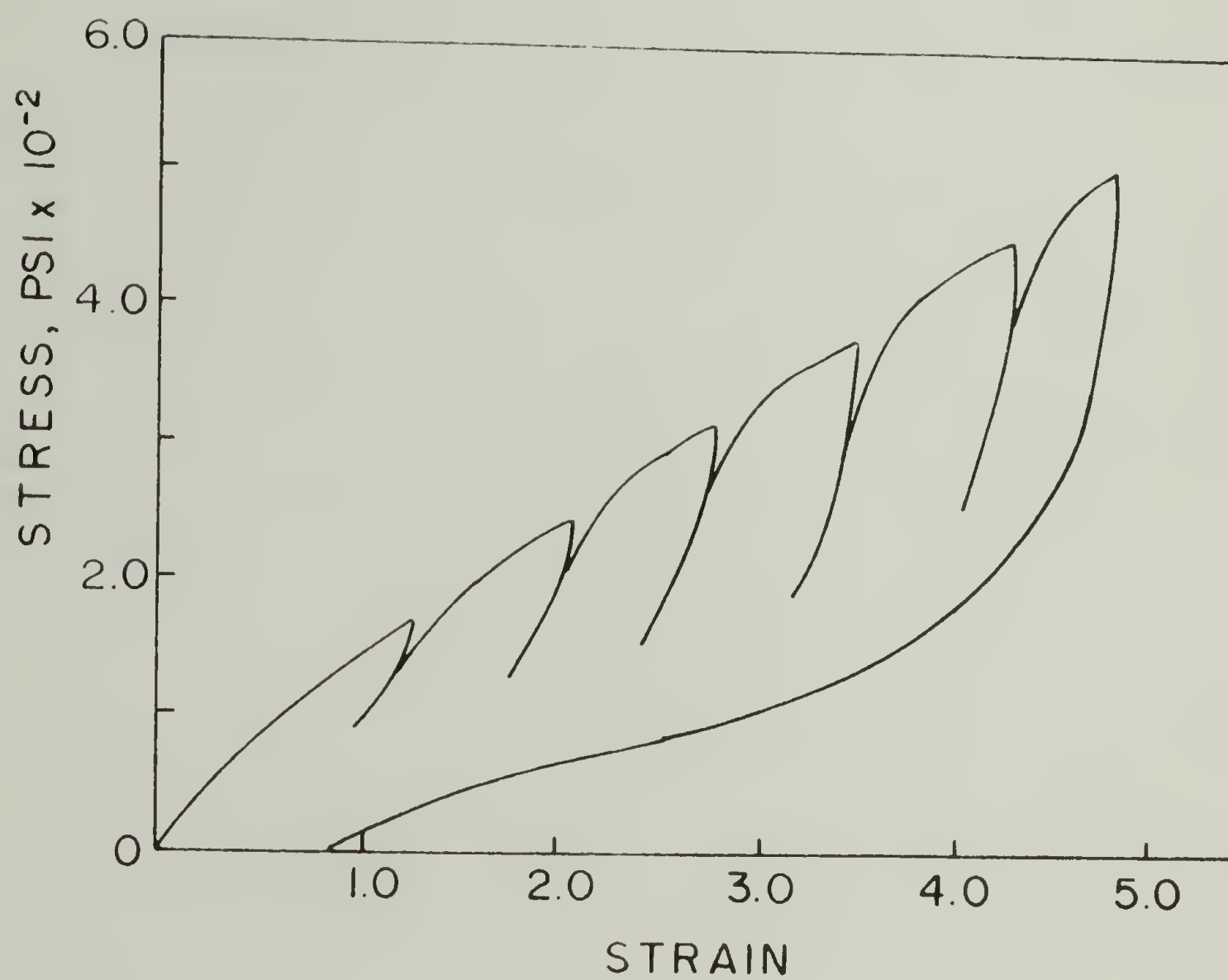


Figure 2. Stress softening in black-filled rubber upon repeated deformation to increasing strain levels.

to some polymer systems. However, the resulting relationships derived for the mechanical response in terms of microstructural parameters generally suffer from their inability to be extended to strain histories other than the limited ones of stress relaxation and creep usually considered.

In the area of continuum mechanics, a few advances have been made by attempts to incorporate mechanical aging features into general constitutive equations. Dong (1964) demonstrated that a constitutive equation of the Green-Rivlin type could be modified by considering a dependence on a general chronological variable,  $s$ , instead of on the time,  $t$ . For example, if  $s$  is defined as

$$(16) \quad s = \int_0^{|\sigma_2^*|} \left| \frac{d\sigma_2}{dt} \right| dt$$

where  $\sigma_2$  is the second invariant of the stress tensor, and  $\sigma_2^*$  is the current value of  $\sigma_2$ , an equation for a plastic material results.

Dong's approach essentially allows the formulation for strain to contain a memory of previous stress states, such that the deformation is plastic only when  $\sigma_2$  is not a constant (otherwise  $s=0$ ). The equations presented by Dong can reflect visco-plastic behavior and as well, reduce to Green-Rivlin fading memory viscoelasticity.

Brereton et al. (1974) proposed a "feedback" constitutive equation, which has the feature of describing in a completely general manner, any strain induced process that modifies a material in a way

which reduces its resistance to stress. The basic equation they presented was of the form

$$(17) \quad AS + BS + CSE = 0$$

where  $S$  is the stress,  $E$  is the strain, and  $A$ ,  $B$ , and  $C$  are material functions. The expressions chosen for the three terms in (17) were linear integrals based on the Green-Rivlin approach, so that (17), although nonlinear at even the smallest strains, is still basically a fading memory formulation. The attempt was made (Brereton et al., 1976) to specify the feedback mechanism in polymers as correlated motions between adjacent monomer units in the polymer chain, but no results were shown that identified any molecular or microstructural parameters with the functions in Equation (17) for a specific material.

McKenna and Zapas (1979) have recently attempted to describe mechanical aging by modifying the BKZ elastic fluid equation (Bernstein et al., 1963) with a generalized time measure,  $t'$ , defined as

$$(18) \quad t' = \int_{\tau}^t \phi(E(t), E(\tau), E(\xi), t-\xi) d\xi$$

where  $\phi$  is a memory function,  $E$  is the strain,  $t$  is the time,  $\tau$  is the past or generic time, and the dot denotes differentiation with respect to  $(t-\xi)$ . The measure  $t'$ , which is obviously a function of  $t$  and  $\tau$ , replaces the usual non-aging fading memory argument  $(t-\tau)$  of the kernel functions in the BKZ integral. The new time measure is dependent on the history of the strains, and the function  $\phi$  was determined from



experimental data on a numerical basis. Limited agreement of this modified BKZ theory was found for the case of torsion of poly(methyl methacrylate) cylinders. No attempt was made to associate the memory function with any specific aging process in the polymer.

The examples presented above are similar to one another from the standpoint that they recognize the need to develop alternative approaches to the Green-Rivlin fading memory viscoelastic theory by considering the microstructural changes in polymers, in either the specific details of models or in general by incorporation of different types of history dependence of past strain states into constitutive equations. Also, none of the above cited works successfully characterize the dependence of specific microstructural changes on the deformation history and then describe the constitutive equation for stress in the body in terms of the changed state of the material.

The first successful attempt to model the microstructural weakening, or damage, that occurs with deformation of the material in order to discover specific strain history functionals that would quantitatively relate the damage state to the stress was due to Farris (1970, 1973). His development of constitutive equations for lightly crosslinked, highly filled solid polyurethane rocket propellant will be discussed in the next section.

### II.3.3. Constitutive equations for materials with permanent memory.

Farris' (1970, 1973) development of constitutive equations for solid rocket propellant was motivated by two distinguishing features of their mechanical behavior. First, he observed that the materials obeyed non-

linear constitutive laws even at very small strains, a fact that necessitated a nonlinear theory. The type of nonlinearity was homogeneity of degree one, i.e., the constitutive functional  $F_{ij}$  satisfied the mathematical requirement

$$(19) \quad F_{ij} \left[ a E_{pq}(t, \tau) \right] = a F_{ij} \left[ E_{pq}(t, \tau) \right]$$

$\tau=0 \qquad \qquad \qquad \tau=t$

where  $E_{pq}$  is the strain and  $a$  is any real number. The condition in (19) was considered to be the simplest type of nonlinearity since it is a requirement that a linear equation also meets. Equation (19) is a degenerate form of the linearity requirement, Equation (1), but satisfaction of (19) in no way implies that (1) holds. This fact has led some researchers to incorrectly classify a material for which the response is doubled if the input is doubled as a linear material.

The second factor which motivated Farris' work was the observation that solid propellants were not primarily fading memory viscoelastic materials. The polymers under consideration did show time dependent effects such as stress relaxation and creep, and as well displayed stress softening with repeated deformation. Also, the materials' mechanical response showed strong history dependence on the previous maximum strain state, as depicted in Figure 3. In this figure it is seen that after a constant tensile strain rate input is applied (curve 1) there is considerable stress softening (curve 2) on reversal of the strain. On restraining (curve 3), the lower modulus curve is followed until the previous maximum strain is surpassed, at which point

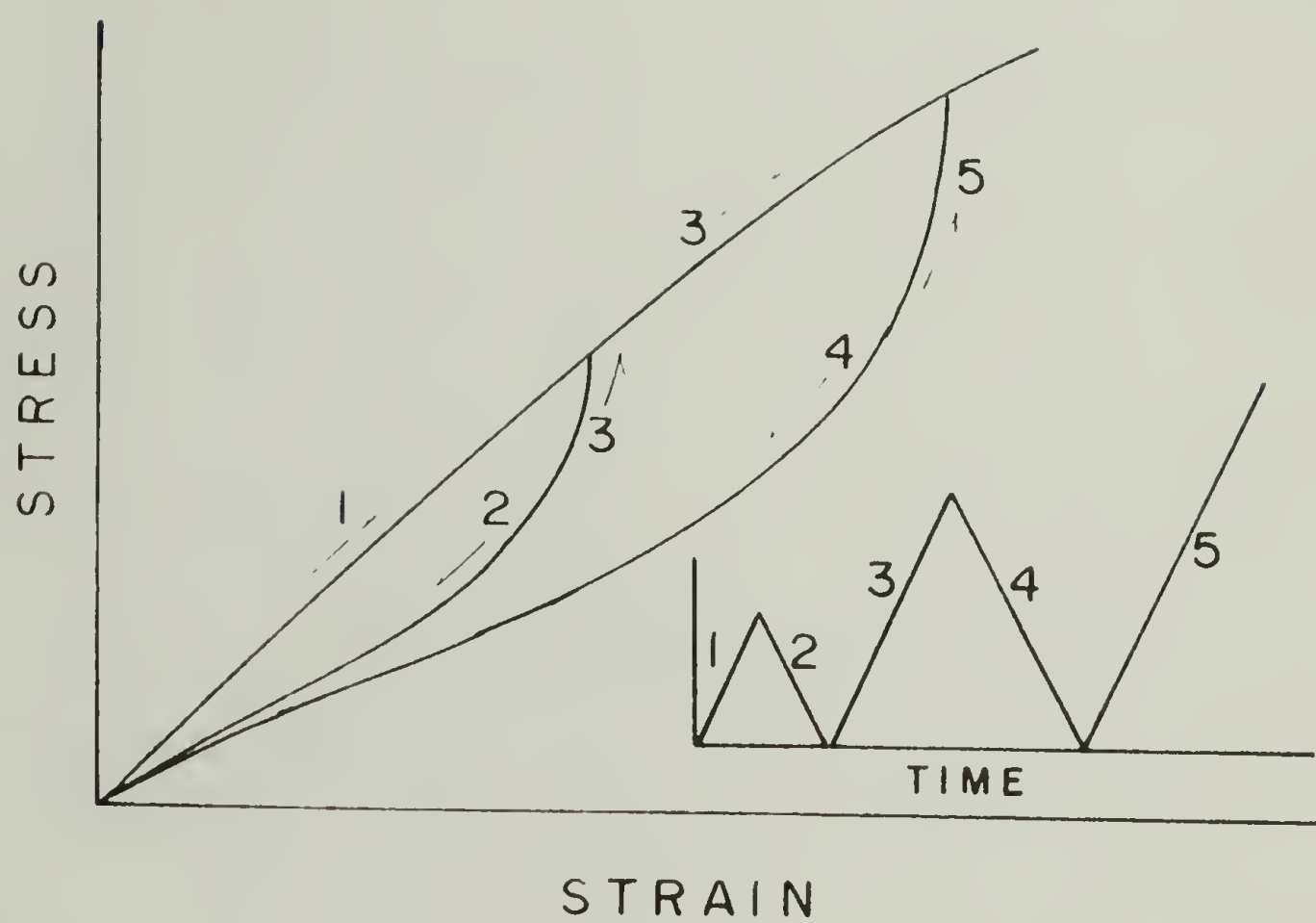


Figure 3. Hysteresis of solid rocket propellant (after Farris, 1970).

the material behaves as if it had not seen any prior deformation. Many other polymers show similar behavior in this type of test, for example, black-filled rubbers (Bueche, 1961; Payne, 1974), foams (Meinecke and Schwaber, 1970), styrene-butadiene-styrene triblock copolymers (Pedemonte et al., 1975), and polyurethanes (Puett, 1967). Farris postulated that some microstructural failure of polymer chains led to the observed perfect or permanent memory of the past strain states, so that any formulation based on linear or nonlinear fading memory viscoelastic theory would be erroneous for solid propellants.

He modelled the time dependent and time independent stress softening of these materials by assuming a system of polymer chain elements, all with the same nonlinear stress-strain law. He assumed that the relative deformation of each element was proportional to the applied strain, but that the proportionality varied from chain to chain. This assumption took into account the rigid filler particles, which move apart in an affine manner with uniaxial strain, for example, and this motion causes large local variations in the strain in the individual attached polymer chains. The hysteresis and permanent memory displayed by this system was dealt with by forming a model of chain failure in which a chain would fail if, at any time in its history, a failure criterion was exceeded. The criterion was the maximum allowable extension for the chain, and was the same criterion for every chain. The time dependence of the mechanical properties was included in the model by assuming that the failure criterion was a time dependent law based on cumulative damage measures (Miner, 1945).

An example of a one-dimensional constitutive equation for the stress,  $S$ , that resulted from Farris' work is

$$(20) \quad S(t) = 100 e \left[ 1 + (e/\|e\|_p)^n \right]$$

where  $n$  is an even integer,  $e$  is the strain, and  $p$  and  $n$  are material constants, and

$$(21) \quad \|e\|_p \equiv \left[ \int_0^t |e(\xi)|^p d\xi \right]^{1/p},$$

which is the definition of the  $p^{\text{th}}$  order Lebesgue norm of  $e$ . A plot of this equation is given in Figure 4 for the constant strain rate cycle shown. Note the similarity of this plot to the response of the solid propellant in Figure 3.

The measure of microstructural damage that arose from Farris' model so happened to have the exact mathematical form as  $p^{\text{th}}$  order Lebesgue norms (see Royden, 1968) and serves as a particular measure of the deformation history. One of the more useful properties of  $p^{\text{th}}$  order Lebesgue norms (hereafter referred to as  $L_p$  norms) is that in the limit as  $p \rightarrow \infty$ , the  $L_p$  norm becomes a time independent quantity which is exactly the maximum, or supremum, of the function argument, i.e.,

$$(22) \quad \|e\|_\infty = \lim_{p \rightarrow \infty} \|e\|_p = \lim_{p \rightarrow \infty} \left[ \int_0^t |e(\xi)|^p d\xi \right]^{1/p} = \max_{\xi=0}^{\xi=t} [e(\xi)]$$

Thus, in general, the  $L_p$  norm integral is a measure of the history that preserves in some sense the maximum value of its argument,



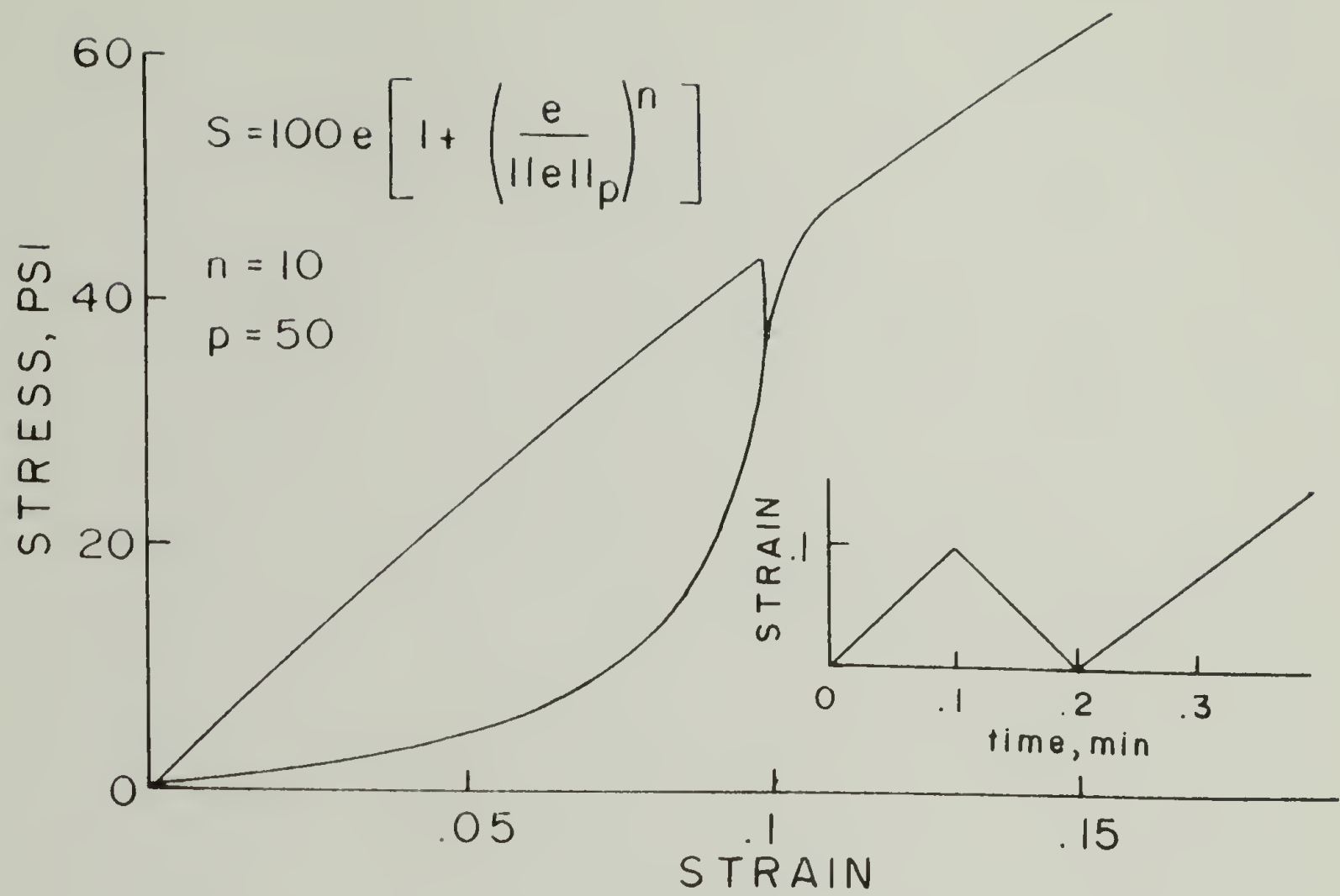


Figure 4. Calculated stress response (Equation 21) to indicated strain history (after Farris, 1970).

regardless of when in the history the maximum occurred. By contrast, the standard fading memory integral (Equation 12) orders events in time and gives recent inputs more weight than inputs far removed in time, regardless of the magnitude of the input. Obviously, the  $L_p$  norm measure is ideally suited to describe irreversible changes in a polymer microstructure that are known to depend on strain maximums rather than on the relative time at which the change occurred. The type of memory of past strain states which can be contained by the  $L_p$  norm measure was termed permanent memory by Farris.

The  $L_p$  norm is a positive functional which is always either constant or increasing, as depicted in Figure 5. It is seen in this figure that after the direction of strain is reversed, the  $L_p$  norm of the strain continues to increase slowly until the previous maximum strain is surpassed. For the limiting case,  $\|e\|_\infty$  is either exactly equal to the strain,  $e(t)$ , or is a constant,  $e_1$ .

If the stress-strain Equation (20) is examined, it will be seen that the ratio  $e/\|e\|_p$  allows the stress softening effect to be accurately predicted. In addition, Equation (20) predicts stress relaxation as shown for the strain history in Figure 6. The  $L_p$  norm of the strain is also dependent on the strain rate, so that it is also possible to construct rate-sensitive equations based on  $L_p$  norms.

Further, it is possible to modify the basic definition of the Lebesgue norm in Equation (21) by including an influence function  $h(t-\xi)$  as part of the kernel (Farris, 1970):

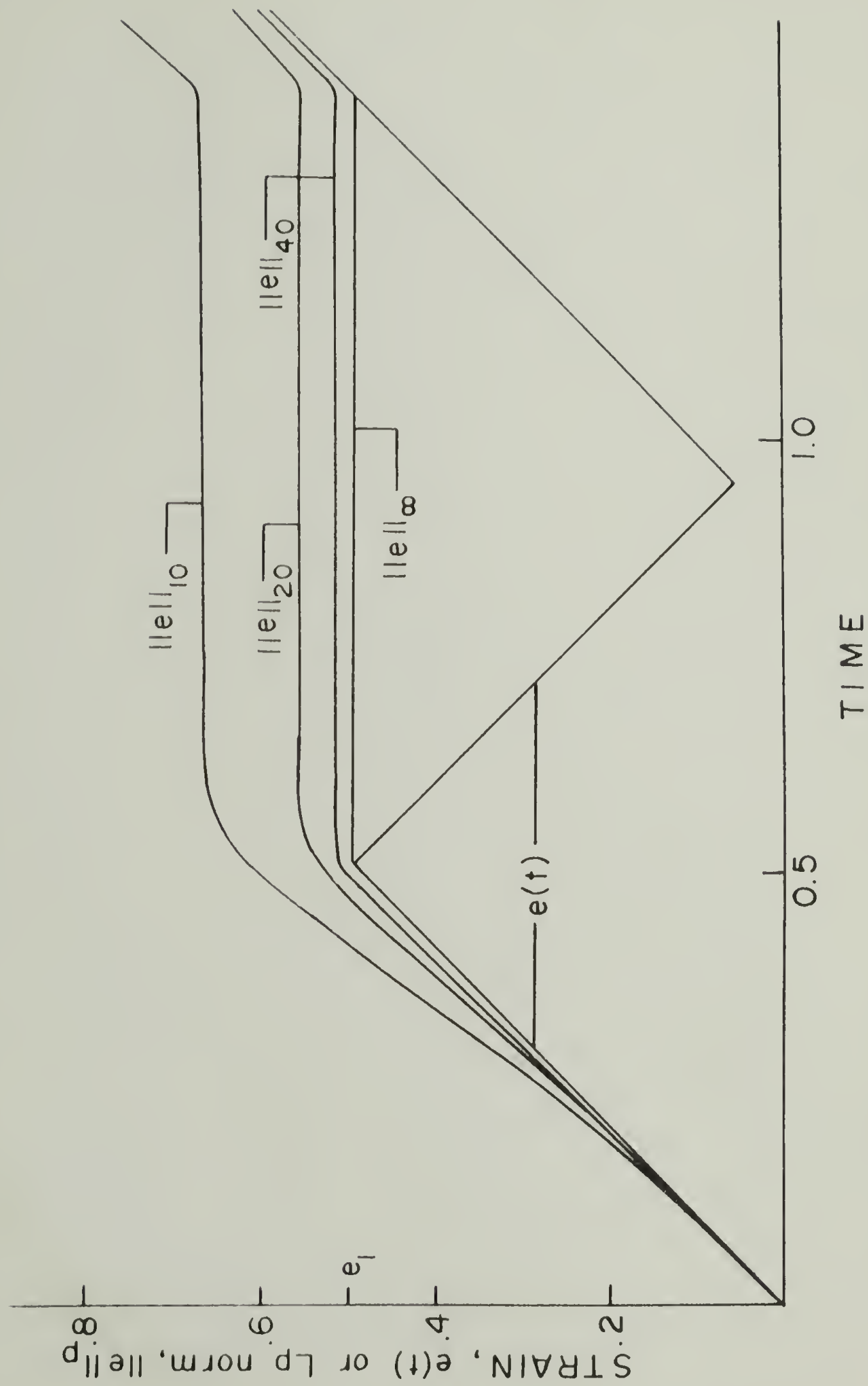


Figure 5. Time dependence of  $p^{\text{th}}$  order Lebesgue norms of the indicated strain history,  $e(t)$ .

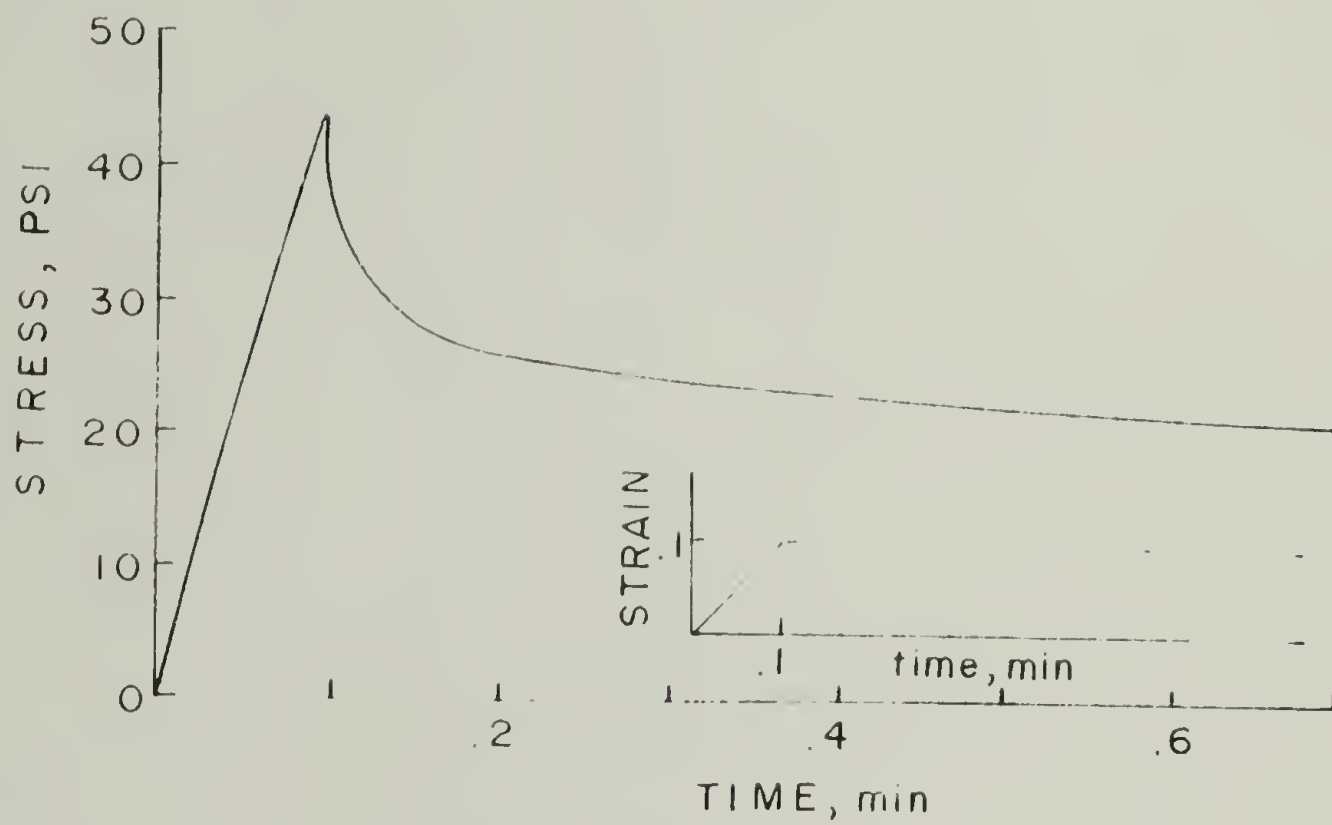


Figure 6. Stress relaxation predicted by Equation 21 for the indicated strain history (after Farris, 1970).

$$(23) \quad \|e\|_{h,p} = \left[ \int_0^t \{h(t-\xi)|e(\xi)|\}^p d\xi \right]^{1/p}$$

The weighted norm defined by Equation (23) may describe several types of material memory, depending on the choice of  $h$ . If an exponential form such as  $h(t-\xi) = \exp(-b(t-\xi))$  is taken, then the  $\|e\|_{h,p}$  measure will describe a rehealing phenomenon wherein the permanent memory of the past strain states will gradually be annihilated. The  $L_{h,p}$  norm may therefore contain a memory of the maximum in the history which fades with time.

Fitzgerald (1973) demonstrated that the  $L_p$  norm may be modified so that aging phenomena of materials like sand asphalt and rocket propellant may be described as well as their permanent memory of maximum strain states. The modified norm was termed a Steklov average of order  $p$ , or  $S_p$ , and defined as

$$(24) \quad \|e\|_{S_p} = \left[ \frac{1}{(1+kt)} \int_0^t |e(\xi)|^p d\xi \right]^{1/p}$$

Despite the fact that many different types of mechanical behavior may be idealized using the various  $L_p$  norm measures, few applications of this type of mathematics has been seen in the literature. Vakili and Fitzgerald (1973) developed equations for asphalt concrete based on  $L_p$  norms, and Chu and Blatz (1972) used Farris' approach to describe hysteresis in living cat tissue. Farris and Herrmann (1971) and Farris and Schapery (1973) extended the initial Farris work to a detailed characterization of solid rocket propellant.



Quinlan and Fitzgerald (1973) obtained theoretical results which showed that Farris' work on defining damage as a microstructural parameter could be generalized by introduction of a damage functional, which is a new internal variable of the material that depends on the deformation history. Then the stress in the body will depend on both the damage, as the measure of irreversible microstructural weakening, and the deformation history itself, i.e.,

$$(25) \quad \underline{S}(t) = G \left[ \int_{\xi=0}^{\xi=t} \underline{E}(t-\xi) ; \underline{D}(t-\xi) \right]$$

where  $G$  is a functional,  $\underline{E}$  is the strain tensor, and  $\underline{D}$  is the damage tensor, with

$$(26) \quad \underline{D}(t) = G_1 \left[ \int_{\xi=0}^{\xi=t} \underline{E}(t-\xi) \right]$$

Now if the functional dependence indicated in Equation (26) is allowed to take on the form

$$(27) \quad G_1[\underline{E}(t-\xi)] = G_1 \left[ \underline{E}(t-\xi), \|\underline{E}(t-\xi)\|_p \right]$$

then the Farris permanent memory equations are seen as a specialization of (25). The form of Equation (25) immediately suggests that a first order approximation of the functional may be made using (Quinlan and Fitzgerald, 1973):

$$(28) \quad \underline{S}(t) = \int_0^t \phi_1(\underline{E}(t), \underline{D}(t), t-\xi) \dot{\underline{E}}(\xi) d\xi \\ + \int_0^t \phi_2(\underline{E}(t), \underline{D}(t), t-\xi) \dot{\underline{D}}(\xi) d\xi$$

where  $\phi_1$  and  $\phi_2$  are tensor-valued material functions, and the dot denotes differentiation with respect to  $\xi$ .

In the characterization of an actual polymer system of highly filled rubber, Farris (1970, 1973) discovered that in addition to permanent memory character, the polymers also displayed some fading memory behavior. These observations led to a constitutive equation of the form

$$(29) \quad \underline{S}(t) = A_1 \left[ \frac{|e|}{\|e\|_{q_1}} \right]^{r_1} e(t) + A_2 \left[ 1 - \left( \frac{|e|}{\|e\|_{q_2}} \right)^{r_2} \right] \int_0^t (t-\xi)^{-n_2} \dot{e}(\xi) d\xi$$

where  $A_1$ ,  $A_2$ ,  $n_2$ ,  $q_1$  and  $q_2$ ,  $r_1$  and  $r_2$  are material constants. If the designations

$$(30) \quad (a) \quad \phi_1 = A_2 \left[ 1 - \left( \frac{|e(t)|}{\|e(t)\|_{q_2}} \right)^{r_2} \right] (t-\xi)^{-n_2} \\ (b) \quad \int_0^t \phi_2(\underline{E}(t), \underline{D}(t), t-\xi) \dot{\underline{D}}(\xi) d\xi = A_1 \left( \frac{|e(t)|}{\|e(t)\|_{q_1}} \right)^{r_1} e(t)$$

are made, then it is seen that the Farris equation may be viewed as a first order permanent memory-fading memory equation.

The results of Farris and Quinlan and Fitzgerald together form

a unique framework for the development of constitutive equations for materials with permanent memory. Farris showed that  $L_p$  norms were the measures necessary to describe permanent memory of past strain states by considering a particular microstructural model of damage taking place in the polymer during deformation. Quinlan and Fitzgerald added that, in general, it was necessary to write the stress functional in terms of some measure of microstructural weakening, as well as the strain. The slight drawback to both sets of results is that there is no way of experimentally determining the damage in the filled polymers as defined by Farris, a situation that would allow the two parameters of strain and damage in Equation (25) to be defined and determined independently.

Unfilled polyurethane elastomers, often called segmented polyurethanes because the individual polymer chains are comprised of alternating hard and soft segments ("hard" and "soft" indicating that one segment is above its glass transition temperature while the other is below) display stress-strain behavior which is quantitatively very similar to the solid propellants examined by Farris. A description of polyurethane mechanical behavior is the subject of the next section.

#### II.4. Mechanical Behavior of Polyurethanes

The stress-strain behavior of a commercial polyurethane elastomer in simple tension is given in Figure 7. The polymer is B.F. Goodrich's Estane 5701 (ES5701); a description of the polymer and of the experimental testing procedure is given in Appendices A and B. If a

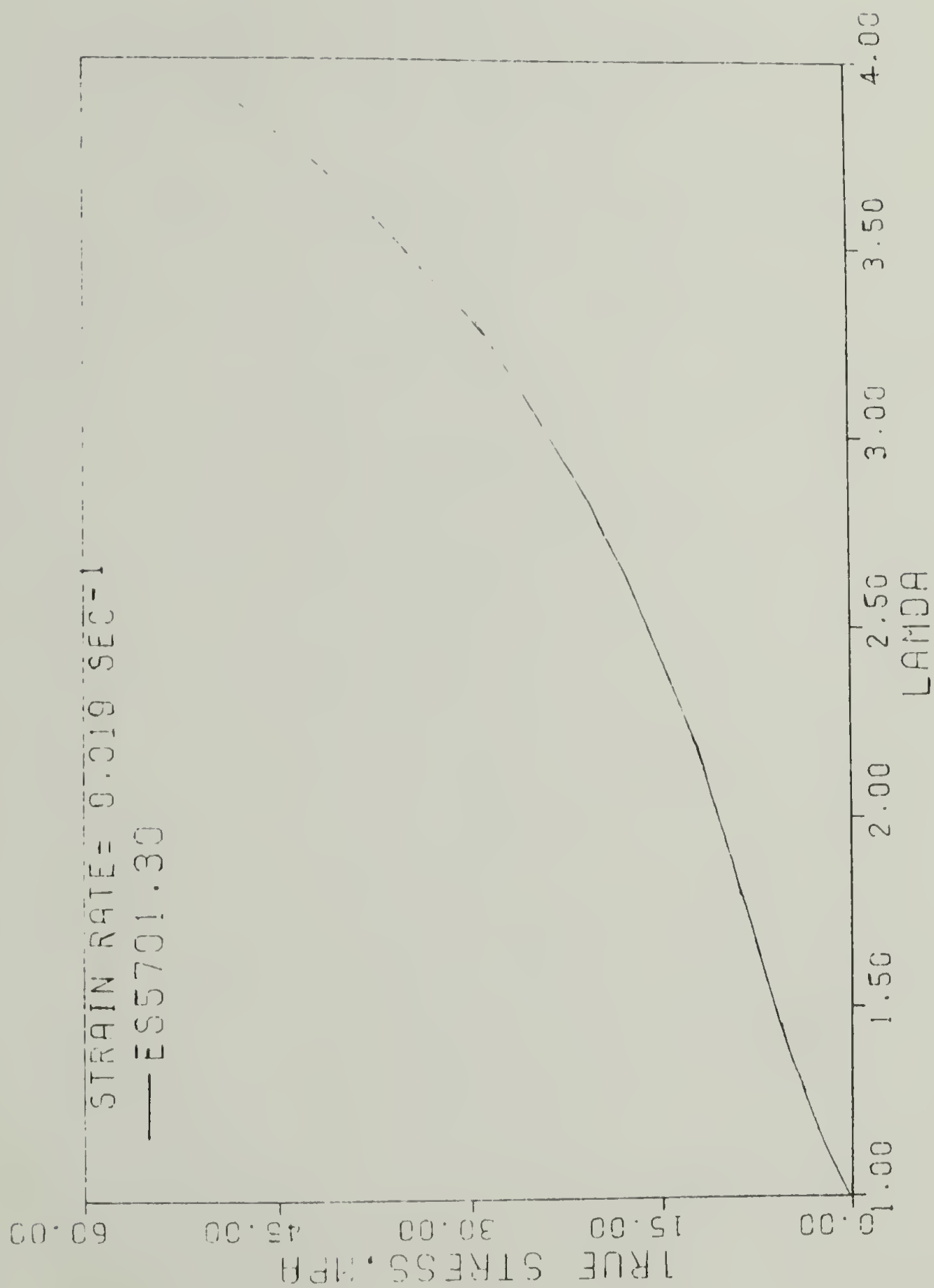


Figure 7. Stress-strain response of ES5701 in simple tension.

strain history such as the one given in Figure 3 is applied, the response of the polyurethane is very similar to the filled system studied by Farris, in that large hysteresis and a sensitivity to strain maximums is observed (Figure 8). The stress softening of ES5701 is given in Figure 9.

The polyurethane also displays stress relaxation (Figure 10). The dependence of the relaxation modulus function,  $E_r(t)$ , defined as

$$(30) \quad E_r(t) = \frac{S(t) \cdot \lambda}{\left(\lambda - \frac{1}{2}\right) \lambda^2}$$

where  $S$  is the stress, and  $\lambda$  is the extension ratio, on strain level is not a simple one, but may be adequately described by the product of a time dependent function and a strain dependent function:

$$(31) \quad E_r(t) = t^{-.089} e^{(.309\lambda + 1.35)}$$

Figure 11 shows the relaxation modulus function at different strain levels along with the curves defined by Equation (31).

If the stress relaxation experiment is repeated on the same sample at increasing strain levels, it is observed that the material again exhibits strong independence of the previous maximum state of strain, i.e., it behaves as the virgin material after each interval of relaxation (Figure 12).

The polyurethane is not a very rate-dependent material, as shown in Figure 13. Also, the material suffers some permanent set, especially if the maximum strain on the sample is above 1 (Figure 14).



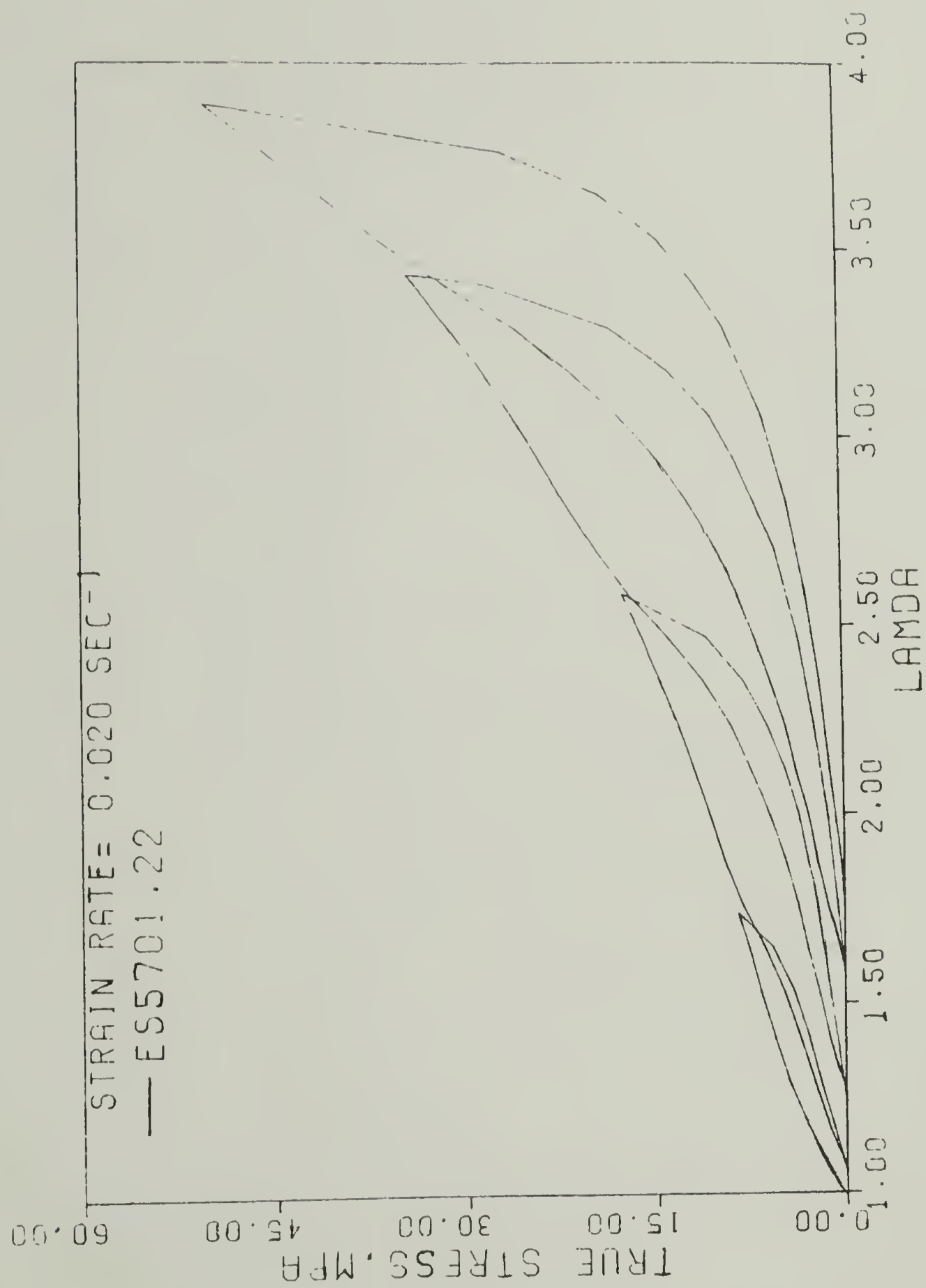


Figure 8. Hysteresis of ES5701 in simple tension.

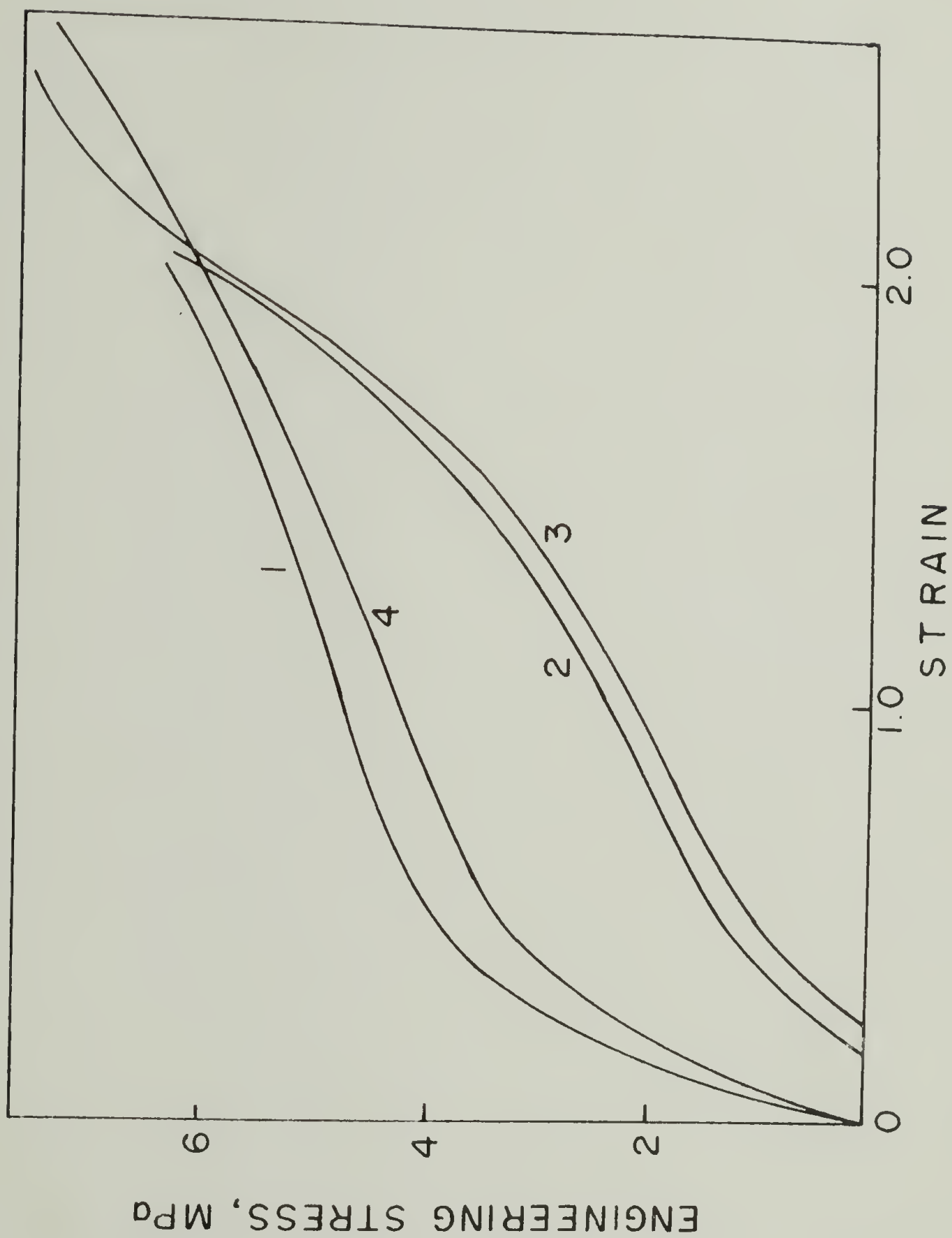


Figure 9. Stress softening of ES5701. Curves 1, 2, and 3 are the first, second, and third tests to strain of 2.0 on the same sample. Curve 4 is the response after heating at 120°C for 30 min., then cooling to room temperature.

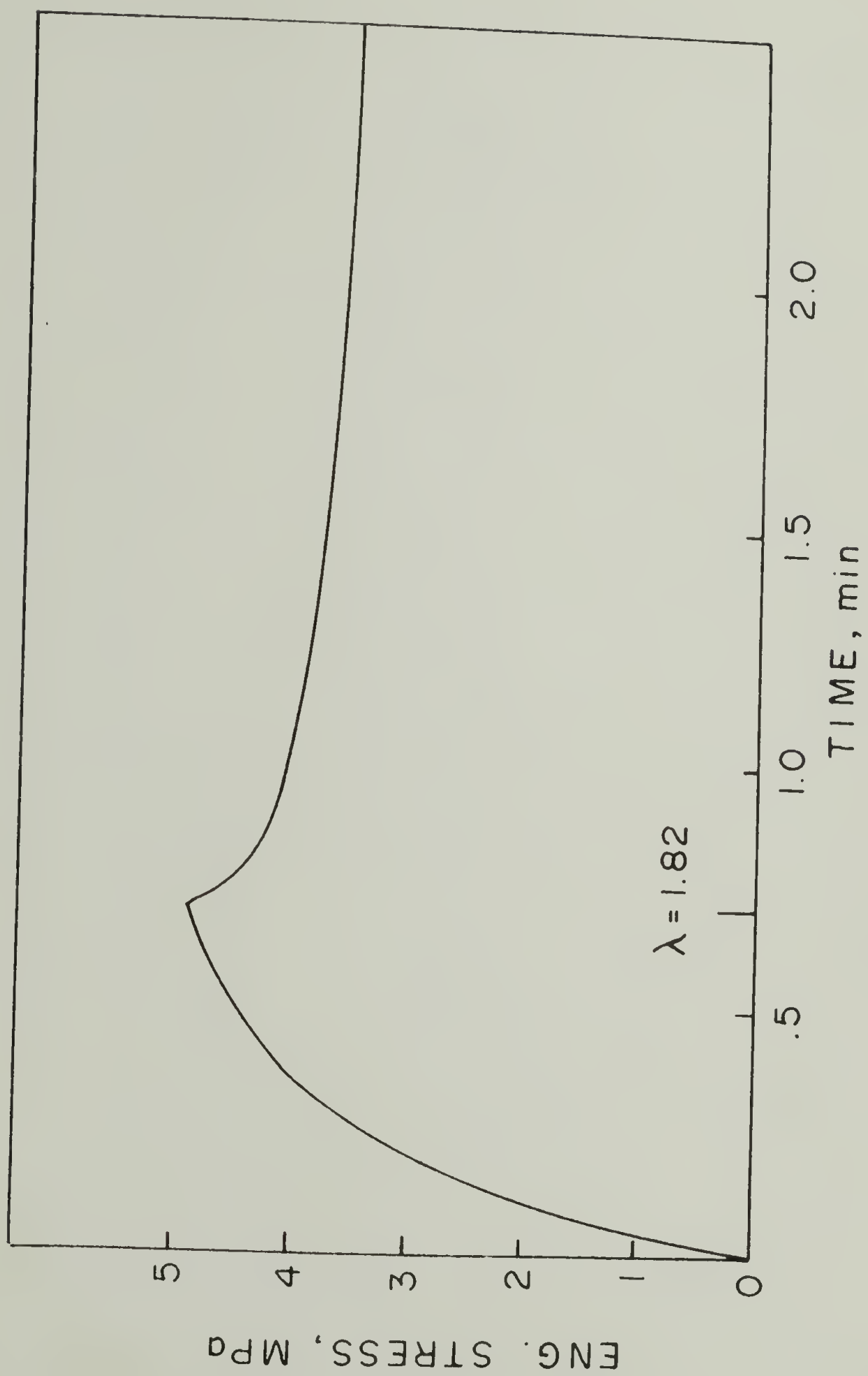


Figure 10. Stress relaxation of ES5701.

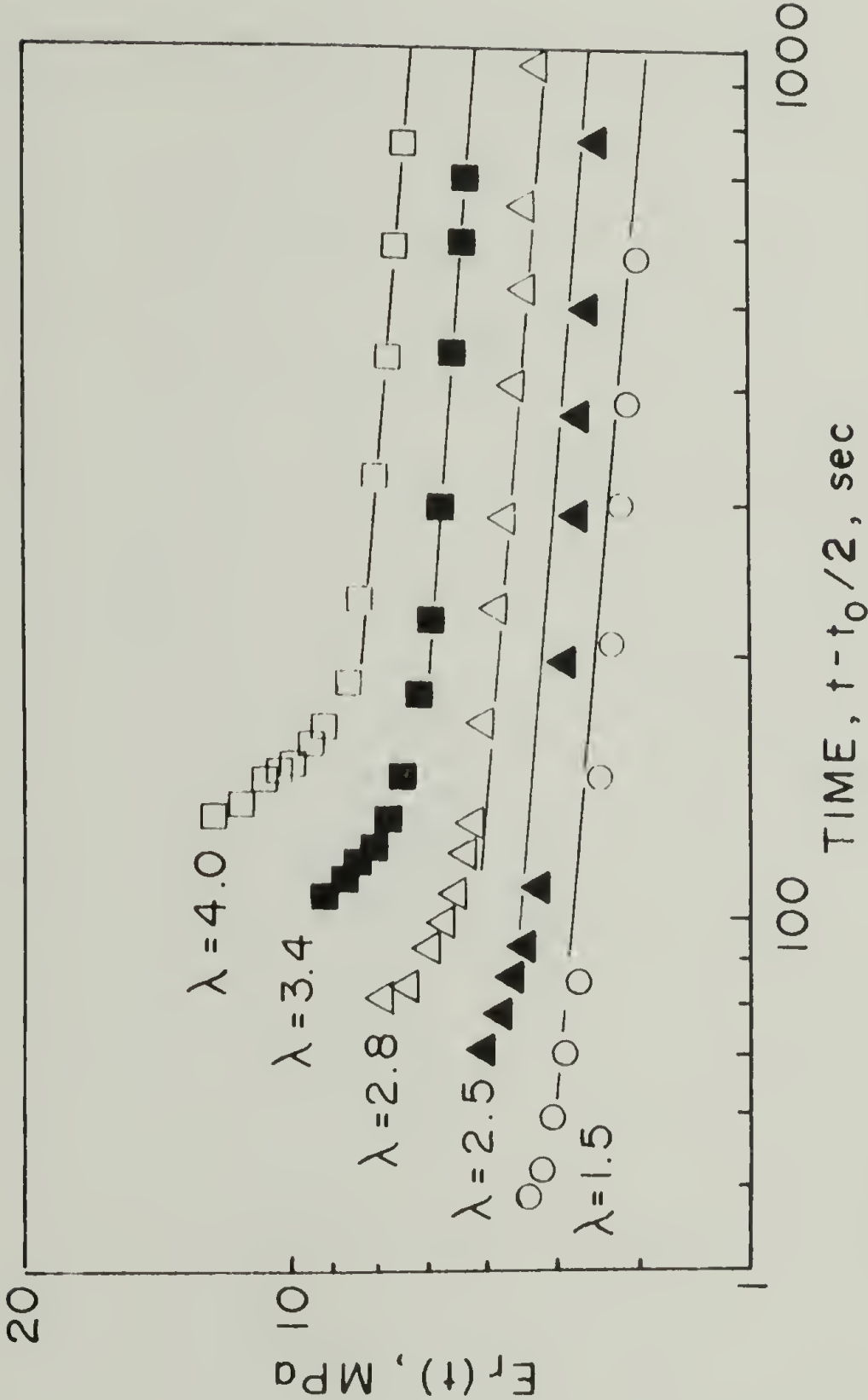


Figure 11. Stress relaxation function defined by Equation 30 of text, for indicated strain levels. Solid curves are given by Equation 31 of text.

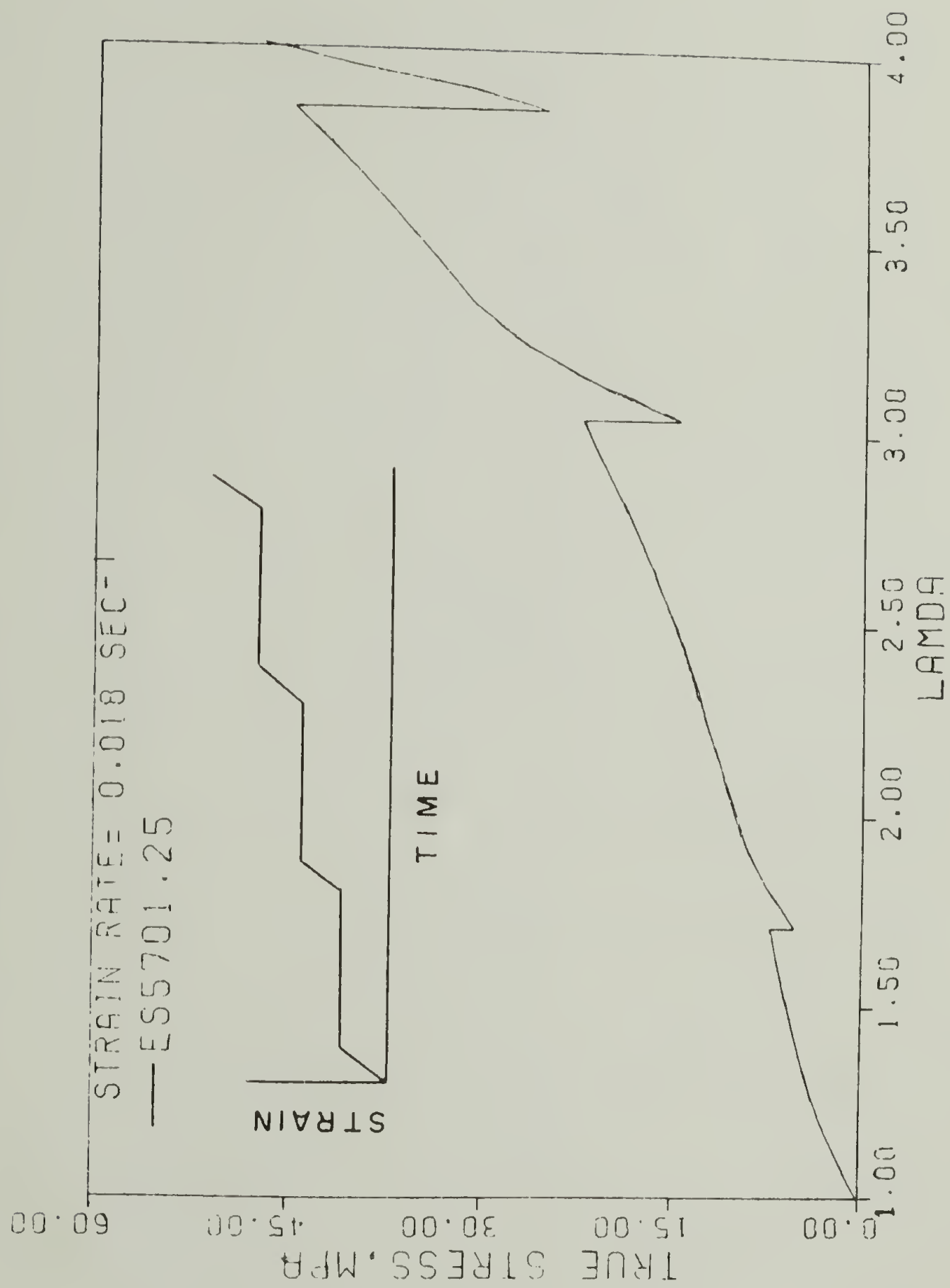


Figure 12. Stress relaxation response of ES5701 to indicated strain history.



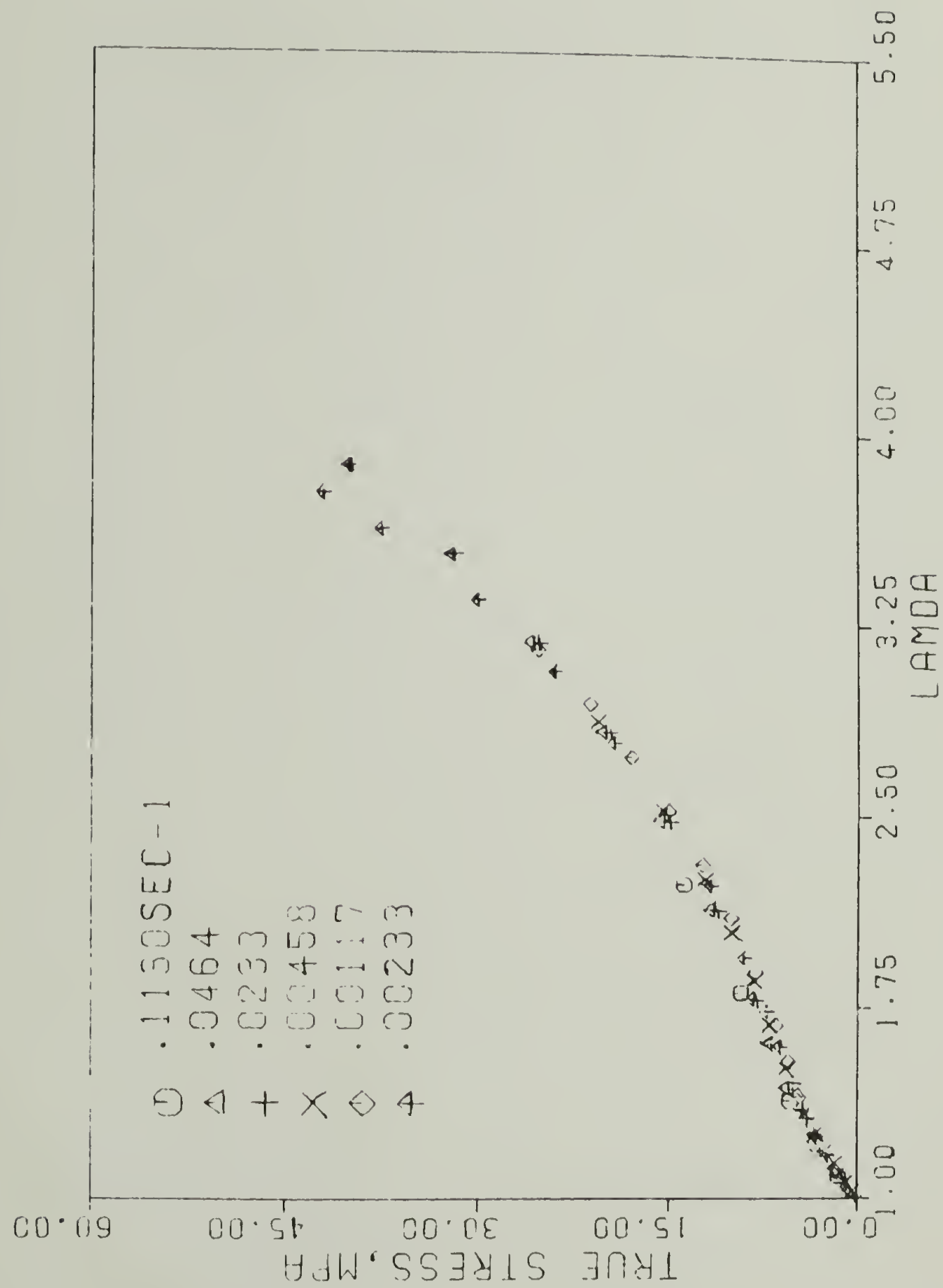


Figure 13. Effect of strain rate on ES5701 in simple tension.

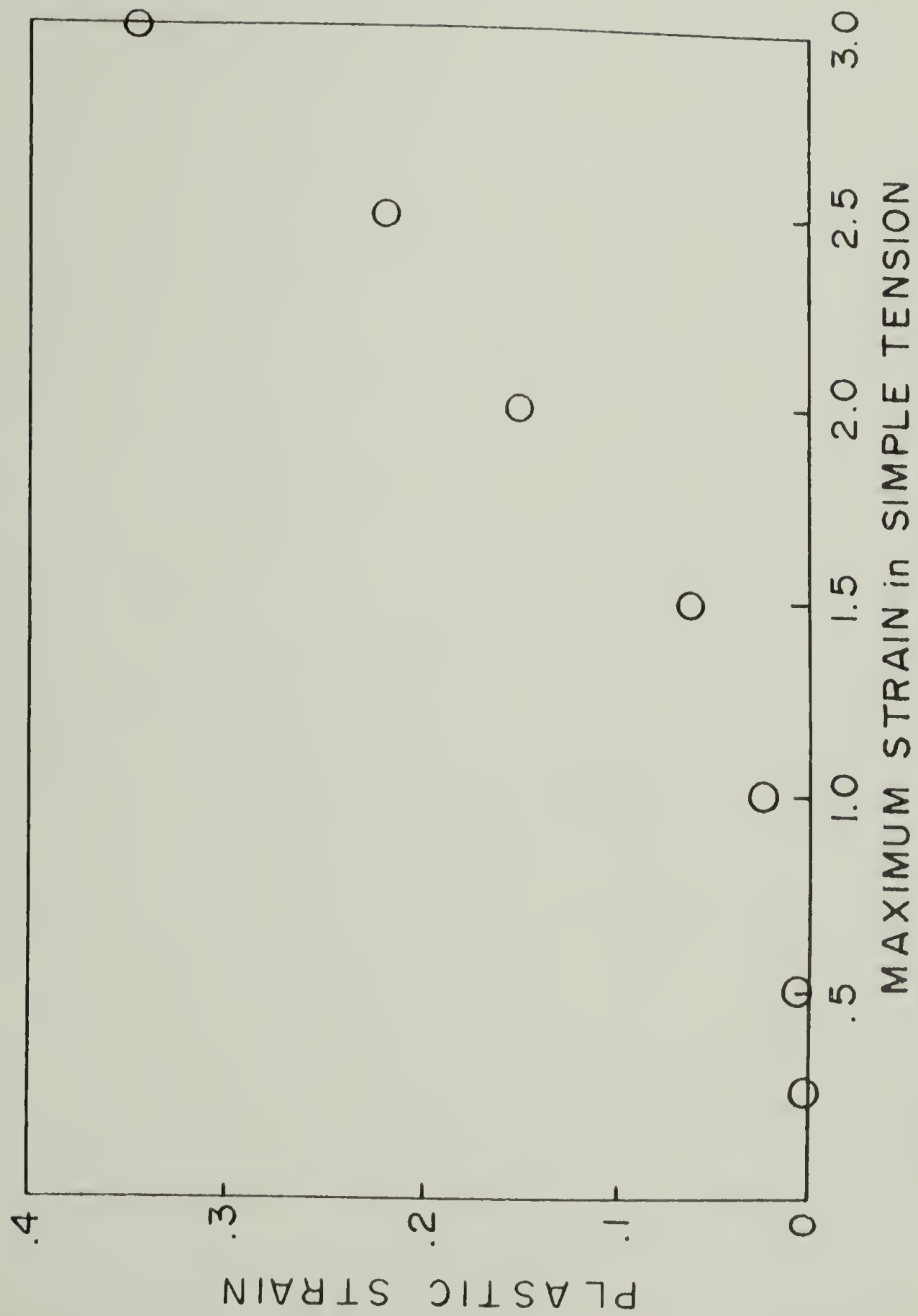


Figure 14. Permanent set in ES5701, as measured by the plastic strain.

The change in mechanical properties with temperature will not be dealt with here except to note that virtually all of the permanent set and mechanical aging recovers upon heating the material to 120°C for a short period (Figure 9).

The permanent memory of polyurethanes for past strain states is seen in the hysteresis and stress relaxation experiments. It can also be observed that the permanent memory is changing its character with time after the test (see the discussion on  $L_{h,p}$  norms above) as indicated in the interrupted test results in Figure 15. It is seen in this figure that although there is some recovery of hysteresis with time, the stress-strain response retains its strong dependence on the previous maximum strain in the history.

These results, together with the failure of the fading memory test presented in Figure 1, are sufficient to demonstrate that Estane polyurethane is a permanent memory material. Even so, it has been characterized as a nonlinear fading memory body by at least one group (deHoff et al., 1966). These authors were satisfied by their agreement of theory to stress relaxation data only. It is evident that a variety of strain histories must be investigated in order to correctly determine what type of functional dependence the stress will have on the strain, and as well the appropriateness of limiting assumptions such as fading memory.

### II.5. Conclusions and Recommendations

The discussion in this chapter has focused on the development

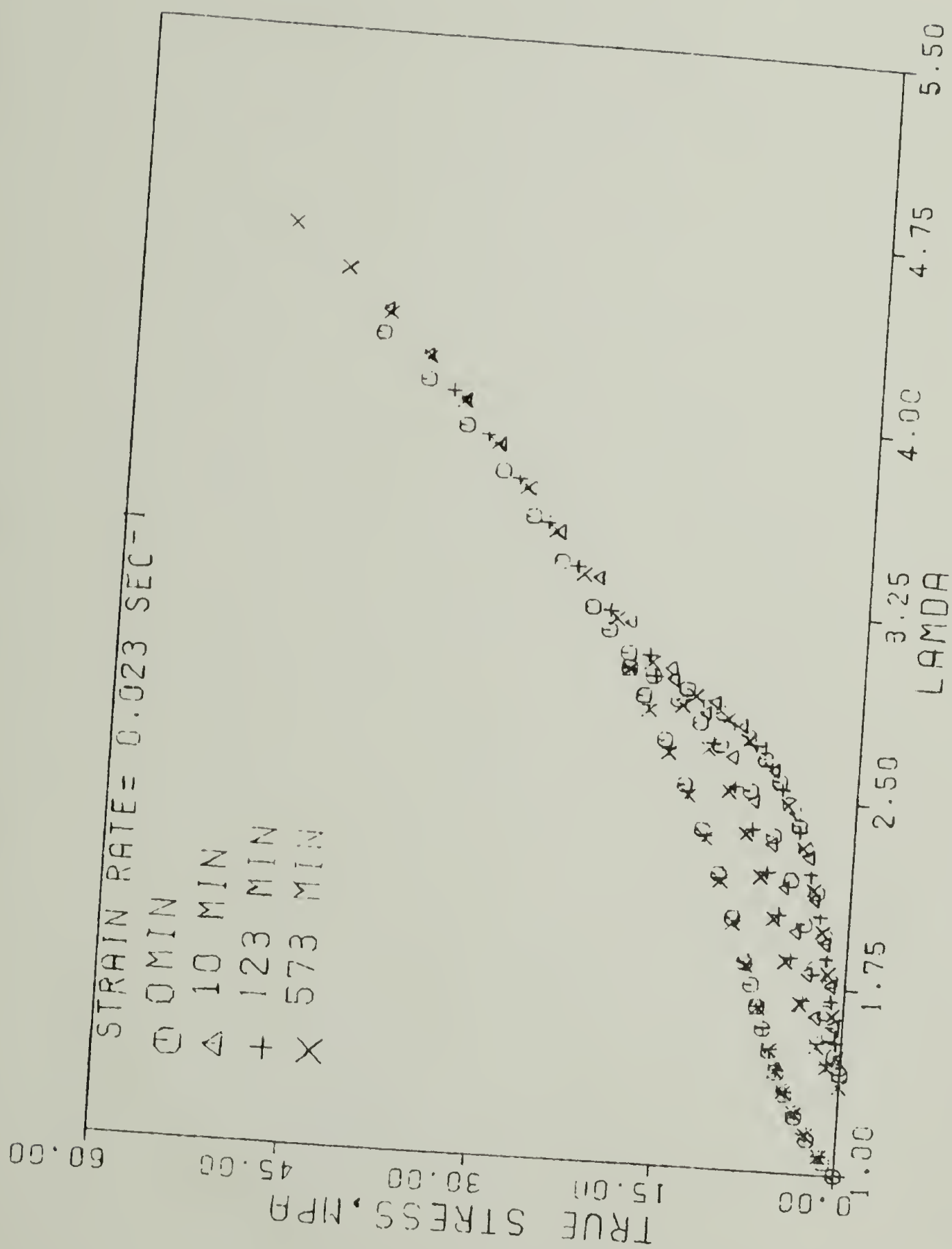


Figure 15. Recovery of hysteresis after straining to 200% and resting for the indicated times.

and application of the fading memory viscoelastic theory as pioneered by Green and Rivlin (1957). It has been shown that the physical implications of fading memory may not be accurate for materials that undergo microstructural changes with deformation. Another class of materials with memory, namely those with permanent memory, has been defined by Farris (1970, 1973); his work represented a departure from the traditional focus of fading memory formulations.

The background information on constitutive equations and material behavior illustrates that the mechanical behavior of polymers may be exceedingly complex, and any attempt at characterization of polymer behavior must begin with an examination of basic assumptions behind the theories in question. In particular, it has been demonstrated that the mechanical behavior of polyurethanes shows permanent memory of the deformation history for which a purely fading memory theoretical description is inappropriate.

Evidence for irreversible microstructural change in polyurethanes is provided by measurements of the orientation in the two separate chain segments during deformation of the material (Estes et al., 1971). The orientation functions determined from IR dichroism show strong dependence on the maximum in the strain history, immediately suggesting the  $L_p$  norm measure of the strain as a significant variable in the orientation-strain constitutive equation. Reasonable models of the orientation-strain behavior may be constructed and compared to experimental data, and fulfillment of this goal will allow the functional dependence of the Quinlan and Fitzgerald Equation (26)



to be examined. The concept of damage may thus be extended to include any microstructural change which alters the material's response to stress, without any restriction to the exact nature of the "damage." Further, the type of strain history dependence of the orientation functions is expected to be an essential feature of the strain history dependence of the stress, as expressed by the functional given in (25).

In general, as more information about the microstructure of polymers becomes available, the opportunity to relate microstructural change to stress-strain behavior in the general framework outlined by Quinlan and Fitzgerald (1973) presents itself. For example, recent work by O'Connor and Wool (1979) on SBS rubber showed that the cavitation in the polymer had a strong dependence on strain history and time, and the stress-strain behavior showed hysteresis similar to that of the polyurethanes. Cavitation may be considered as a measure of damage in the polymer, making the SBS system an ideal candidate for analysis of equations like (25). A large number of other polymers may be treated in the same manner as long as measurements on the polymer microstructure can be made simultaneously with the measurements of stress and strain. Spectrographic and optical measurements, as well as some resonance techniques like electron paramagnetic resonance (see Devries and Farris, 1970), are obvious choices for this type of study. The construction of adequate constitutive equations for polymers is certain to be simplified by this approach since it is a step in the direction of narrowing down the scope of the hopelessly general expression of material memory in Equation (7) by consideration of observed physical

changes in the material.

The next chapter will contain the results obtained from a model of the polyurethane microstructure which leads to a characterization of the strain history dependence of orientation, which is essentially a characterization of Equation (26). The final chapter will show the results of characterizing polyurethane mechanical behavior based on the results of Chapter III.

## CHAPTER III

### POLYURETHANE MICROSTRUCTURAL MODELS

A large body of work in the polymer science field has been devoted to increasing the knowledge of polymer microstructure and morphology as a function of composition, temperature, and deformation histories. For the class of polymers under consideration, segmented polyurethane elastomers, the microstructure has been investigated in considerable detail, and as well, it is known that irreversible orientation of the hard and soft segment domains of this polymer occurs with deformation (Estes et al., 1971; West et al., 1975). As discussed in the previous chapter, irreversible events produced by deformation history of a material may lead to permanent memory of past deformation states in the constitutive equation for stress. The goal of this chapter is to examine in detail the available information on the morphology and orientation of polyurethanes during deformation in order to help construct microstructural models that will enable one to predict the orientation-strain behavior of polyurethanes. Since the microstructural behavior is expected to be intimately associated with the bulk stress-strain response measured during mechanical testing, the relationship between the microstructure and bulk properties will be clarified. The model predictions will be compared to the experimental data of Cooper (1978).

### III.1. Microstructure of Polyurethane Elastomers

Segmented polyurethane elastomers are block copolymers produced by joining alternate blocks of two different polymer chains. At room temperature one of the polymer chains of the polyurethane is viscoelastic or rubbery in nature (soft segment); the other is below its glass transition (hard segment). In the following discussion reference will be made to several general types of segmented polyurethanes. Polymers in which the soft segments are a polyester will be designated ES and those in which the soft segments are polyether, ET. The hard urethane segments are based either on 4,4'-diphenylmethane diisocyanate (MDI) or toluene diisocyanate (TDI). A detailed description of the composition of the polyurethanes discussed in this thesis is given in Appendix A. The polymers mentioned here have urethane content low enough to render the hard domains noncrystalline (Estes et al., 1971).

It is currently accepted that many of the desirable properties of polyurethanes may be attributed to micro-separation of hard segments into domains dispersed in the soft segment matrix (Estes et al., 1970). These two domains of the polymer are frequently referred to as phases since the polyurethane, while homogeneous in the chemical sense, is not physically homogeneous. The domains are small, with a characteristic size of  $50 \text{ \AA}$ , as seen in the transmission electron microscope (Koutsky et al., 1970). The hard segment domains act as stiff filler particles and as physical crosslink points and thus reinforce the soft matrix. Above the softening temperature of the higher modulus hard



segments, polyurethanes behave as thermoplastics and may be processed as such; they then regain their elastomeric properties upon cooling.

A subject of much discussion in the recent literature has been the role of hydrogen bonding in determining the mechanical properties of polyurethanes. The polymers under discussion in this thesis are extensively hydrogen bonded; the donor group is the N-H of the hard urethane segment while the acceptor group for the hydrogen bond is either the carbonyl (C=O) in the urethane segment or the ether oxygen (in the case of ET polymers) or the polyester carbonyl (in the case of ES polymers) of the soft segment. The hydrogen bonding is therefore divided between intra- and inter-domain bonding, as shown schematically in Figure 16.

Studies by Seymour et al. (1970) indicate that about 85% of the urethane NH groups are hydrogen bonded, while about 60% of the urethane carbonyls act as acceptors for bonding. Thus, about 30% of the bonded NH are involved with bonding to acceptors in the soft segment (ET polymer). The conclusion drawn from this study is either that the domain separation is incomplete in the polyurethane, so that a substantial amount of soft segments are mixed into the hard domains, and vice versa; or that the interface between the two domains is a diffuse one, essentially giving rise to a boundary phase between the soft and hard domains; or that the domain structure is such that the surface area between the domains is large enough to account for all the hard segment to soft segment hydrogen bonding.

Recent small angle x-ray scattering (SAXS) results by Kober-



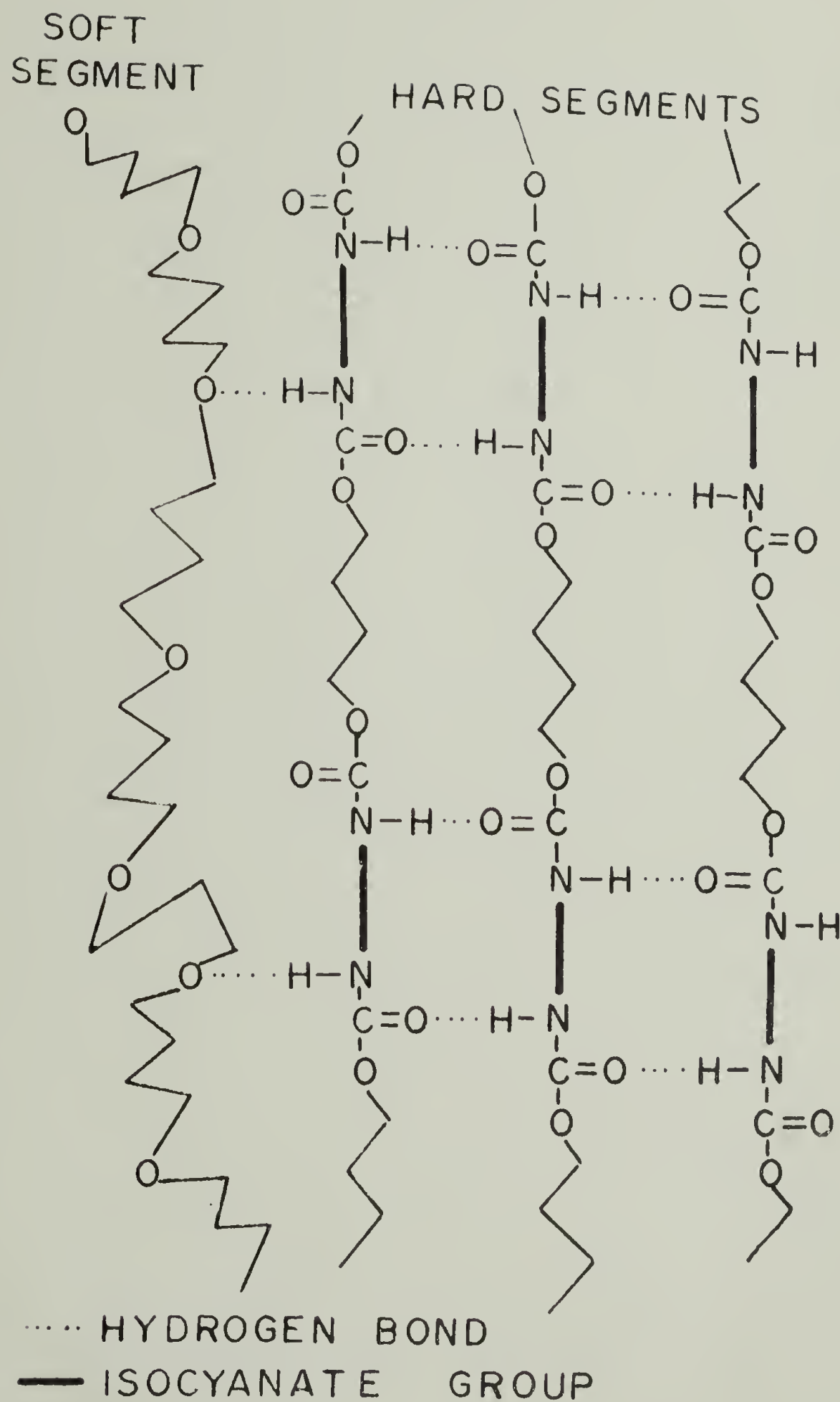


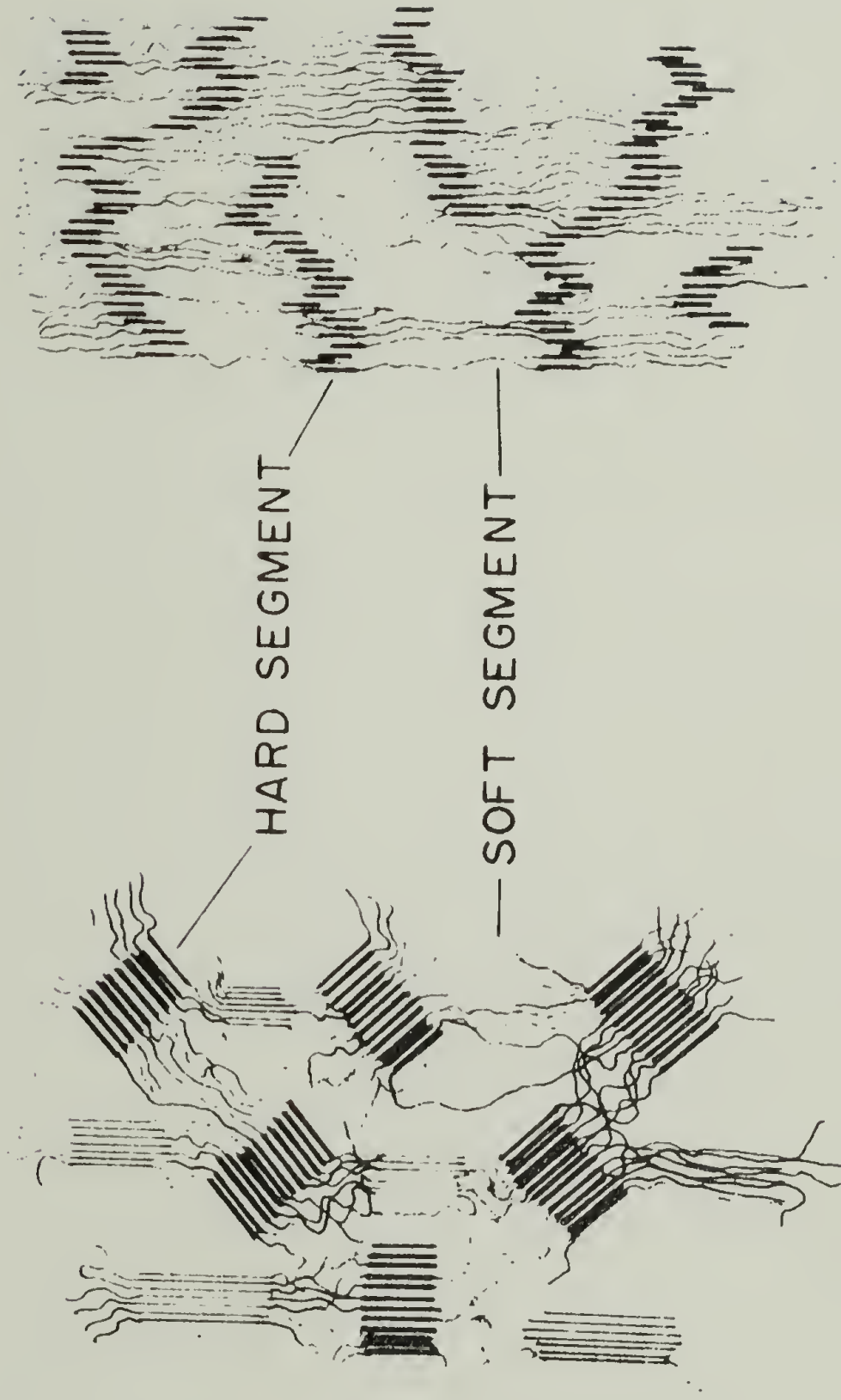
Figure 16. Schematic of polyurethane microstructure showing hydrogen bonding in the hard chain segments and between the hard and soft chain segments.

stein (1979) on MDI and TDI based polyurethanes indicate that MDI polymers are 40-45% domain separated while the TDI polymers are only about 25% separated. The nature of the domain separation was different for the two types of polymers, with mixing in the MDI polymers occurring predominantly in the interface between hard and soft domains, while in the TDI based systems there was considerable inter-domain mixing as well as boundary mixing. The major conclusions of this study were that considerable amounts of the two different types of polyurethane chains are mixed together, and also that the domain sizes are small. These conclusions were also reached by Bonart and Müller (1974).

Investigations into the morphology of segmented polyurethanes have also received much attention in the recent literature. Bonart (1968) and Bonart et al. (1969) determined from SAXS that the hard segment domains in MDI-based polymers contain considerable order, while the soft domain did not. He explained the SAXS spacings in terms of a reasonable arrangement of hydrogen bonding bridges between hard domain segments. Two reports by Clough and Schneider (1968) and Clough et al. (1968) on B.F. Goodrich Estanes (MDI-type) contained similar conclusions based on SAXS and scanning thermal methods.

Of central concern to this thesis is the change in the polyurethane microstructure with deformation. The original ideas of Bonart (1968, 1969) have received wide acceptance and confirmation by other workers. His model for the changes in the morphology of polyurethanes with deformation is shown in Figure 17. At small strains,

# BONART MODEL



A. ~ 200% STRAIN

B. ~ 500% STRAIN

Figure 17. Schematic of polyurethane microstructure undergoing deformation. After Bonart (1968, 1969).

the lamellar hard segment domains retain their original order but can orient as a more or less rigid unit in the direction of strain. There is also considerable soft segment crystallization with stretch. At elongations over about 200%, the original hard domain structure breaks up, but reforms in a lamellar fashion that retains most, if not all, of the essential domain character of the original structure.

The restructuring of the original network configuration is supported by other studies. Koberstein (1979) assumed a lamellar structure of the two domains in his SAXS work. Seymour et al. (1970) demonstrated that the extent of hydrogen bonding in polyurethanes remains essentially constant to 325% elongation. This result indicates that not only are changes in the amount of hydrogen bonding with deformation unimportant to the mechanical response of the polymers, but also that reorganization and orientation occurring with stretch is accomplished while preserving the character and amount of the initial inter- and intra-domain interactions. The SAXS work of Wilkes and Yusek (1973) supports the idea that the hard domains are lamellar in nature and orient perpendicular to the stretch direction while retaining considerable order.

Further insight into the microstructural mechanical behavior has been gained by studies that focus on strain histories other than simple extension of a virgin sample. The stress softening seen on repeated stretching of polyurethanes was first considered by Puett (1967), who showed excellent insight into the microstructure of these polymers even before the X-ray results of Bonart were published. Puett



attributed the modulus reduction on second stretch to a "decrease in the effective number of network chains, resulting from a modification of physical crosslinkages. Such an effect can result from an irreversible detachment of certain segments from the network junction points or even by readjustment within the crosslinkage" (added emphasis). Puett's results also demonstrated that the birefringence, a measure of the total orientation in the polyurethane, did not show hysteresis corresponding to the stress-strain hysteresis. The plot of birefringence vs. strain was linear up to an extension of 100% for both the first and second stretches. This observation was also made by Estes et al. (1969) for an Estane polyurethane (MDI-type) up to strains of 200%.

Further clarification of the deformation behavior of the polyurethane microstructure was gained by Estes et al. (1971) through the use of infrared (IR) dichroism experiments, in which the orientation of specific polymer chain segments was monitored for different strain histories. In particular, the NH stretching vibration was recorded as representing the orientation of the hard segments, while the asymmetric C-H stretching absorption was used to indicate soft segment orientation. Some error was introduced in the determination of the soft segment orientation since 16% of the CH groups of an ET type polymer reside in the hard domain (22% in the case of an ES polymer). The results of this investigation showed that the orientation of the two different backbone segments depends strongly on strain history. In particular, the hard segment orientation for ES-38 (see Appendix A)



showed some irreversible part when the samples were strained to a particular level, then relaxed for 5 minutes, while the soft segment orientation was nearly reversible. Also, when the samples were prestrained to 200% elongation, then relaxed and retested, the hard segment orientation displayed the reverse hysteresis shown in Figure 18 (replot of Estes et al., 1971 data). Note that after the previous maximum state of strain (200%) is surpassed, the orientation-strain behavior was comparable to a virgin sample. The soft segment orientation (Figure 19) appeared to have the same behavior for both the prestrained and virgin samples. With reference to the previous chapter, it is evident that the hard domain orientation process possesses the same type of permanent memory of deformation states as does the stress. Obviously the restructuring of the polyurethane lamellar network is accomplished by some irreversible deformation of the hard segment domains which leads to the observed orientation-strain behavior.

In another publication (Seymour et al., 1973) the time-dependence of the orientation process in ET-31 (see Appendix A) was demonstrated by monitoring the IR dichroism of the two domains during a stress relaxation test (Figure 20). After initial straining to 150%, the soft segment orientation decreased rapidly with time at constant strain by about 25% while the hard segment orientation increased in the same manner by about 20%. This behavior clearly demonstrates how the two chain segments act in cooperation since the more flexible soft chains relax toward a disordered state while exerting tension on the hard segments, allowing them to become more oriented in

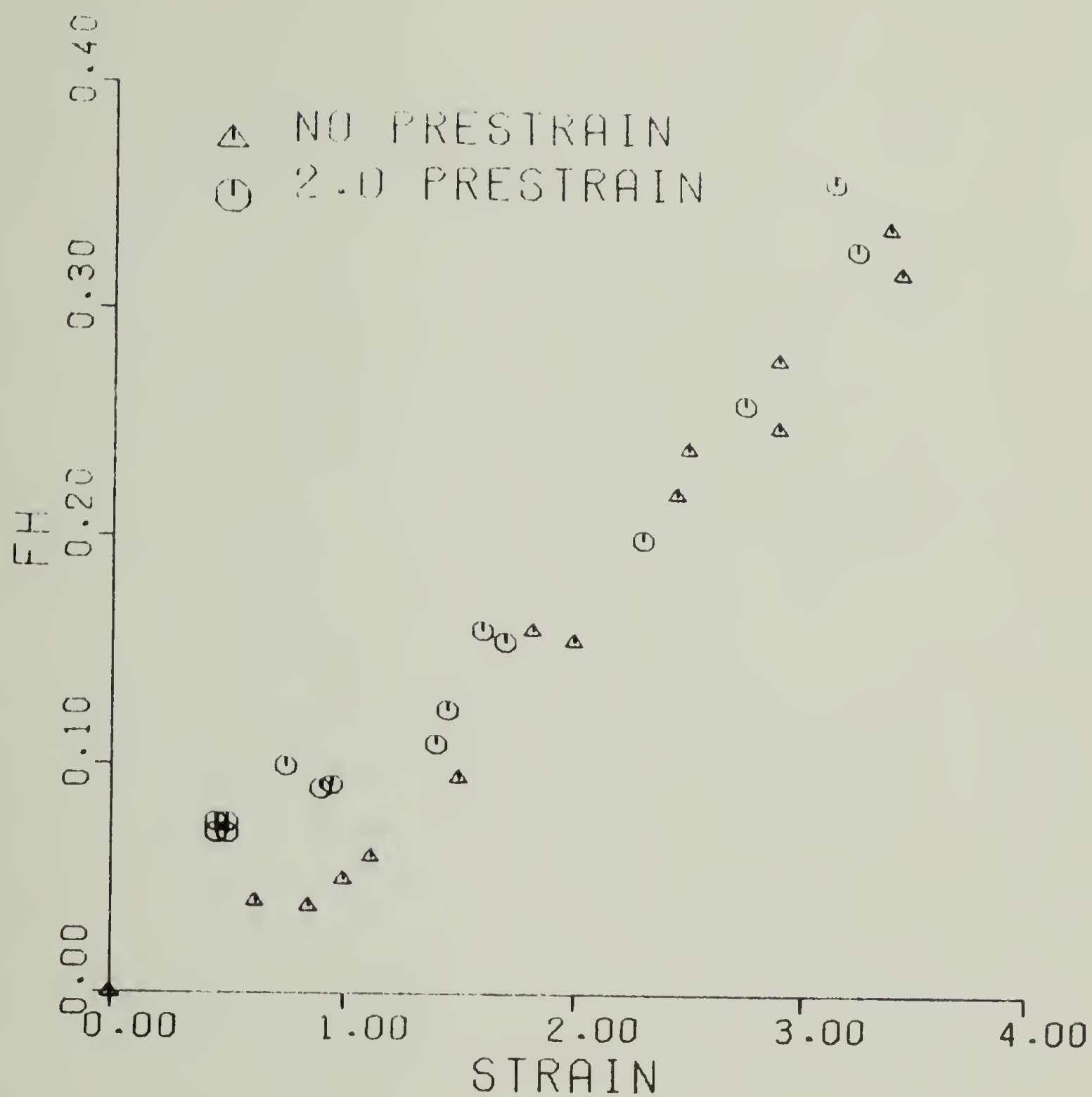


Figure 18. Orientation function of hard segments (FH) vs. strain for virgin samples and samples with prestrain of 2.0. Data of Estes et al. (1971).

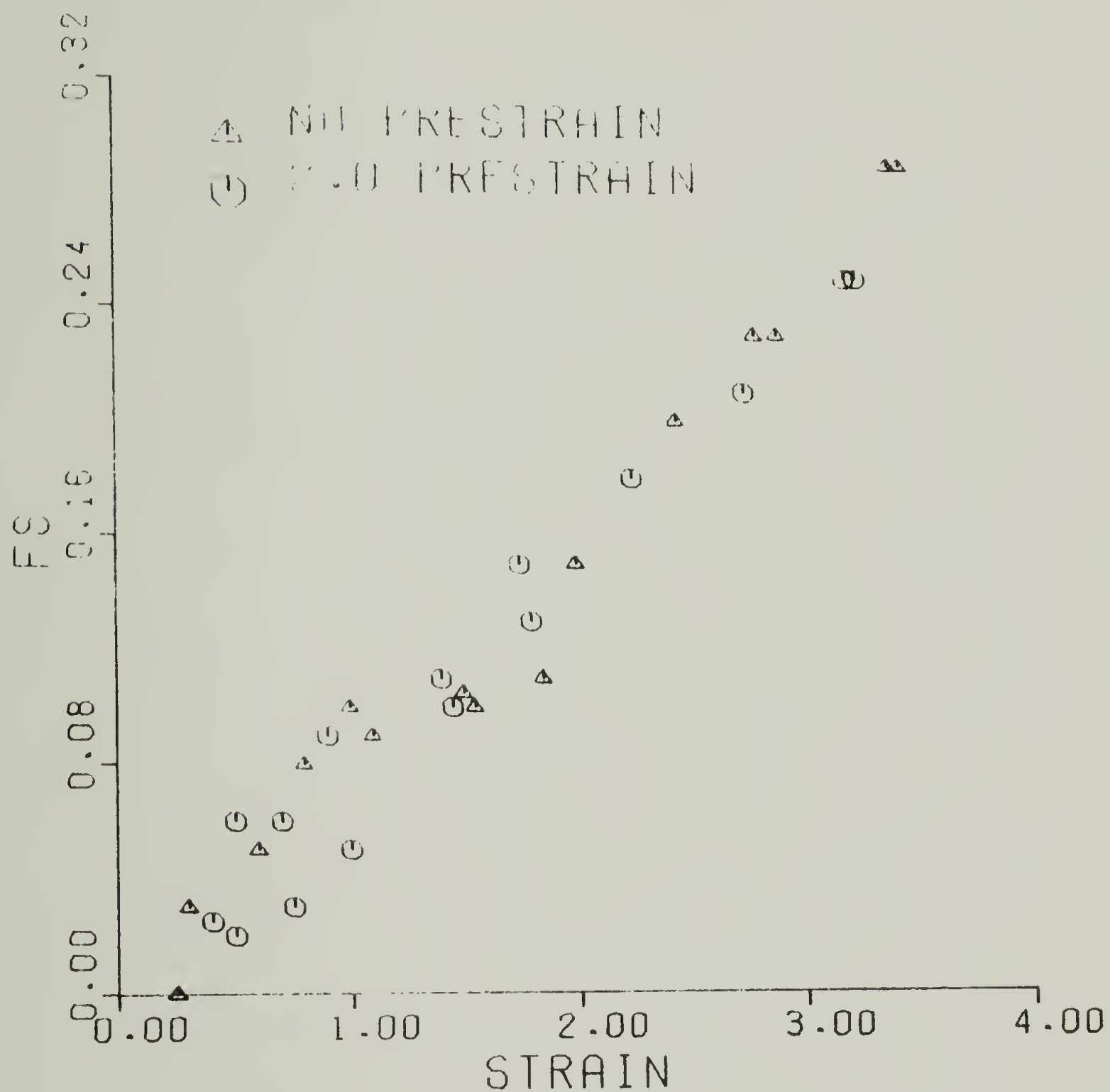


Figure 19. Orientation function of soft segments (FS) vs. strain for virgin samples and samples with prestrain of 2.0. Data of Estes et al. (1971).

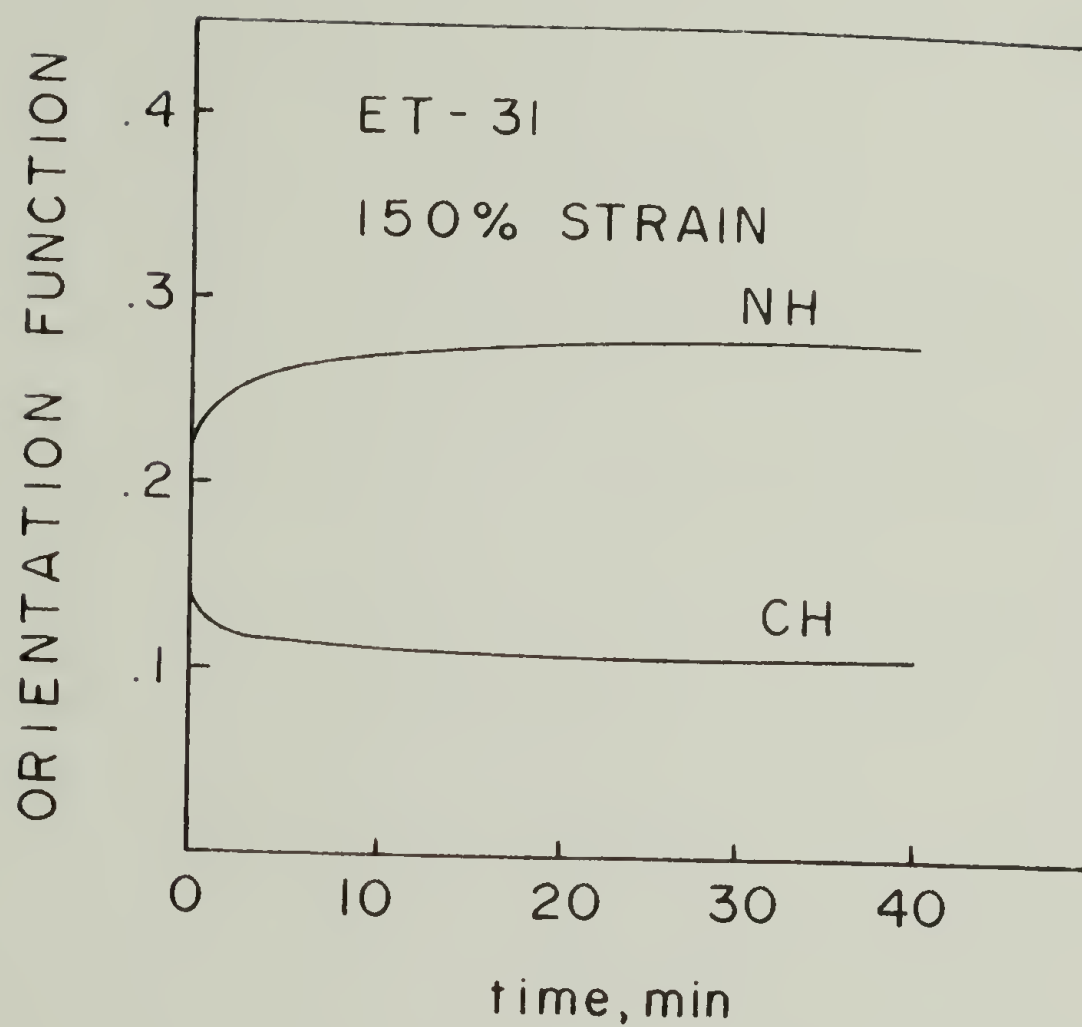


Figure 20. Hard (NH) and soft (CH) segment orientation functions as a function of time after straining quickly to 150% strain. After Seymour and Cooper, 1974.

the stretch direction. West et al. (1975) showed the results of a more sophisticated IR dichroism technique for orientation-strain studies of ET-38 (see Appendix A) in which the characteristic spectrum for each domain was recorded continuously during a constant strain rate history such as the one in Figure 21. In the earlier study (Estes et al., 1971), a different sample was used to obtain each data point, creating considerable scatter in the data (Figures 18 and 19). The continuous test on the ET polymer showed the same type of hard segment orientation as the earlier work did; additionally, the soft segment orientation showed hysteresis in the same direction as the stress-strain hysteresis.

A complete set of stress-strain-orientation data (Figures 22, 23, 24) for the ET-38 polyurethane discussed in West et al. (1975) was obtained from Dr. S.L. Cooper, University of Wisconsin, and will be discussed in detail below. In Figure 22, the orientation function,  $f_h$ , determined from the NH stretching vibration, is plotted versus strain for the strain history shown in Figure 21. In Figure 23, the orientation function,  $f_{CO}$ , was determined from the hydrogen-bonded urethane carbonyl (C=O) group of the polymer, and thus is also indicative of hard segment orientation. In Figure 24, the orientation function,  $f_s$ , of the soft segments, as indicated by the CH group, is plotted for the same history. Note that the orientation functions determined from the NH and bonded CO groups display hysteresis which is complementary to the soft domain orientation hysteresis.

To summarize, the important points concerning the changes in



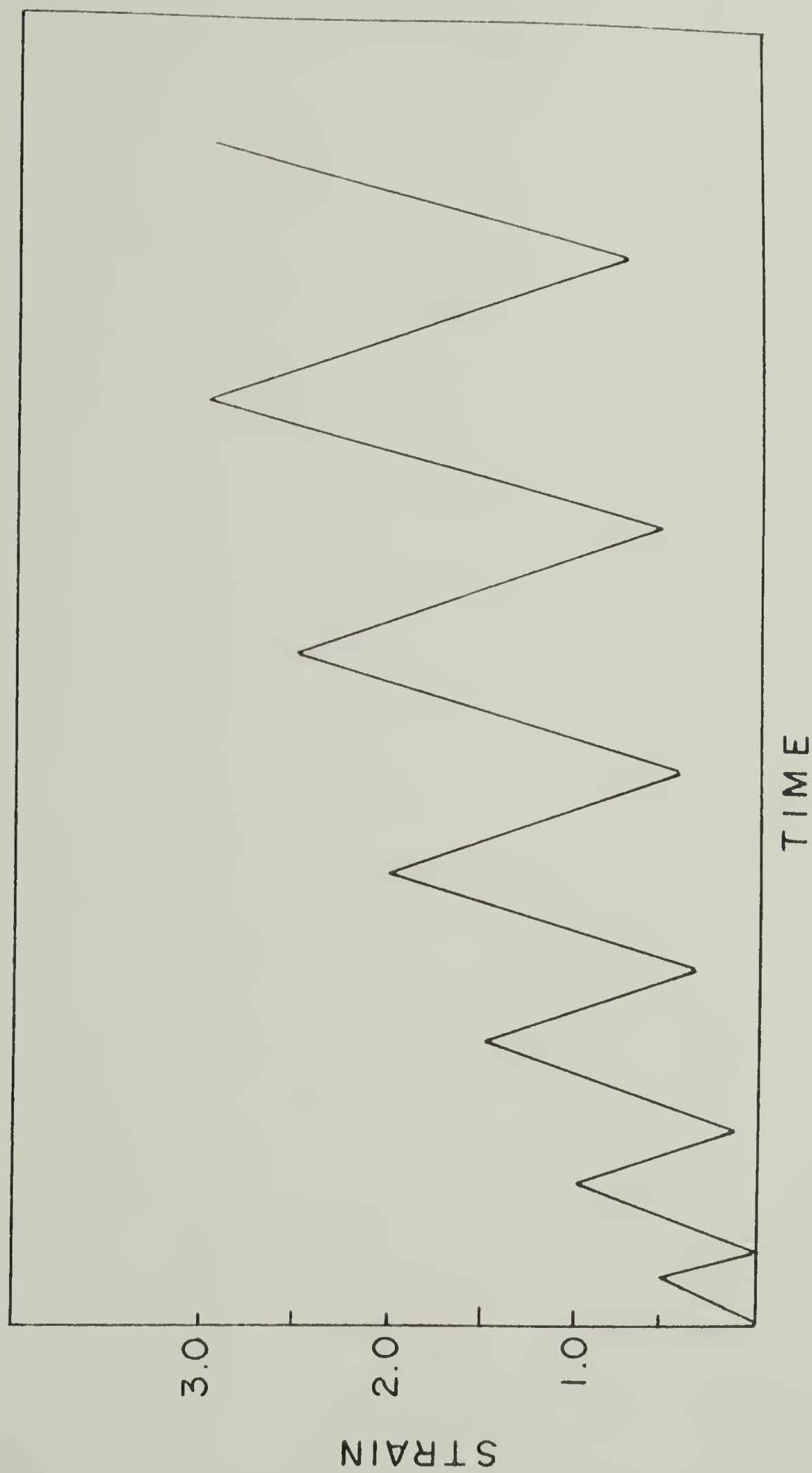


Figure 21. Constant strain rate history.

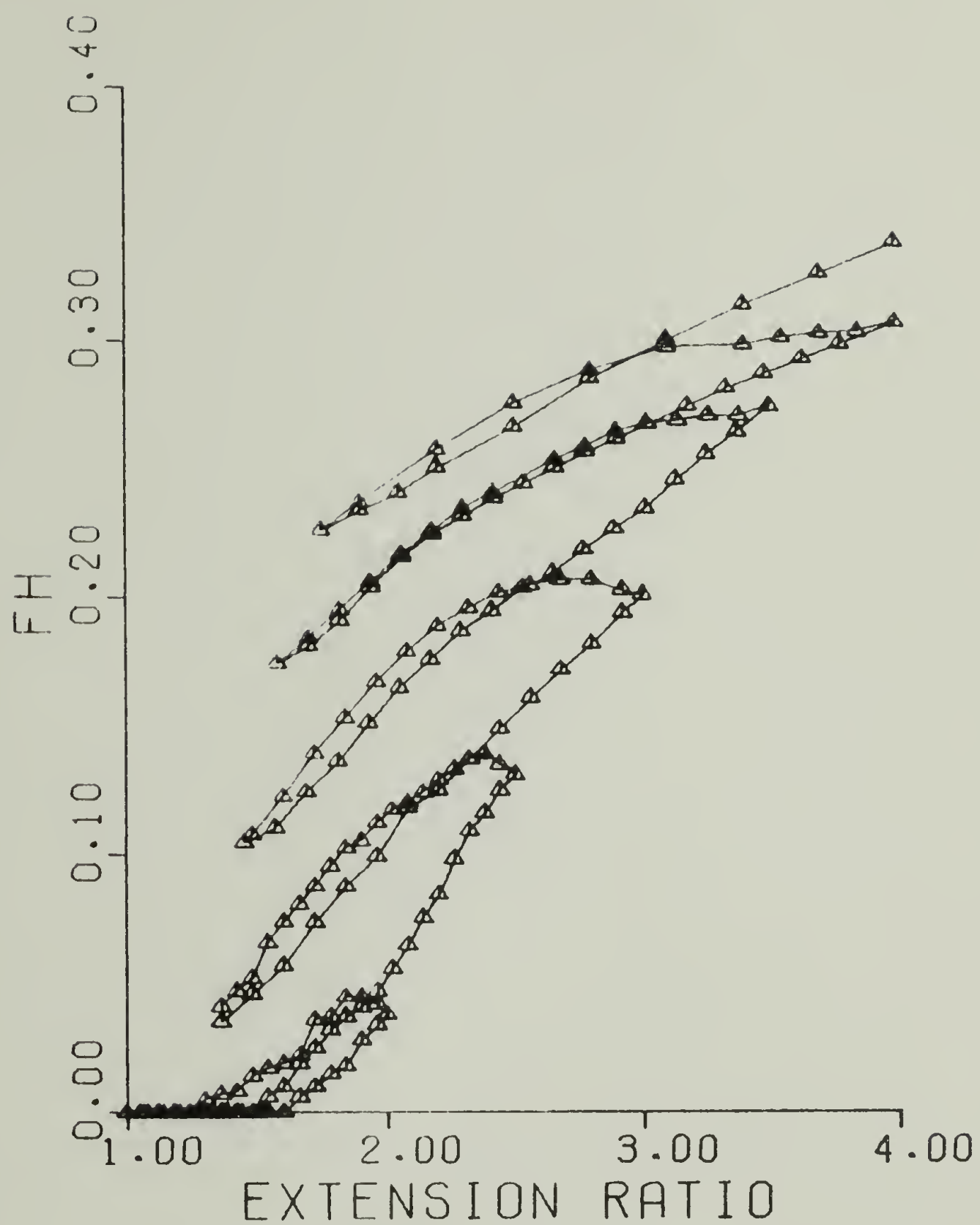


Figure 22. Hard segment orientation as indicated by NH stretching (FH) vs. extension ratio for ET-38 (data of Cooper). Strain history given in Figure 21.

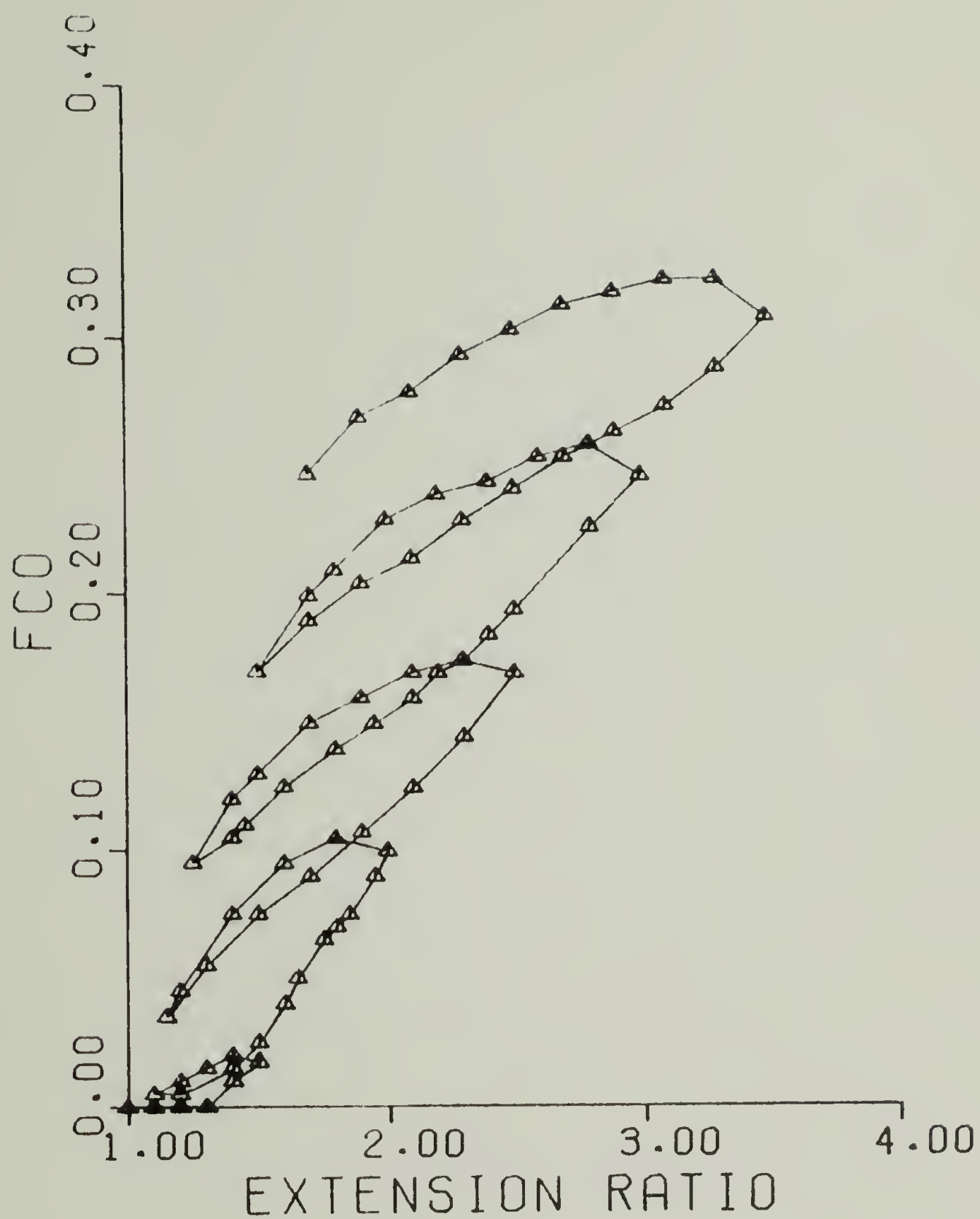


Figure 23. Hard segment orientation as indicated by CO stretching (FCO) vs. extension ratio for ET-38 (data of Cooper). Strain history given in Figure 21.

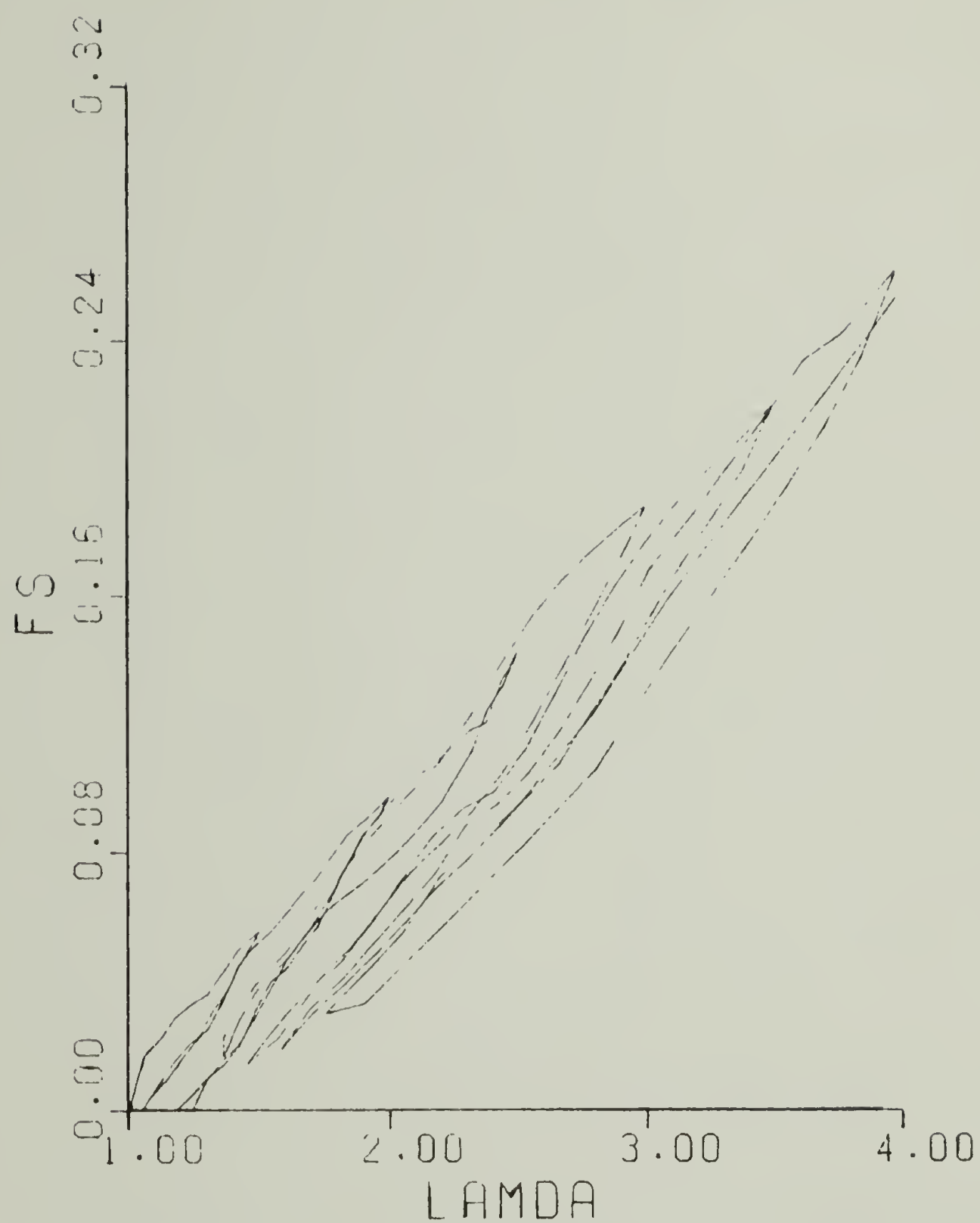


Figure 24. Soft segment orientation as indicated by CH stretching vibration (FS) vs. extension ratio for ET-38 (data of Cooper). Strain history given in Figure 21. Data points omitted for clarity.

the microstructure of polyurethanes during deformation are:

- (1) The morphology of polyurethanes has been shown to consist of two partially segregated domains of soft and hard segments. The structure is lamellar in nature, and the lamellar structure is conserved in deformation through reorganization of the hard domains.
- (2) The deformation of the hard domains, as evidenced by the orientation function of the hard chain segment, does not proceed reversibly in a cyclic straining test.
- (3) The orientation-strain behavior of the hard and soft segments exhibits the same type of sensitivity to the previous maximum state of strain as does the stress.
- (4) The total orientation, as measured by the birefringence, shows no hysteresis.
- (5) The orientation functions of the two separate domains show time-dependence in a stress-relaxation test.

The conclusion drawn from the above studies is that the orientation functions of the hard and soft chain segments may serve as measures of the change in the microstructure during deformation, in the manner suggested by the use of the damage tensor of Quinlan and Fitzgerald (1973), discussed in the previous chapter. This concept will be developed in the next section.

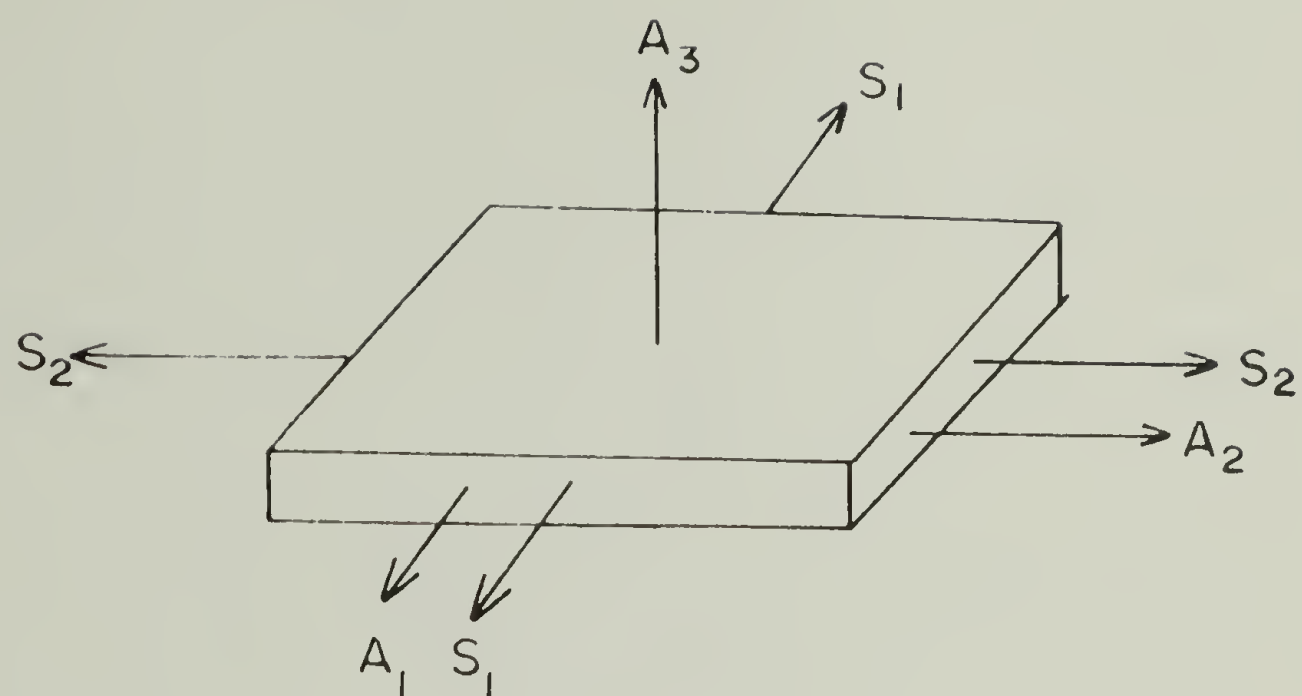


### III.2. Orientation Function as a Measure of Microstructural Change

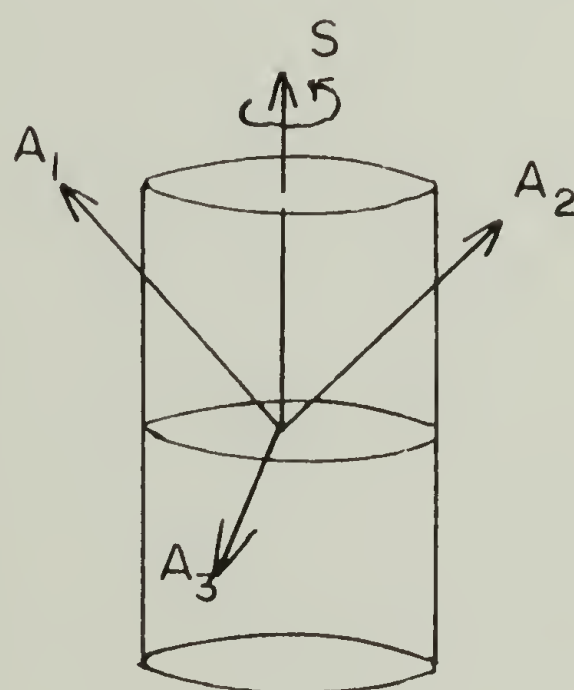
In the infrared (IR) dichroism experiments discussed above, the orientation function measured in the direction of stretch is defined as the normalized difference between the IR absorbances in the directions parallel ( $A_{||}$ ) and perpendicular ( $A_{\perp}$ ) to the stretching direction (Gotoh et al., 1965):

$$(32) \quad f = \frac{A_{||} - A_{\perp}}{A_{||} + 2A_{\perp}}$$

The two absorbances in Equation (32) are two components of the absorbance tensor, which, since the absorbances are normally determined in the principle directions of stress and strain, has only three nonzero components. The absorbance components for simple test configurations such as unequal biaxial stress, simple torsion, and simple tension are depicted in Figures 25 and 26. From those diagrams it may be concluded that the denominator of (32) is simply the first invariant of the absorbance tensor, and that the definition in (32) may be generalized, yielding the result that the orientation function is itself a second rank tensor, with diagonal components:



A.



B.

Figure 25. Example test configurations with indicated stresses,  $S_i$ , and IR absorbances,  $A_i$ , in the principle directions.  
 A. unequal biaxial B. simple torsion.

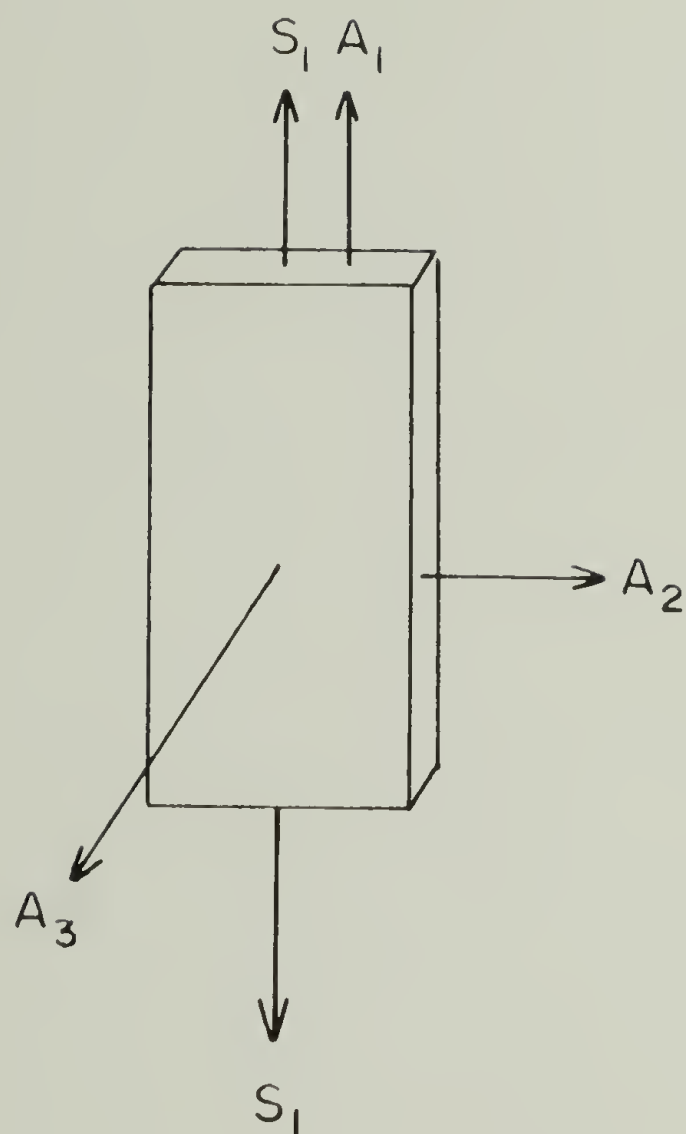


Figure 26. Principle directions of IR absorbances,  $A_i$ , for the case of simple tension.

$$(33) \quad f_1 = \frac{A_1 - \bar{A}/3}{\bar{A}}$$

$$f_2 = \frac{A_2 - \bar{A}/3}{\bar{A}}$$

$$f_3 = \frac{A_3 - \bar{A}/3}{\bar{A}}$$

where  $\bar{A} = A_1 + A_2 + A_3 = \text{tr}\underline{A}$ . The orientation functions in the principle directions are thus seen as the normalized distortional part of the absorbance tensor.

Since the absorbances are measured on the deformed sample, it is necessary to express any orientation function-strain relation in terms of the strain in the deformed coordinate system. The first order term of the Eulerian strain, which is a strain measure referred to the deformed coordinates of the sample, for the case of simple tension, may be written in terms of the extension ratio  $\lambda$  (see Appendix C):

$$(34) \quad \epsilon = \frac{\lambda - 1}{\lambda} = 1 - \frac{1}{\lambda}$$

In the ensuing development of orientation function-strain relations, the strain measure  $\epsilon$  will be used. For comparison to the way in which the orientation function is usually plotted, namely versus nominal strain or extension ratio (both measures are referred to the original sample coordinate system), a plot is given in Figure 27 of the orientation function of the hard chain segments of the polyurethane (data of Figure 22) multiplied by the extension ratio  $\lambda$ , versus the nominal strain  $(\lambda-1)$ . Multiplication of  $f_h$  by  $\lambda$  is equivalent to plotting  $f_h$  versus  $(\lambda-1)/\lambda$  directly.

For consistency with other work, however, all plots of orientation function will be given versus nominal strain  $(\lambda-1)$  or extension ratio  $\lambda$ , with the understanding that the strain measure used in the constitutive relations for  $f_h$  is given by Equation (34).

### III.3. Series Model for Polyurethane Domains

Since this report deals with the mechanical behavior of polyurethanes, it is desirable to formulate a model of the polyurethane microstructure which will lend itself to simple analysis. Based on the above investigations into the microstructure and morphology of polyurethanes, a series composite model is proposed which represents in an idealized fashion the lamellar nature of the hard and soft domains (see Figure 17). The series model is sketched in Figure 28.

Other researchers have used composite models of various types to combine the properties of two phase polymer systems. Takayanagi



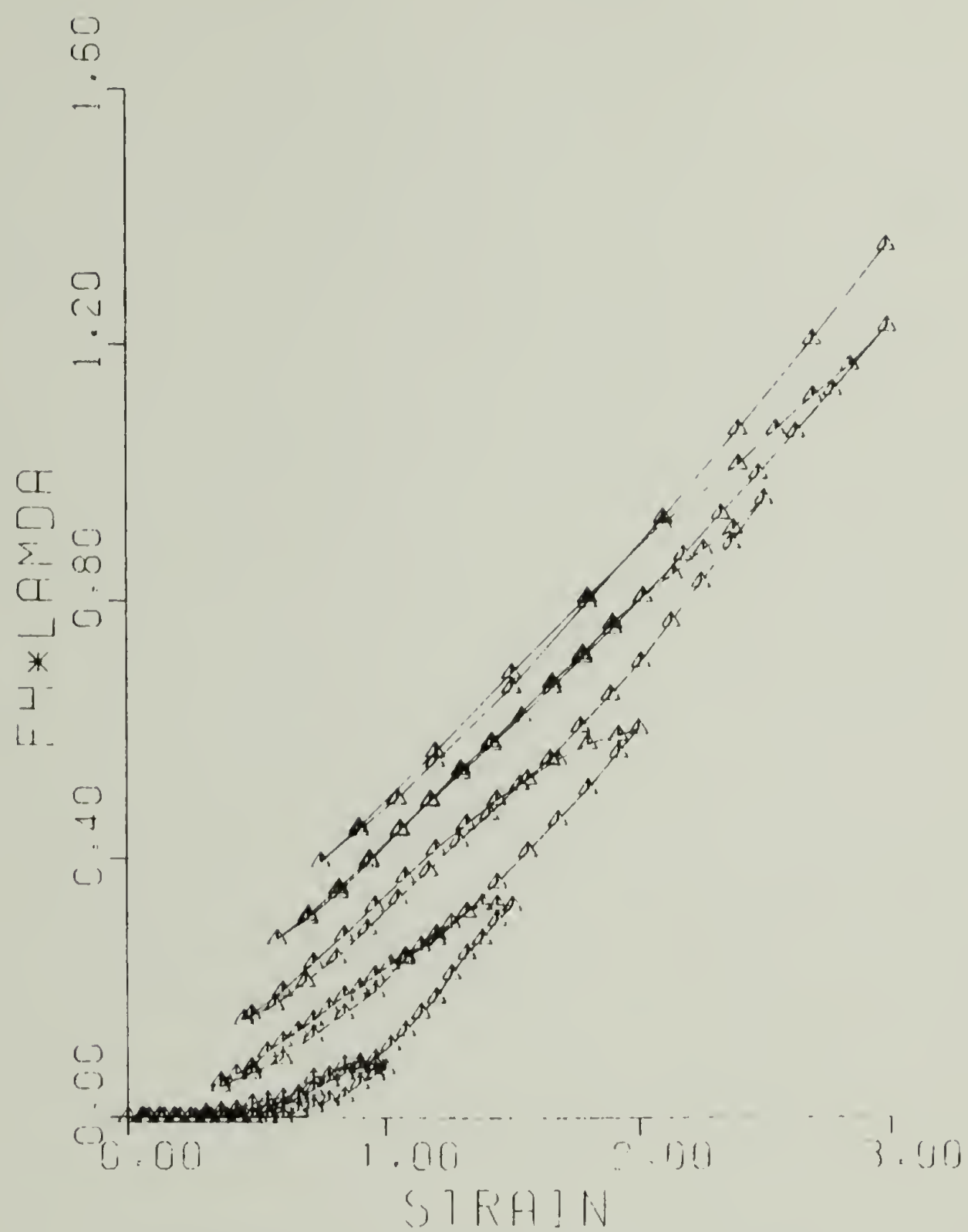


Figure 27. Hard segment orientation function multiplied by extension ratio  $\lambda$  vs. nominal strain. Data from Figure 22.

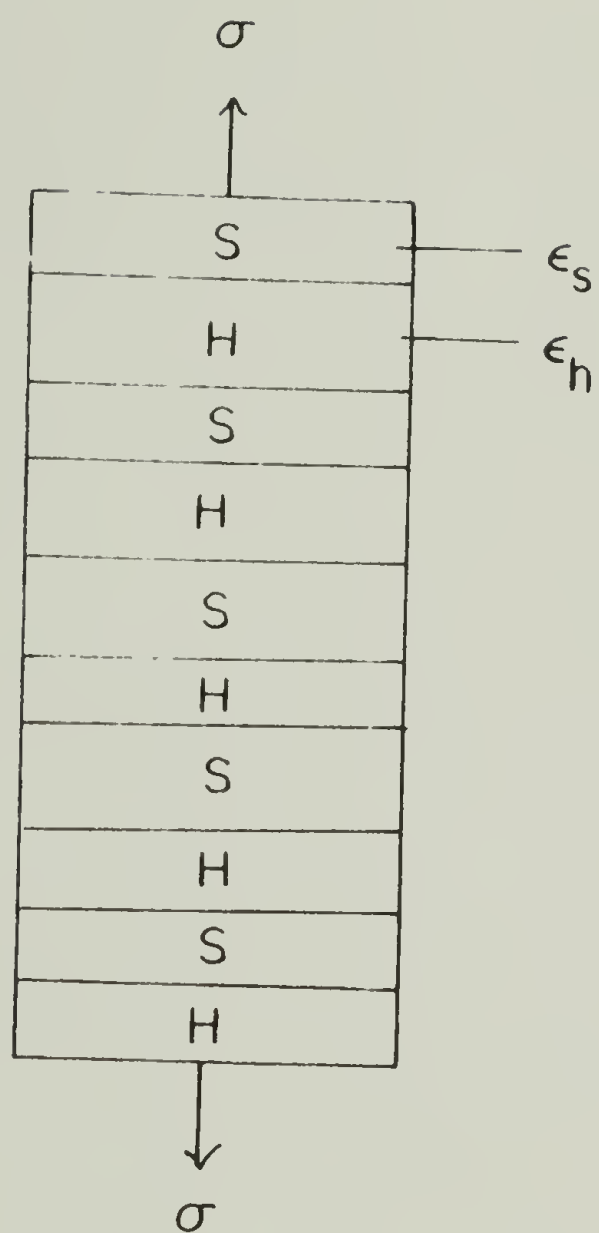


Figure 28. Series model of soft and hard domains in polyurethanes.

et al. (1966) and Onogi and Asada (1971) have used series models and combination series-parallel models to combine crystalline and amorphous properties and compute moduli for semicrystalline polymers. Seferis et al. (1976, 1977) used the assumption of a uniform distribution of stress (series model) to add compliance tensors for the two phases of polypropylene.

The series model assumes constant stress throughout the composite, and provides a relationship between strain in the two separate domains to the total strain on the sample, derived as follows:

Define the total strain on the composite,  $\epsilon_T$ , as

$$(35) \quad \epsilon_T = \Delta L_T / L_{0T}$$

where  $\Delta L_T = L_T - L_{0T}$ ;  $L_{0T}$  is the initial sample length and  $L_T$  is the deformed length. The average strain in the hard domains,  $\epsilon_h$ , is

$$(36) \quad \epsilon_h = \frac{\Delta L_h}{L_{0h}}$$

and the average strain in the soft matrix,  $\epsilon_s$ , is

$$(37) \quad \epsilon_s = \frac{\Delta L_s}{L_{0s}}$$

where  $\Delta L_h$ ,  $\Delta L_s$ ,  $L_{0h}$ , and  $L_{0s}$  are defined in a similar manner to  $\Delta L$  and

$L_0$  above.

The series model provides for additivity of strains such that for the initial configuration of the composite,

$$(38) \quad L_{0T} = L_{0S} + L_{0h}$$

and after some deformation  $\Delta L$ ,

$$(39) \quad \Delta L_T = \Delta L_S + \Delta L_h$$

Using (35), (36), and (37), (39) may be expressed

$$(40) \quad \Delta L_T = \epsilon_S L_{0S} + \epsilon_h L_{0h} = \epsilon_T L_{0T}$$

This yields

$$(41) \quad \epsilon_T = \epsilon_S L_{0S}/L_{0T} + \epsilon_h L_{0h}/L_{0T}$$

Now the ratios  $L_{0S}/L_{0T}$  and  $L_{0h}/L_{0T}$  represent the soft domain and hard domain line fractions in the composite which would be computed if a random vector were passed through the sample. Using a well-known result from scattering theory (Appendix D), the line fractions may be related to the volume fractions as follows:

$$(42) \quad \frac{L_{0S}}{L_{0T}} = \frac{V_{0S}}{V_{0T}} \equiv V_S; \quad \frac{L_{0h}}{L_{0T}} = \frac{V_{0h}}{V_{0T}} \equiv V_h$$

Where  $V_{0h}$ ,  $V_{0S}$  are the initial volumes of the hard and soft domains,  $V_{0T}$  is the initial volume of the composite, and  $V_S$ ,  $V_h$  are the volume

fractions of the soft and hard domains, respectively. Using (42), (41) may be rewritten

$$(43) \quad \epsilon_T = V_S \epsilon_S + V_h \epsilon_h$$

Equation (43) gives the simple result that the total strain in the sample is a weighted sum of the average strains in the individual domains.

Now, it is proposed that the orientation in the two individual domains is a function of the strain in that domain, i.e.,

$$(44) \quad f_h = g_h(\epsilon_h); \quad f_s = g_s(\epsilon_s)$$

where  $f_h$ ,  $f_s$  are the orientation functions of the hard and soft domains;  $g_h$  and  $g_s$  are unspecified functions of the strains. The simplest form for the functions  $g_h$  and  $g_s$  is a linear one, which has been mentioned by Onogi and Asada (1971) for orientation functions for blends of polyethylene and polypropylene:

$$(45) \quad f_h = C_h \epsilon_h; \quad f_s = C_s \epsilon_s$$

where  $C_h$ ,  $C_s$  are constants of the material domains. Using (11), Equation (43) becomes

$$(46) \quad \epsilon_T = \frac{V_S}{C_s} f_s + \frac{V_h}{C_h} f_h$$

Equation (46) may also be written as



$$(47) \quad \epsilon_T = Af_s + Bf_h$$

where  $A = V_s/C_s$ ;  $B = V_h/C_h$ .

Equation (47) yields a relationship between the measured orientation functions of the soft and hard segments of the polyurethane and the total strain on the sample. Deviations from (47) may be expected since the series model used is a gross simplification of the morphology found in the polyurethanes. Also, if  $f_s$  is determined from the CH transition moment, as discussed above, error will be introduced because some of the CH groups belong to the hard segments. Agreement of experimental data to equation (47) would indicate, however, that the two different chain segments, regardless of where they reside in the microstructure and regardless of previous strain history, react cooperatively to strain. An encouraging feature of the series composite model is that since the two types of chain segments are chemically bonded together, there is no failure at the domain boundaries, which may occur in blends, for example.

The theoretical predictions above were checked by analysis of data presented in Figures 22, 23, and 24. In order to determine the constants A and B in equation (47), values of  $f_s$  and  $f_h$  corresponding to the same strain level must be used, which required interpolation of the  $f_s$  data. The constants A and B were determined by a nonlinear least squares regression analysis for a function of two independent variables yielding

$$A = 9.0 \pm .1$$

$$B = 2.24 \pm .04$$

Details of the regression analysis may be found in Appendix E. The error indicated is  $\pm$  one standard deviation.

For this case,  $f_s$  was chosen as the dependent variable in the regression analysis, since it is known with much less accuracy than are  $f_h$  or  $\epsilon_T$ . As mentioned above, 16% of the C-H groups in an ET polymer are in the hard chain segments, so that use of the CH signal to indicate soft segment orientation is subject to this error, in addition to experimental error.

The values of A and B were used to recompute  $f_s$ ,  $f_h$  and  $\epsilon_T$  as listed in Table 1. In Figures 29, 30, and 31 the calculated vs. observed values of  $f_s$ ,  $f_h$  and  $\epsilon_T$  are plotted to graphically illustrate the goodness of fit to (47). The same analysis was performed using the urethane carbonyl orientation function,  $f_{CO}$ , to represent hard segment orientation. The result for the two constants in Equation (47) is:

$$A = 8.2 \pm .1$$

$$B = 2.09 \pm .09$$

The theoretical predictions for the strain and orientation functions are presented in Table 2 and Figures 32, 33, and 34. The predictions of the series model for  $f_s$  and  $\epsilon_T$  are excellent; although the predictions for  $f_h$  and  $f_{CO}$  are less impressive, they are adequate considering the above-mentioned errors and also the fact that the measurements for  $f_s$  and  $f_h$  were taken on two different samples. The predictions for  $f_h$  and  $f_{CO}$  improve considerably if  $f_h$  and  $f_{CO}$  are taken to be the dependent variables in Equation (47), as would be expected.

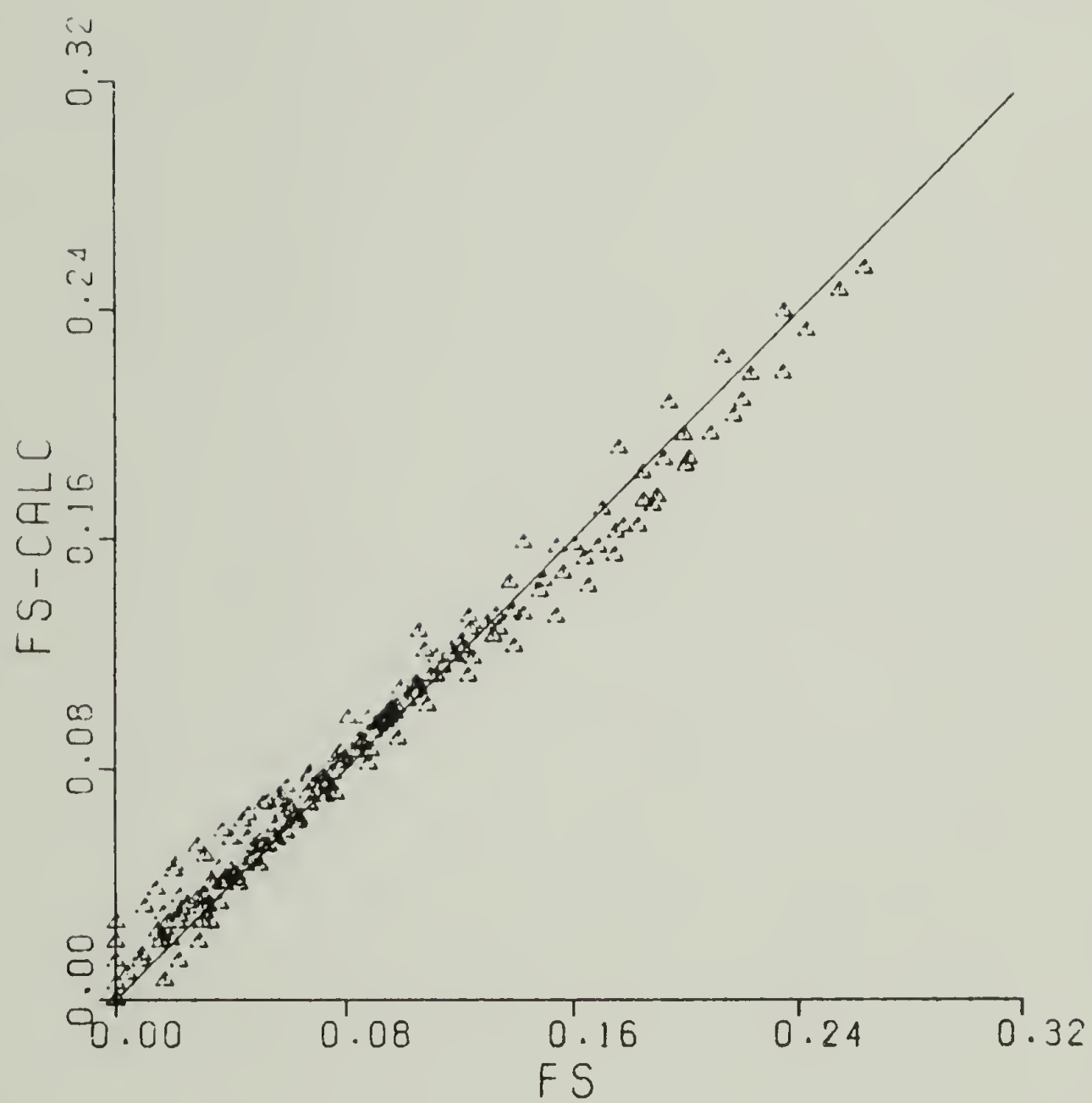


Figure 29. Calculated (Equation 47) vs. observed values of soft segment orientation (FS).

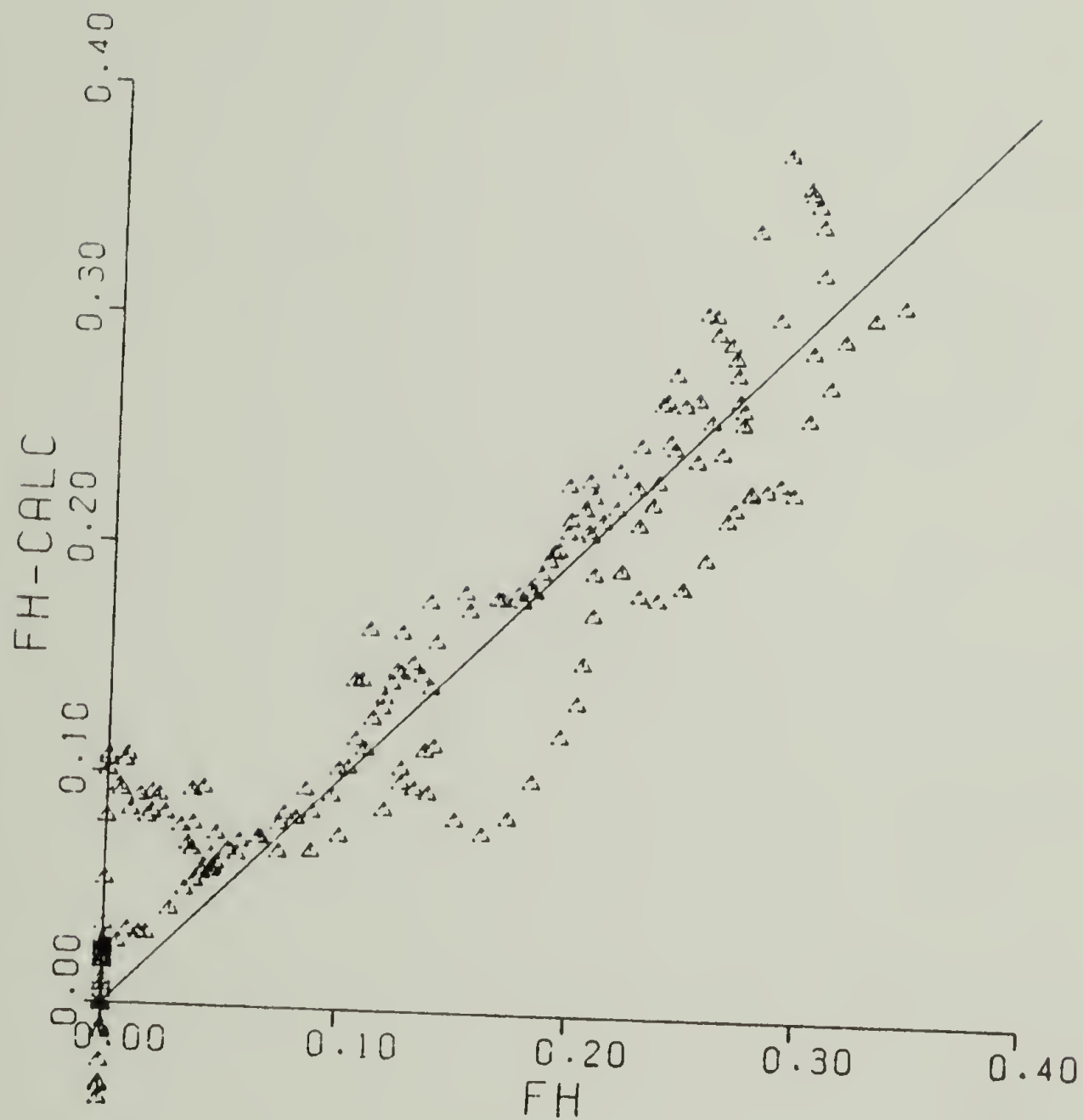


Figure 30. Calculated (Equation 47) vs. observed values of hard segment orientation (FH).

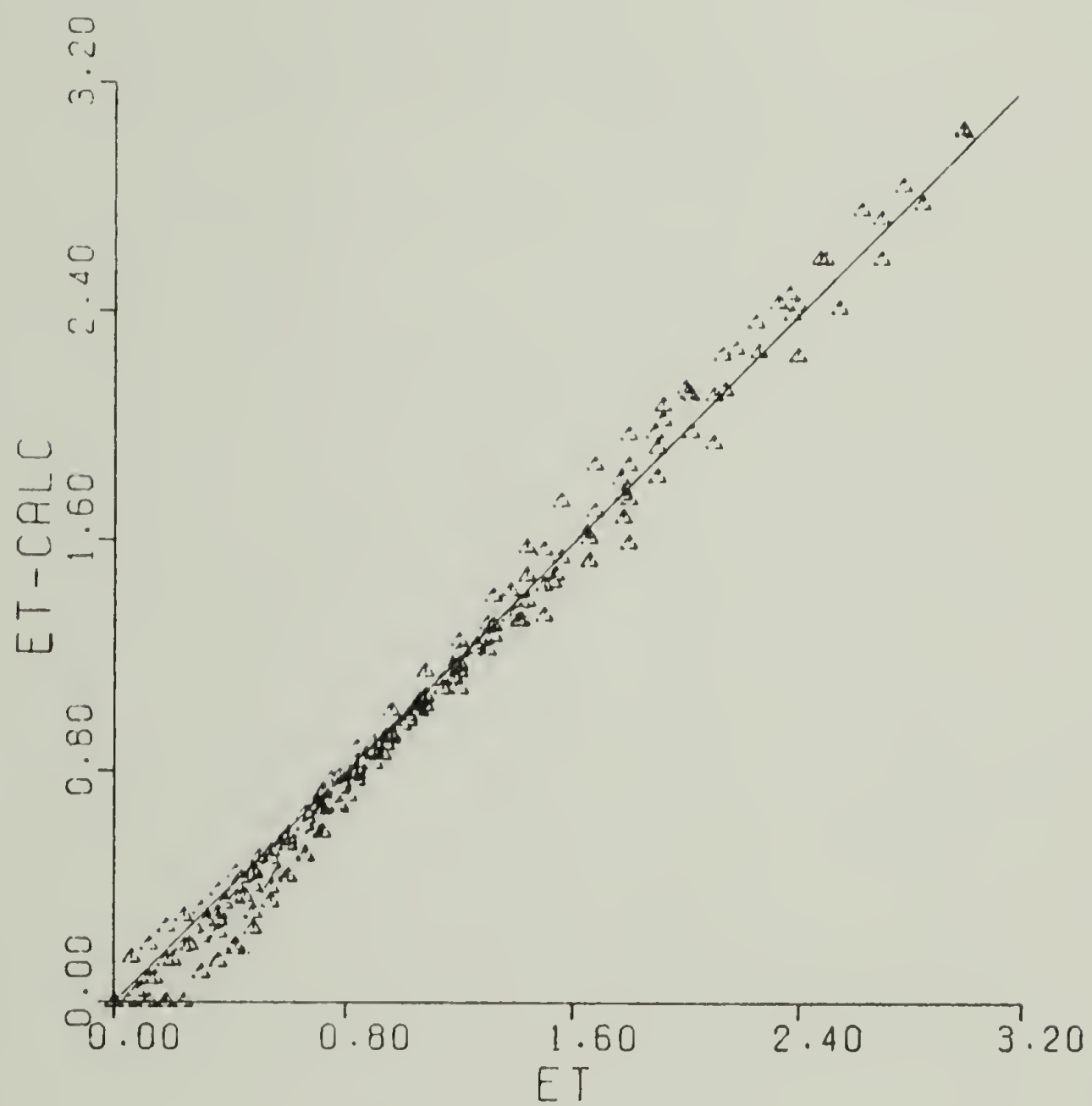


Figure 31. Calculated (Equation 47) vs. observed values of total strain (ET).







TABLE 1 (continued)

$f_s$	$f_{s\text{-calc}}$	% error	$f_h$	$f_{h\text{-calc}}$	% error	$\epsilon_T$	$\epsilon_{T\text{-calc}}$	% error
6768	7843	16	0033	0067	14	784	677	-13
6766	7840	9	0034	0065	11	790	683	-4
6716	7859	4	0045	0060	30	802	690	4
6720	7841	2	0065	0080	17	840	706	17
6000	7840	0	0076	0090	18	840	706	17
6004	7840	0	0089	0094	5	840	706	17
6000	7840	0	0099	0099	0	840	706	17
6004	7840	0	0110	0099	11	840	706	17
6000	7840	0	0125	0099	20	840	706	17
6000	7840	0	0136	0099	26	840	706	17
6000	7840	0	0150	0099	34	840	706	17
6000	7840	0	0162	0099	39	840	706	17
6000	7840	0	0176	0099	43	840	706	17
6000	7840	0	0190	0099	47	840	706	17
6000	7840	0	0206	0099	51	840	706	17
6000	7840	0	0220	0099	55	840	706	17
6000	7840	0	0236	0099	59	840	706	17
6000	7840	0	0250	0099	63	840	706	17
6000	7840	0	0266	0099	67	840	706	17
6000	7840	0	0280	0099	71	840	706	17
6000	7840	0	0296	0099	75	840	706	17
6000	7840	0	0310	0099	79	840	706	17
6000	7840	0	0326	0099	83	840	706	17
6000	7840	0	0340	0099	87	840	706	17
6000	7840	0	0356	0099	91	840	706	17
6000	7840	0	0370	0099	95	840	706	17
6000	7840	0	0386	0099	99	840	706	17
6000	7840	0	0400	0099	103	840	706	17
6000	7840	0	0416	0099	107	840	706	17
6000	7840	0	0430	0099	111	840	706	17
6000	7840	0	0446	0099	115	840	706	17
6000	7840	0	0460	0099	119	840	706	17
6000	7840	0	0476	0099	123	840	706	17
6000	7840	0	0490	0099	127	840	706	17
6000	7840	0	0506	0099	131	840	706	17
6000	7840	0	0520	0099	135	840	706	17
6000	7840	0	0536	0099	139	840	706	17
6000	7840	0	0550	0099	143	840	706	17
6000	7840	0	0566	0099	147	840	706	17
6000	7840	0	0580	0099	151	840	706	17
6000	7840	0	0596	0099	155	840	706	17
6000	7840	0	0610	0099	159	840	706	17
6000	7840	0	0626	0099	163	840	706	17
6000	7840	0	0640	0099	167	840	706	17
6000	7840	0	0656	0099	171	840	706	17
6000	7840	0	0670	0099	175	840	706	17
6000	7840	0	0686	0099	179	840	706	17
6000	7840	0	0700	0099	183	840	706	17
6000	7840	0	0716	0099	187	840	706	17
6000	7840	0	0730	0099	191	840	706	17
6000	7840	0	0746	0099	195	840	706	17
6000	7840	0	0760	0099	199	840	706	17
6000	7840	0	0776	0099	203	840	706	17
6000	7840	0	0790	0099	207	840	706	17
6000	7840	0	0806	0099	211	840	706	17
6000	7840	0	0820	0099	215	840	706	17
6000	7840	0	0836	0099	219	840	706	17
6000	7840	0	0850	0099	223	840	706	17
6000	7840	0	0866	0099	227	840	706	17
6000	7840	0	0880	0099	231	840	706	17
6000	7840	0	0896	0099	235	840	706	17
6000	7840	0	0910	0099	239	840	706	17
6000	7840	0	0926	0099	243	840	706	17
6000	7840	0	0940	0099	247	840	706	17
6000	7840	0	0956	0099	251	840	706	17
6000	7840	0	0970	0099	255	840	706	17
6000	7840	0	0986	0099	259	840	706	17
6000	7840	0	1000	0099	263	840	706	17
6000	7840	0	1016	0099	267	840	706	17
6000	7840	0	1030	0099	271	840	706	17
6000	7840	0	1046	0099	275	840	706	17
6000	7840	0	1060	0099	279	840	706	17
6000	7840	0	1076	0099	283	840	706	17
6000	7840	0	1090	0099	287	840	706	17
6000	7840	0	1106	0099	291	840	706	17
6000	7840	0	1120	0099	295	840	706	17
6000	7840	0	1136	0099	299	840	706	17
6000	7840	0	1150	0099	303	840	706	17
6000	7840	0	1166	0099	307	840	706	17
6000	7840	0	1180	0099	311	840	706	17
6000	7840	0	1196	0099	315	840	706	17
6000	7840	0	1210	0099	319	840	706	17
6000	7840	0	1226	0099	323	840	706	17
6000	7840	0	1240	0099	327	840	706	17
6000	7840	0	1256	0099	331	840	706	17
6000	7840	0	1270	0099	335	840	706	17
6000	7840	0	1286	0099	339	840	706	17
6000	7840	0	1300	0099	343	840	706	17
6000	7840	0	1316	0099	347	840	706	17
6000	7840	0	1330	0099	351	840	706	17
6000	7840	0	1346	0099	355	840	706	17
6000	7840	0	1360	0099	359	840	706	17
6000	7840	0	1376	0099	363	840	706	17
6000	7840	0	1390	0099	367	840	706	17
6000	7840	0	1406	0099	371	840	706	17
6000	7840	0	1420	0099	375	840	706	17
6000	7840	0	1436	0099	379	840	706	17
6000	7840	0	1450	0099	383	840	706	17
6000	7840	0	1466	0099	387	840	706	17
6000	7840	0	1480	0099	391	840	706	17
6000	7840	0	1496	0099	395	840	706	17
6000	7840	0	1510	0099	399	840	706	17
6000	7840	0	1526	0099	403	840	706	17
6000	7840	0	1540	0099	407	840	706	17
6000	7840	0	1556	0099	411	840	706	17
6000	7840	0	1570	0099	415	840	706	17
6000	7840	0	1586	0099	419	840	706	17
6000	7840	0	1600	0099	423	840	706	17
6000	7840	0	1616	0099	427	840	706	17
6000	7840	0	1630	0099	431	840	706	17
6000	7840	0	1646	0099	435	840	706	17
6000	7840	0	1660	0099	439	840	706	17
6000	7840	0	1676	0099	443	840	706	17
6000	7840	0	1690	0099	447	840	706	17
6000	7840	0	1706	0099	451	840	706	17
6000	7840	0	1720	0099	455	840	706	17
6000	7840	0	1736	0099	459	840	706	17
6000	7840	0	1750	0099	463	840	706	17
6000	7840	0	1766	0099	467	840	706	17
6000	7840	0	1780	0099	471	840	706	17
6000	7840	0	1796	0099	475	840	706	17
6000	7840	0	1810	0099	479	840	706	17
6000	7840	0	1826	0099	483	840	706	17
6000	7840	0	1840	0099	487	840	706	17
6000	7840	0	1856	0099	491	840	706	17
6000	7840	0	1870	0099	495	840	706	17
6000	7840	0	1886	0099	499	840	706	17
6000	7840	0	1900	0099	503	840	706	17
6000	7840	0	1916	0099	507	840	706	17
6000	7840	0	1930	0099	511	840	706	17
6000	7840	0	1946	0099	515	840	706	17
6000	7840	0	1960	0099	519	840	706	17
6000	7840	0	1976	0099	523	840	706	17
6000	7840	0	1990	0099	527	840	706	17
6000	7840	0	2006	0099	531	840	706	17
6000	7840	0	2020	0099	535	840	706	17
6000	7840	0	2036	0099	539	840	706	17
6000	7840	0	2050	0099	543	840	706	17
6000	7840	0	2066	0099	547	840	706	17
6000	7840	0	2080	0099	551	840	706	17
6000	7840	0	2096	0099	555	840	706	17
6000	7840	0	2110	0099	559	840	706	17
6000	7840	0	2126	0099	563	840	706	17
6000	7840	0	2140	0099	567	840	706	17
6000	7840	0	2156	0099	571	840	706	17
6000	7840	0	2170	0099	575	840	706	17
6000	7840	0	2186	0099	579	840	706	17
6000	7840	0	2200	0099	583	840	706	17
6000	7840	0	2216	0099	587	840	706	17
6000	7840	0	2230	0099	591	840	706	17
6000	7840	0	2246	0099	595	840	706	17
6000	7840	0	2260	0099	599	840	706	17
6000	7840	0	2276	0099	603	840	706	17
6000	7840	0	2290	0099	607	840	706	17
6000	7840	0	2306	0099	611	840	706	17
6000	7840	0	2320	0099	615	840	706	17
6000	7840	0	2336	0099	61			





TABLE 1 (continued)

$f_s$	$f_{s\text{-calc}}$	% error	$f_h$	$f_{h\text{-calc}}$	% error	$\varepsilon_T$	$\varepsilon_{T\text{-calc}}$	% error
0	754	1.4	0	49	0	0	1	1.8
420	555	40	800	59	37	98	93	54
600	555	20	400	65	13	72	67	23
1000	555	6	300	75	4	42	50	8
1400	555	4	200	87	2	28	43	2
1800	555	3	100	100	0	15	50	0
2200	555	2	50	115	1	8	57	0
2600	555	1	0	135	0	5	62	0
3000	555	0	0	157	0	3	67	0
3400	555	0	0	180	0	2	72	0
3800	555	0	0	205	0	1	77	0
4200	555	0	0	230	0	0	82	0
4600	555	0	0	258	0	0	87	0
5000	555	0	0	287	0	0	92	0
5400	555	0	0	317	0	0	97	0
5800	555	0	0	348	0	0	100	0
6200	555	0	0	380	0	0	100	0
6600	555	0	0	413	0	0	100	0
7000	555	0	0	447	0	0	100	0
7400	555	0	0	482	0	0	100	0
7800	555	0	0	517	0	0	100	0
8200	555	0	0	553	0	0	100	0
8600	555	0	0	590	0	0	100	0
9000	555	0	0	627	0	0	100	0
9400	555	0	0	665	0	0	100	0
9800	555	0	0	704	0	0	100	0
10000	555	0	0	743	0	0	100	0



TABLE 1 (continued)

$f_s$	$f_{s\text{-calc}}$	% error	$f_h$	$f_{h\text{-calc}}$	% error	$\varepsilon_T$	$\varepsilon_{T\text{-calc}}$	% error
1548	1578	2.0	2690	2811	4.5	2.02	1.99	1.3
1386	1453	5.7	2600	2949	10.9	1.90	1.84	-3.4
1230	1327	12.1	2550	3080	15.0	1.78	1.65	-7.2
1080	1197	11.0	2420	2810	16.1	1.66	1.54	-6.5
920	1065	15.2	2270	2675	17.4	1.53	1.33	-12.4
760	943	24.1	2070	2492	19.9	1.43	1.23	-15.4
600	805	34.0	1870	2338	25.6	1.30	1.10	-16.4
440	633	43.9	1670	2235	35.9	1.18	1.09	-7.6
280	453	61.8	1470	2104	46.9	1.06	1.01	-4.6
120	233	93.3	1270	1921	52.7	0.94	0.99	5.3
60	133	121.7	1070	1824	70.1	0.82	0.86	4.9
0	73	152.7	870	1624	86.7	0.70	0.70	0.0
0	33	190.0	670	1438	111.8	0.58	0.57	-1.7
0	13	250.0	470	1235	160.5	0.46	0.43	-6.5
0	3	320.0	270	1035	281.9	0.34	0.32	-5.9
0	0	400.0	70	835	1078.6	0.22	0.21	-4.5
0	0	500.0	0	635	1577.6	0.10	0.10	0.0
0	0	600.0	0	435	2076.6	0.08	0.08	0.0
0	0	700.0	0	235	2575.6	0.06	0.06	0.0
0	0	800.0	0	35	2974.6	0.04	0.04	0.0
0	0	900.0	0	0	3373.6	0.02	0.02	0.0
0	0	1000.0	0	0	3772.6	0.01	0.01	0.0
0	0	1100.0	0	0	4171.6	0.00	0.00	0.0
0	0	1200.0	0	0	4570.6	0.00	0.00	0.0
0	0	1300.0	0	0	4969.6	0.00	0.00	0.0
0	0	1400.0	0	0	5368.6	0.00	0.00	0.0
0	0	1500.0	0	0	5767.6	0.00	0.00	0.0
0	0	1600.0	0	0	6166.6	0.00	0.00	0.0
0	0	1700.0	0	0	6565.6	0.00	0.00	0.0
0	0	1800.0	0	0	6964.6	0.00	0.00	0.0
0	0	1900.0	0	0	7363.6	0.00	0.00	0.0
0	0	2000.0	0	0	7762.6	0.00	0.00	0.0
0	0	2100.0	0	0	8161.6	0.00	0.00	0.0
0	0	2200.0	0	0	8560.6	0.00	0.00	0.0
0	0	2300.0	0	0	8959.6	0.00	0.00	0.0
0	0	2400.0	0	0	9358.6	0.00	0.00	0.0
0	0	2500.0	0	0	9757.6	0.00	0.00	0.0
0	0	2600.0	0	0	10156.6	0.00	0.00	0.0
0	0	2700.0	0	0	10555.6	0.00	0.00	0.0
0	0	2800.0	0	0	10954.6	0.00	0.00	0.0
0	0	2900.0	0	0	11353.6	0.00	0.00	0.0
0	0	3000.0	0	0	11752.6	0.00	0.00	0.0
0	0	3100.0	0	0	12151.6	0.00	0.00	0.0
0	0	3200.0	0	0	12550.6	0.00	0.00	0.0
0	0	3300.0	0	0	12949.6	0.00	0.00	0.0
0	0	3400.0	0	0	13348.6	0.00	0.00	0.0
0	0	3500.0	0	0	13747.6	0.00	0.00	0.0
0	0	3600.0	0	0	14146.6	0.00	0.00	0.0
0	0	3700.0	0	0	14545.6	0.00	0.00	0.0
0	0	3800.0	0	0	14944.6	0.00	0.00	0.0
0	0	3900.0	0	0	15343.6	0.00	0.00	0.0
0	0	4000.0	0	0	15742.6	0.00	0.00	0.0
0	0	4100.0	0	0	16141.6	0.00	0.00	0.0
0	0	4200.0	0	0	16540.6	0.00	0.00	0.0
0	0	4300.0	0	0	16939.6	0.00	0.00	0.0
0	0	4400.0	0	0	17338.6	0.00	0.00	0.0
0	0	4500.0	0	0	17737.6	0.00	0.00	0.0
0	0	4600.0	0	0	18136.6	0.00	0.00	0.0
0	0	4700.0	0	0	18535.6	0.00	0.00	0.0
0	0	4800.0	0	0	18934.6	0.00	0.00	0.0
0	0	4900.0	0	0	19333.6	0.00	0.00	0.0
0	0	5000.0	0	0	19732.6	0.00	0.00	0.0
0	0	5100.0	0	0	20131.6	0.00	0.00	0.0
0	0	5200.0	0	0	20530.6	0.00	0.00	0.0
0	0	5300.0	0	0	20929.6	0.00	0.00	0.0
0	0	5400.0	0	0	21328.6	0.00	0.00	0.0
0	0	5500.0	0	0	21727.6	0.00	0.00	0.0
0	0	5600.0	0	0	22126.6	0.00	0.00	0.0
0	0	5700.0	0	0	22525.6	0.00	0.00	0.0
0	0	5800.0	0	0	22924.6	0.00	0.00	0.0
0	0	5900.0	0	0	23323.6	0.00	0.00	0.0
0	0	6000.0	0	0	23722.6	0.00	0.00	0.0
0	0	6100.0	0	0	24121.6	0.00	0.00	0.0
0	0	6200.0	0	0	24520.6	0.00	0.00	0.0
0	0	6300.0	0	0	24919.6	0.00	0.00	0.0
0	0	6400.0	0	0	25318.6	0.00	0.00	0.0
0	0	6500.0	0	0	25717.6	0.00	0.00	0.0
0	0	6600.0	0	0	26116.6	0.00	0.00	0.0
0	0	6700.0	0	0	26515.6	0.00	0.00	0.0
0	0	6800.0	0	0	26914.6	0.00	0.00	0.0
0	0	6900.0	0	0	27313.6	0.00	0.00	0.0
0	0	7000.0	0	0	27712.6	0.00	0.00	0.0
0	0	7100.0	0	0	28111.6	0.00	0.00	0.0
0	0	7200.0	0	0	28510.6	0.00	0.00	0.0
0	0	7300.0	0	0	28909.6	0.00	0.00	0.0
0	0	7400.0	0	0	29308.6	0.00	0.00	0.0
0	0	7500.0	0	0	29707.6	0.00	0.00	0.0
0	0	7600.0	0	0	30106.6	0.00	0.00	0.0
0	0	7700.0	0	0	30505.6	0.00	0.00	0.0
0	0	7800.0	0	0	30904.6	0.00	0.00	0.0
0	0	7900.0	0	0	31303.6	0.00	0.00	0.0
0	0	8000.0	0	0	31702.6	0.00	0.00	0.0
0	0	8100.0	0	0	32101.6	0.00	0.00	0.0
0	0	8200.0	0	0	32500.6	0.00	0.00	0.0
0	0	8300.0	0	0	32899.6	0.00	0.00	0.0
0	0	8400.0	0	0	33298.6	0.00	0.00	0.0
0	0	8500.0	0	0	33697.6	0.00	0.00	0.0
0	0	8600.0	0	0	34096.6	0.00	0.00	0.0
0	0	8700.0	0	0	34495.6	0.00	0.00	0.0
0	0	8800.0	0	0	34894.6	0.00	0.00	0.0
0	0	8900.0	0	0	35293.6	0.00	0.00	0.0
0	0	9000.0	0	0	35692.6	0.00	0.00	0.0
0	0	9100.0	0	0	36091.6	0.00	0.00	0.0
0	0	9200.0	0	0	36490.6	0.00	0.00	0.0
0	0	9300.0	0	0	36889.6	0.00	0.00	0.0
0	0	9400.0	0	0	37288.6	0.00	0.00	0.0
0	0	9500.0	0	0	37687.6	0.00	0.00	0.0
0	0	9600.0	0	0	38086.6	0.00	0.00	0.0
0	0	9700.0	0	0	38485.6	0.00	0.00	0.0
0	0	9800.0	0	0	38884.6	0.00	0.00	0.0
0	0	9900.0	0	0	39283.6	0.00	0.00	0.0
0	0	10000.0	0	0	39682.6	0.00	0.00	0.0



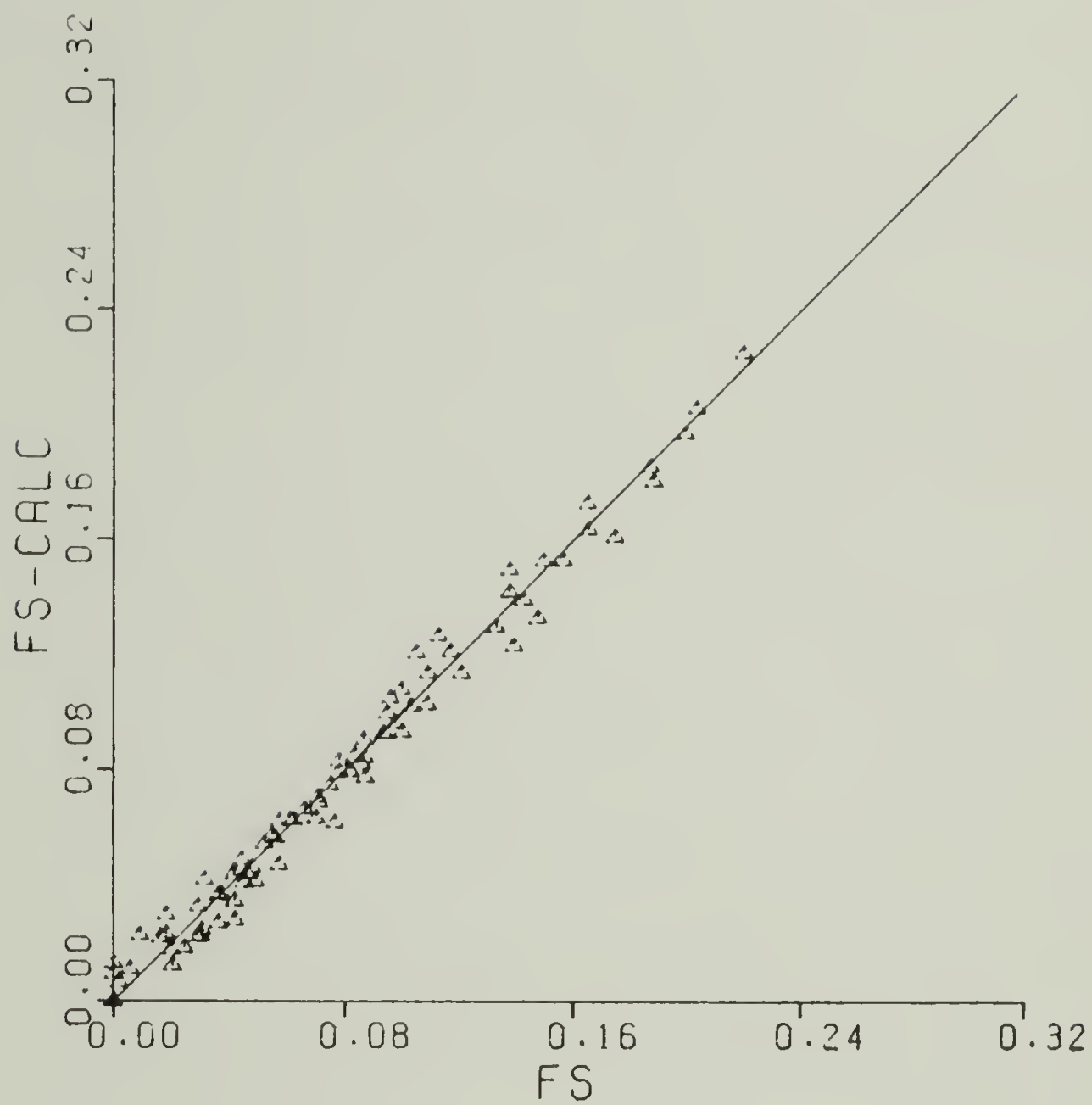


Figure 32. Calculated (Equation 47) vs. observed values of soft segment orientation (FS).

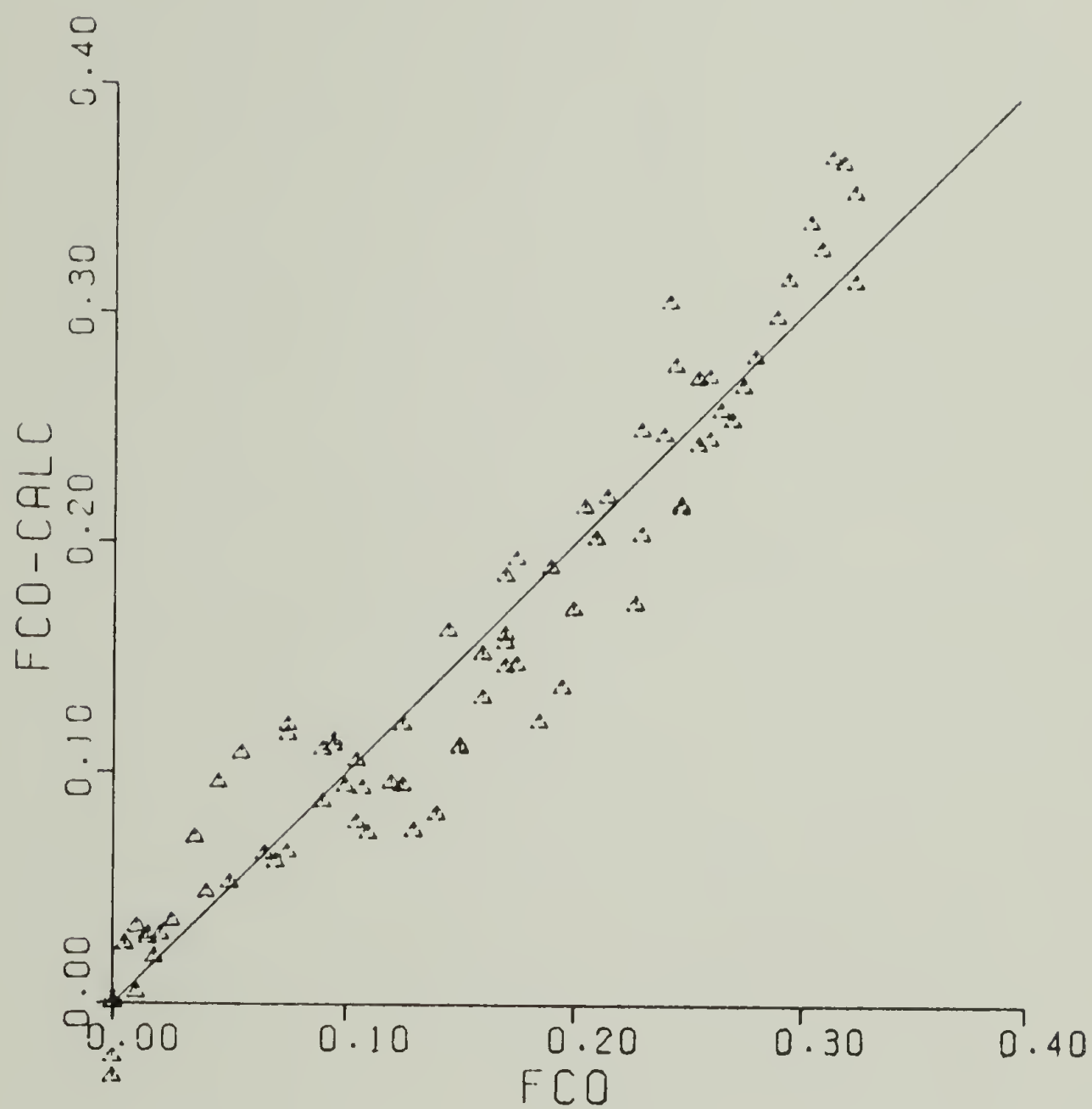


Figure 33. Calculated (Equation 47) vs. observed values of hard segment orientation (FCO).

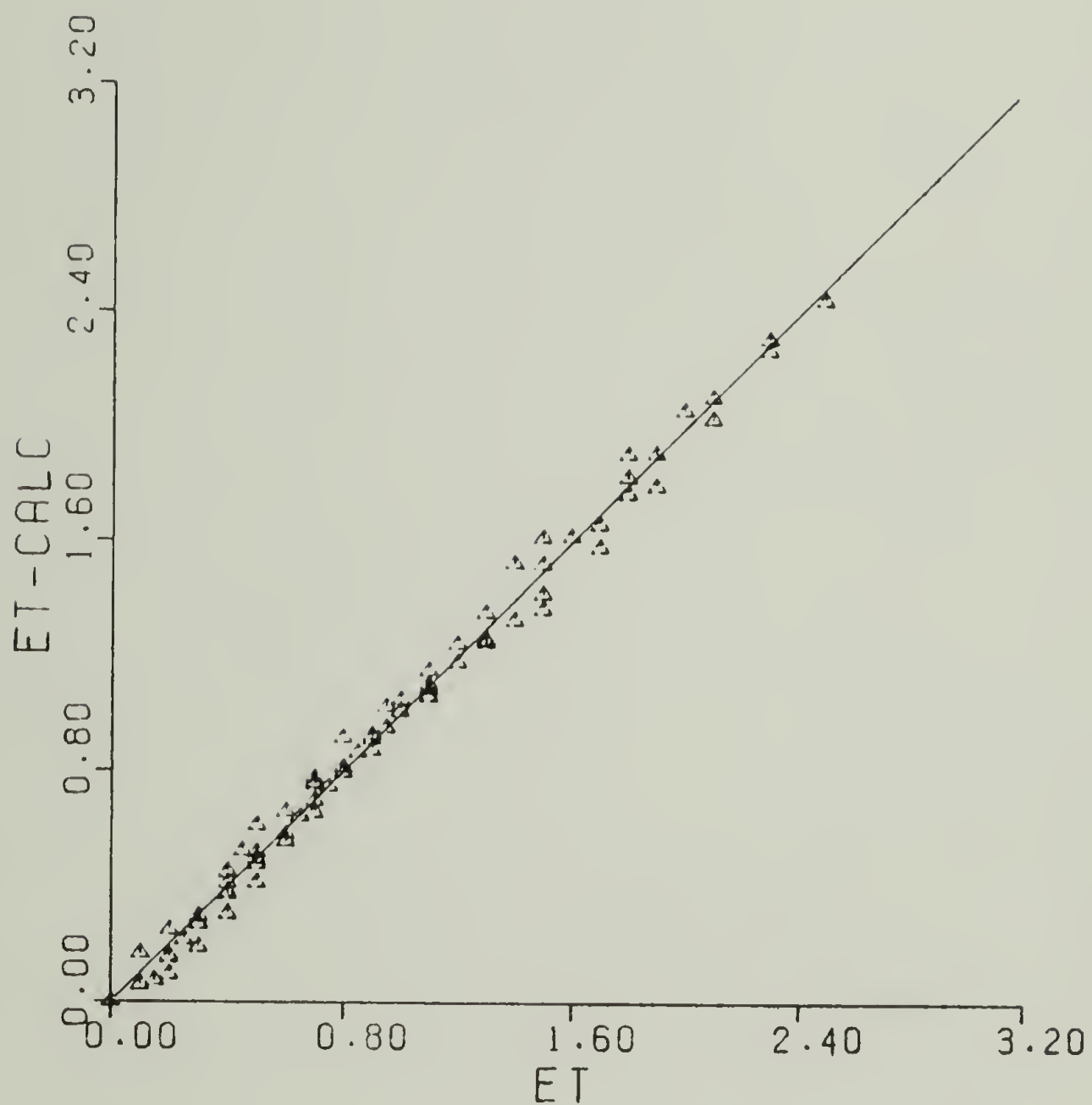


Figure 34. Calculated (Equation 47) vs. observed values of total strain (ET).



TABLE 2

OBSERVED AND CALCULATED VALUES OF ORIENTATION  
FUNCTIONS AND STRAIN

$f_s$	$f_s$ -calc	% error	$f_{co}$	$f_{co}$ -calc	% error	$\epsilon_T$	$\epsilon_T$ -calc	% error
0.0000	0.0000	0.0	0.0000	0.0000	0.0	0.0000	0.0000	0.0
0.0003	0.0002	-39.0	0.0000	0.0000	0.0	0.0000	0.0000	0.0
0.0033	0.0012	-19.4	0.0000	0.0031	-3.0	0.0000	0.0000	0.0
0.0036	0.0024	-33.7	0.0000	0.0023	-2.0	0.0000	0.0000	0.0
0.0047	0.0036	-23.0	0.0000	0.0044	-5.0	0.0000	0.0000	0.0
0.0056	0.0045	-19.0	0.0000	0.0047	-12.0	0.0000	0.0000	0.0
0.0070	0.0053	-23.9	0.0000	0.0059	-14.7	0.0000	0.0000	0.0
0.0093	0.0067	-28.0	0.0000	0.0067	-27.3	0.0000	0.0000	0.0
0.0107	0.0089	-16.9	0.0000	0.0089	-16.9	0.0000	0.0000	0.0
0.0120	0.0103	-13.3	0.0000	0.0103	-13.3	0.0000	0.0000	0.0
0.0141	0.0123	-12.8	0.0000	0.0123	-12.8	0.0000	0.0000	0.0
0.0158	0.0135	-13.9	0.0000	0.0135	-13.9	0.0000	0.0000	0.0
0.0180	0.0154	-14.4	0.0000	0.0154	-14.4	0.0000	0.0000	0.0
0.0200	0.0170	-15.0	0.0000	0.0170	-15.0	0.0000	0.0000	0.0
0.0216	0.0185	-14.3	0.0000	0.0185	-14.3	0.0000	0.0000	0.0
0.0240	0.0205	-14.6	0.0000	0.0205	-14.6	0.0000	0.0000	0.0
0.0261	0.0219	-16.1	0.0000	0.0219	-16.1	0.0000	0.0000	0.0
0.0280	0.0234	-16.8	0.0000	0.0234	-16.8	0.0000	0.0000	0.0
0.0300	0.0249	-16.7	0.0000	0.0249	-16.7	0.0000	0.0000	0.0
0.0316	0.0265	-16.5	0.0000	0.0265	-16.5	0.0000	0.0000	0.0
0.0336	0.0283	-15.8	0.0000	0.0283	-15.8	0.0000	0.0000	0.0
0.0350	0.0298	-14.9	0.0000	0.0298	-14.9	0.0000	0.0000	0.0
0.0360	0.0309	-13.9	0.0000	0.0309	-13.9	0.0000	0.0000	0.0
0.0370	0.0318	-13.3	0.0000	0.0318	-13.3	0.0000	0.0000	0.0
0.0380	0.0324	-13.0	0.0000	0.0324	-13.0	0.0000	0.0000	0.0
0.0390	0.0329	-12.8	0.0000	0.0329	-12.8	0.0000	0.0000	0.0
0.0400	0.0333	-13.6	0.0000	0.0333	-13.6	0.0000	0.0000	0.0
0.0410	0.0335	-13.9	0.0000	0.0335	-13.9	0.0000	0.0000	0.0
0.0420	0.0337	-14.3	0.0000	0.0337	-14.3	0.0000	0.0000	0.0
0.0430	0.0339	-14.6	0.0000	0.0339	-14.6	0.0000	0.0000	0.0
0.0440	0.0341	-14.9	0.0000	0.0341	-14.9	0.0000	0.0000	0.0
0.0450	0.0343	-15.0	0.0000	0.0343	-15.0	0.0000	0.0000	0.0
0.0460	0.0345	-15.1	0.0000	0.0345	-15.1	0.0000	0.0000	0.0
0.0470	0.0347	-15.1	0.0000	0.0347	-15.1	0.0000	0.0000	0.0
0.0480	0.0349	-15.1	0.0000	0.0349	-15.1	0.0000	0.0000	0.0
0.0490	0.0351	-15.1	0.0000	0.0351	-15.1	0.0000	0.0000	0.0
0.0500	0.0353	-15.1	0.0000	0.0353	-15.1	0.0000	0.0000	0.0
0.0510	0.0355	-15.1	0.0000	0.0355	-15.1	0.0000	0.0000	0.0
0.0520	0.0357	-15.1	0.0000	0.0357	-15.1	0.0000	0.0000	0.0
0.0530	0.0359	-15.1	0.0000	0.0359	-15.1	0.0000	0.0000	0.0
0.0540	0.0361	-15.1	0.0000	0.0361	-15.1	0.0000	0.0000	0.0
0.0550	0.0363	-15.1	0.0000	0.0363	-15.1	0.0000	0.0000	0.0
0.0560	0.0365	-15.1	0.0000	0.0365	-15.1	0.0000	0.0000	0.0
0.0570	0.0367	-15.1	0.0000	0.0367	-15.1	0.0000	0.0000	0.0
0.0580	0.0369	-15.1	0.0000	0.0369	-15.1	0.0000	0.0000	0.0
0.0590	0.0371	-15.1	0.0000	0.0371	-15.1	0.0000	0.0000	0.0
0.0600	0.0373	-15.1	0.0000	0.0373	-15.1	0.0000	0.0000	0.0
0.0610	0.0375	-15.1	0.0000	0.0375	-15.1	0.0000	0.0000	0.0
0.0620	0.0377	-15.1	0.0000	0.0377	-15.1	0.0000	0.0000	0.0
0.0630	0.0379	-15.1	0.0000	0.0379	-15.1	0.0000	0.0000	0.0
0.0640	0.0381	-15.1	0.0000	0.0381	-15.1	0.0000	0.0000	0.0
0.0650	0.0383	-15.1	0.0000	0.0383	-15.1	0.0000	0.0000	0.0
0.0660	0.0385	-15.1	0.0000	0.0385	-15.1	0.0000	0.0000	0.0
0.0670	0.0387	-15.1	0.0000	0.0387	-15.1	0.0000	0.0000	0.0
0.0680	0.0389	-15.1	0.0000	0.0389	-15.1	0.0000	0.0000	0.0
0.0690	0.0391	-15.1	0.0000	0.0391	-15.1	0.0000	0.0000	0.0
0.0700	0.0393	-15.1	0.0000	0.0393	-15.1	0.0000	0.0000	0.0
0.0710	0.0395	-15.1	0.0000	0.0395	-15.1	0.0000	0.0000	0.0
0.0720	0.0397	-15.1	0.0000	0.0397	-15.1	0.0000	0.0000	0.0
0.0730	0.0399	-15.1	0.0000	0.0399	-15.1	0.0000	0.0000	0.0
0.0740	0.0401	-15.1	0.0000	0.0401	-15.1	0.0000	0.0000	0.0
0.0750	0.0403	-15.1	0.0000	0.0403	-15.1	0.0000	0.0000	0.0
0.0760	0.0405	-15.1	0.0000	0.0405	-15.1	0.0000	0.0000	0.0
0.0770	0.0407	-15.1	0.0000	0.0407	-15.1	0.0000	0.0000	0.0
0.0780	0.0409	-15.1	0.0000	0.0409	-15.1	0.0000	0.0000	0.0
0.0790	0.0411	-15.1	0.0000	0.0411	-15.1	0.0000	0.0000	0.0
0.0800	0.0413	-15.1	0.0000	0.0413	-15.1	0.0000	0.0000	0.0
0.0810	0.0415	-15.1	0.0000	0.0415	-15.1	0.0000	0.0000	0.0
0.0820	0.0417	-15.1	0.0000	0.0417	-15.1	0.0000	0.0000	0.0
0.0830	0.0419	-15.1	0.0000	0.0419	-15.1	0.0000	0.0000	0.0
0.0840	0.0421	-15.1	0.0000	0.0421	-15.1	0.0000	0.0000	0.0
0.0850	0.0423	-15.1	0.0000	0.0423	-15.1	0.0000	0.0000	0.0
0.0860	0.0425	-15.1	0.0000	0.0425	-15.1	0.0000	0.0000	0.0
0.0870	0.0427	-15.1	0.0000	0.0427	-15.1	0.0000	0.0000	0.0
0.0880	0.0429	-15.1	0.0000	0.0429	-15.1	0.0000	0.0000	0.0
0.0890	0.0431	-15.1	0.0000	0.0431	-15.1	0.0000	0.0000	0.0
0.0900	0.0433	-15.1	0.0000	0.0433	-15.1	0.0000	0.0000	0.0
0.0910	0.0435	-15.1	0.0000	0.0435	-15.1	0.0000	0.0000	0.0
0.0920	0.0437	-15.1	0.0000	0.0437	-15.1	0.0000	0.0000	0.0
0.0930	0.0439	-15.1	0.0000	0.0439	-15.1	0.0000	0.0000	0.0
0.0940	0.0441	-15.1	0.0000	0.0441	-15.1	0.0000	0.0000	0.0
0.0950	0.0443	-15.1	0.0000	0.0443	-15.1	0.0000	0.0000	0.0
0.0960	0.0445	-15.1	0.0000	0.0445	-15.1	0.0000	0.0000	0.0
0.0970	0.0447	-15.1	0.0000	0.0447	-15.1	0.0000	0.0000	0.0
0.0980	0.0449	-15.1	0.0000	0.0449	-15.1	0.0000	0.0000	0.0
0.0990	0.0451	-15.1	0.0000	0.0451	-15.1	0.0000	0.0000	0.0
0.1000	0.0453	-15.1	0.0000	0.0453	-15.1	0.0000	0.0000	0.0

TABLE 2 (continued)

$f_s$	$f_{s\text{-calc}}$	% error	$f_{co}$	$f_{co\text{-calc}}$	% error	$\varepsilon_T$	$\varepsilon_{T\text{-calc}}$	% error
.0573	.0625	9.4	.0900	.105	22.2	.70	.663	-6.3
.0860	.0824	-4.1	.1075	.136	26.5	.90	.93	3.3
.1033	.1219	18.0	.1450	.1543	6.4	.1300	.1163	-10.5
.1173	.1134	-3.3	.1700	.1573	-7.5	.5300	.553	4.3
.1430	.1191	-16.7	.1750	.1938	10.7	.5300	.5267	-0.6
.1867	.1912	2.4	.1700	.1867	9.8	.1900	.1928	1.4
.0051	.0047	-7.7	.1500	.1525	1.7	.70	.7028	0.4
.0418	.0479	14.6	.1300	.1165	-10.4	.50	.615	23.0
.0243	.0218	-10.3	.1200	.1095	-8.8	.40	.42	5.0
.0269	.0263	-2.2	.1050	.1079	2.8	.25	.245	-2.0
.0021	.0026	23.8	.1050	.1074	2.3	.40	.42	5.0
.0049	.0042	-14.3	.1250	.125	0.0	.60	.62	3.3
.0075	.0073	-2.7	.1500	.1525	1.7	.80	.83	3.8
.0090	.0093	3.3	.1600	.165	3.1	.90	.96	6.7
.0111	.0111	0.0	.1700	.1737	2.2	.1000	.105	5.0
.0140	.0149	6.4	.1750	.1774	1.4	.2000	.23	15.0
.0170	.0185	8.8	.1700	.1749	2.9	.3000	.35	16.7
.0200	.0217	8.5	.1800	.1873	4.1	.4000	.45	12.5
.0230	.0243	5.7	.1900	.1973	3.8	.5000	.58	16.0
.0260	.0275	5.8	.2000	.223	11.5	.6000	.65	8.3
.0290	.0307	5.9	.2100	.237	12.9	.7000	.76	8.6
.0320	.0337	5.3	.2200	.246	11.4	.8000	.86	8.0
.0350	.0367	4.9	.2300	.254	10.4	.9000	.94	4.4
.0380	.0397	4.5	.2400	.261	8.8	.1000	.11	1.0
.0410	.0427	4.1	.2500	.278	11.2	.2000	.22	10.0
.0440	.0457	3.9	.2600	.281	7.7	.3000	.32	6.7
.0470	.0487	3.6	.2700	.291	7.0	.4000	.42	5.0
.0500	.0517	3.4	.2800	.301	7.1	.5000	.52	4.0
.0530	.0547	3.2	.2900	.311	6.9	.6000	.62	3.3
.0560	.0577	3.0	.3000	.321	7.0	.7000	.72	2.9
.0590	.0607	2.9	.3100	.331	6.8	.8000	.82	2.5
.0620	.0637	2.7	.3200	.341	6.6	.9000	.92	2.2
.0650	.0667	2.6	.3300	.351	6.4	.1000	.11	1.0
.0680	.0697	2.5	.3400	.361	6.2	.2000	.22	10.0
.0710	.0727	2.4	.3500	.371	6.0	.3000	.32	6.7
.0740	.0757	2.3	.3600	.381	5.8	.4000	.42	5.0
.0770	.0787	2.2	.3700	.391	5.7	.5000	.52	4.0
.0800	.0817	2.1	.3800	.401	5.5	.6000	.62	3.3
.0830	.0847	2.0	.3900	.411	5.4	.7000	.72	2.9
.0860	.0877	1.9	.4000	.421	5.3	.8000	.82	2.5
.0890	.0907	1.8	.4100	.431	5.1	.9000	.92	2.2
.0920	.0937	1.7	.4200	.441	5.0	.1000	.11	1.0
.0950	.0967	1.6	.4300	.451	4.9	.2000	.22	10.0
.0980	.0997	1.5	.4400	.461	4.8	.3000	.32	6.7
.1010	.1027	1.4	.4500	.471	4.7	.4000	.42	5.0
.1040	.1057	1.3	.4600	.481	4.6	.5000	.52	4.0
.1070	.1087	1.2	.4700	.491	4.5	.6000	.62	3.3
.1100	.1117	1.1	.4800	.501	4.4	.7000	.72	2.9
.1130	.1147	1.0	.4900	.511	4.3	.8000	.82	2.5
.1160	.1177	0.9	.5000	.521	4.2	.9000	.92	2.2
.1190	.1207	0.8	.5100	.531	4.1	.1000	.11	1.0
.1220	.1237	0.7	.5200	.541	4.0	.2000	.22	10.0
.1250	.1267	0.6	.5300	.551	3.9	.3000	.32	6.7
.1280	.1297	0.5	.5400	.561	3.8	.4000	.42	5.0
.1310	.1327	0.4	.5500	.571	3.7	.5000	.52	4.0
.1340	.1357	0.3	.5600	.581	3.6	.6000	.62	3.3
.1370	.1387	0.2	.5700	.591	3.5	.7000	.72	2.9
.1400	.1417	0.1	.5800	.601	3.4	.8000	.82	2.5
.1430	.1447	0.1	.5900	.611	3.3	.9000	.92	2.2
.1460	.1477	0.1	.6000	.621	3.2	.1000	.11	1.0
.1490	.1507	0.1	.6100	.631	3.1	.2000	.22	10.0
.1520	.1537	0.1	.6200	.641	3.0	.3000	.32	6.7
.1550	.1567	0.1	.6300	.651	2.9	.4000	.42	5.0
.1580	.1597	0.1	.6400	.661	2.8	.5000	.52	4.0
.1610	.1627	0.1	.6500	.671	2.7	.6000	.62	3.3
.1640	.1657	0.1	.6600	.681	2.6	.7000	.72	2.9
.1670	.1687	0.1	.6700	.691	2.5	.8000	.82	2.5
.1700	.1717	0.1	.6800	.701	2.4	.9000	.92	2.2
.1730	.1747	0.1	.6900	.711	2.3	.1000	.11	1.0
.1760	.1777	0.1	.7000	.721	2.2	.2000	.22	10.0
.1790	.1807	0.1	.7100	.731	2.1	.3000	.32	6.7
.1820	.1837	0.1	.7200	.741	2.0	.4000	.42	5.0
.1850	.1867	0.1	.7300	.751	1.9	.5000	.52	4.0
.1880	.1897	0.1	.7400	.761	1.8	.6000	.62	3.3
.1910	.1927	0.1	.7500	.771	1.7	.7000	.72	2.9
.1940	.1957	0.1	.7600	.781	1.6	.8000	.82	2.5
.1970	.1987	0.1	.7700	.791	1.5	.9000	.92	2.2
.2000	.2017	0.1	.7800	.801	1.4	.1000	.11	1.0
.2030	.2047	0.1	.7900	.811	1.3	.2000	.22	10.0
.2060	.2077	0.1	.8000	.821	1.2	.3000	.32	6.7
.2090	.2107	0.1	.8100	.831	1.1	.4000	.42	5.0
.2120	.2137	0.1	.8200	.841	1.0	.5000	.52	4.0
.2150	.2167	0.1	.8300	.851	0.9	.6000	.62	3.3
.2180	.2197	0.1	.8400	.861	0.8	.7000	.72	2.9
.2210	.2227	0.1	.8500	.871	0.7	.8000	.82	2.5
.2240	.2257	0.1	.8600	.881	0.6	.9000	.92	2.2
.2270	.2287	0.1	.8700	.891	0.5	.1000	.11	1.0
.2300	.2317	0.1	.8800	.901	0.4	.2000	.22	10.0
.2330	.2347	0.1	.8900	.911	0.3	.3000	.32	6.7
.2360	.2377	0.1	.9000	.921	0.2	.4000	.42	5.0
.2390	.2407	0.1	.9100	.931	0.1	.5000	.52	4.0
.2420	.2437	0.1	.9200	.941	0.1	.6000	.62	3.3
.2450	.2467	0.1	.9300	.951	0.1	.7000	.72	2.9
.2480	.2497	0.1	.9400	.961	0.1	.8000	.82	2.5
.2510	.2527	0.1	.9500	.971	0.1	.9000	.92	2.2
.2540	.2557	0.1	.9600	.981	0.1	.1000	.11	1.0
.2570	.2587	0.1	.9700	.991	0.1	.2000	.22	10.0
.2600	.2617	0.1	.9800	.101	0.1	.3000	.32	6.7
.2630	.2647	0.1	.9900	.111	0.1	.4000	.42	5.0
.2660	.2677	0.1	.1000	.121	0.1	.5000	.52	4.0
.2690	.2707	0.1	.1100	.131	0.1	.6000	.62	3.3
.2720	.2737	0.1	.1200	.141	0.1	.7000	.72	2.9
.2750	.2767	0.1	.1300	.151	0.1	.8000	.82	2.5
.2780	.2797	0.1	.1400	.161	0.1	.9000	.92	2.2
.2810	.2827	0.1	.1500	.171	0.1	.1000	.11	1.0
.2840	.2857	0.1	.1600	.181	0.1	.2000	.22	10.0
.2870	.2887	0.1	.1700	.191	0.1	.3000	.32	6.7
.2900	.2917	0.1	.1800	.201	0.1	.4000	.42	5.0
.2930	.2947	0.1	.1900	.211	0.1	.5000	.52	4.0
.2960	.2977	0.1	.2000	.221	0.1	.6000	.62	3.3
.2990	.3007	0.1	.2100	.231	0.1	.7000	.72	2.9
.3020	.3037	0.1	.2200	.241	0.1	.8000	.82	2.5
.3050	.3067	0.1	.2300	.251	0.1	.9000	.92	2.2
.3080	.3097	0.1	.2400	.261	0.1	.1000	.11	1.0
.3110	.3127	0.1	.2500	.271	0.1	.2000	.22	10.0
.3140	.3157	0.1	.2600	.281	0.1	.3000	.32	6.7
.3170	.3187	0.1	.2700	.291	0.1	.4000	.42	5.0
.3200	.3217	0.1	.2800	.301	0.1	.5000	.52	4.0
.3230	.3247	0.1	.2900	.311	0.1	.6000	.62	3.3
.3260	.3277	0.1	.3000	.321	0.1	.7000	.72	2.9
.3290	.3307	0.1	.3100	.331	0.1	.8000	.82	2.5
.3320	.3337	0.1	.3200	.341	0.1	.9000	.92	2.2
.3350	.3367	0.1	.3300	.351	0.1	.1000	.11	1.0
.3380	.3397	0.1	.3400	.361	0.1	.2000	.22	10.0
.3410	.3427	0.1	.3500	.371	0.1	.3000	.32	6.7
.3440	.3457	0.1	.3600	.381	0.1	.4000	.42	5.0
.3470	.3487	0.1	.3700	.391	0.1	.5000	.52	4.0
.3500	.3517	0.1	.3800	.401	0.1	.6000	.62	3.3
.3530	.3547	0.1	.3900	.411	0.1	.7000	.72	2.9
.3560	.3577	0.1	.4000	.421	0.1	.8000	.82	2.5
.3590	.3607	0.1	.4100	.431	0.1	.9000	.92	2.2
.3620	.3637	0.1	.4200	.441	0.1	.1000	.11	1.0
.3650	.3667	0.1	.4300	.451	0.1	.2000	.22	10.0
.3680	.3697	0.1	.4400	.461	0.1	.3000	.32	6.7
.3710	.3727	0.1	.4500	.471	0.1	.4000	.42	5.0
.3740	.3757	0.1	.4600	.481	0.1	.5000	.52	4.0
.3770	.3787	0.1	.4700	.491	0.1	.6000	.62	3.3
.3800	.3817	0.1	.4800	.501	0.1	.7000	.72	2.9
.3830	.3847	0.1	.4900	.511	0.1	.8000	.82	2.5
.3860	.3877	0.1	.5000	.521	0.1	.9000	.92	2.2
.3890	.3907	0.1	.5100	.531	0.1	.1000	.11	1.0
.3920	.3937	0.1	.5200	.541	0.1	.2000	.22	10.0
.3950	.3967	0.1	.5300	.551	0.1	.3000	.32	6.7
.3980	.3997	0.1	.5400	.561	0.1	.4000	.42	5.0
.4010	.4027	0.1	.5500	.571	0.1	.5000	.52	4.0
.4040	.4057	0.1	.5600	.581	0.1	.6000	.62	3.3
.4070	.4087	0.1	.5700	.591	0.1	.7000	.72	2.9
.4100	.4117	0.1	.5800	.601	0.1	.8000	.82	2.5
.4130	.4147	0.1	.5900	.611	0.1	.9000	.92	2.2
.4160	.4177	0.1	.6000	.621	0.1	.1000	.11	1.0
.4190	.4207	0.1	.6100	.631	0.1	.2000	.22	10.0
.4220	.4237	0.1	.6200	.641	0.1	.30		



Further, it is possible to determine the orientation-strain moduli  $C_h$  and  $C_s$  from A and B, since the volume fractions  $V_h$  and  $V_s$  are known from the chemical composition. The polyurethane studied is about 50/50 hard/soft segment by weight, and the corresponding densities are 1.4 for the hard segment, 1.0 for the soft. These values yield volume fractions of  $V_s = .583$ ,  $V_h = .417$ , so that

$$C_s = \frac{V_s}{A} = .065$$

$$C_h = \frac{V_h}{B} = .186$$

for the constants determined from the first analysis based on the N-H absorbance as characteristic of the hard segment; and

$$C_s = \frac{V_s}{A} = .071$$

$$C_h = \frac{V_h}{B} = .200$$

for the constants determined from the analysis based on the carbonyl absorbance as characteristic of the hard segment. That the set of constants determined by using two different IR bands to characterize the hard segment orientation are not very different is proof that the series model is an adequate description of the material microstructure. This simple analysis gives the anticipated result that the soft segments have a lower resistance to strain-induced orientation than do the hard segments.

The series model also lends some insight into the phenomenon of permanent set in polyurethanes. The equation relating the sample



strain to the two orientation functions (Equation 47) should be valid for all strain states; therefore the plastic part of the strain should be calculable from knowledge of the values of the two orientation functions in the deformed sample after tractions are removed. Figure 35 illustrates the data given by Estes et al. (1971) on the ES-38 material for the two orientation functions after straining to the indicated level, releasing the samples, and resting them for 5 minutes. The soft segment orientation relaxes to a very small value, while considerable hard segment orientation remains, indicating that the greatest part of the observed plasticity in the sample is due to the hard phase residual orientation. Comparison of the figure data with the observed permanent set in ES5701 (Figure 14) shows that there is a rough correspondence between permanent set and  $f_h$ . Below strains of about 100%, there is little permanent set and little residual  $f_h$ . Above 100%, both the residual  $f_h$  and the permanent set increase with prestrain in roughly the same manner.

The series model is also consistent with the observed birefringence-strain behavior of polyurethanes, as presented, for example, by Puett (1967) and Estes et al. (1969). The birefringence,  $\Delta n$ , is a measure of the total orientation in the sample, which, consistent with the above discussion, may be taken as some weighted average of the orientations in the two separate domains. If this is true, then it immediately follows that the strain-birefringence relationship is a linear one, i.e.,

$$(48) \quad \epsilon_T = C \Delta n$$



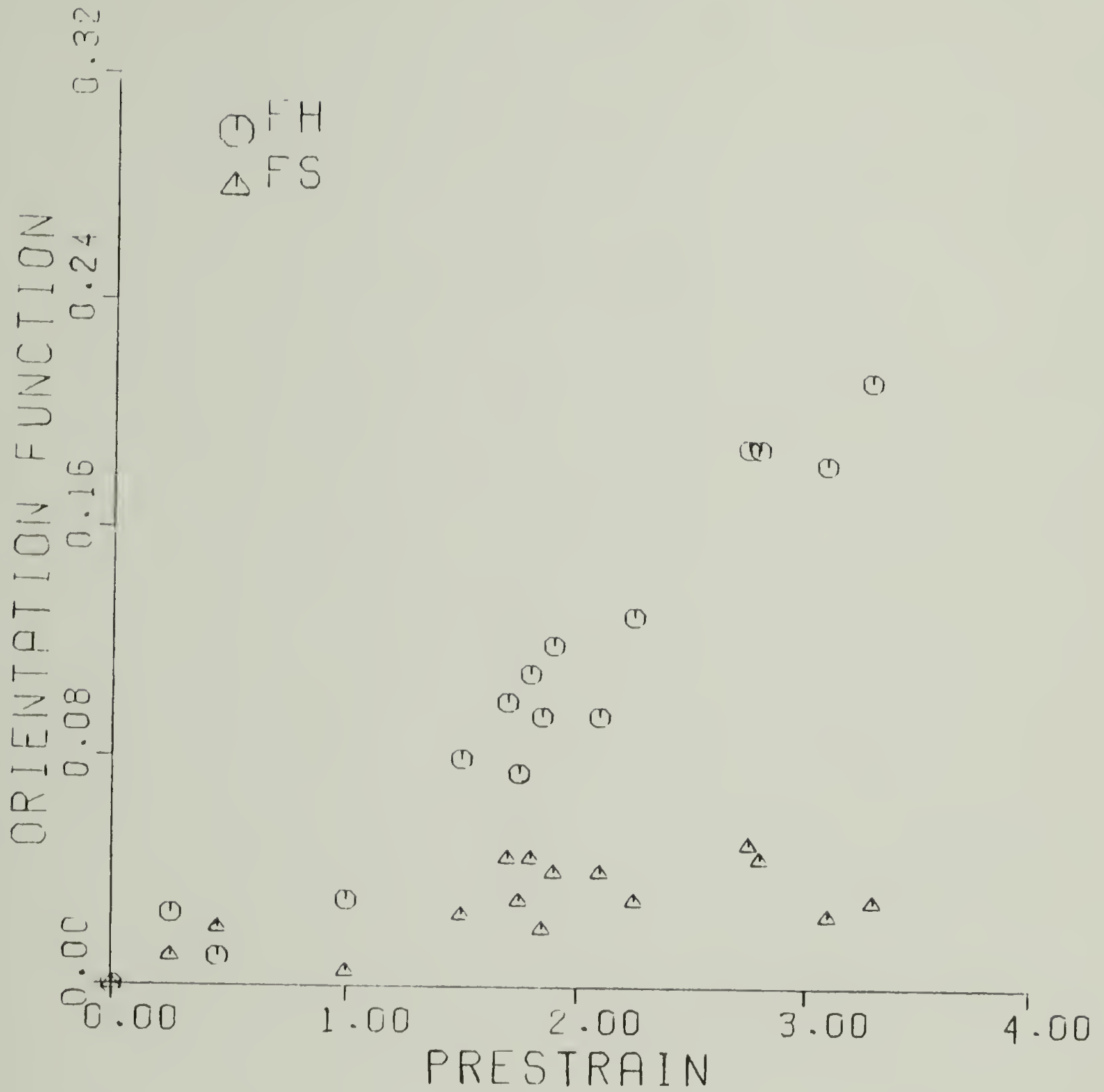


Figure 35. Residual orientation in hard (FH) and soft (FS) segments after indicated prestrain and 5 minutes at zero stress. Data of Estes et al. (1971).

which is the experimental result shown in the two papers mentioned above.

#### III.4. Microstructural Models for Orientation in Polyurethanes

The results of the previous section provide a relationship between the strain in the sample and the strains, or equivalently the orientations, in the hard and soft domains. In this section models are developed which quantitatively describe the dependence of the orientation function on strain history.

Other workers have related the orientation functions of semi-crystalline polymers to sample strain level. Kratky's "floating rod" model (Kratky, 1933) is a description of cellulose as a system of right prisms deforming and orienting in an isotropic medium. His goal was to relate the change in orientation function of the "rods" with strain to the changes in x-ray scattering patterns. More recent results by Sasaguri et al. (1964), Nomura et al. (1971), Yoon et al. (1974) and Petraccone et al. (1975) for spherulitic polymers treat the microstructure as a more sophisticated system of spheres of crystalline lamellae deforming into ellipsoids. These results, although they correlate calculations of birefringence-strain behavior with data taken at discrete strain levels, do not attempt to describe any strain history-dependence of the orientation functions other than a monotonically increasing one.

##### III.4.1. Time-independent orientation of hard segment domains. The

orientation function-strain data taken by Estes et al. (1971) indicates that there is some irreversible orientation of the hard segments after deformation, while the orientation of the soft phase is reversible. In order for some irreversible orientation to be present, some of the work done in straining the sample must be nonrecoverable. The nonrecoverable part of the work may be accounted for, as discussed above, by the readjustment of the hard domains as a whole in the soft matrix, or some slip process such as the pulling out of a hard chain segment from its surrounding environment of other hydrogen-bonded hard segments. In both cases, the restoring force of the soft chains when traction is removed is not great enough to disrupt the hard segment from its new position, which will be stabilized by the reforming of hydrogen bonds, van der Waals forces, and the driving force for domain segregation.

As a first approximation, the irreversible orientation of the hard segments will be considered as a time independent but history dependent process. The history dependence will be introduced by use of infinite Lebesgue norms of the strain, as discussed in Chapter II. The following physical assumptions will be considered in developing a model for the orientation of hard segments. The treatment is for the one-dimensional case, and will emphasize the behavior of some characteristic elements of the hard domain, without specifying precisely the molecular composition of the elements.

#### Model assumptions.

- A. The polyurethane system is considered a collection of hard

urethane elements randomly distributed in the soft, continuous matrix. Each hard element consists of many urethane chain segments connected by hydrogen bond bridges, in the manner described by Bonart (1968).

- B. The  $i^{\text{th}}$  hard element reacts independently to strain in the following manner: after a critical yield strain,  $\epsilon_{yi}$ , is reached, the orientation function increases linearly with strain. This assumption is equivalent to stating that the hard segment strain is a linear function of the applied strain. This stochastic model is similar to the one described by Farris (1968) for vacuole formation in filled elastomers. In that example, an individual vacuole was assumed to begin its growth at some critical strain, and the total volume change in the material computed as the sum of the volume of all the vacuoles.

Additionally, all elements will have the same orientation-strain behavior once their individual yield strain is surpassed.

- C. The orientation in the hard segments displays strain-hardening and permanent memory of the previous maximum strain state. Thus, after the material has been deformed and relaxed to zero stress, the hard segments will have an increased resistance to further orientation, i.e., the slope of the orientation function-strain curve will be lower. Further, the previous maximum state of strain will be preserved as an

important point in the strain history through use of Lebesgue norms.

- D. It is assumed that there exists a distribution of yield strains for the different elements, so that the total orientation function measured at any point in the strain history will be the sum of all the  $F_i$ 's for the elements, averaged over a normalized distribution function of yield strains,  $N(\epsilon_y)$ .

Assumptions B and C may be given a precise mathematical meaning if the orientation function of the  $i^{\text{th}}$  element has the following form:

$$(49) \quad f_i = \begin{cases} 0 & \|\epsilon\| < \epsilon_{yi} \\ C \frac{\epsilon}{\|\epsilon\|} [\|\epsilon\| - \epsilon_{yi}] & \|\epsilon\| \geq \epsilon_{yi} \end{cases}$$

where  $\epsilon_{yi}$  is the yield strain of the  $i^{\text{th}}$  element,  $C$  is a material constant,  $\epsilon$  is the applied strain, and  $\|\epsilon\|$  is the infinite Lebesgue norm of the strain, i.e., the maximum strain in the deformation history (the notation  $\|\epsilon\|$  will be used instead of  $\|\epsilon\|_\infty$  for simplicity). The strain measure  $\epsilon$  used here is the strain in the deformed coordinate system defined as  $\epsilon = (\lambda - 1)/\lambda$  where  $\lambda$  is the extension ratio (see Section II.2).

The function  $f_i$  in Equation (49) is graphically illustrated in Figure 36. For a monotonic, increasing strain history  $\|\epsilon\| = \epsilon$ , so that after the yield strain  $\epsilon_{yi}$  is surpassed,  $f_i$  follows the linear relation  $f_i = C(\epsilon - \epsilon_{yi})$ . This relation is depicted by the AB portion of the curve in Figure 36, which corresponds to the first leg of the



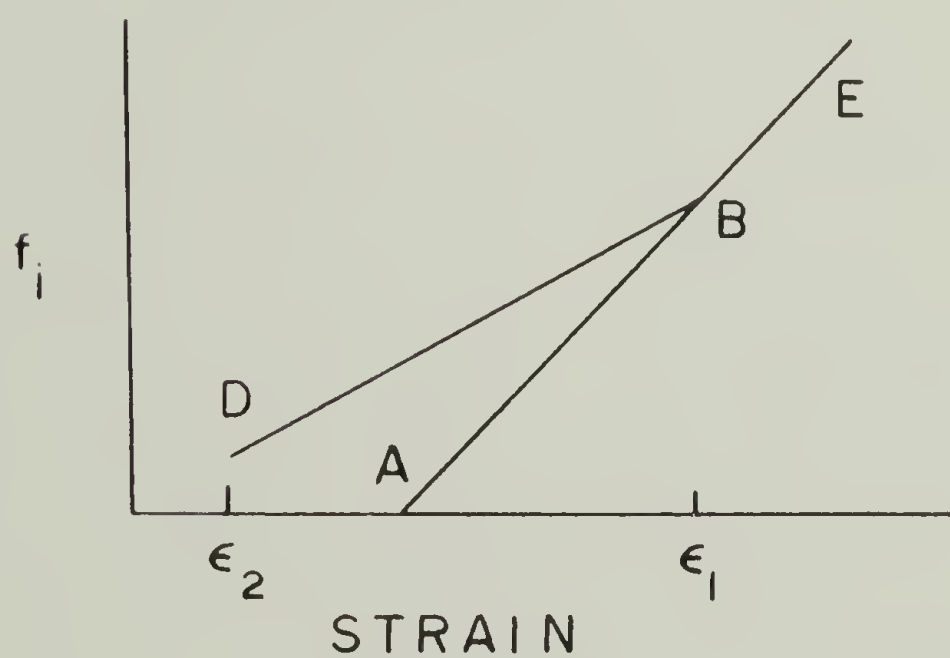
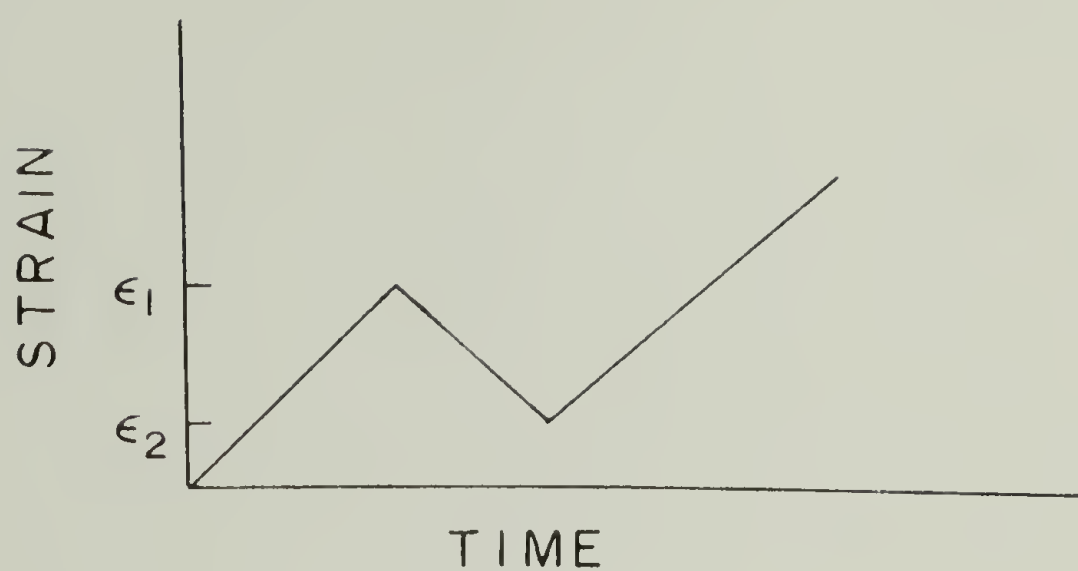


Figure 36. Orientation function of the  $i^{\text{th}}$  hard element,  $f_i$ , vs. strain for the indicated strain history, given by Equation (49) of text.

indicated strain history, up to strain  $\epsilon_1$ . As the strain decreases to  $\epsilon_2$  in the given history,  $\|\epsilon\| = \epsilon_1$  and  $f_i$  will follow the curve BD according to the relation  $f_i = C \epsilon (1 - \epsilon_{yi}/\epsilon_1)$ . The slope of DB therefore will always be less than  $C$ , the original slope of the orientation function curve. Thus the first condition of assumption C is fulfilled.

If the strain direction is reversed at  $\epsilon_2$ , the curve DB will be followed until  $\epsilon_1$  is surpassed, at which point  $\|\epsilon\| = \epsilon$  again, and path BE is followed. This behavior is obtained through use of the ratio  $\epsilon/\|\epsilon\|$  to multiply the linear equation for  $f_i$ . As already shown,  $\epsilon/\|\epsilon\|$  will be unity for any monotonic increasing strain histories, while for other histories it will depend on both  $\epsilon$  and  $\|\epsilon\|$ .

The use of  $\|\epsilon\|$  to indicate the range of the function insures that once the element has yielded, it remains yielded, and the orientation thus induced by strain will return to zero only for zero strain. Since the polymers under consideration exhibit permanent set, a return to zero orientation will theoretically only be possible for compressive stress states, which will not be treated here.

In order to compute the total orientation function from the contribution of all the individual hard segments, it is assumed (see D above) that the  $\epsilon_{yi}$  comprise a continuous spectrum,  $\epsilon_y$ , and that the fraction of elements with yield strains between  $\epsilon_y$  and  $\epsilon_y + d\epsilon_y$  is given by the distribution function  $N(\epsilon_y)d\epsilon_y$ . Then it follows that the total orientation function of the hard domains,  $f_h$ , is

$$(50) \quad f_h = \int_{-\infty}^{\|\epsilon\|} N(\epsilon_y) f_i(\epsilon_y) d\epsilon_y \quad 0 < \epsilon_y < \|\epsilon\|$$

The upper limit of the integral in (50) stems from the fact that  $f_i(\epsilon_y)$  is zero for  $\epsilon_y > \|\epsilon\|$ . Using (49), the integral becomes

$$(51) \quad f_h = C \frac{\epsilon}{\|\epsilon\|} \int_{-\infty}^{\|\epsilon\|} N(\epsilon_y) (\|\epsilon\| - \epsilon_y) d\epsilon_y$$

It is possible to roughly determine the form of  $N(\epsilon_y)$  by noting that, for a monotonic strain history,

$$(52) \quad \frac{d^2 f_h}{d\|\epsilon\|^2} = C N(\|\epsilon\|)$$

Thus the second derivative of the orientation function with respect to the maximum strain should be proportional to the instantaneous frequency of elements yielding at that strain. In Figure 37 a plot is given of the points from Figure 22 that correspond to the monotonic increasing portion of the test. It is seen that  $f_h$  is first zero, then increases rapidly over a small range of strain. This orientation-strain behavior shows a striking resemblance to the volume change-strain behavior of filled elastomers determined by Farris (1968). He showed that the frequency distribution for the case of vacuole formation was Gaussian, based on the appearance of the second derivative curves (see Figure 38) and also by simply considering a random process dealing with a large number of individual vacuoles forming.

For the purpose of this analysis it is thus assumed that the



Figure 37. Orientation function of hard segment (FH) vs. strain for the monotonic portion of the strain history given in Figure 21.

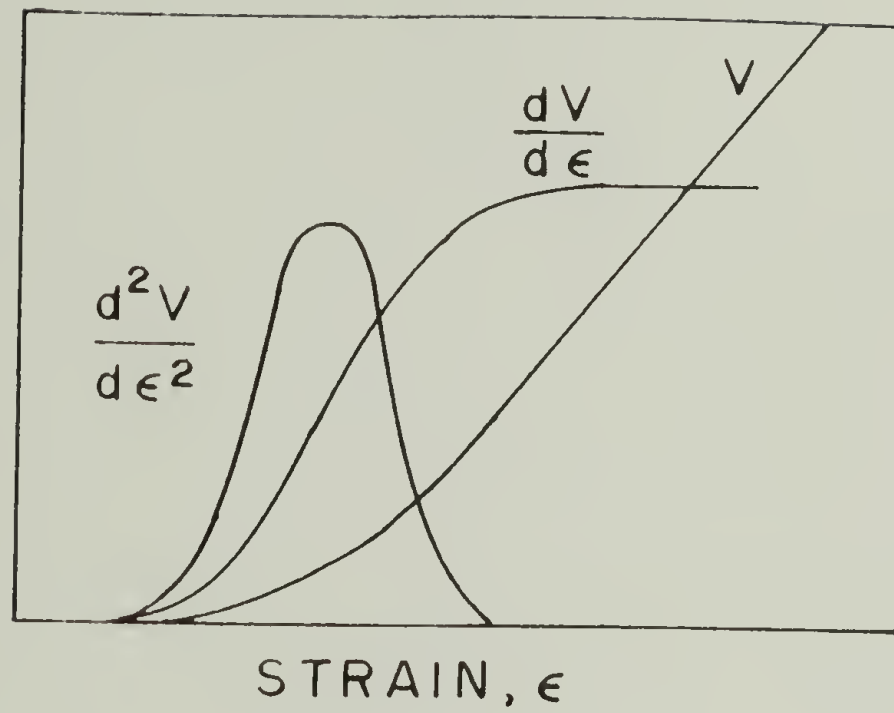


Figure 38. Schematic representation of dilatation,  $V$ , vs. strain relationship and its first and second derivatives (after Farris, 1968).



distribution function is the normalized Gaussian distribution, of mean  $\bar{\epsilon}$  and standard deviation  $S$ :

$$(53) \quad N(\epsilon_y) = \frac{1}{S\sqrt{2\pi}} e^{-\frac{(\epsilon_y - \bar{\epsilon})^2}{2S^2}}$$

Equation (51) then becomes

$$(54) \quad f_h = C \frac{\epsilon}{\|\epsilon\|} \cdot \frac{1}{S\sqrt{2\pi}} \int_{-\infty}^{\|\epsilon\|} e^{-\frac{(\epsilon_y - \bar{\epsilon})^2}{2S^2}} (\|\epsilon\| - \epsilon_y) d\epsilon_y$$

Equation (54) may be solved analytically (see Appendix F) to yield

$$(55) \quad f_h = \frac{C}{2} \frac{\epsilon}{\|\epsilon\|} \left\{ \|\epsilon\| - \bar{\epsilon} \left[ 1 + \operatorname{erf}\left(\frac{\|\epsilon\| - \bar{\epsilon}}{S\sqrt{2}}\right) \right] + S\sqrt{\frac{2}{\pi}} e^{-\frac{(\|\epsilon\| - \bar{\epsilon})^2}{2S^2}} \right\}$$

The material constants  $C$ ,  $\bar{\epsilon}$  and  $S$  determined by nonlinear regression analysis of the data in Figure 21 are:

$$C = .673 \pm .008$$

$$S = .28 \pm .02$$

$$\bar{\epsilon} = 1.00 \pm .01$$

The best-fit values of  $S$  and  $\bar{\epsilon}$  correspond to the distribution centered about  $\epsilon_y = 1.00$ , with standard deviation  $S = .28$ , as plotted in Figure 39. It is interesting to note that the cumulative distribution, from  $\epsilon_y = 0$  to  $\epsilon_y = +\infty$ , contains 99.98% of the yield events under consideration, indicating that some elements begin yielding even at very small strains. The small error (.02%) introduced into the theory by allowing some elements to begin in a compressive strain state

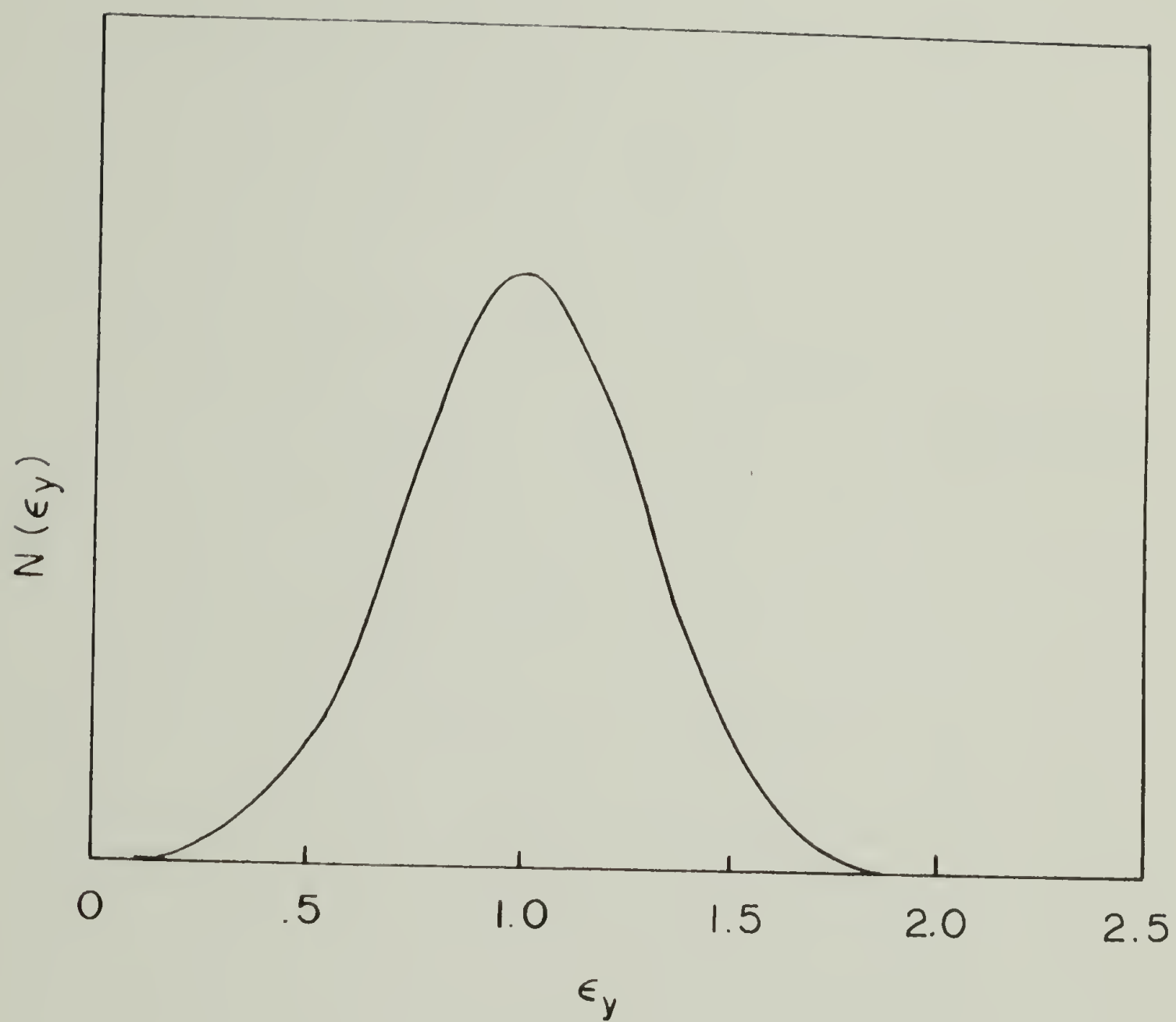


Figure 39. Distribution function of yield strains,  $N(\epsilon_y)$ , determined from data of Figure 22.

( $\epsilon_y < 0$ ) is a consequence of choosing a distribution function that is defined over the range  $-\infty$  to  $+\infty$ .

The theoretical curve from Equation (55) is plotted with the data in Figure 40. Since the two orientation functions  $f_s$  and  $f_h$  are related to the strain by Equation (47), it is also possible to predict  $f_s$  using Equation (55). The predicted curve is shown alone in Figure 41 and superimposed on the data in Figure 42.

It is seen that the theory successfully predicts the hysteresis and permanent memory features of both the  $f_s$ - and  $f_h$ -strain behavior.

III.4.2. Time-dependent orientation of hard segment domains. In the previous section, the time-independent permanent memory characteristics in the orientation function-strain response of polyurethanes were described by a simple equation based on the infinite Lebesgue norm of the strain,  $\|\epsilon\|_\infty$ . In this section it will be demonstrated that time-dependent orientation may be described through use of lower order norms (see Chapter II).

The time-dependence of the orientation in polyurethanes has been demonstrated mostly by monitoring of the IR dichroism during stress relaxation experiments. Seymour and Cooper (1974) noted that after straining to 150% and holding the strain level constant, the hard segment orientation function increased rapidly at first but quickly leveled off at a new value about 20% higher than the value at the start of the relaxation portion of the test (Figure 20). The soft segment orientation showed similar behavior except that it decreased where the hard segment orientation increased.

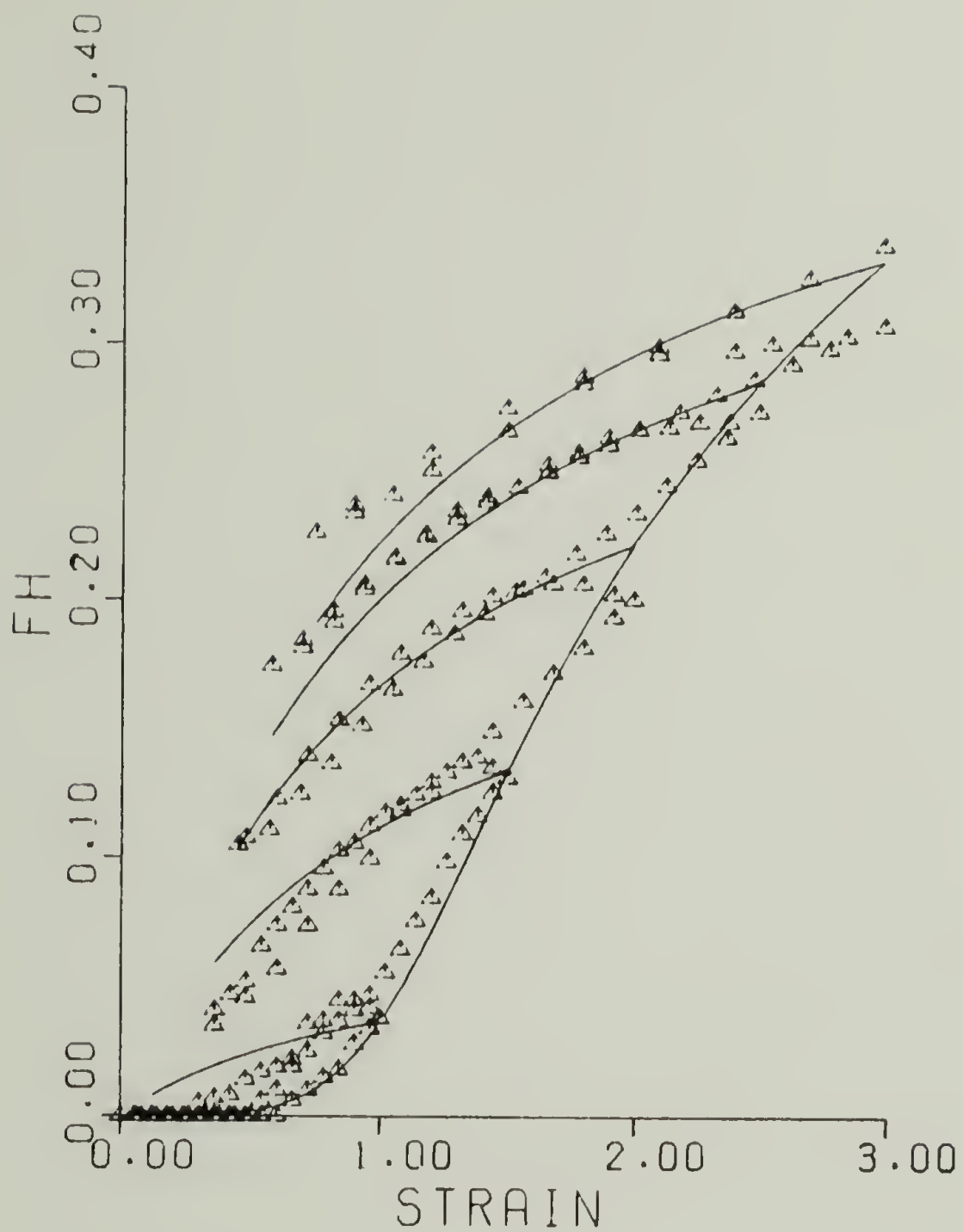


Figure 40. Hard segment orientation function vs. strain. Points are experimental data of Cooper (Figure 22), curve is Equation 55 of text.

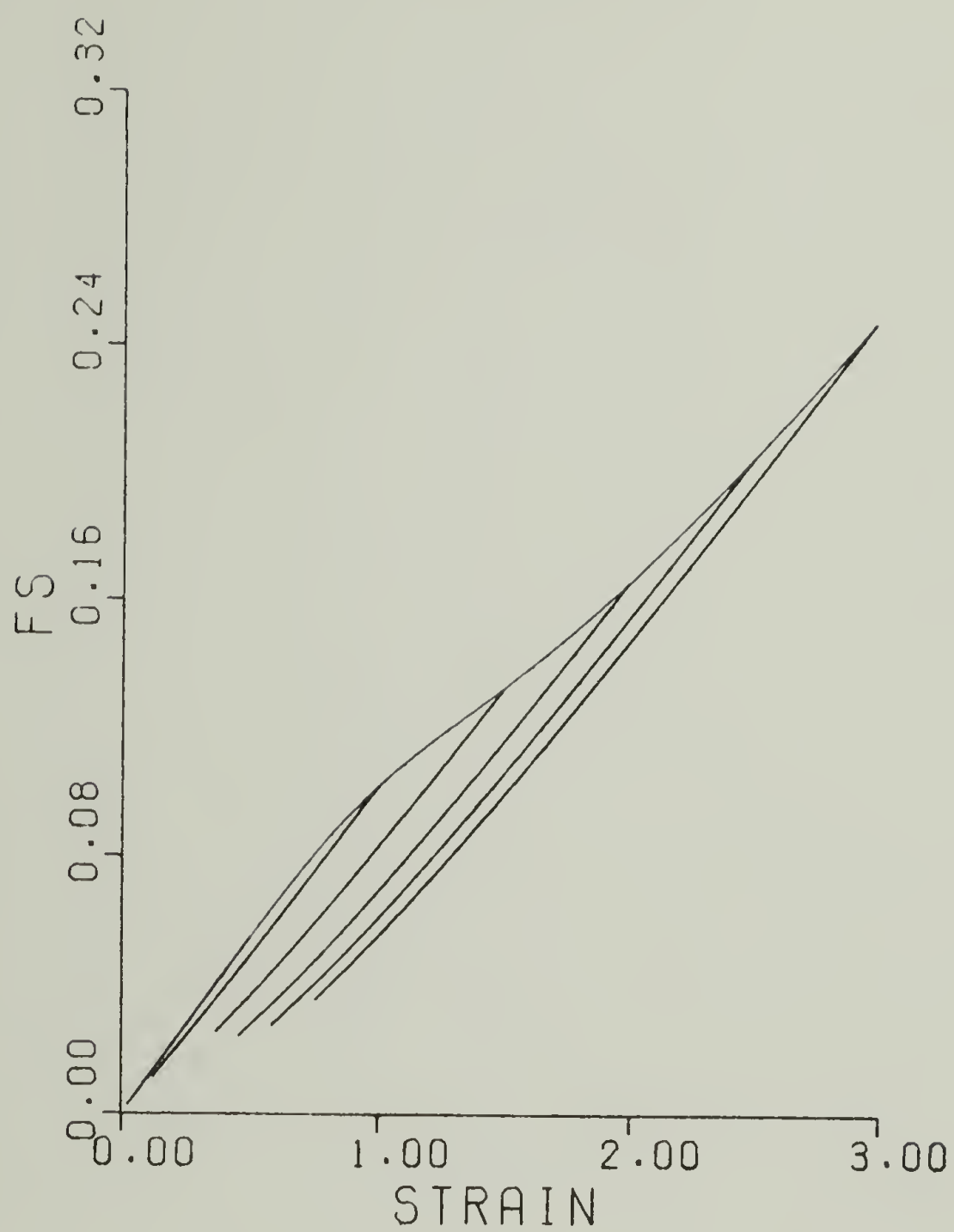


Figure 41. Soft segment orientation function predicted by Equations 55 and 47 of text.



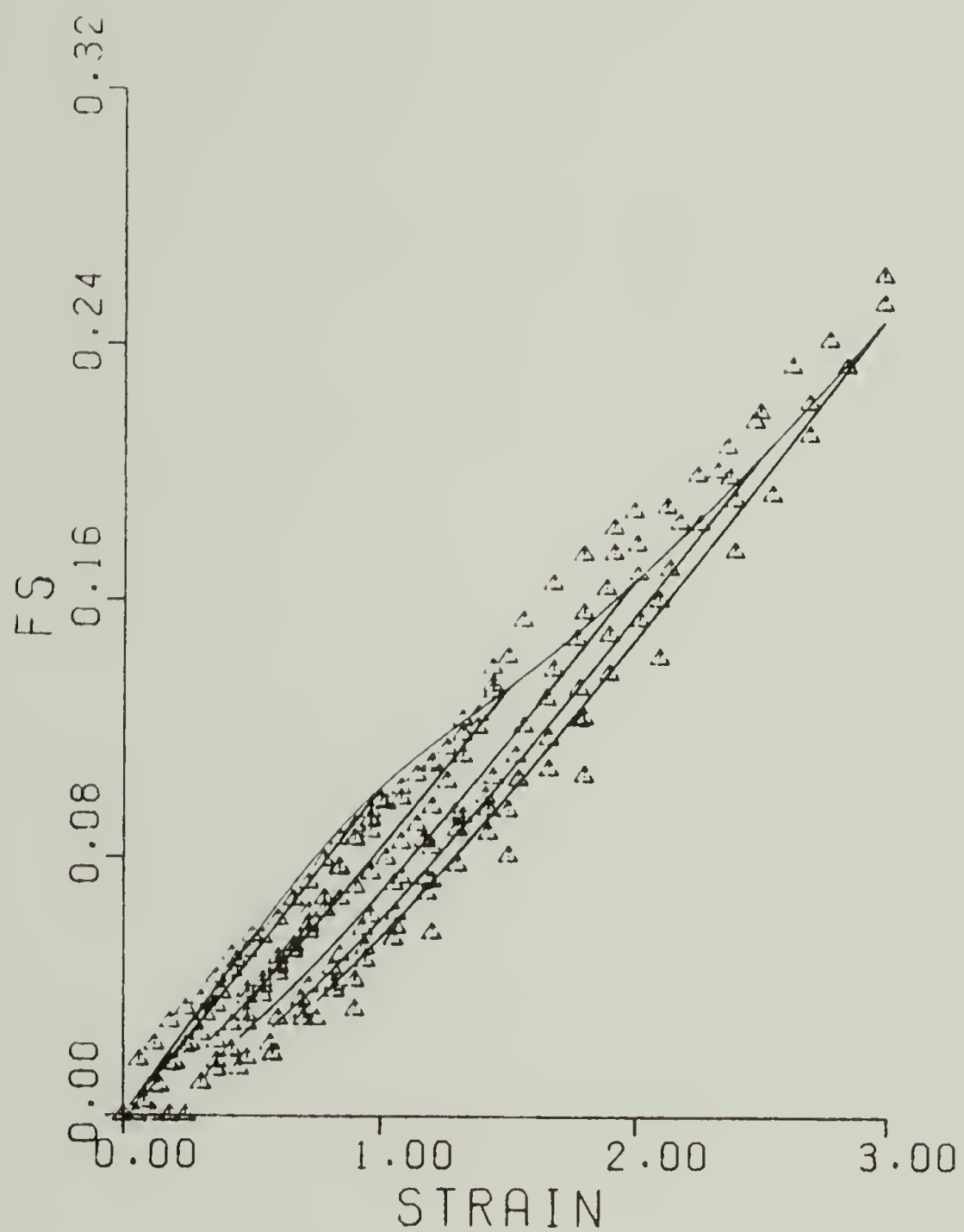


Figure 42. Soft segment orientation data (points) and prediction (curve) of Equations 55 and 47 of text.

This type of time-dependence may be easily described by extension of the time-independent model in the previous section. The infinite norm of the strain, a time-independent quantity, is the limiting case of the general  $p^{\text{th}}$  order norm,  $\|\epsilon\|_p$ , described in Chapter II. By simple replacement of  $\|\epsilon\|_\infty$  in equation 26 by  $\|\epsilon\|_p$ , the model for the orientation of the hard segments becomes both history and time-dependent. Equation 26, then, in its more general form, is

$$(56) \quad f_h = \frac{C}{2} \frac{\epsilon}{\|\epsilon\|_p} \left\{ (\|\epsilon\|_p - \bar{\epsilon}) \left[ 1 - \operatorname{erf} \left( \frac{\|\epsilon\|_p - \bar{\epsilon}}{S\sqrt{2}} \right) \right] + S\sqrt{\frac{2}{\pi}} e^{-\frac{(\|\epsilon\|_p - \bar{\epsilon})^2}{2S^2}} \right\}$$

and obviously contains the time-independent case in the limit as  $p \rightarrow \infty$ .

The improvement in the model through use of  $\|\epsilon\|_p$  is immediately seen when Equation (56) is applied to the hysteresis data of the previous section. In Figure 43, the data for  $f_h$  vs. strain are plotted together with the best fit of Equation (56) for  $p = 10$ . Analytical expressions for  $\|\epsilon\|_p$  for this strain history are given in Appendix G. The new equation successfully predicts the delay in rejoining the virgin curve behavior seen in the data, while the permanent memory of the previous maximum strain state is preserved. In Figure 44 the corresponding plot for  $f_s$  is given; the data are omitted for clarity. It may be seen that, in comparison to Figure 41, the predicted soft segment orientation also has an imperfect rejoining of the original curve. It appears that the data for  $f_s$  (Figure 24) also shows this feature; however, the scatter in the data makes the

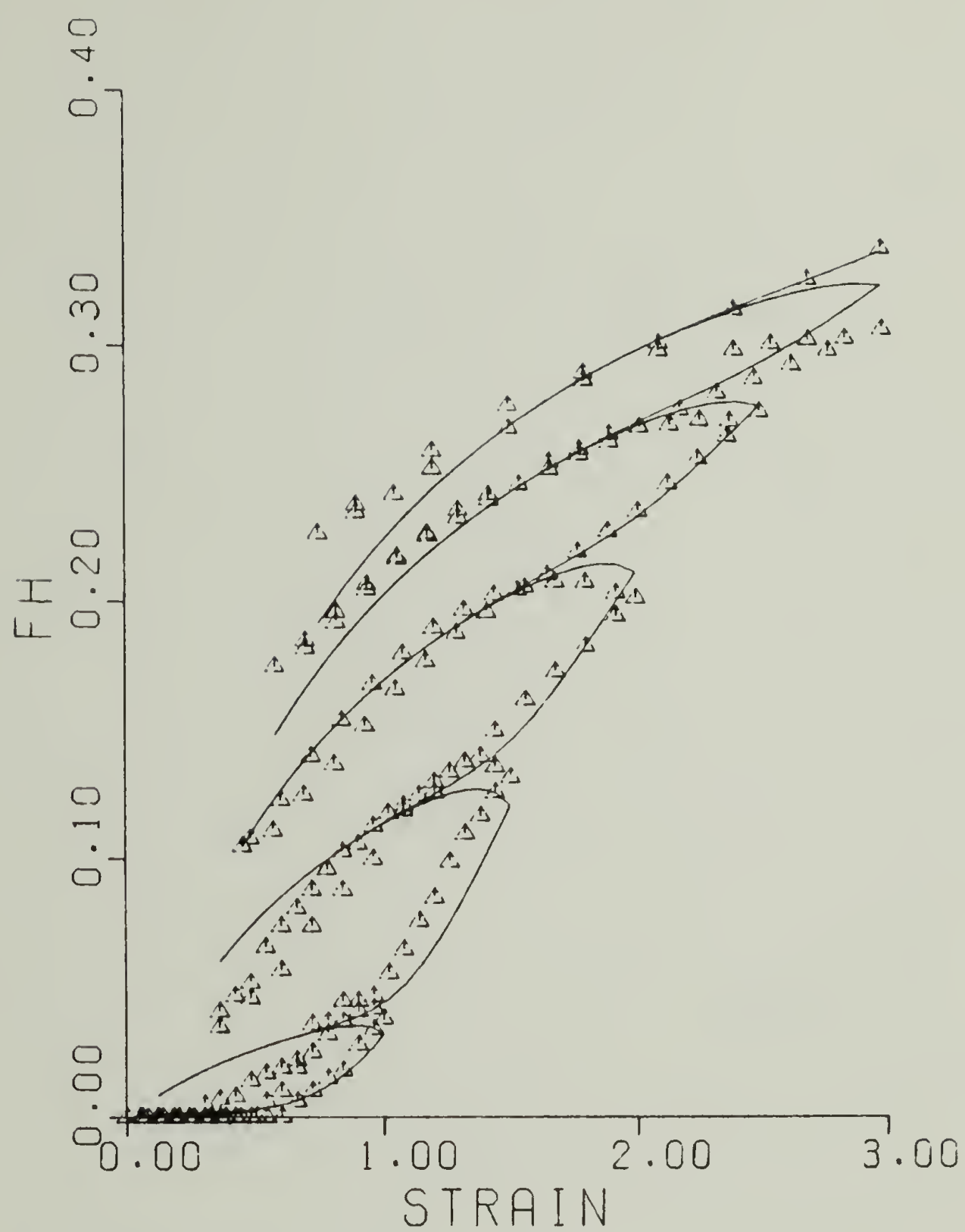


Figure 43. Hard segment orientation function vs. strain. Points are data of Figure 22; curve is Equation 56 of text with  $p=10$ .

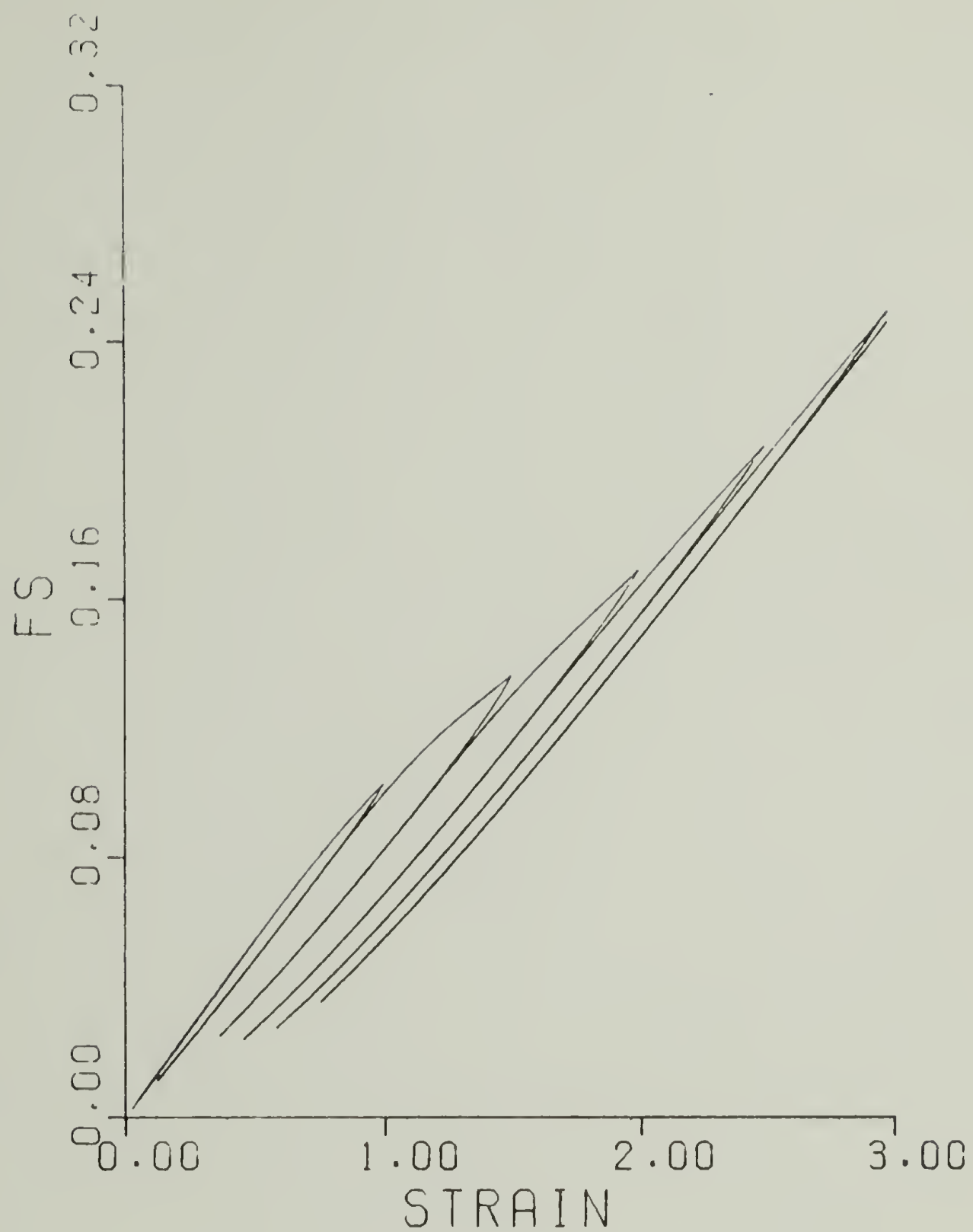


Figure 44. Soft segment orientation function vs. strain. Equations 56 and 47 of text, with  $p=10$ .

comparison of theory to experiment for the soft segment difficult.

In Figures 45 and 46 graphs are given for the case of  $p = 20$  in Equation (56). When  $p$  is increased, the unloading portion of the curve rejoins the original curve more quickly; i.e., the predicted behavior is approaching the  $p = \infty$  case seen in Figures 40 and 41.

By examining the predictions of Equation (56) for a stress relaxation test further agreement is seen between theory and experiment. In Figure 47, the orientation function-strain response is plotted for the indicated strain history in which the strain rate is constant (Zone 1), then zero (the stress relaxation step at 150% strain, Zone 2), and then constant again (Zone 3). The analytical expressions for  $\|\epsilon\|_p$  for this strain history are given in Appendix H. In agreement with the observations of Seymour and Cooper (1974), the hard segment orientation increases during the relaxation step, while the soft segment orientation decreases. There is also great similarity between the shape of the two predicted orientation curves and those given by Seymour and Cooper (1974) (Figure 20).

The determination of the order of the Lebesgue norm appropriate to any particular material may be determined by examining the relaxation test response. In Figures 48 and 49, the orientation-strain output is plotted for the relaxation step only, as a function of  $p$ . The order of  $p$  therefore is an indication of the relative speed with which the orientation becomes constant during the relaxation test.

The effect of strain level on the relaxation step response is displayed in Figures 50 and 51. Again, equation (56) is plotted for



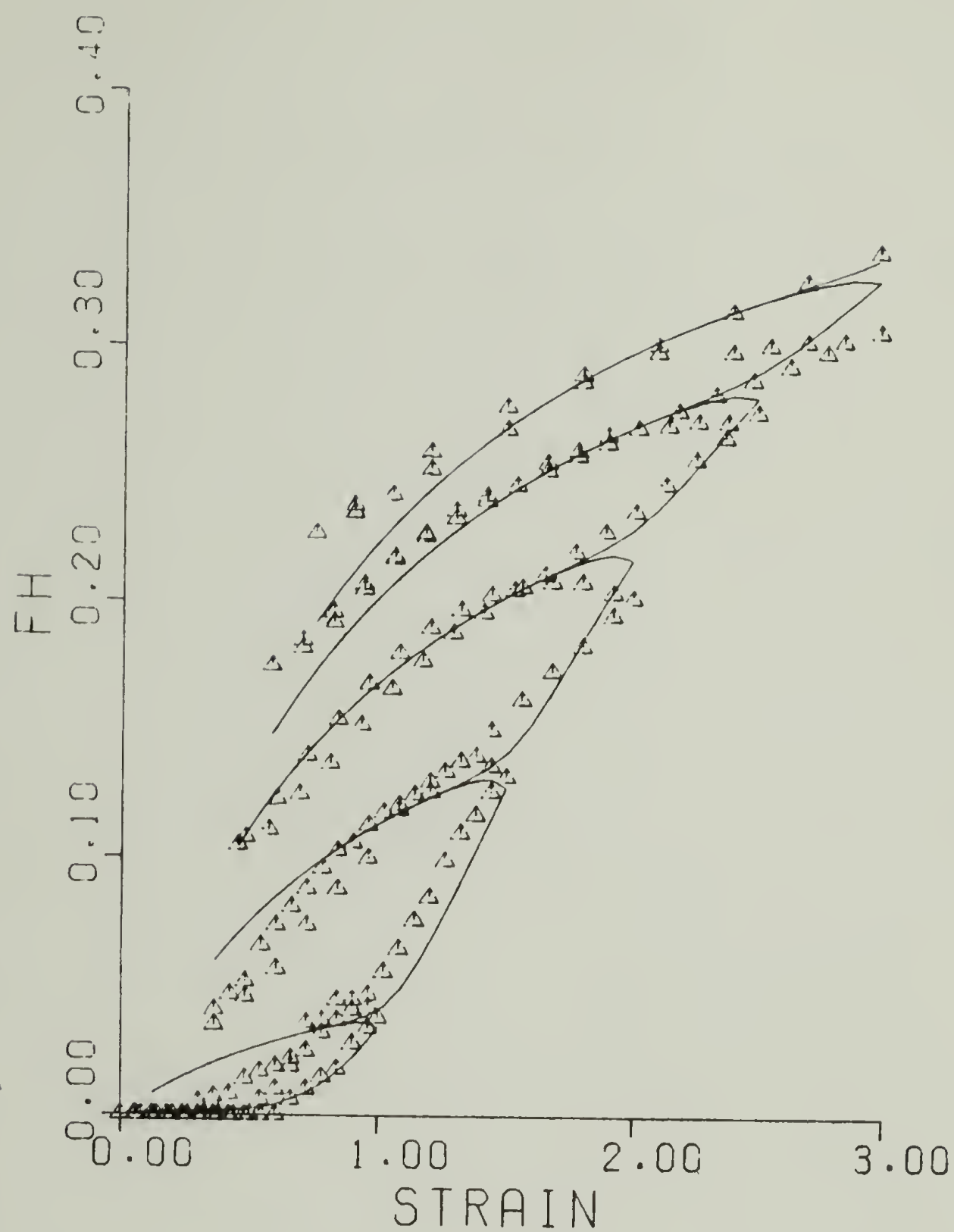


Figure 45. Hard segment orientation function. Points are data of Figure 22; curve is Equation 56 of text with  $p=20$ .

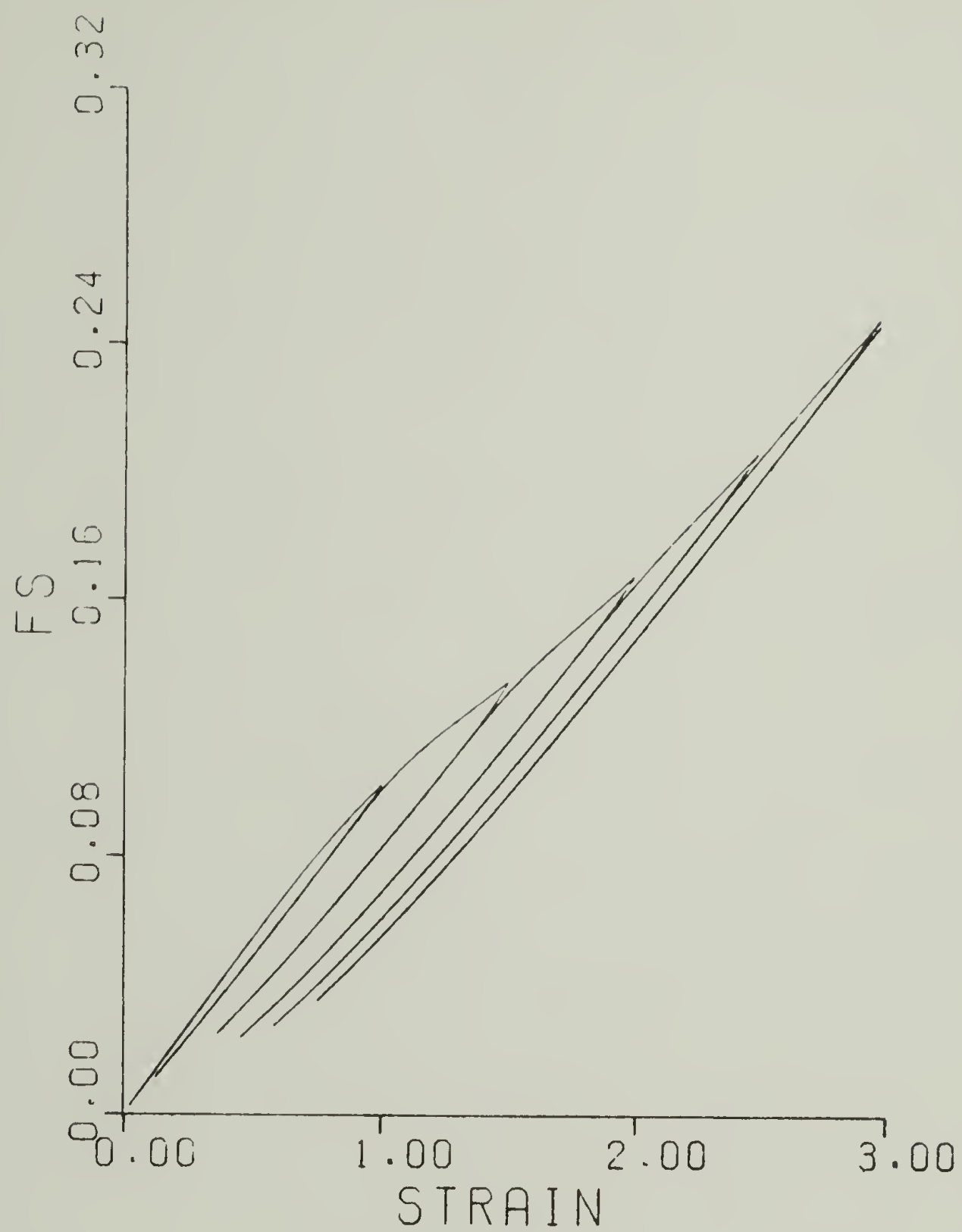


Figure 46. Soft segment orientation function vs. strain. Curve is Equations 56 and 47 of text with  $p=20$ .

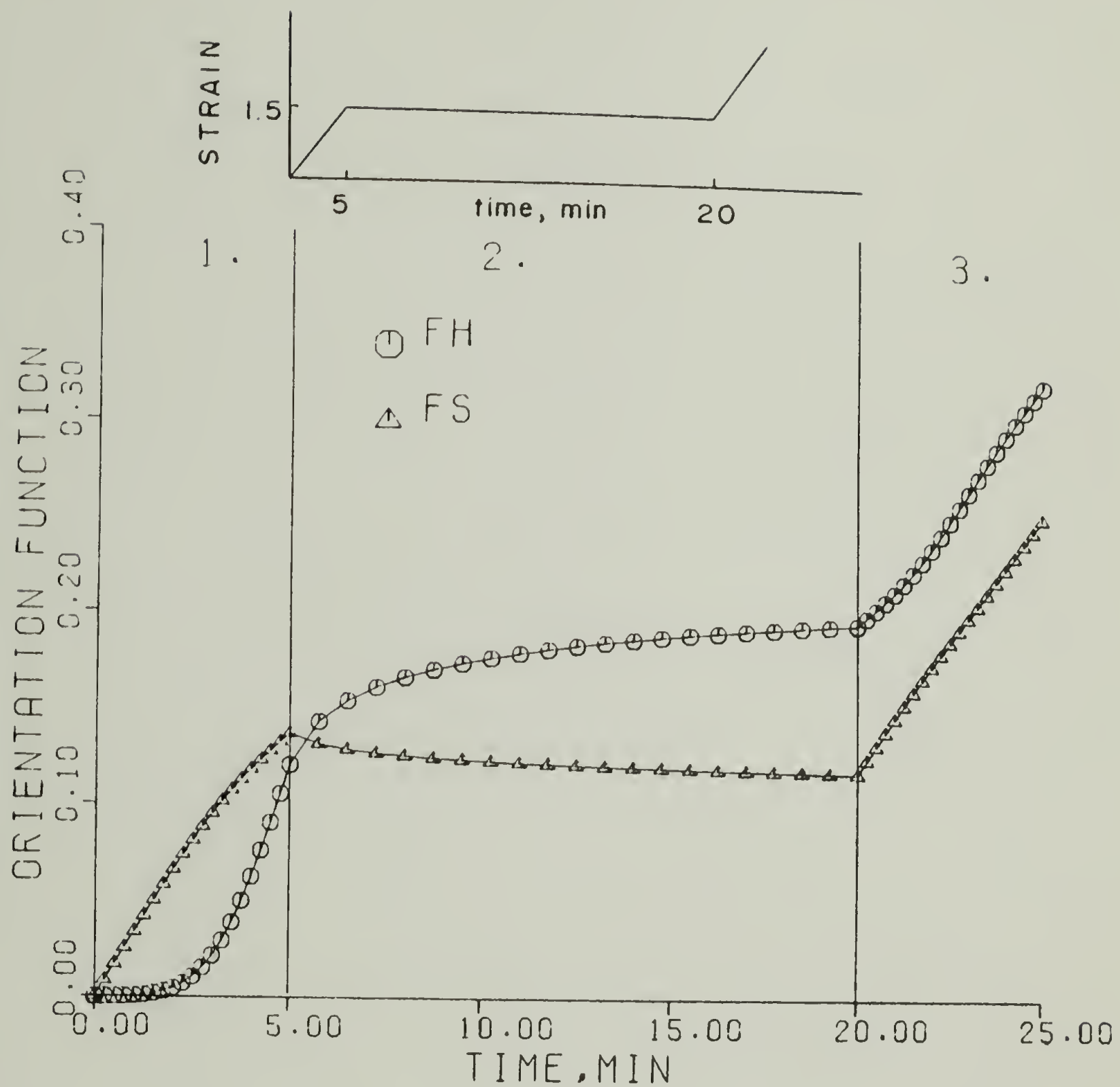


Figure 47. Soft and hard segment orientation functions for the indicated strain history, predicted by Equation 56 of text, with  $p=10$ .

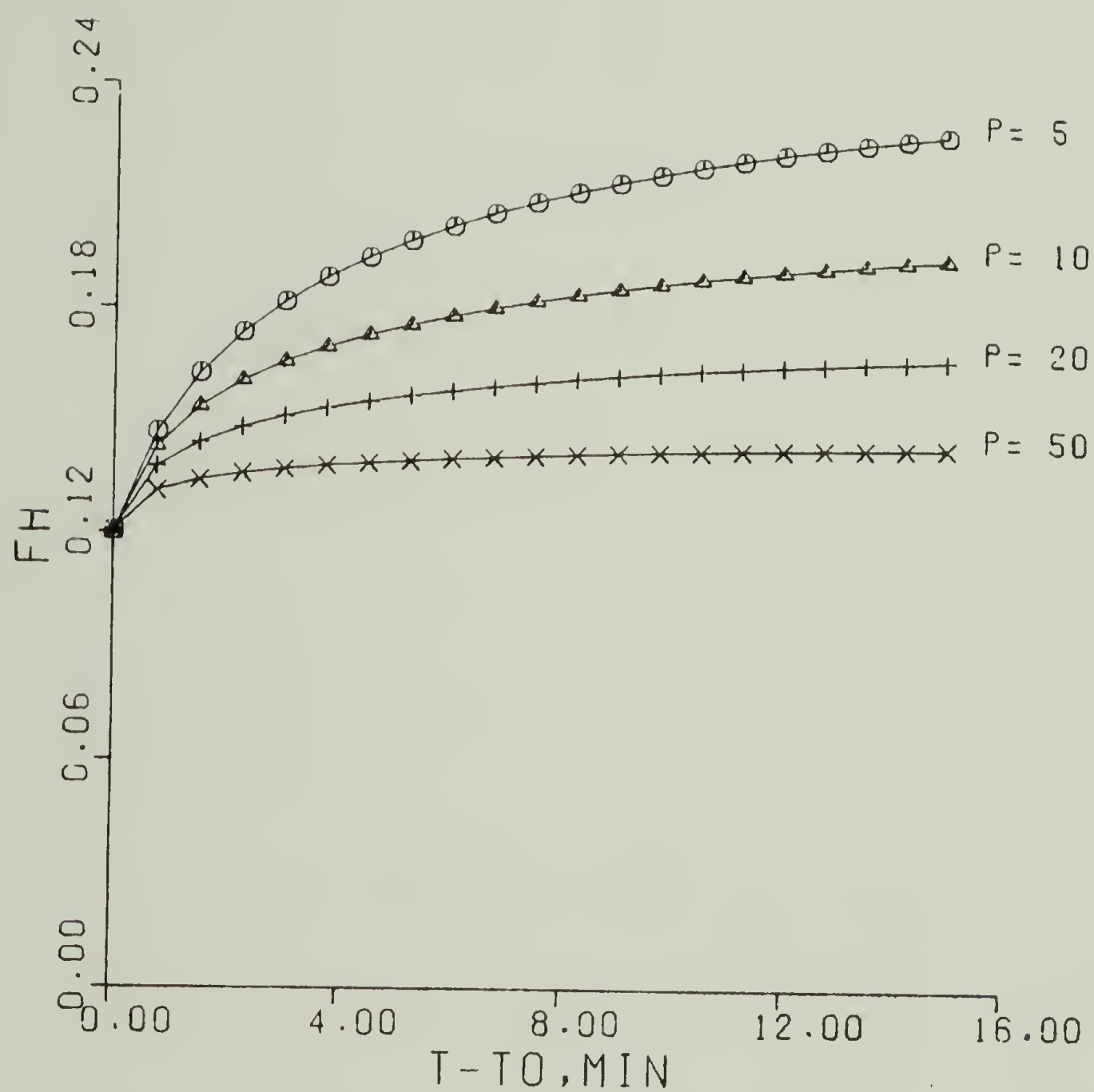


Figure 48. Hard segment orientation function vs. time in stress relaxation test at 150% strain, for indicated values of  $p$  (Equation 56).

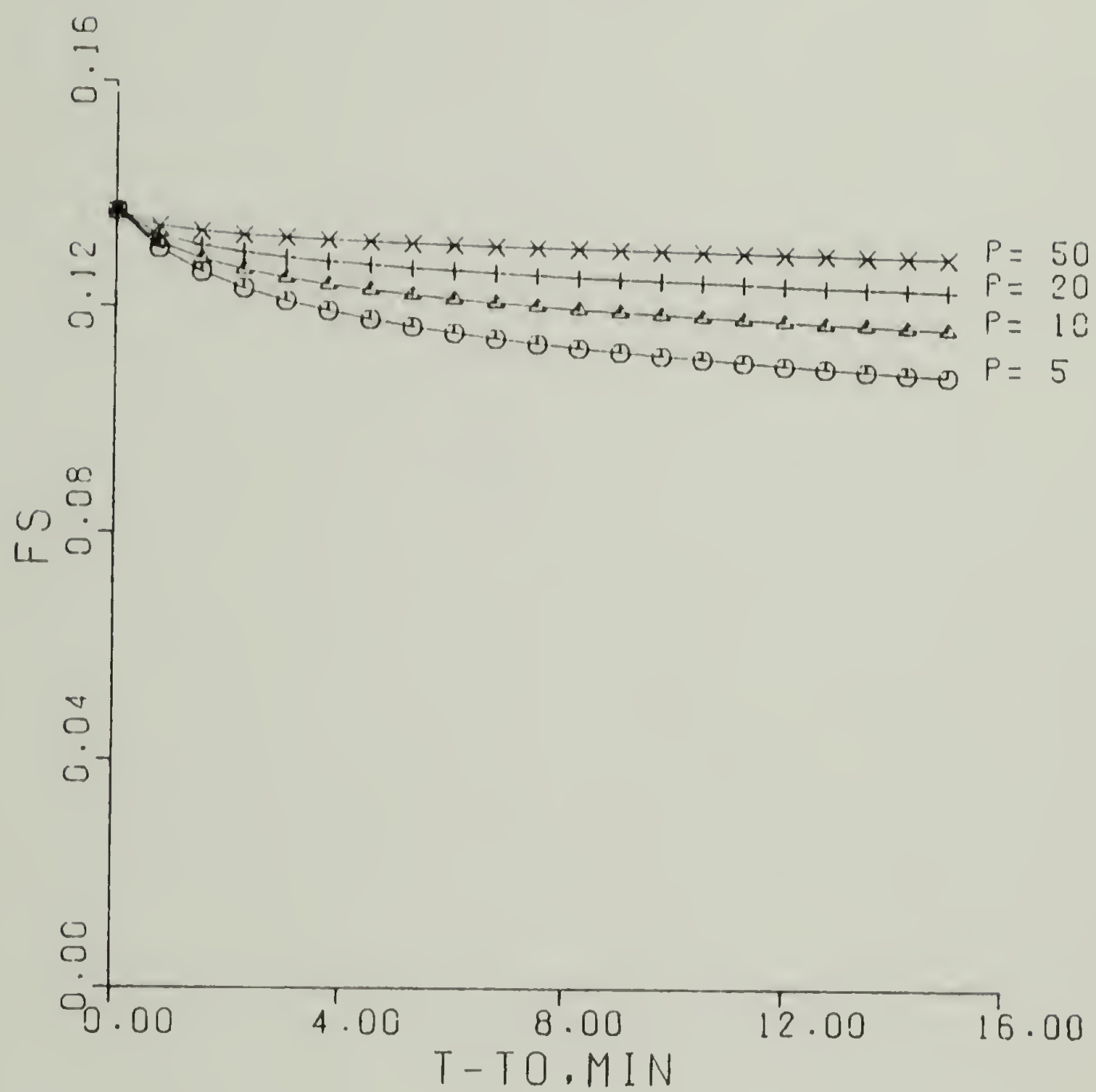


Figure 49. Soft segment orientation function vs. time in stress relaxation at 150% strain, for indicated values of  $p$  (Equation 56).



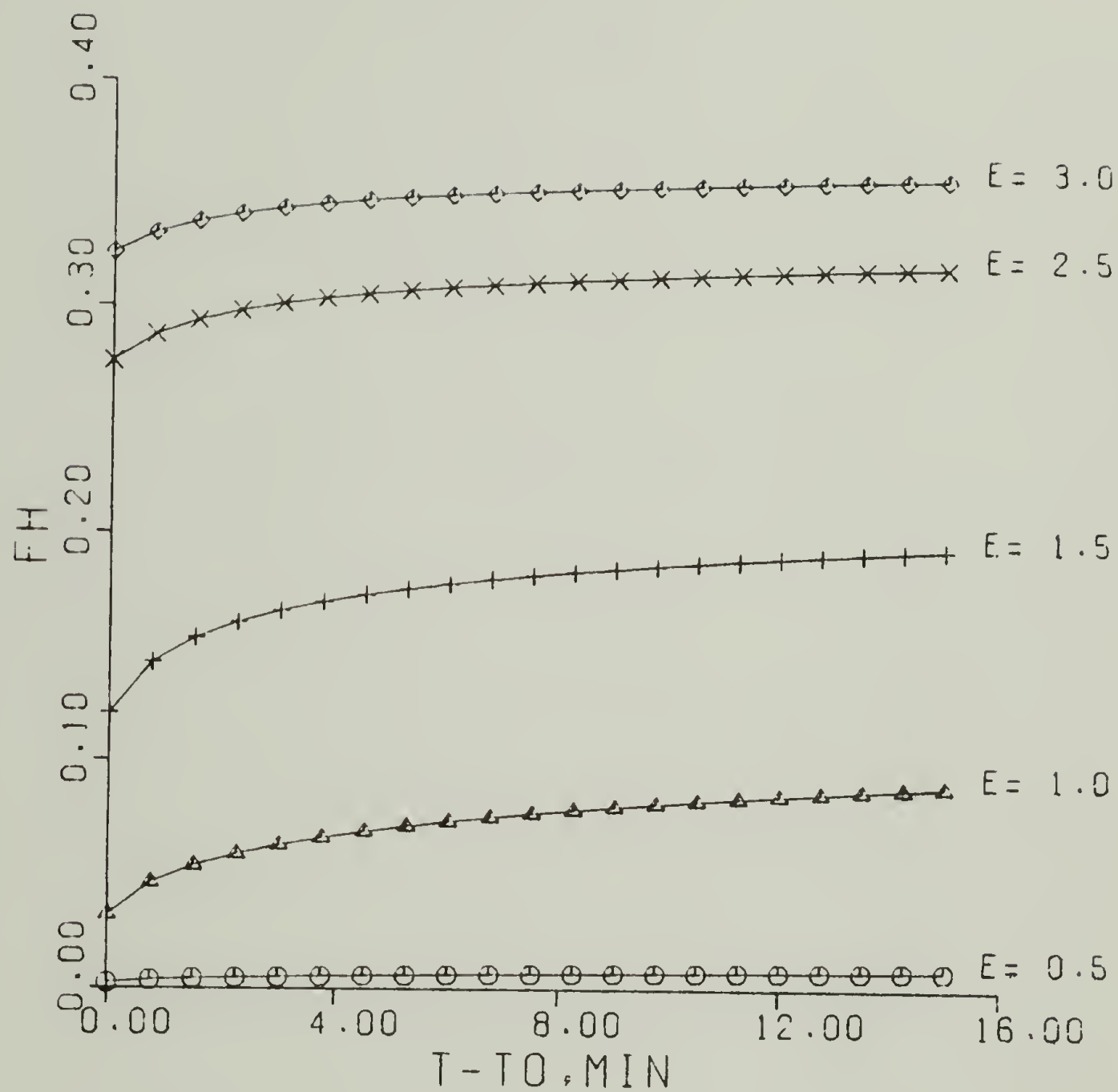


Figure 50. Hard segment orientation function vs. time in stress relaxation at indicated strain levels; prediction of Equation 56 with  $p=10$ .

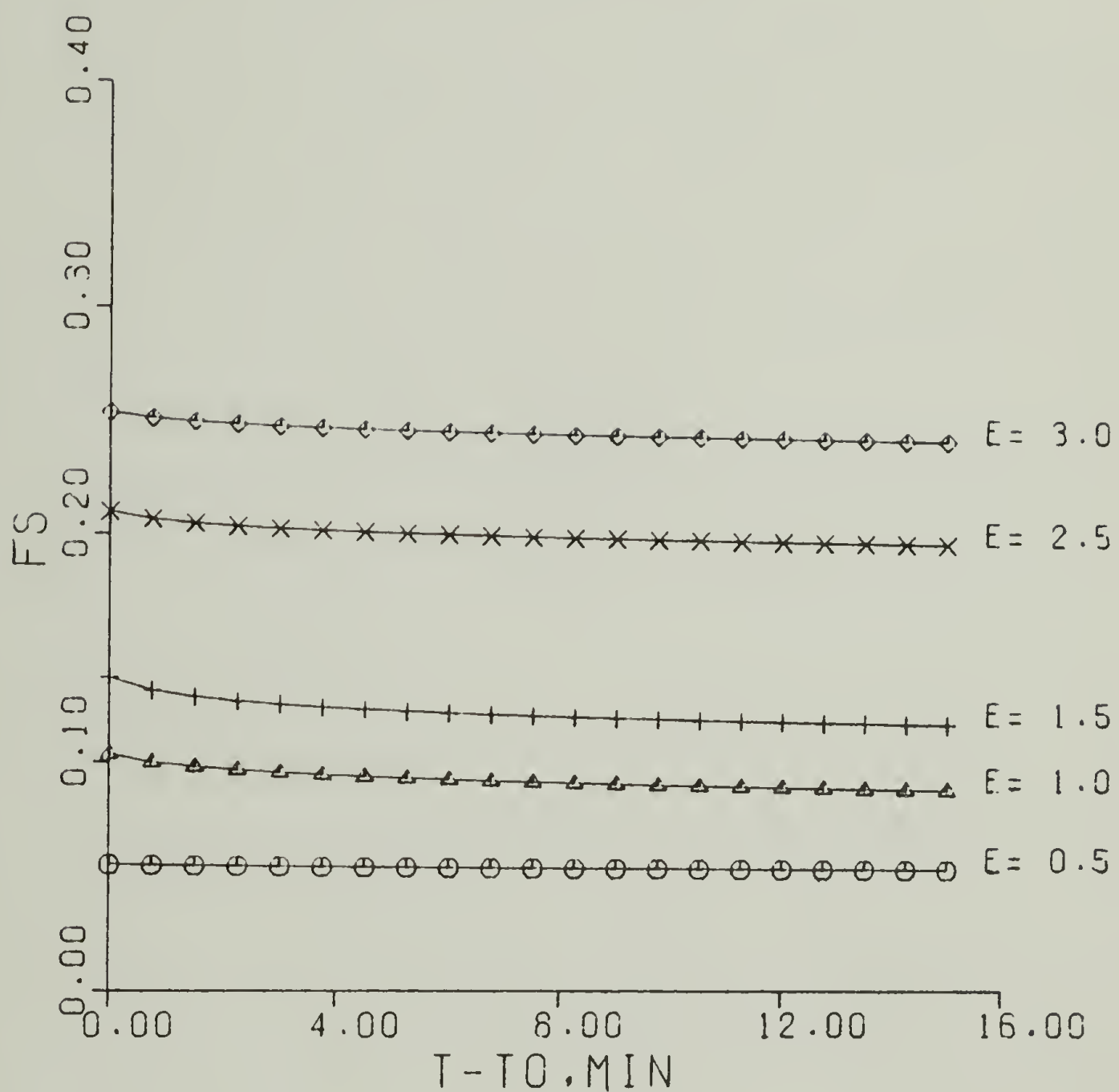


Figure 51. Soft segment orientation function vs. time in stress relaxation at indicated strain levels; prediction of Equation 56 with  $p=10$ .

the case  $p = 10$ , for relaxation step at 150% strain. It is seen that at low strains, before a significant fraction of elements have yielded (see Figure 37), the increase (in the case of  $f_h$ ) in the orientation function during relaxation is not great. At intermediate strain levels there is a rapid increase in orientation, followed by a leveling off of the curve with time, since a substantial fraction of elements are yielding in this region of strain. At higher strain levels, the relative increase in orientation with time diminishes again since most of the elements have yielded.

### III.5. Conclusions and Recommendations

A model for the orientation produced in the two separate domains of polyurethanes has been presented which successfully describes both the observed interaction of the hard and soft domains and the observed time-independent and time-dependent response of orientation to strain history. The morphology of the two domains are shown to be accurately represented by a series model at all levels of strain. The fact that the series model is accurate lends additional proof to the theory that the polyurethane network of hard and soft domains stays together and any restructuring of the network with deformation preserves the original character of the interdomain interactions.

The series model may be tested further by strain-dichroism experiments on polyurethanes for strain histories different from the single example given here. Experiments involving stress-relaxation, creep, and a combination of many different strain rates and steps may

be tried to see if the two domains act in series at all times. More accurate measurements may be taken on the orientation function behavior with a Fourier transform infrared spectrometer equipped with a tensile test unit, and as well this type of apparatus would enable simultaneous measurement of many different IR bands on the same sample.

Compositional changes in the hard and soft segments of polyurethane elastomers are easy to achieve and may be analyzed in the context of the series model. For example, it would be interesting to determine whether the orientation-strain compliance of a given soft segment remained the same when the hard segment content or composition is changed.

Here it must be mentioned that orientation-strain and stress-strain behavior very similar to that of the polyurethanes mentioned here has been seen for other block copolymers, for example the polyether-ester system studied by Lilaonitkul et al. (1976). Their observations add further fuel to the argument that it is the interactions between the two domains of the block copolymers that determine most of their properties, rather than any particular feature of chemical nature, such as the presence of hydrogen bonding sites. This point is also made by consideration that the series model presented requires only that the two domains be intimately connected, as they are by chemical bonding between hard and soft segments in the polymer chain, without specification of the nature of the connection.

It has been shown that the strain response of the hard segment orientation itself could be viewed in terms of a distribution of

yielding hard elements, with the strain history dependence of the yield events contained in Lebesgue norms of the strain in the constitutive relation for orientation. It is seen that the infinite Lebesgue norm provides a suitable measure of the history-dependence of the microstructural changes in the material, while use of the lower order norms provides the correct type of time-dependence needed to describe the orientation function behavior observed in a stress relaxation experiment. Thus all of the observed time dependent memory effects in this polymer may be accounted for by a model of time dependent plasticity of the microstructure, without considering any type of viscous mechanisms. This example of a model for the irreversible microstructural change in polyurethane illustrates the need for different routes of analysis of the mechanical behavior of polymers than that provided by viscoelasticity theory.

There is a paucity of literature data on the orientation response to other strain histories, for example the change in relaxation response of the orientation with varying strain level (Figures 49 and 50), which could be used to further corroborate the theory outlined here. However, the agreement of the theory to the limited data available serves to demonstrate the applicability of Lebesgue norm measures to the description of history-dependent microstructural changes.

It is immediately apparent that whatever changes occur in the microstructure of a polymer as it undergoes deformation will influence the ultimate mechanical properties of the material. In a more precise



sense, if the history of the microstructural changes is known or calculable, then the mechanical properties and mechanical response should be calculable. In this light, the relationship of the orientation function-strain response of the two separate domains in polyurethanes to the stress-strain response will be explored in the next chapter.

## C H A P T E R   I V

### CONSTITUTIVE EQUATIONS FOR STRESS

The development of a constitutive equation for stress for a material such as polyurethane which undergoes microstructural change with deformation must take into account the changing nature of the material as a function of deformation history. As discussed in Chapter II, this approach allows the basic assumptions made in the mathematical idealizations of the mechanical behavior of materials to be examined. For the case of polymers, it was shown that a fading memory viscoelastic relation for stress is particularly inappropriate if the material behavior shows strong dependence on maximums in the deformation history.

The permanent memory of past strain states may be described by consideration of the state of microstructural change in the material, as shown first by Farris (1970, 1973). He introduced a model of strain-induced damage which led to a constitutive equation for stress that included the Lebesgue norm of the strain as the measure of strain history that contained the permanent memory behavior of the material. Quinlan and Fitzgerald (1973) gave the essential result that the general stress functional for a material with memory suggested by Volterra, i.e.,

$$(57) \quad \underline{S}(t) = G \left[ \int_{\xi=0}^{\xi=t} \underline{E}(t, \xi) d\xi \right]$$

may be specialized by considering a measure of microstructural change, the damage  $\underline{D}$ , in the constitutive relation:

$$(58) \quad \underline{S}(t) = G \int_{\xi=0}^{\xi=t} [\underline{E}(t,\xi), \underline{D}(t,\xi)]$$

In the previous chapter it was demonstrated that the orientation function of the hard chain segment of polyurethane elastomers is irreversible and contains permanent memory of past deformation states which may be described through use of the Lebesgue norm measures suggested by Farris. In this chapter the concept that the orientation function of the hard segments may serve as a measure of damage in the material in the sense of the Quinlan and Fitzgerald Equation (58) will be explored in order to obtain a specialization of (58) for the polyurethane system.

#### IV.1. Stress as a Function of Strain and Orientation

The degree of orientation in polymers is known to have a tremendous effect on the mechanical properties, as is seen in the excellent tensile strength of highly oriented fibers of polyamides and polyesters. Attempts to compute mechanical properties from the state of orientation have been made; a good example of this is seen in the work of Seferis et al. (1976, 1977), who calculated dynamic and static moduli of polypropylene sheet based on its state of bi-axial orientation. There are few examples, however, of theories to

predict mechanical behavior in terms of orientation in the polymer.

An example of the use of orientation in polymers to describe the stress in the material has been developed by Hsiao (1959, 1971) and Hsiao and Moghe (1971). Hsiao attempted to bridge the gap between continuum mechanics and molecular models by developing failure criteria and constitutive equations for materials exhibiting molecular orientation with deformation. He analyzed a system of randomly oriented elements embedded in an arbitrary domain (very similar to Kratky's (1933) model) to produce a stress-strain equation for a point in the body:

$$(59) \quad \sigma_{ij}(e,t) = \int \rho(\theta,\phi,e)f(\theta,\phi,t)\psi(\theta,\phi,t) s_i s_j d\Omega$$

where  $\rho$  is a density of probability distribution function of orientation,  $f$  is the fraction of unbroken elements at time  $t$ ,  $\psi$  is the local stress acting on a group of parallel elements,  $s_i$ ,  $s_j$  are unit vectors and  $d\Omega$  is the infinitesimal solid angle of integration containing the parallel elements. Failure times were calculated using (59) and a reaction rate model for  $f$ . In this respect the approach is similar to Farris's (1971), who used a cumulative damage model instead of a reaction rate model for element failure. The orientation function  $\rho$  is derived by assuming deformation of a sphere of linear elements to an ellipsoid. Therefore, no time or history dependence is introduced into (59) by the expression for  $\rho$ . Rather, time dependent failure and mechanical response is achieved by the reaction rate equation for  $f$  and assumption of a Voigt model for  $\psi$ . In later work Hsiao (1971) uses

equation (59) to show how general stress-strain curves for polymers may be obtained, but he does not pursue the relationship of  $\rho$  to orientation-strain data for specific polymers.

For the specific case of polyurethanes, it is contended that the orientation function of the hard segments serves as a measure of the microstructural change in the material as it undergoes deformation. This contention is supported mainly by the results of the previous chapter in which it was demonstrated that the orientation functions of the hard and soft segments were simply related to the relative strain in the hard and soft domains of the polyurethane. The idea immediately presents itself that the stress in the polyurethane will depend not only on the state of total sample strain but also on the relative strains, or equivalently the orientations, in the two domains of the polymers. Since the hard and soft domain orientation functions may be related to each other by the series model (Equation 47), only one of these two functions is needed as a new parameter in the constitutive equation.

The Quinlan and Fitzgerald Equation (58) may therefore be applied to yield a constitutive equation for stress for polyurethanes of the form

$$(60) \quad \underline{S}(t) = G \int_{\xi=0}^{\xi=t} \underline{E}(t-\xi), \underline{f}(t-\xi) d\xi$$

where  $\underline{f}$  is the orientation function tensor of either domain.

The stress-strain-orientation data of Cooper on ET-38 may be



examined to discover the particular form of (60) for the case of simple tension. The stress-strain response corresponding to the strain history given in Figure 21 is shown in Figure 52. The orientation function for the hard segments in the polymer during the same deformation history is given in Figure 22. The hard segment orientation function will be chosen to represent  $\underline{f}$  in equation (60) since the soft segment orientation function is calculated from the CH stretching IR absorption band, and approximately 16% error is introduced because the hard segments also contain this group.

A simple form of Equation (60) is derived for the case of simple tension by assuming that the stress depends only on a second order polynomial expansion of the current values of  $\underline{E}$  and  $\underline{f}$ :

$$(61) \quad S = AE + Bf_h + CEf_h$$

where A, B, and C are material constants, S is the tensile true stress, E is the strain, and  $f_h$  is the orientation function of the hard domains. Since polyurethanes are capable of large deformations, a suitable finite strain measure is needed in Equation (61): the particular measure found to be suitable was derived from the neo-Hookean, or ideal rubber, constitutive equation, to yield:

$$(62) \quad E \equiv \left( \lambda - \frac{1}{\lambda^2} \right)$$

where  $\lambda$  is the extension ratio. Using (62), the true stress is given by

$$(63) \quad S\lambda = \left( \lambda^2 - \frac{1}{\lambda} \right) (A + Cf_h) + Bf_h\lambda$$

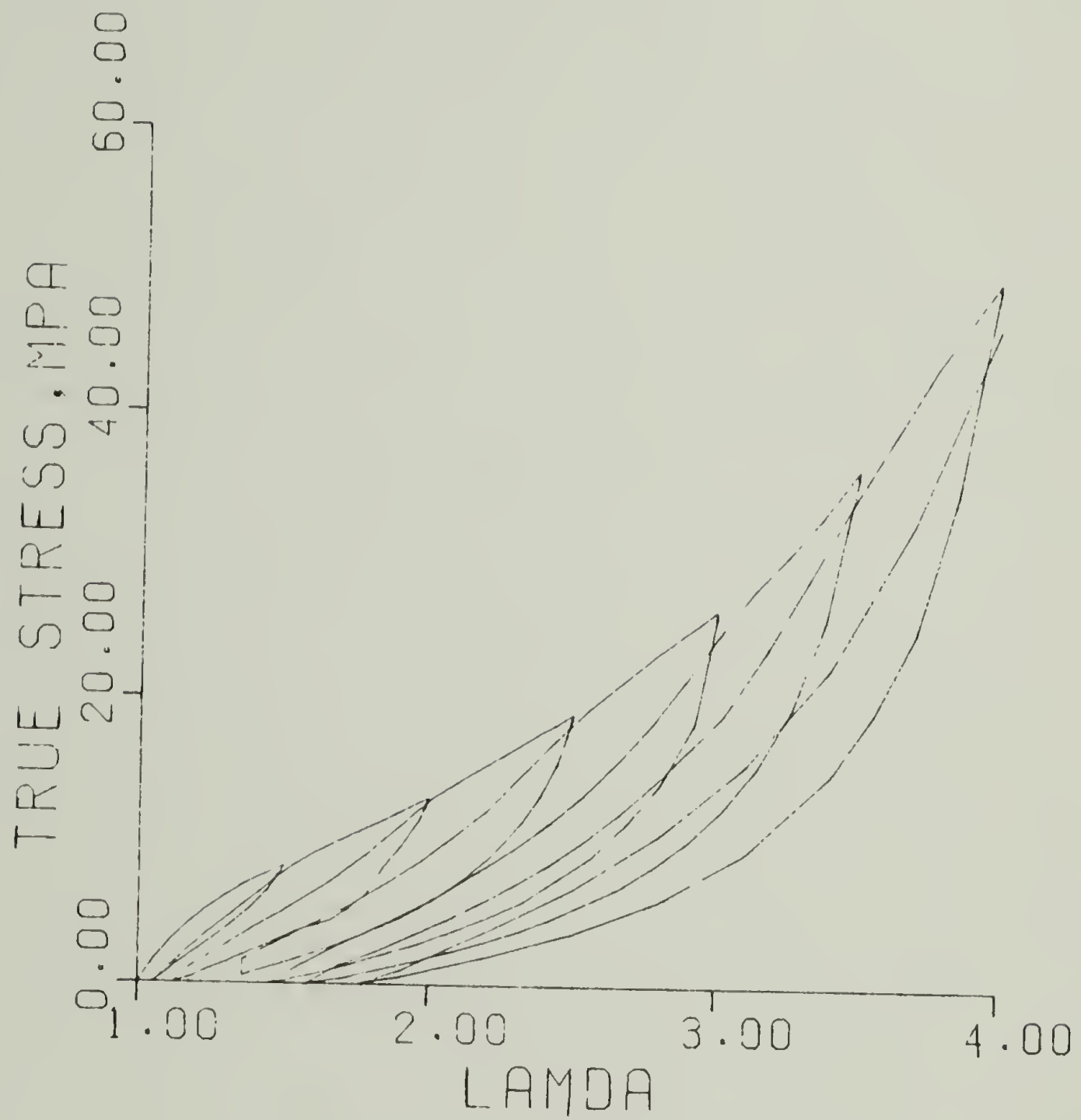


Figure 52. Stress-strain response of ET-38 corresponding to the strain history in Figure 21 and the orientation functions in Figures 22, 23, and 24.

The data indicated in Figures 22 and 52 were analyzed using the non-linear regression scheme discussed in Appendix E. The constants in Equation (63) were determined to be:

$$A = 48 \pm 1$$

$$B = 54 \pm 4$$

$$C = -426 \pm 17$$

The stress predicted by Equation (63) with these constants is plotted with the corresponding data from Figure 52 in Figure 53. In this figure, the output corresponding to the unloading or negative strain rate portions of the strain history is omitted for clarity. The agreement of Equation (63) with the data demonstrates that all of the hysteresis in the polyurethane may be accounted for by knowledge of the level of orientation in the hard domains. The result given in Equation (63) thus quantifies and supports the qualitative contention of Estes et al. (1971) and others that the hysteresis in the stress-strain curve is due to the orientation in the two separate domains of polyurethanes.

Further, in Chapter III a relationship for  $f_h$  in terms of current strain and strain history was developed from a model of the polyurethane microstructure. The result given there in Equations (55) and (56) may be abbreviated as

$$(64) \quad f_h = F[\epsilon(t), \|\epsilon(t)\|_p]$$

and is essentially the characterization of the Quinlan and Fitzgerald damage functional indicated by Equation (26).

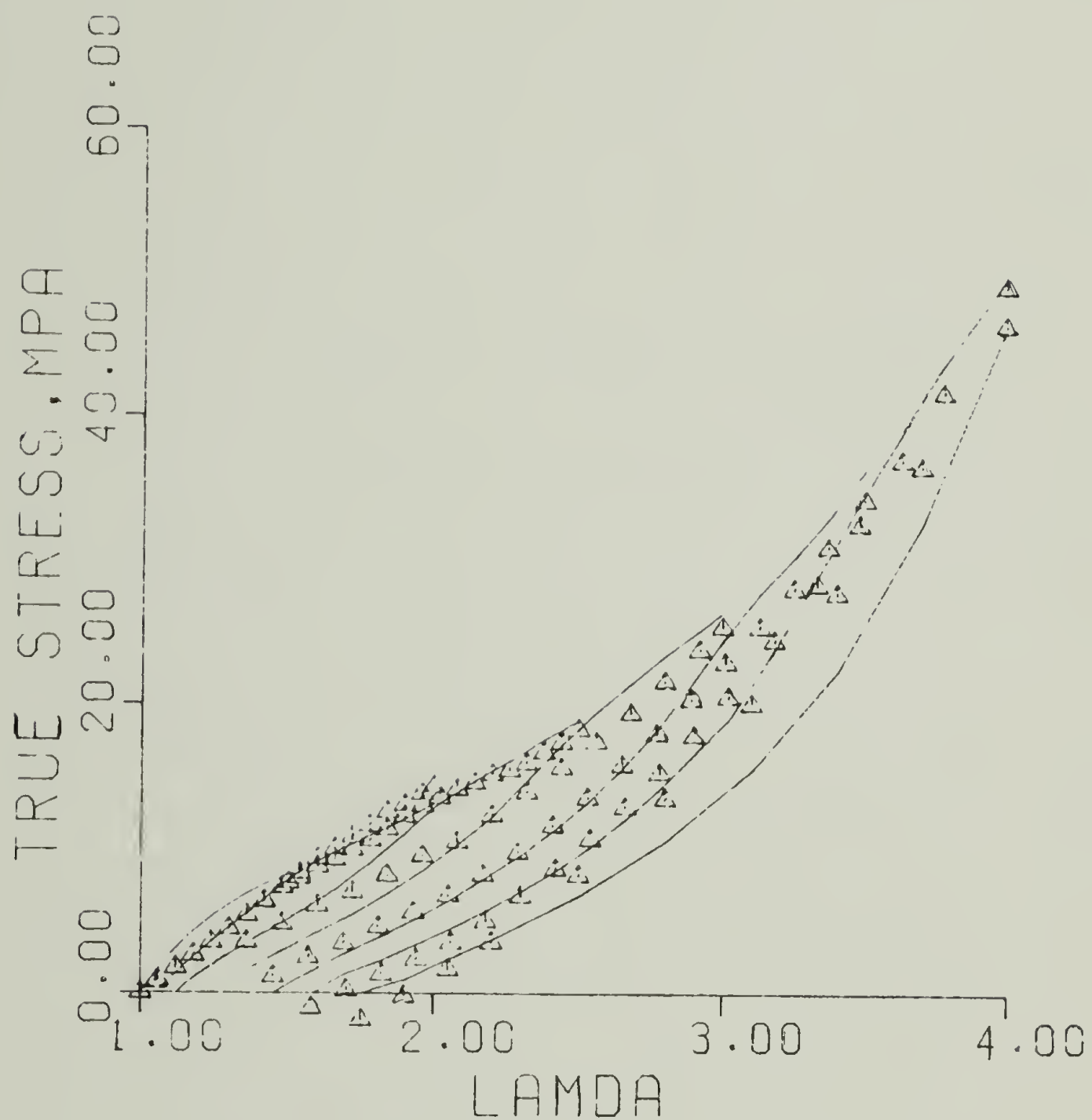


Figure 53. Stress predicted by Equation (63) of text (points) compared to data of Figure 52 (curves). The unloading or negative strain rate portion of the data is omitted.

If Equation (55) is used in (63), the result is an equation for the stress in terms of strain history and current strain and the result is plotted in Figure 54. In this figure the curve is the prediction given by Equation (63) if  $f_h$  is given by Equation (55). The points are the data from Figure 52, and again the negative strain rate data are omitted. The constants used for Equation (55) are the ones determined from the analysis of the  $f_h$  vs. strain data.

The agreement of theory to data in Figure 54 demonstrates that in principle, if the state of orientation of the hard domains can be determined or idealized in terms of strain history, then the stress may be predicted by simple equations like (63). Further corroboration of the ideas presented in this section must await more detailed simultaneous information on the stress, strain, and orientation in this system.

The various polyurethane elastomers mentioned in Chapters II and III have different chemical compositions (see Appendix A) but possess the basic physical similarity of being copolymers of alternating hard and soft chain segments. By comparison of the general features in the different polyurethane tensile stress-strain curves (e.g., Figures 8 and 52), it may be concluded that the permanent memory features and hysteresis are due largely to irreversible changes in the orientation of the two chain segments. The approach to developing constitute equations for stress for any polyurethane would then logically proceed by characterizing the orientations. In the absence of this information, however, it is possible to use the more general



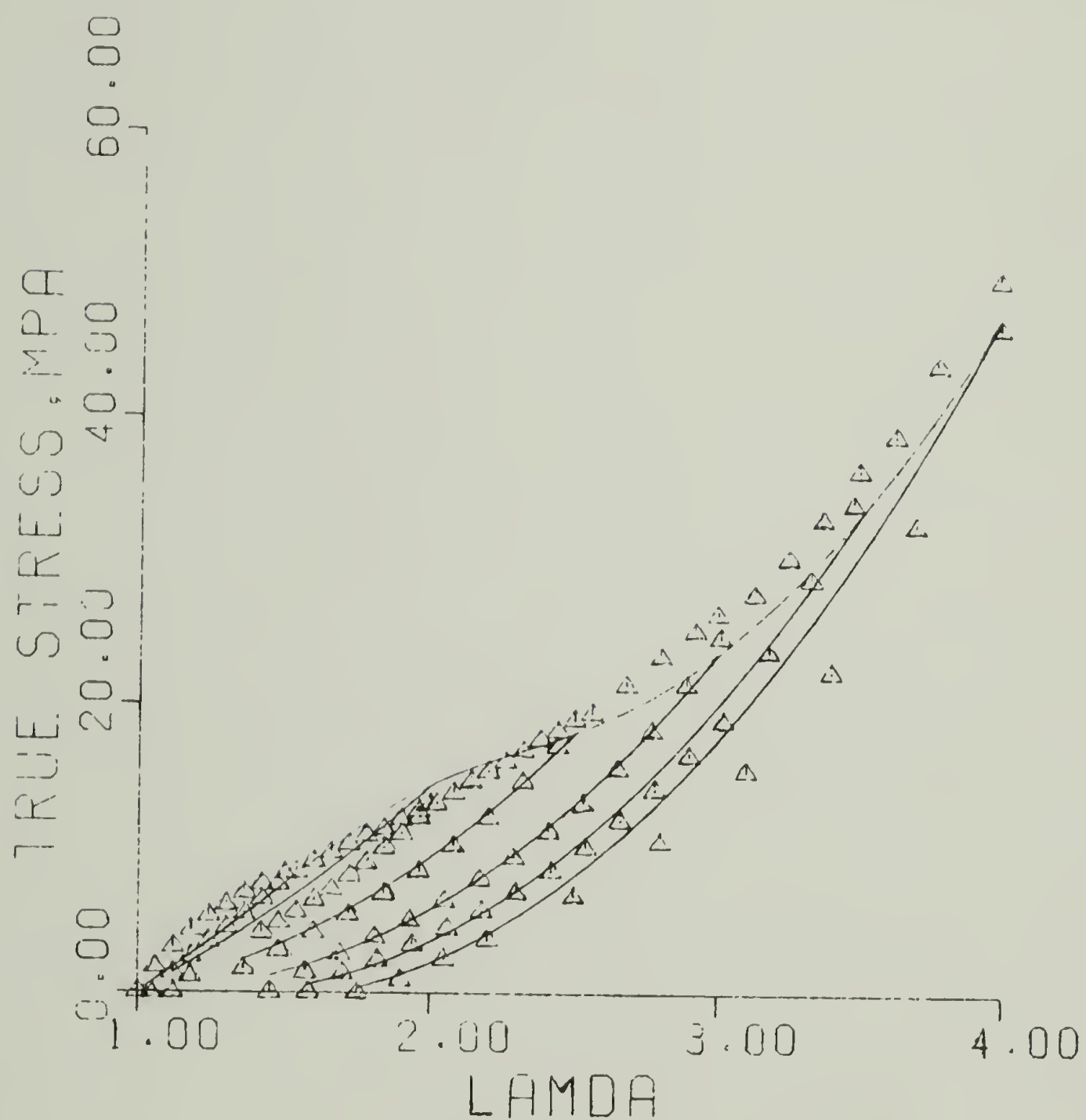


Figure 54. Stress response predicted by Equations (55) and (63) of text (curve). Points are data from Figure 52.

result that permanent memory of past strain states can be contained by Lebesgue norms of the strain. Essentially, then, it is possible to consider that since the orientation function will be some function of strain and the norms of the strain (Equation 64), then the stress will also have this dependence by virtue of Equation (60), i.e.,

$$(65) \quad \underline{S}(t) = G\left\{\left[\int_{\xi=0}^{\xi=t} \underline{E}(t-\xi) d\xi\right], \|\underline{E}\|_{p_1}, \|\underline{E}\|_{p_2}, \dots\right\}$$

The next section will discuss applications of (65) to specific polymers.

#### IV.2. Material Characterization

The development of a constitutive equation for stress for a nonlinear material with memory like polyurethane which will correctly predict the response to any arbitrary strain history over a large range of strains is a formidable task. What will be demonstrated in this section is that modification of nonlinear elastic equations by permanent memory and fading memory measures is a step toward meeting this goal for several polyurethane elastomers.

The first example will be du Pont's Lycra 2240 fiber (see Appendix A). The tensile stress-strain response for this material is given in Figure 55. A nonlinear elastic equation that suitably describes this behavior may be derived from the following general elastic constitutive equation:

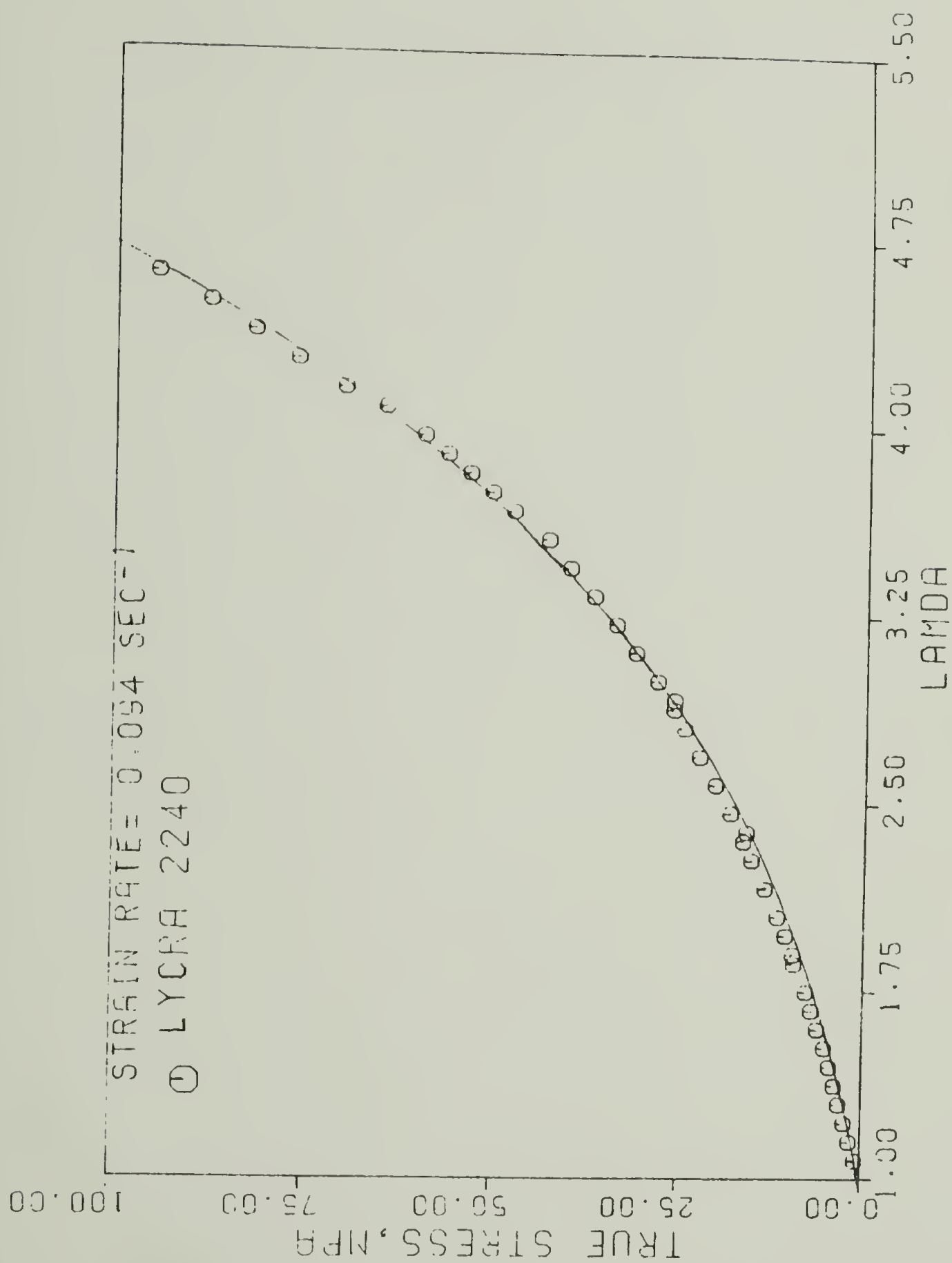


Figure 55. Stress-strain response of Lycra 2240 in simple tension. Points are experimental data; curve is prediction of Equation (70) of text.

$$(66) \quad \underline{S} = \psi_0 \underline{I} + \psi_1 \underline{E} + \psi_2 \underline{E}^2$$

where  $\underline{S}$  is the true stress,  $\underline{E}$  is the strain,  $\underline{I}$  is the unit tensor, and  $\psi_0$ ,  $\psi_1$ , and  $\psi_2$  are material functions of the three strain invariants. For simple tension, the tensile stress,  $S_{11}$ , can be calculated from (66) by subtracting the  $S_{22}$  component, which is zero:

$$(67) \quad S_{11} - S_{22} = S_{11} = \psi_1 (E_{11} - E_{22}) + \psi_2 (E_{11}^2 - E_{22}^2)$$

If  $\underline{E}$  is taken to be the Lagrangian strain, then in terms of the principle extension ratios  $\lambda_1$  and  $\lambda_2$ , Equation (67) becomes

$$(68) \quad S_{11} = \frac{\psi_1}{2} (\lambda_1^2 - \lambda_2^2) + \frac{\psi_2}{4} [(\lambda_1^2 - 1)^2 - (\lambda_2^2 - 1)^2]$$

Applying the incompressibility condition ( $\lambda_2^2 = 1/\lambda_1$ ) gives the result

$$(69) \quad S_{11} = \frac{\psi_1}{2} (\lambda_1^2 - \frac{1}{\lambda_1}) + \frac{\psi_2}{4} [\lambda_1^4 - 2\lambda_1^2 - \frac{1}{\lambda_1^2} + \frac{2}{\lambda_1}]$$

or equivalently

$$(70) \quad S_{11} = (\lambda^2 - \frac{1}{\lambda}) [C_1 + C_2(\lambda^2 - 2 + \frac{1}{\lambda})] = F(\lambda)$$

where  $\lambda$  is the extension ratio in the stretching direction, and  $\psi_1$  and  $\psi_2$  are taken as constants. Equation (70) is plotted with the data in Figure 55, with  $C_1 = 2.54$  and  $C_2 = .099$ .

Lycra 2240 also exhibit stress relaxation, which by virtue of the above discussion on time-dependent orientation of the hard domains in polyurethanes, may be described solely through  $L_p$  norm measures.

Using the ideas of Farris (1970, 1973), the elastic equation (70) may be modified by a term containing the ratio of the strain to the  $L_p$  norm of the strain, i.e.,

$$(71) \quad S_{11} = F(\lambda) \left( 1 + \left[ \frac{(\lambda-1)}{\|\lambda-1\|_p} \right]^n \right)$$

where  $p$  is the order of the Lebesgue norm and  $n$  is a material constant. The order of the norm in (71) may be determined by analysis of stress relaxation data (see Appendix H for the appropriate analytical expression for the norm measure). Equation (71) for the case  $p = 34$  is plotted in Figure 56 along with stress relaxation data at nominal strain of  $\lambda = 3.5$ . This simple analysis then allows fairly accurate prediction of the stress response to a multiple ramp input such as the one given in Figure 21, as shown in Figure 57.

The Estane polyurethane, ES5701, described in detail in Chapter II, represents a material with even more complex mechanical behavior. The simple tensile data may be fit with an extension of the Mooney-Rivlin equation due to Tschoegl (1971):

$$(72) \quad S = 2\left(\lambda^2 - \frac{1}{\lambda}\right) (C_1 + C_2/\lambda + C_3 F_{22}) = G(\lambda)$$

where  $S$  is the stress,  $\lambda$  is the extension ratio;  $C_1$ ,  $C_2$ , and  $C_3$  are material constants, and  $F_{22}$  is defined as

$$(73) \quad F_{22} = 6(\lambda - 1)^6 (1 + 2/\lambda) (2 + 1/\lambda) (1 + 1/\lambda) \lambda^{-2}$$

The tensile test data on ES5701 is plotted in Figure 58 along with



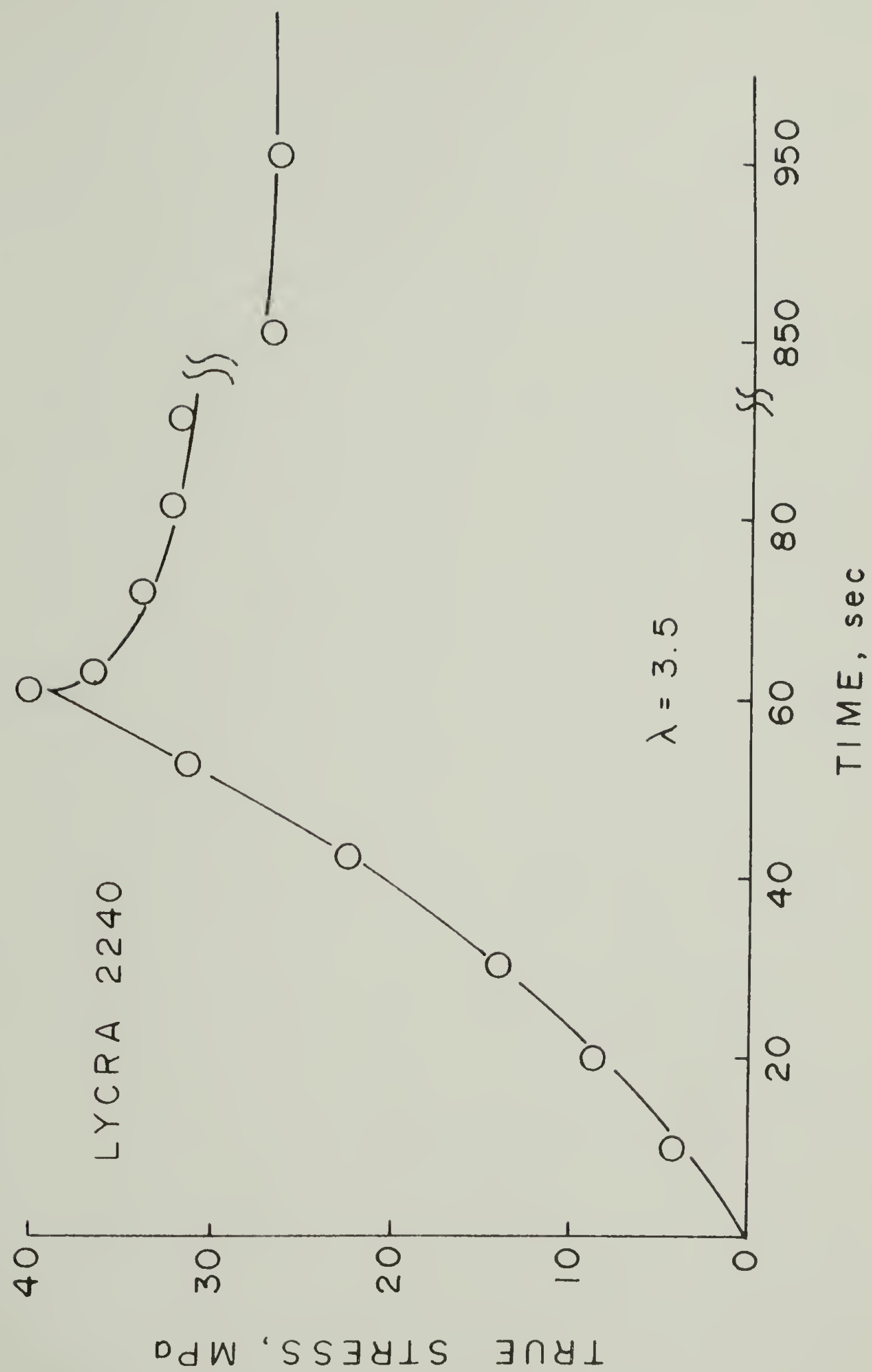


Figure 56. Stress relaxation of Lycra 2240 at extension ratio of 3.5. Points are experimental data; curve is Equation (71) of text.

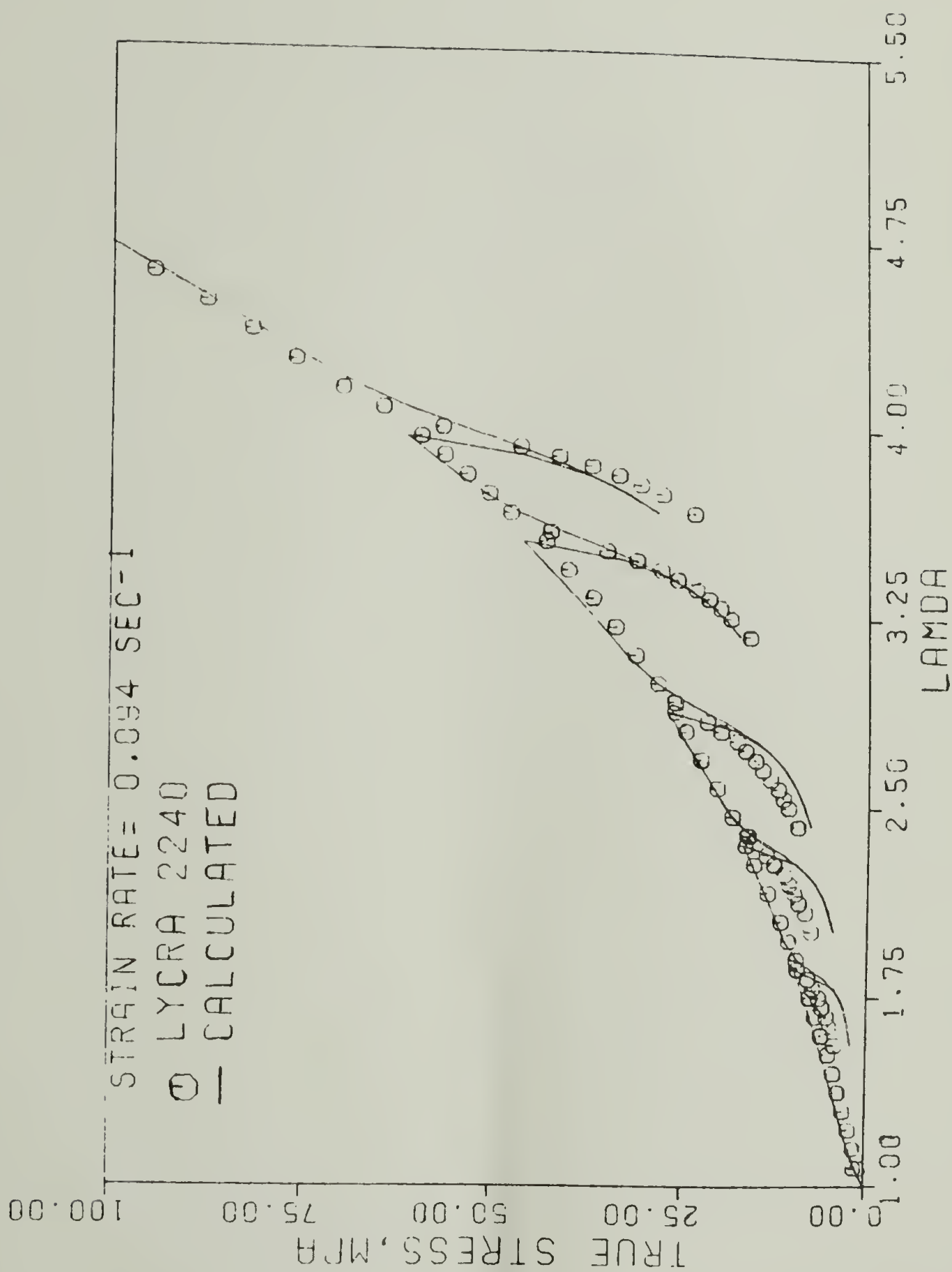


Figure 57. Stress response of Lycra 2240 for strain history similar to Figure 21. Points are experimental data; curve is prediction of Equation (71) of text.

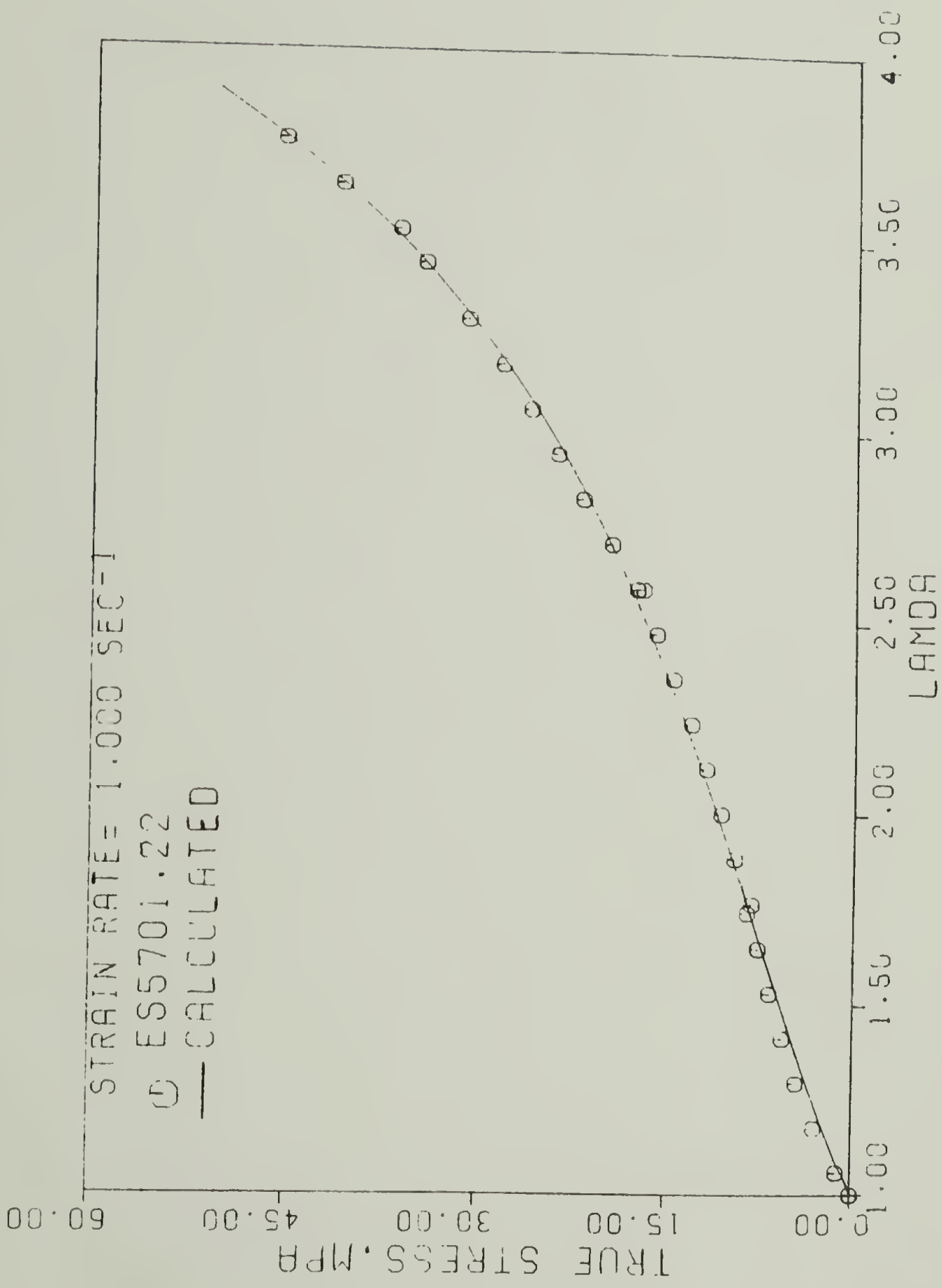


Figure 58. Stress-strain response of ES5701 in simple tension. Points are experimental data; curve is prediction of Equation (72) of text.

Equation (72), with  $C_1 = 1.48$ ,  $C_2 = 3.31$ ,  $C_3 = .00108$ .

The  $L_p$  norm term in Equation (71) is not able to describe the difference in the unloading and reloading curves seen in Figure 8. The strain history for this plot is similar to the one in Figure 21 except that each cycle returns to zero stress. For ES5701 it is also necessary to consider that some part of the mechanical response may have fading memory character as well as permanent memory character. This combination of memory effects was shown to be true of the filled propellants treated by Farris (1970).

By combining a permanent memory term similar to Equation (71) with a fading memory - permanent memory term, the following equation results:

$$(74) \quad S = G(\lambda) \left( C_4 + \left[ \frac{\lambda-1}{\|\lambda-1\|_\infty} \right]^{n_1} \right) + C_5 \left( 1 - \left[ \frac{\lambda-1}{\|\lambda-1\|_p} \right]^{n_2} \right) \int_0^t (t-\tau)^{n_3} \frac{d(\lambda-1)}{d\tau} d\tau$$

where  $n_1$ ,  $n_2$ ,  $n_3$ ,  $C_4$ ,  $C_5$  and  $p$  are material constants. The analytical expressions for the fading memory integral term for this strain history are given in Appendix I. Equation (74) is plotted in Figure 59 along with the tensile test data on Figure 8, for  $C_4 = .2$ ,  $C_5 = 16.3$ ,  $n_1 = 13$ ,  $n_2 = 10$ ,  $n_3 = -.3$ ,  $p = 8$ . It is seen that the addition of the fading memory term can account for most of the difference between the unloading and reloading portions of the curve, while the norm terms preserve the maximum strain points.

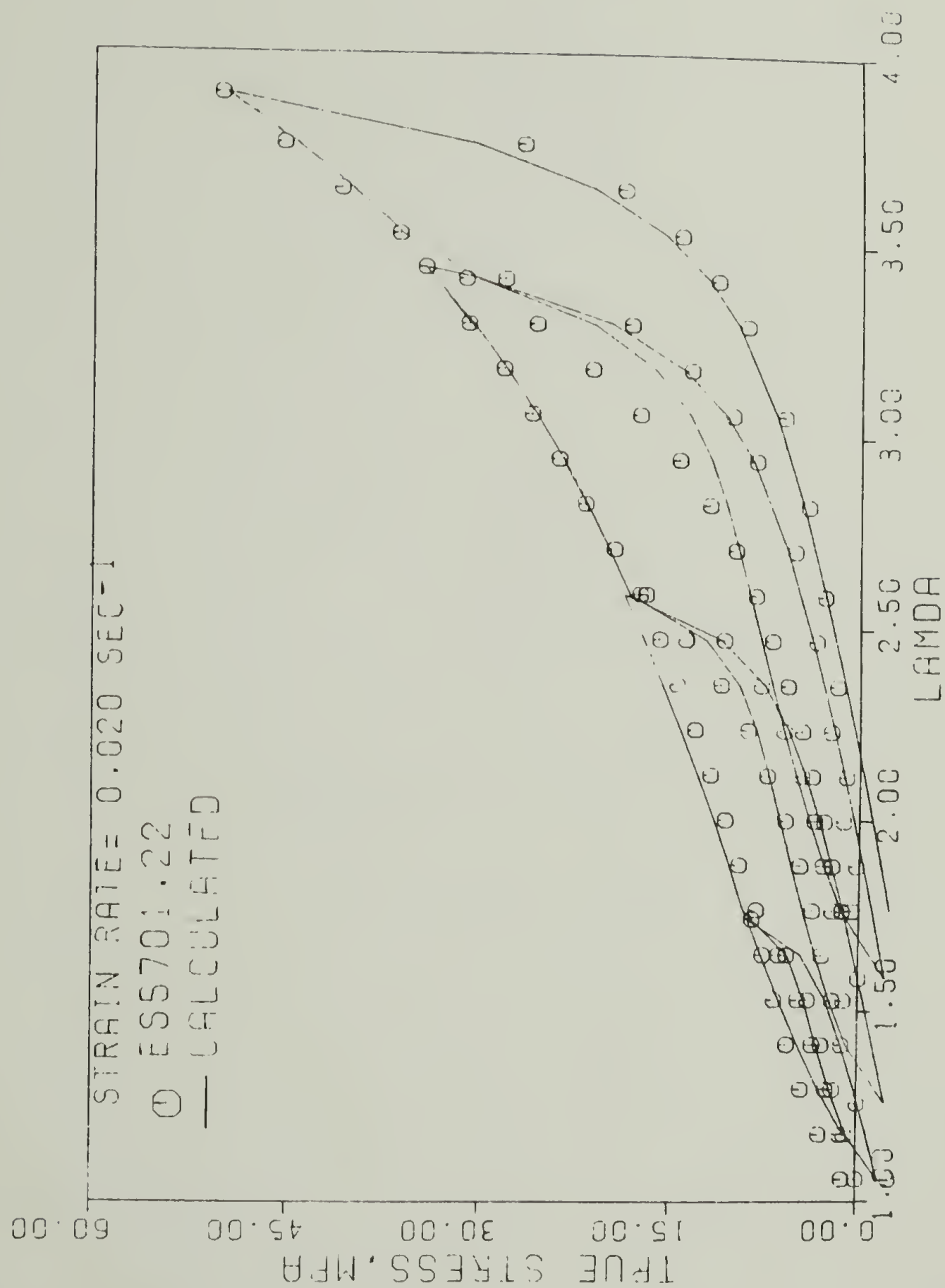


Figure 59. Stress response of ES5701 to strain history similar to Figure 21. Points are experimental data; curve is prediction of Equation (74) of text.



The two limited examples of constitutive equations presented here are meant only to illustrate the complexity of polyurethane mechanical behavior and the corresponding complexity needed in their nonlinear constitutive equations for stress. By a purely continuum mechanical approach, approximations to (65) may be made with an eye to practical application, since it is obvious that the Lebesgue norm measures are needed to describe permanent memory phenomena accurately.

#### IV.3. Conclusions and Recommendations

It has been demonstrated that the problem of determining a constitutive relation for stress for polyurethanes may be separated into two problems, one of determining the constitutive equation for the orientation as a measure of microstructural change in the material and one of determining the constitutive equation for stress in terms of the strain and orientation history. For the limited data available it is seen that the stress depends only on the current state of strain and orientation, with the orientation measure itself containing all of the material's memory of past deformation states. This result is somewhat surprising in that if the polymer behavior is approached from the "black box" point of view of a simple material with memory, some very complex history-dependent expressions is the strain result as shown in the last section. Thus the conclusion may be drawn that the state of stress in a body which undergoes changes in microstructure with deformation may be described simply by introduction of a new internal parameter of the material which contains the history dependence

of the microstructural change in question.

The example given here of orientation as a measure of microstructural change is the first known case in which quantitative information on such an internal parameter was related to the stress state. As stated before, the damage model developed by Farris and generalized by Quinlan and Fitzgerald contained the internal damage parameter which was unable to be determined experimentally. The results given here demonstrate, then, that material response to deformation is predictable on a quantitative basis through knowledge of the microstructural reaction to deformation. Changing the orientation behavior of the hard segments in polyurethanes would therefore be expected to change the material's hysteresis, stress softening, and permanent set under known deformation histories.

Future work on polyurethanes and other polymers is recommended to corroborate and extend the results presented here. Particular studies that may be undertaken include:

1. For polyurethanes, detailed IR work on polymers with varying formulations under a variety of strain histories to check the applicability of the series model and the orientation function-strain model given in Chapter III is suggested. Simultaneous measurement of stress and orientation would allow the predictions of equations like (61) to be checked.
2. For other polymer systems, extensions of the meaning of Quinlan and Fitzgerald damage tensor to include other microstructural changes such as cavitation and crystallization may

be made, and the stress in the material then could be calculated by discovering the dependence of the stress functional on the state of change in the microstructure.

Finally, it will be emphasized again that use of a purely continuum mechanic approach to the development of constitutive equations can be fruitful if the assumptions that the theory is based on are accurate for the system under study. For polymers, the easiest and most direct way of insuring the assumptions are correct is by considering the microstructure and morphology of the material in question. In that way errors such as application of the fading memory viscoelastic theory to non-fading memory materials will be avoided.

## REFERENCES

- Askan, S. and Zurek, W. (1975), "A Rheological Model of Viscose Rayon," J. Appl. Polym. Sci. 19, 3129.
- Bernstein, B., Kearsley, A., and Zapas, L.J. (1963), "A Study of Stress Relaxation with Finite Strain," Trans. Soc. Rheol. 7, 391.
- Bonart, R. (1968), "X-ray Investigations Concerning the Physical Structure of Cross-Linking in Segmented Urethane Elastomers," J. Macromol. Sci. Phys. B2, 115.
- Bonart, R., Morbitzer, L. and Hentze, G. (1969), "X-ray Investigations Concerning the Physical Structure of Cross-Linking in Urethane Elastomers. II. Butanediol as Chain Extender." J. Macromol. Sci. Phys. B3, 337.
- Bonart, R. and Müller, E.H. (1974), "Phase Separation in Urethane Elastomers as Judged by Low Angle X-ray Scattering. II. Experimental Results," J. Macromol. Sci. Phys. B10, 345.
- Brereton, M.G., Croll, S.G., Duckett, R.A., and Ward, I.M. (1974), "Nonlinear Viscoelastic Behavior of Polymers: An Implicit Equation Approach," J. Mech. Phys. Solids 22, 97.
- Brereton, M.G., Duckett, R.A., Joseph, S.H., and Spence, P.J. (1976), "An Interpretation of the Yield Behavior of Polymers in Terms of Correlated Motion," J. Mech. Phys. Solids 25, 127.
- Bueche, F. (1960), "Molecular Basis for the Mullins' Effect," J. Appl. Polym. Sci. 4, 107.
- Chang, W.V., Bloch, R., and Tschoegl, N.W. (1976), "On The Theory of the Viscoelastic Behavior of Soft Polymers in Moderately Large Deformations," Rheol. Acta 15, 367.
- Christensen, R.M., and Naghdi, P.M. (1966), "Linear Non-Isothermal Viscoelastic Solids," Acta Mech. 3, 1.
- Chu, B.M. and Blatz, P.J. (1972), "Cumulative Microdamage Model to Describe the Hysteresis of Living Tissue," Ann. Biomed. Eng. 1, 204.



- Clough, S.B. and Schneider, N.S. (1968), "Structural Studies on Urethane Elastomers," J. Macromol. Sci. Phys. B2, 553.
- Clough, S.B., Schneider, N.S., and King, A.O. (1968), "Small Angle X-ray Scattering from Polyurethane Elastomers," J. Macromol. Sci. Phys. B2, 641.
- Coleman, B.D. and Mizel, V.J. (1966), "Norms and Semi-Groups in the Theory of Fading Memory," Arch. Rat. Mech. Anal. 23, 87.
- Coleman, B.D. and Mizel, V.J. (1968), "On The General Theory of Fading Memory," Arch. Rat. Mech. Anal. 29, 18.
- Coleman, B.D. and Noll, W. (1960), "An Approximation Theorem for Functionals, with Applications in Continuum Mechanics," Arch. Rat. Mech. Anal. 6, 355.
- Coleman, B.D. and Noll, W. (1961), "Foundations of Linear Viscoelasticity," Rev. Mod. Phys. 33, 239.
- Davis, W.M. and Macosko, C.W. (1978), "Nonlinear Dynamic Mechanical Moduli for Polycarbonate and PMMA," J. Rheol. 22, 53.
- deHoff, P.H., Lianis, G., and Goldberg, W. (1966), "An Experimental Program for Finite Linear Viscoelasticity," Trans. Soc. Rheol. 10, 385.
- Devries, K.L. and Farris, R.J. (1970), "Strain Inhomogeneities, Molecular Chain Scission, and Stress-Deformation in Polymers," Int. J. Fract. Mech. 6, 411.
- Dong, R.G. (1964), "Constitutive Equations Involving Chronological Variables," Univ. of California Lawrence Radiation Laboratory, Report UCRL-12228.
- Eringen, A.C. (1962), Nonlinear Theory of Continuous Media, McGraw-Hill, New York, 144-154.
- Eringen, A.C. (1967), Mechanics of Continua, Wiley, New York, 153-155.
- Estes, G.M., Cooper, S.L. and Tobolsky, A.V. (1970), "Block Polymers and Related Heterophase Elastomers," J. Macromol. Sci. Rev. Macro. Chem. C4, 313.
- Estes, G.M., Seymour, R.W., Huh, D.S. and Cooper, S.L. (1969), "Mechanical and Optical Properties of Block Polymers. I. Polyester-Urethanes," Polym. Eng. Sci. 9, 383.



- Estes, G.M., Seymour, R.W., and Cooper, S.L. (1971), "Infrared Studies of Segmented Polyurethane Elastomers. II. Infrared Dichroism," *Macromol.* 4, 452.
- Farris, R.J. (1968), "The Influence of Vacuole Formation on the Response and Failure of Filled Elastomers," *Trans. Soc. Rheol.* 12, 315.
- Farris, R.J. (1969), "Applications of Viscoelasticity to Filled Materials," M.S. Thesis, Dept. Civil Eng., Univ. of Utah.
- Farris, R.J. (1970), "Homogeneous Constitutive Equations for Materials with Permanent Memory," Ph.D. Dissertation, Dept. Civil Eng., Univ. of Utah.
- Farris, R.J. (1973), "The Stress-Strain Behavior of Mechanically Degradable Polymers," *Polymer Networks: Structural and Mechanical Properties*, A.J. Chompff, S. Newman, eds., Plenum, New York.
- Farris, R.J. (1978), "Problems with the Popular Theory of Linear Viscoelasticity," *J. Poly. Sci. Polym. Symp.* 63, 185.
- Farris, R.J. and Herrmann, L.R. (1971), "Application of Nonlinear Viscoelasticity and Cumulative Damage (A Realistic Evaluation of Real Propellant Behavior)," Final Report to the Naval Ordnance Systems Command (ORD-0331), Contract No. N00017-70-C-4441, Aerojet Solid Propulsion Co. No. 1565-26F.
- Farris, R.J., and Schapery, R.A. (1973), "Development of a Solid Rocket Propellant Nonlinear Viscoelasticity Constitutive Theory," Final Report to the Air Force Rocket Propulsion Lab., Contract No. F04611-71-C-0046, TR-73-50.
- Feughelman, M. (1973), "Mechanical Hysteresis in Wool Keratin Fibers," *J. Macromol. Sci. Phys.* 87, 569.
- Fitzgerald, J.E. (1973), "On The General Theory of Steklov Aging," *Rheol. Acta* 12, 311.
- Foot, C.J. and Ward, I.M. (1972), "The Nonlinear Viscoelastic Behavior of Isotropic PET," *J. Mech. Phys. Solids* 20, 165.
- Fraser, R.D.B. (1956), "Interpretation of Infrared Dichroism in Fibrous Proteins--the  $2\mu$  Region," *J. Chem. Phys.* 24, 89.
- Frechét, M.M. (1910), "Sur Les Fonctionnelles Continues," *Ann. Sci. de l'Ecole Norm. Sup.* (3) 27, 193.

- Goldberg, N. and Lianis, G. (1968), "Behavior of Viscoelastic Media under Small Sinusoidal Oscillations Superposed on Finite Strain," J. Appl. Mech. 35, 433.
- Gotoh, R., Takenaka, T., and Hayama, N. (1965), "Simultaneous Measurements of Stress and Infrared Dichroism on Polymers. I. Stress Relaxation of Vulcanized Natural Rubber," Kolloid Z.-Z. Polym. 205, 18.
- Green, A.E., and Rivlin, R.S. (1957), "The Mechanics of Nonlinear Materials with Memory. Part I," Arch. Rat. Mech. Anal. 1, 1.
- Hadley, D.W. and Ward, I.M. (1975), "Anisotropic and Nonlinear Viscoelastic Behavior in Solid Polymers," Rep. Prog. Phys. 38, 1143.
- Hermans, P.H. and Platzek, P. (1939), "Beiträge zur Kenntnis des Deformation mechanismus und der Feinstruktur der Hydratzellulose," Kolloid Z. 88, 68.
- Herrmann, L.R. (1965), "On a General Theory of Viscoelasticity," J. Frank. Inst. 280, 244.
- Hsiao, C.C. (1959), "Theory of Mechanical Breakdown and Molecular Orientation of a Model Linear High-Polymer Solid," J. Appl. Phys. 30, 1492.
- Hsiao, C.C. (1971), "Simple Continuum Constitutive Representation of Systems with Random Microstructure," J. Macromol. Sci. Phys. B5, 293.
- Hsiao, C.C. and Moghe, S.R. (1971), "Theory of Deformational Behavior of Polymers," J. Macromol. Sci. Phys. B5, 263.
- Huang, W.N. and Aklonis, J.J. (1978), "Creep of Polymer Networks Undergoing Scission Reactions," J. Macromol. Sci. Phys. B15, 45.
- Koberstein, J.T. (1979), "Small Angle X-ray Scattering Studies of Interstitial Composites," Ph.D. Dissertation, Dept. Polymer Sci. & Eng., Univ. of Mass.
- Koutsky, J.A., Hein, N.V., and Cooper, S.L. (1970), "Some Results on Electron Microscopic Investigations of Polyether-urethane and Polyester-urethane Block Copolymers," J. Poly. Sci. B8, 353.
- Kratky, O. (1933), "Zum Deformations Mechanismus der Faserstoffe," Kolloid Z. 64, 213.

- Leaderman, H. (1962), "Large Longitudinal Retarded Elastic Deformation of Rubber-like Network Polymers," *Trans. Soc. Rheol.* 6, 361.
- Lilaonitkul, A., West, J.C. and Cooper, S.L. (1976), "Properties of Poly(tetramethylene Oxide)-Poly(tetramethylene Terephthalate) Block Polymers," *J. Macromol. Sci. Phys.* B12, 563.
- Lockett, F.J. (1965), "Creep and Stress-Relaxation Experiments for Non-Linear Materials," *Int. J. Eng. Sci.* 3, 59.
- Lockett, F.J. and Stafford, R.O. (1969), "On Special Constitutive Relations in Nonlinear Viscoelasticity," *Int. J. Eng. Sci.* 7, 917.
- Lubliner, J. and Sackman, J.L. (1966), "On Aging Viscoelastic Materials," *J. Mech. Phys. Solids* 14, 25.
- McGuirt, C.W. and Lianis, G. (1969), "Experimental Investigation of Non-Linear, Non-Isothermal Viscoelasticity," *Int. J. Eng. Sci.* 7, 579.
- McKenna, G.B., and Zapas, L.J. (1979), "Nonlinear Viscoelastic Behavior of Poly(methyl Methacrylate) in Torsion," *J. Rheol.* 23, 151.
- Meinecke, E.A. and Schwaber, D.M. (1970), "Energy Absorption in Polymeric Foams," *J. Appl. Polym. Sci.* 14, 2239.
- Miner, M.A. (1945), "Cumulative Damage in Fatigue," *J. Appl. Mech.* 12, 159.
- Moacanin, J., Aklonis, J.J., and Landel, R.F. (1975), "Viscoelastic Behavior of Elastomers Undergoing Scission Reactions," *J. Macromol. Sci. Phys.* B11, 41.
- Mullins, L.J. (1947), "Studies in the Absorption of Energy by Rubber," *J. Rubber Res.* 16, 180.
- Mullins, L.J. (1948), "Effect of Stretching on the Properties of Rubber," *Rubber Chem. Tech.* 21, 281.
- Nakamura, K. (1976), "A Phenomenological Relation in Anisotropic Viscoelastic and Aging Materials," *J. Phys. Soc. Japan* 41, 2091.
- Noll, W. (1958), "A Mathematical Theory of the Mechanical Behavior of Continuous Media," *Arch. Rat. Mech. Anal.* 2, 197.
- Nomura, S., Asanuma, A., Suehiro, S. and Kawai, H. (1971), "Crystal Orientation in a Semicrystalline Polymer in Relation to Deformation of Spherulites," *J. Poly. Sci. A2* 9, 199.



- O'Connor, K.M. and Wool, R.P. (1979), "Mechanical Recovery in SBS Block Copolymers," *Bull. Am. Phys. Soc.* 24, 289.
- Onogi, S. and Asada, T. (1971), "Rheo-Optical Studies of High Polymers by the Infrared Dichroism Method," *Prog. Polym. Sci. Japan* 2, 290.
- Park, J.B., Devries, K.L., and Statton, W.O. (1978), "Chain Rupture During Tensile Deformation of Nylon 6 Fibers," *J. Macromol. Sci. Phys.* B15, 205.
- Payne, A.R. (1974), "Hysteresis in Rubber Vulcanizates," *J. Poly. Sci. Symp.* 48, 169.
- Pedemonte, E., Dondero, G., Alfonso, G.C., and de Candia, F. (1975), "Three-block Copolymers: Morphologies and Stress-Strain Properties of Samples Prepared Under Various Experimental Conditions," *Polymer* 16, 531.
- Peng, S.T.J., Valanis, K.C., and Landel, R.F. (1977), "Nonlinear Viscoelasticity and Relaxation Phenomena of Polymer Solids," *Acta Mech.* 25, 229.
- Petraccone, V., Sanchez, I.C., and Stein, R.S. (1975), "The Orientation of Amorphous Chains in Spherulites," *J. Poly. Sci. PP* 13, 1991.
- Pipkin, A.C. (1964), "Small Finite Deformations of Viscoelastic Solids," *Rev. Mod. Phys.* 36, 1034.
- Pipkin, A.C. and Rogers, T.G. (1968), "A Non-linear Integral Representation for Viscoelastic Behavior," *J. Mech. Phys. Solids* 16, 59.
- Predeleanu, M. (1973), "Mathematical Models in Rheology of the Bodies with Memory and Aging," *Rheol. Acta* 12, 479.
- Puett, D. (1967), "Network Behavior of Polyurethane Elastomers," *J. Poly. Sci. A-2* 5, 839.
- Quinlan, M.H., and Fitzgerald, J.E. (1973), "The Mechanics of Materials with Permanent Memory. Part I." UTEC Report CE 73-129, Dept. Civil Eng., Univ. of Utah.
- Rigby, B.J., Mitchell, T.W., and Robinson, M.S. (1974), "Changes with Time in Mechanical Properties of Wool Fibers," *J. Macromol. Sci. Phys.* B10, 255.
- Rivlin, R.S. (1965), "Nonlinear Viscoelastic Solids," *SIAM Rev.* 7, 323.

- Royden, H.L. (1968), Real Analysis III. 2nd ed., MacMillan, N.Y.
- Sasaguri, K., Hoshino, S., and Stein, R.S. (1964), "Relationship Between Morphology and Deformation Mechanisms of Polyolefins," J. Appl. Phys. 35, 47.
- Schapery, R.A. (1969), "On The Characterization of Nonlinear Viscoelastic Materials," Polym. Eng. Sci. 9, 295.
- Seferis, J.C., McCullough, R.L. and Samuels, R.J. (1976), "Constitutive Relationship for the Mechanical Properties of Anisotropic, Partially Crystalline Polymers," Polym. Eng. Sci. 16, 334.
- Seferis, J.C., McCullough, R.L. and Samuels, R.J. (1977), "Influence of Structure on the Dynamic Mechanical Properties of Crystalline Polymers," J. Macromol. Sci. Phys. B13, 357.
- Seymour, R.W., Allegrezza, A.E. and Cooper, S.L. (1973), "Segmental Orientation Studies of Block Polymers. I. Hydrogen-bonded Polyurethanes," Macromol. 6, 896.
- Seymour, R.W., Estes, G.M., and Cooper, S.L. (1970), "Infrared Studies of Segmented Polyurethane Elastomers. I. Hydrogen Bonding," Macromol. 3, 579.
- Seymour, R.W., and Cooper, S.L. (1974), "Viscoelastic Properties of Polyurethane Block Polymers," Rubber Chem. Tech. 47, 19.
- Smart, J. and Williams, J.G. (1972), "A Power Law Model for the Multiple-Integral Theory of Non-linear Viscoelasticity," J. Mech. Phys. Solids 20, 325.
- Smith, T.L. (1962), "Nonlinear Viscoelastic Response of Amorphous Elastomers to Constant Strain Rates," Trans. Soc. Rheol. 6, 61.
- Stafford, R.O. (1969), "On Mathematical Forms for the Material Functions in Non-Linear Viscoelasticity," J. Mech. Phys. Solids 17, 339.
- Takayanagi, M., Ingada, K. and Kajiyama, T. (1966), "Mechanical Properties and Fine Structure of Drawn Polymers," J. Poly. Sci. C 16, 334.
- Tschoegl, N.W. (1971), "Constitutive Equations for Elastomers," J. Poly. Sci. A1, 9, 1959.
- Vakili, J. and Fitzgerald, J.E. (1973), "Nonlinear Characterization of Sand Asphalt Concrete by Means of Permanent Memory Norms," Exp. Mech. 13, 504.



- Volterra, V. (1959), Theory of Functionals and of Integral and Integro-Differential Equations, Dover, New York.
- West, J.C., Koberstein, J.T., Lilaonitkul, A., Cooper, S.L. (1975), "Stress and Orientation Hysteresis in Block Copolymer Elastomers," ACS Polymer Preprints 16, 523.
- Wilkes, C.E. and Yusek, C.S. (1973), "Investigation of Domain Structure in Urethane Elastomers by X-ray and Thermal Methods," J. Macromol. Sci. Phys. B7, 157.
- Wu, J.B.C., and Brown, N. (1979), "An Equation for Stress Relaxation During Crazing," J. Rheol. 23, 231.
- Yannas, I.V., and Lunn, A.C. (1970), "Transition from Linear to Non-linear Viscoelastic Behavior. Part I. Creep of Polycarbonate," J. Macromol. Sci. Phys. B4, 603.
- Yoon, D.Y., Chang, C., and Stein, R.S. (1974), "An Improved Model for Crystalline Orientation of Spherulitic Polymers," J. Poly. Sci. PP 12, 2091.
- Zapas, L.J., and Craft, T. (1965), "Correlation of Large Longitudinal Deformations with Different Strain Histories," J. Res. Nat. Bur. Stds., part A 69A, 541.

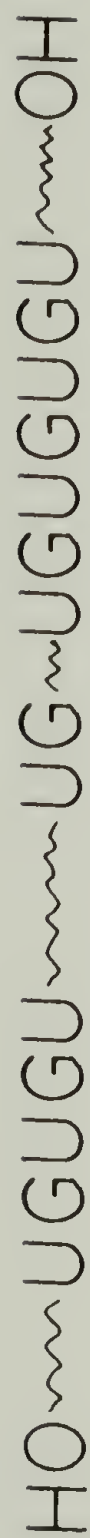
## A P P E N D I X    A

### DESCRIPTION OF POLYURETHANE CHEMISTRY

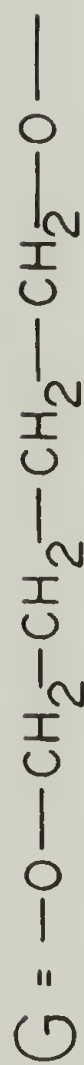
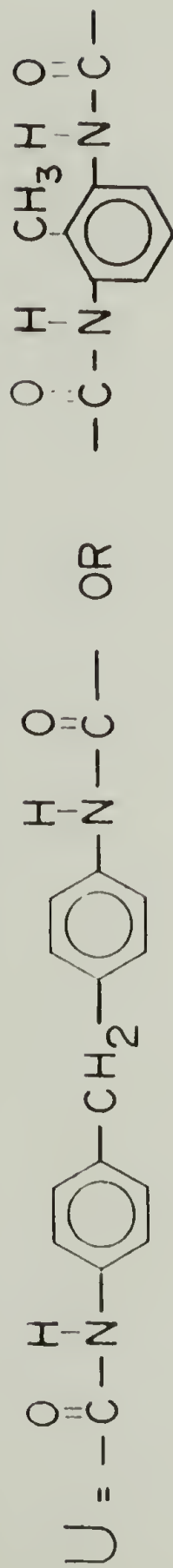
Segmented polyurethane elastomers have the basic chemistry given in Figure 60. They are produced by first preparing a relatively low molecular weight (1000-3000) polyester (ES-type) or polyether (ET-type) segment which is referred to as the soft segment of the polyurethane. The commonly used soft segments are poly(tetramethylene oxide), or PTO, for the ET-types, and poly(tetramethylene adipate), or PTA, for the ES-types. These two basic soft segments are given in Figure 60.

The polyurethane is then synthesized by reaction of an excess of diisocyanate with the soft segment polymer to form an isocyanate-capped prepolymer. The diisocyanates most commonly used are p,p'-diphenylmethane diisocyanate (MDI) and a mixture of the 2,4- and 2,6-isomers of tolylene diisocyanate, as depicted in Figure 60. The final polymer is formed by a reaction of the prepolymer with a chain extender such as butanediol. The portion of the polymer formed during this reaction step consists of alternating isocyanate and chain extender groups and is termed the hard segment of the polyurethane.

In Table 3, the main polyurethanes discussed in this report are listed along with their soft and hard segment compositions and weight fractions.



# SEGMENTED POLYURETHANE



or

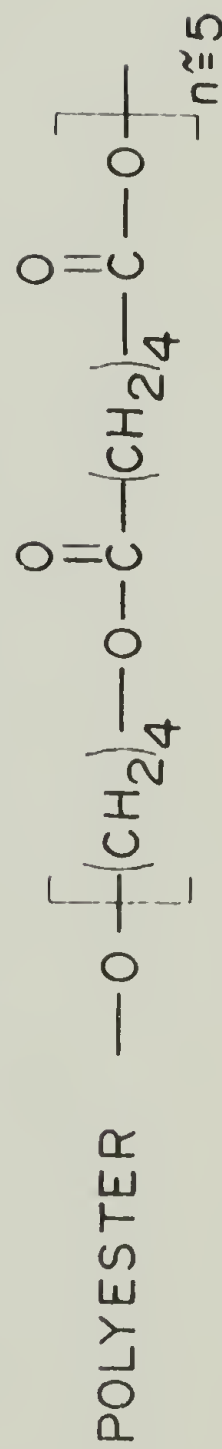


Figure 60. Polyurethane chemistry.

TABLE 3  
POLYURETHANE COMPOSITION

Polymer	Soft Segment	Soft Segment m. wt.	Hard Segment	wt. % hard segment
ES-38	PTA	1000	MDI	38
ET-31	PTO	1000	MDI	31
ET-38	PTO	1000	MDI	38
ES5701	PTA	1000	MDI	30
Lycra 2240	PTO	2000	TDI	18

## A P P E N D I X B

### EXPERIMENTAL PROCEDURE FOR STRESS-STRAIN TESTING

Samples of Estane 5701 were obtained in the form of injection molded 3" x 6" x 1/8" plaques from B.F. Goodrich Company. The author gratefully acknowledges the assistance of Dr. Larry Hewitt, who provided the samples. Tensile test specimens were cut from the as-received plaques with an Xacto knife. A soap solution was used to wet the surface of the polymer to facilitate cutting. The samples were then rinsed with water to remove the soap and air dried. A typical specimen was 8 cm x 0.8 cm x 0.3 cm in size. The ends of the specimens were flattened to provide increased surface area for bonding by melting the ends on a metal plate heated by a laboratory hot plate.

The samples were bonded to machined aluminum tabs (see Figure 61) according to the following regimen: the tabs were sanded with coarse emery paper, cleaned with toluene, and coated with Thixon Bonding Agent #AB-1153/55 one-coat bonding agent for metals to polyethylenes (Dayton Coatings and Chemicals, W. Alexandria, OH 45381). The tabs were dried overnight, then the samples were bonded to the tabs with a second coat of Thixon. After the tab-sample assembly dried overnight, the bond was cured in a forced air oven for one hour at 120°C.

The tensile samples were tested on the Instron Universal Testing Instrument, model TTBM. Only the Instron crosshead was used



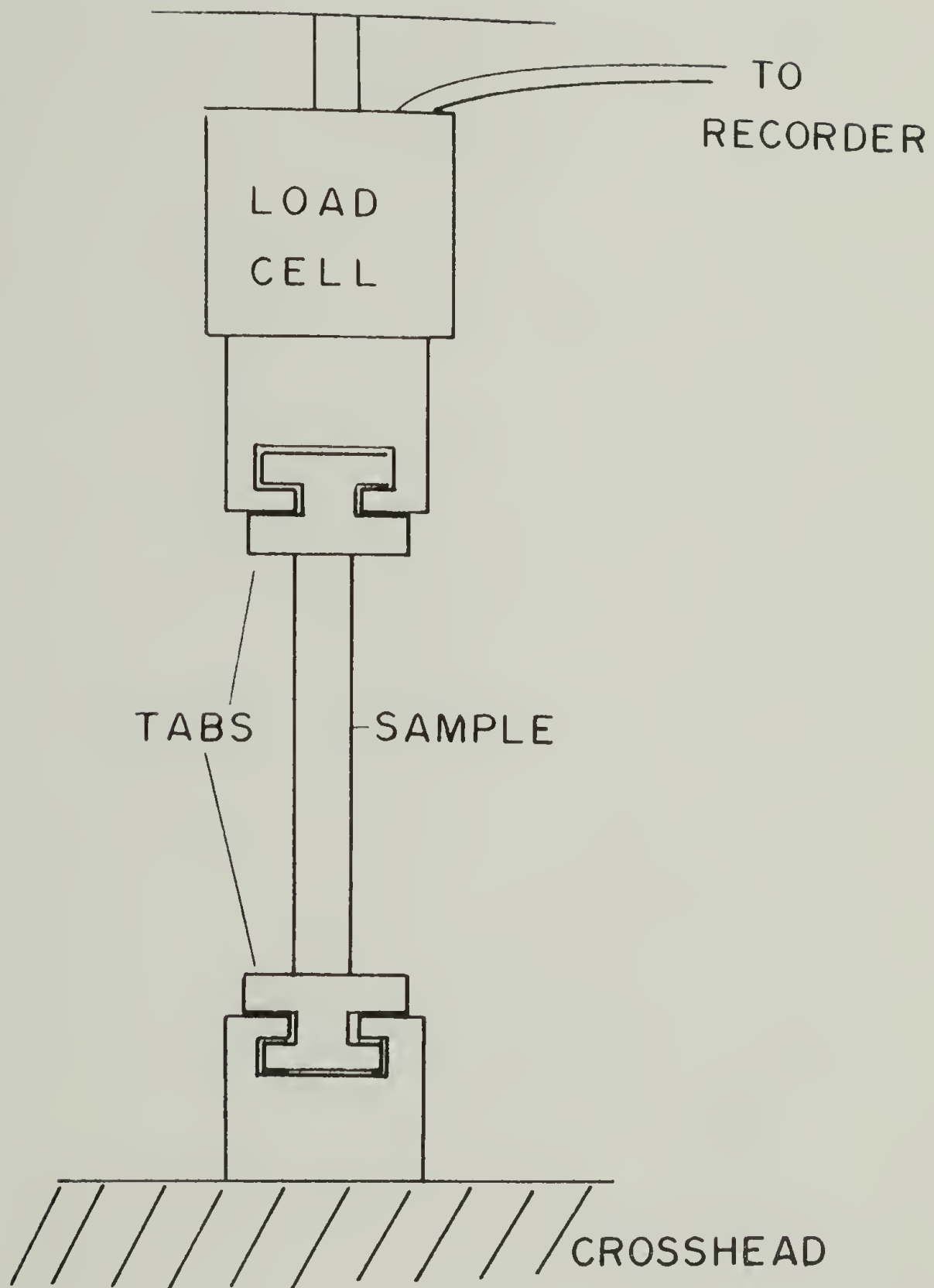


Figure 61. Experimental configuration for tensile testing of ES5701.

for the testing; a Tyco Bytrex Load Cell, model JP-200 (Tyco Laboratories, Inc., Watertown, MA) was connected to the Instron frame to register the stress, and the measurements were recorded on a Perkin-Elmer recorder (model 56). The electronic interfacing between chart and load cell was designed by Farris Instruments (428 Chesterfield Rd., Northampton, MA).

Samples of Lycra 2240 were tested on the same Instron instrument. The tensile test specimen were prepared by cutting 10 feet of the fiber, knotting the ends together, then doubling the resulting loop four times to obtain a hank with 32 fibers in the cross-section. The hank was looped over two pins between the load cell and Instron crosshead. Lycra 2240 is a 2240 denier fiber produced by E.I. duPont deNemours Company.

## A P P E N D I X    C

### STRAIN MEASURES IN THE DEFORMED COORDINATE SYSTEM

Let the reference configuration of all points in a body be  $X_i$  and the deformed configuration  $x_i$ . Two points, a distance  $ds_0^2$  apart in the reference system are a distance  $ds^2$  apart in the deformed system, with the relative change in the two distances expressed by

$$\frac{ds^2 - ds_0^2}{ds^2} = 2 e_{ij} \frac{dx_i}{ds} \frac{dx_j}{ds} \quad i, j = 1, 2, 3$$

in the deformed coordinate system. The second rank tensor  $e_{ij}$  is commonly referred to as the Eulerian strain tensor.

Consider the above definition for the two-dimensional case with strains in the principle directions only. Then

$$\frac{ds^2 - ds_0^2}{ds^2} = 2 e_{11} \left( \frac{dx_1}{ds} \right)^2 + 2 e_{22} \left( \frac{dx_2}{ds} \right)^2$$

The two squared quantities  $(dx_1/ds)^2$  and  $(dx_2/ds)^2$  are the squares of the cosines of the angles between the vector  $ds$  and the  $x_1$  and  $x_2$  axes. These cosine squared quantities appear in the commonly used Hermans orientation function (Hermans and Platzek, 1939; Fraser, 1956), which is defined for the case of simple tension as

$$f_1 = \frac{3\langle \cos^2 \theta \rangle - 1}{2}$$

where  $\theta$  is the angle between the stretching direction and the vector of the orienting body under discussion. The brackets denote average value. Thus it is seen that the definition of the orientation function is a natural one based on the consideration of the relative change in the distance between two points in the body, referred to as the deformed coordinate system. Also, it may be seen that the orientation function naturally is a second rank tensor since it is defined by the tensor

$$\frac{dx_i}{ds} \frac{dx_j}{ds}$$

and the contraction of the orientation tensor with the strain tensor  $e_{ij}$  leads to the scalar quantity

$$\frac{ds^2 - ds_0^2}{ds^2}$$

The strain measure which naturally arises from this discussion is the Eulerian strain, which for the two dimensional case above has the principle components

$$e_{11} = \frac{\partial u_1}{\partial x_1} - \frac{1}{2} \left( \frac{\partial u_1}{\partial x_1} \right)^2$$

$$e_{22} = \frac{\partial u_2}{\partial x_2} - \frac{1}{2} \left( \frac{\partial u_2}{\partial x_2} \right)^2$$

where  $u_1$  and  $u_2$  are the displacements defined by

$$u_1 = x_1 - X_1$$

$$u_2 = x_2 - X_2$$

The displacements may also be written in terms of the extension ratios,  $\lambda_1$  and  $\lambda_2$ , to yield

$$u_1 = \frac{(\lambda_1 - 1)}{\lambda_1} x_1$$

$$u_2 = \frac{(\lambda_2 - 1)}{\lambda_2} x_2$$

since  $x_1 = \lambda_1 X_1$  and  $x_2 = \lambda_2 X_2$ . Now the Eulerian strain components become

$$e_{11} = \frac{\lambda_1 - 1}{\lambda_1} - \frac{1}{2} \left( \frac{\lambda_1 - 1}{\lambda_1} \right)^2$$

$$e_{22} = \frac{\lambda_2 - 1}{\lambda_2} - \frac{1}{2} \left( \frac{\lambda_2 - 1}{\lambda_2} \right)^2$$

and a first order, linear strain measure arising from this treatment, for the principle stretch direction, is

$$\epsilon = \frac{\lambda - 1}{\lambda}$$

where  $\lambda$  is the principle extension ratio in the stretching direction.



## A P P E N D I X   D

### EQUIVALENCE OF LINE, AREA, AND VOLUME FRACTIONS

The system in question has two components, a and b, of volume fractions  $X_a$  and  $X_b$ , where

$$X_a = \frac{\bar{V}_a}{V} \quad ; \quad X_b = \frac{\bar{V}_b}{V} \quad ; \quad X_a + X_b = 1$$

where  $V$  is the volume of the system and  $\bar{V}_a$  and  $\bar{V}_b$  are the volumes of the two components.

If a plane section of the system is considered, the total areas of a and b represented will be  $\bar{A}_a$  and  $\bar{A}_b$ . Now  $\bar{V}_a$  and  $\bar{V}_b$  may be calculated if the changes in  $A_a$  and  $A_b$  with linear dimension  $x$  are known:

$$\bar{V}_a = \int_0^L A_a(x) dx$$

$$\bar{V}_b = \int_0^L A_b(x) dx$$

where  $L$  is the sample thickness. But since

$$\bar{A}_a = \frac{1}{L} \int_0^L A_a(x) dx$$

$$\bar{A}_b = \frac{1}{L} \int_0^L A_b(x) dx$$

we have

$$\bar{A}_a L = \bar{V}_a$$

$$\bar{A}_b L = \bar{V}_b$$

Then, using  $AL = V$ , where  $A$  is the total area,

$$\frac{\bar{A}_a L}{V} = \frac{\bar{A}_a L}{AL} = \frac{\bar{A}_a}{A} = \frac{\bar{V}_a}{V}$$

$$\frac{\bar{A}_b L}{V} = \frac{\bar{A}_b L}{AL} = \frac{\bar{A}_b}{A} = \frac{\bar{V}_b}{V}$$

Thus the area fractions of  $a$  and  $b$  equal the volume fractions. A similar argument shows that the line fractions of  $a$  and  $b$  obtained by passing a random vector through the system are equal to the area fractions and therefore also equal to the volume fractions.

# A P P E N D I X   E

## NONLINEAR REGRESSION ANALYSIS

The data were fit to the equations indicated in the text by using a non-linear least squares algorithm as follows.

Definitions:

$y_j$  =  $j^{\text{th}}$  observed value

$B_i$  = unknown material constant

$B_i^{\circ}$  = initial guess of  $B_i$

$X_{ji}$  = input data for  $j^{\text{th}}$  observation, summation on  $i$   
implied

$f_j = f_j(B_i^{\circ}, X_{ji})$  = known equation to be evaluated for the  
 $B_i$ 's using the data  $X_{ji}$ .

Procedure:  $y_j$  is expanded about the initial guesses  $B_i^{\circ}$  in a Taylor series of  $i$  variables of the known function  $f_j$ . Only first order terms are used and an approximate expression for  $y_j$ , called  $\tilde{y}_j$ , is obtained.

$$y_j \approx \tilde{y}_j = f_j(B_i^{\circ}, X_{ji}) + \left. \frac{\partial f_j}{\partial B_1} \right|_{B_1^{\circ}} (B_1 - B_1^{\circ}) + \left. \frac{\partial f_j}{\partial B_2} \right|_{B_2^{\circ}} (B_2 - B_2^{\circ}) + \dots \quad (75)$$

or

$$\tilde{y}_j = f_j + \sum_i \left. \frac{\partial f_j}{\partial B_i} \right|_{B_i^{\circ}} (B_i - B_i^{\circ}), \quad \text{or} \quad (76)$$

$$\tilde{y}_j = f_j + \sum_i P_{ij} \Delta B_i \quad (77)$$

where

$$P_{ij} \equiv \left. \frac{\partial f_i}{\partial B_i} \right|_{B_i^0}, \quad \Delta B_i = B_i - B_i^0 \quad (78)$$

The error,  $E$ , between this approximate expression and the exact expression is given by the sum of the squares of the differences between  $y_j$  and  $\tilde{y}_j$ :

$$E = \sum_j (y_j - \tilde{y}_j)^2 \quad (79)$$

Using Equation (77), we obtain

$$E = \sum_j [y_j - (f_j + \sum_i P_{ij} \Delta B_i)]^2 \quad (80)$$

To minimize the error, the partial derivatives of  $E$  with respect to the  $\Delta B_i$ 's are set to zero to form a system of equations:

$$\frac{\partial E}{\partial \Delta B_1} = -2 \sum_i P_{1j} [y_j - (f_j + \sum_i P_{ij} \Delta B_i)] = 0 \quad (81)$$

$$\frac{\partial E}{\partial \Delta B_2} = -2 \sum_j P_{2j} [y_j - (f_j + \sum_i P_{ij} \Delta B_i)] = 0$$

etc. These equations yield the following system:

$$\begin{aligned} \sum_j P_{1j} (\sum_i P_{ij} \Delta B_i) &= \sum_j y_j P_{1j} - \sum_j f_j P_{1j} \\ \sum_j P_{2j} (\sum_i P_{ij} \Delta B_i) &= \sum_j y_j P_{2j} - \sum_j f_j P_{2j} \end{aligned} \quad (82)$$

etc. Expanding the left-hand side of the first equation in (82) reveals that:

$$\begin{aligned} \sum_j P_{1j} (P_{1j} \Delta B_1 + P_{2j} \Delta B_2 + P_{3j} \Delta B_3 + \dots) = \\ \Delta B_1 \left( \sum_j P_{1j} P_{1j} \right) + \Delta B_2 \left( \sum_j P_{1j} P_{2j} \right) + \Delta B_3 \left( \sum_j P_{1j} P_{3j} \right) + \dots \end{aligned} \quad (83)$$

The unknowns are the  $\Delta B_i$  and the coefficients of the matrix are the  $P_{ij}$  products. This can be expressed as the matrix equation:

$$[P]\{\Delta B\} = \{Y\} \quad (84)$$

and is solved by inversion of the  $[P]$  matrix to obtain:

$$\{\Delta B\} = [P]^{-1}\{Y\} \quad (85)$$

If the function  $f_j$  is linear in  $\Delta B_i$ , then Equation (85) gives the exact solution. If not, as in the case of the equations in the text, the partial derivative  $[P]$  and, hence,  $[P]^{-1}$ , will depend on the  $\Delta B_i$ 's, and in the usual trial-and-error methods for computing least squares estimates,  $\{\Delta B\}$  is re-evaluated at each iteration, using the maximum neighborhood, until one of several convergence criteria are met.

A copy of an example program using the nonlinear least squares algorithm, together with the output, follows. In this example, the equation was (27) with  $p = 10$ .  $X(I,1)$  is the orientation function  $f_h$ ,  $X(I,2)$  is the strain,  $e$ , and the coefficients  $B_i$  are as follows:



$$B(1) = C$$

$$B(2) = S$$

$$B(3) = \bar{e}$$

$$B(4) = p = 10 \text{ (held constant)}$$

Documentation of the non-linear regression code was obtained from D.F. Vronay, Aerojet General Corp., P.O. Box 13400, Sacramento, CA 95813.

```

      PROGRAM FHYST(TAPE5,TAPE4,TAPE7,OUTPUT,TAPE6=OUTPUT
1      TAPE8)
1-22-79 MODIFIED TO FIT ORIENTATION STRAIN DATA
4/7/79 MODIFIED TO USE EXTENSION RATIO LAMDA
      X(I,1)=STRESS
      X(I,2)=STRAIN
      X(I,3)=ORIENTATION
      LAST(I)=FLAG
1      DIMENSION B(50),IB(50),ITITLE(4)
COMMON/DATA/X(50,3),Y(500),NT
COMMON/RATE/R,ELEG(15),EEND(15),NL,INDEX(15)
      REAL LAST
      REWIND 5
      REWIND 4
      REWIND 7
      READ IN THE DATA
      ITER=NO. OF ITERATIONS ASKED FOR,N= NO. OF UNKNOWN
      I=NO. OF VARIABLES, IDVT=PARTIAL DERIV. OPTION
      ENTER 1 FOR ESTIMATED PARTIALS ENTER 1 TO OMIT
      ICON=1 FOR ESTIMATION LIMIT CALC. ENTER 0(ZERO)
      IPRINT=CONFINING OPTION, ENTER 0 TO OMIT DATA LIST,
      NECHO=PRINTING OPTION, ENTER 0 OTHERWISE
      ENTER NONZERO INTEGER OTHERWISE
      READ(7,*) ITER,N,M,IDVT,ICON,IPRINT,NECHO
      WRITE(8,53) ITER,N,M,IDVT,ICON,IPRINT,NECHO
      FORMAT(I3,1X,6(I2,1X))
      IG0=0
      IP=1
      IB(1)=4
      IB(2)=2
      NT=0
      R=0.005
53
      INITIAL GUESSES OF PARAMETERS
      READ(7,*) (B(I),I=1,N)
100 CONTINUE
      NT=NT+1

```

```

C DATA IS ENTERED AS Y,X,FLAG
C NON-ZERO FLAG IS THE END OF DATA *****
C
C READ(5,*) DUM,X(NT,2),X(NT,1),LAST(NT)
C
C Y(NT)=X(NT,1)
C IF(LAST(NT).LT.0.0) GO TO 90
C GO TO 100
C PRINT OUT INPUT
C
90 NT=NT-1 ITER,N,M, IDVT,ICON,IPRINT
WRITE(6,8) (I,I=1,N)
WRITE(6,9) (B(I),I=1,N)
WRITE(6,10) (EQ(I),I=1,N)
DO 110 I=1,NT
WRITE(6,3) X(I,1), X(I,2)
110 CONTINUE
50 IGO=1
C FIND STARTING AND STOPPING POINTS
C
EBEG(1)=0.0
INDEX(1)=1
NL=1
DO 20 I=1,NT
IF(LAST(I).EQ.1.0.AND.LAST(I+1).EQ.2.0) GO TO 11
IF(LAST(I).EQ.2.0.AND.LAST(I+1).EQ.1.0) GO TO 11
GO TO 20
EEND(NL)=X(I,2)
EBEG(NL+1)=X(I,2)
INDEX(NL+1)=I
NL=NL+1
CONTINUE
20 EEND(NL)=X(NT,2)
INDEX(NL+1)=NT
C CALL GUTS
C

```





SUBROUTINE LSQENP

74/175 OPT=1

FTN 4.7+485

```

C**REVIS 11-20-72 TO ADD OPTION FOR NOT PRINTING OBSERVED AND CALCULAT
C**VALUES AFTER 6-12-70 TO REARRANGE LEAST SQUARES
C**REVIS 6-12-70 TO REARRANGE LEAST SQUARES
C**REVIS 6-12-70 TO REARRANGE LEAST SQUARES
C**

```

```

SUBROUTINE LSQENP(N,K,M,Y,X,B,IP,IB,IDVT,ICON,IQUIT,IPRNT)
  DIMENSION BS(50),DB(50),BA(50),G(50),W(51),SA(50),P(50),A(50,51)
  DIMENSION X(50,1),Y(1),B(1),IB(1)
  COMMON /INT/ N7,K7,M7,IP7
  COMMON /PLOT/ IFF,I,E,TAU,XL,GAMCR,DEL,ZETA,IPA
  COMMON /AFCLSQ/ BS,DB,BA,G,M,SA,P,A,

```

```

  1 I,IBKP,WS,PHIZ,STE,SPL,WS1,DO,XK2,BL,PU,SE,OPL,SPU,PKN,PHID,XK3,
  1 IBKA,IBK2,J1,KST,IWS6,JJ,J,IBKM,KEND,IFSS3,IFSS2,IBOUT,
  1 PL,HJTD,OPU,PC,D,XK1,BC,BU,PHI
  1 DOUBLE PRECISION PHD
  LOGICAL JBCH,JOCH,JXCH,JYCH/1H,1H0,1HP,1HX,1HY/
  FIN=.FALSE.
  IWS2=IQUIT
  IWS3=IQUIT
  IWS4=IQUIT
  IWS6=IQUIT
  IN7=N
  K7=M
  M7=M
  IP7=IP
  YMN=YMIN
  IF (IFP .NE. 1) IFP=0
  IF (IFP .EQ. 1) SPRD=YMAX-YMIN
  IF (XL .LT. 0.0) XL=0

```

```

C**MAX NO OF OBSERVATIONS IS K=50
C**MAX NO OF OBSERVATIONS IS N=500
C**IWHHER=-1 MEANS DO ANY SPECIAL INITIALIZING FOR CASE
C**IWHHER=0 MEANS START NEW CASE OR END RUN
C**IWHHER=1 MEANS GET P S AND F
C**IWHHER GREATER THAN 1 MEANS GET F ONLY

```

23 IWHHER = 0



```

24 GO TO 39
25 IWHER = IWHER
   IF (IWHER.GT.0) GO TO 31
   IF (IWHER.EQ.0) GO TO 38
26 CONTINUE
   IF (IBOUT.EQ.0) GO TO 24
   GO TO 23
31 CONTINUE

C** CODING TO MAKE F GOES HERE
C** F IS Y HAT (I)
C** NPRINT IS THE NO OF OTHER WORDS TO BE PRINTED
C** THE WORDS TO BE PRINTED ARE IN PRNT(1)...PRNT(5)
C**
C** CALL FCODE(Y,X,B,F,I,IWHER)
C**
C** IF (IWHER.NE.1) GO TO 24
C** IF (IFSS2.NE.0) GO TO 24
34 CONTINUE

C** CODING TO MAKE DF/DB GOES HERE
C** MAKE K OF THEM. CALL THEM P(J)
C** THEY ARE MADE FROM X(I,L) AND B(J)
C**
CALL PCODE(P,X,B,F,I)
GO TO 24
38 RETURN

C** THIS IS THE END OF THE MAIN ROUTINE
C**
IWHER = IWHER
-
IF (IWHER.LT.0) GO TO 80
IF (IWHER.EQ.0) GO TO 43
GO TO (106,363,114,125), IWHER
42 ITCT=0
43 IBOUT=0
   IF (FIN) RETURN
   FIN=.TRUE.

C** END OF LAST PROBLEM
   IF (IFP.LE.0) GO TO 55
48 CONTINUE
49 IBCH=JECH
   IOCH=JOCH

```

```

IPCH=JPCH
IXCH=JXCH
IYCH=JYCH
55 IF(IP.LE.0)GOTO 62
DO 61 I=1,IP
58 IF (IB(I):GT.0)GO TO 61
59 WRITE(6,402)
61 CONTINUE
IBOUT=1
61 CONTINUE
C**
C**
62 CONTINUE
IF (IPA.EQ.1) GO TO 76
FF=4.
T=2.00005
E=.00001
TAU=.001
XL=0.01
GAMCR=45.
DEL = 1.E-02
ZETA = 1E-30
76 XKDB = 1.
77 CONTINUE
IWHER=-1
GO TO 25
C**
C**
C**
.....START THE CALCULATION OF THE PIP MATRIX.....
80 IBKA=1
WRITE(6,383)N,K,IP,M,IFP,GAMCR,DEL,FF,T,E,TAU,XL,ZETA
82 CONTINUE
DO 86 I=1,K
G (I) = 0.
DO 86 J=1,K
86 A (I,J)=0.
GO TO(88,91,91),IBKA
88 IFSS3=IWS3
IFSS2=IWS2
GO TO 92
91 IFSS3=1
92 WRITE(6,384) (B(J),J=1,K)

```

SUBROUTINE LSQENP      74/175    OPT=1      FTN 4.7+485

C\*\*  
C\*\*

IF (IFSS3 .LE. 0 .OR. IWS3 .LT. 0) GO TO 99  
IF (IFP.LE.0) GO TO 98

WS = YMN+SPRD  
WRITE(6,382) YMN,WS

GO TO 99

98 WRITE (6,386)

99

IHI=1

PHI=0  
IF (IFSS2.EQ.0) GO TO 104  
GO TO 111

103 IF (IFSS2.EQ.1) GO TO 112

C\*\*

104 IMHER=1      THIS IS THE ANALYTICAL P S ROUTINE

C\*\*

GET P S AND F

GO TO 25

106 IF (IP.LE.0) GO TO 132

107

DO 109 I=1,IP

IWS=IB(II)

109

P(IWS)=0.

GO TO 132

C\*\*

.....THIS IS THE ESTIMATED P S ROUTINE.....

C\*\*

CONTINUE

111 IMHER=3

112 GO TO 25

114

FWS=F

J=1

116 IF (IP.LE.0) GO TO 120

117

DO 119 I=1,IP

IF ((J-IB(II)).EQ.0) GO TO 128

119

CONTINUE

OBW=B(J)\*DEL

120 IF (B(J) .EQ. 0.) DBW = DEL

TWS=B(J)

B(J)=B(J)+DBW

IMHER=4

GO TO 25

125

B(J)=TWS

P(J)=(F-FWS)/DBW

GO TO 129

```

SUBROUTINE LSQEMP      74/175   OPT=1      FTN 4.7+485

128 P(J)=0.
129 J=J+1
131 IF ((J-K).LE.0)GO TO 116
131 F=FWS
C**
C**
C**
      END OF ESTIMATED P S ROUTINE
      NOW, USE THE P S TO MAKE PARTIALS MATRIX
132 DO 136 JJ=1,K
      G(JJ)=G(JJ)+(Y(I)-F)*P(JJ)
      DO 136 II=J,K
      A(II,JJ)=A(II,JJ)+P(II)*P(JJ)
136 A(JJ,II)=A(II,JJ)
      IF (IFP.LE.0)GO TO 184
138 IF (IFSS3.LE.0)GO TO 188
      IO = (Y(I)-YMN)*100./SPRD
      IPP = (F-YMN)*100./SPRD
      IF (IO.EQ. IPP)GO TO 148
      IF (IO.GT. IPP)GO TO 153
      Y(I) OUT FIRST
C**
143 IP1=IOCH
      IP2=IPCH
      I1=IO
      I2=IPP
      GO TO 157
C**
148 IP1=IYCH
      IP2=IBCH
      I1=IO
      I2=IPP
      GO TO 157
C**
153 IP1=IPCH
      IP2=IPOCH
      I1=IPP
      I2=IO
      ZERO PLOTS IN THE LEFT HAND COLUMN, SO I1 IS ITS
      OWN BLANK COUNTER
      OVERFLOWS PLOT X IN COLUMN 182
      UNDERFLOWS ALSO PLOT X IN COLUMN ZERO
157 IF (I2.LE.101)GO TO 165
158 I2=101

```

SUBROUTINE LSQENP 74/175 OPT=1

FTN 4.7+485

```

161 IP2=IXCH
    IF (I1.LT.101)GO TO 165
    I1=101
    IP1=IXCH
    IP2=IBCH
    GO TO 171
165 IF (I1.GE.0)GO TO 171
166 I1=0
    IP1=IXCH
    IF (I2.GT.0)GO TO 171
169 I2=1
    IP2=IBCH
171 I1M1=I1
    I1M2=I2-I1-1
    IF (I1M1.GT.0)GO TO 179
    IF (I1M2.GT.0)GO TO 177
174 WRITTO (6,404)IP1,IP2
175 GOITTO 183
177 WRITTO (6,404)IP1,(IBCH,II=1,I1M2),IP2
179 IF (I1M2.GT.0)GO TO 182
180 WRITTO (6,404)(IBCH,II=1,I1M1),IP1,IP2
182 WRITTO (6,404)(IBCH,II=1,I1M1),IP1,(IBCH,II=1,I1M2),IP2
183 GOITTO 188
184 WS=Y(I)-F
    IF (IFSS3.LE.0.OR.IWS3.LT.0)GO TO 188
186 IF (INUE(6,401)X(I,1),Y(I),F,WS
187 CONTINUE(6,401)X(I,1),Y(I),F,WS
188 PHI=PHI+WS*WS
    IF I=1
    IF (I.LE.N)GO TO 103
    IF (IP.LE.0)GO TO 199
192 DO IWS=IB(JJ)
193 DO I=198(JJ)
    DO IWS=197(JJ)
    A(IWS,I)=0.
197 A(IWS,I)=1.
198 A(IWS,I)=1.
    C* A(IWS,I)=1.
199 IF (IBKA.EQ.1)GO TO 204

```



```

      IBKS=1
      CALL CONLIM(IBKS,IBD,Y,X,B,IB)
      GO TO(82,314,23,359,43),IBD
      SAVE SQUARE ROOTS OF DIAGONAL ELEMENTS
C** 204 CONTINUE
      DO 206 I=1,K
      SA(I)=SQRT(A(I,I))
      DO 219 I=1,K
      DO 214 J=1,K
      WS=SA(I)*SA(J)
      IF(WS.GT.0.)GOTO 213
      A(I,J)=0.
      GO TO 214
213 A(I,J)=A(I,J)/WS
214 CONTINUE
      IF(SA(I).GT.0.)GOTO 218
      G(I)=0.
      GO TO 219
218 G(I)=G(I)/SA(I)
219 CONTINUE
      DO 221 I=1,K
      A(I,I)=1.
      PHIZ=PHI
C** 221 PHIZ=PHI
C** ..... WE NOW HAVE PHI ZERO
C** .....
C** .....
C** .....
C** .....
      IF(ITCT.GT.0)GO TO 230
      FIRST ITERATION
225 IF(IPA.EQ.1) GO TO 227
226 XL=0.01
227 ITCT=1
      DO 229 J=1,K
      BS(J)=B(J)
C** 229 BS(J)=B(J)
C** ..... BS(J) CORRESPONDS TO PHIZ
C** .....
230 IBK1=1
      WS=N-K+IP
      SE=SQRT(PHIZ/WS)
      IF(IFSS3.GT.0)GO TO 239
      IF(IFSS2.EQ.0)GO TO 237
234 WRITE(6,387)PHIZ,SE,XLL,GAMMA,XL
235 GO TO 243
237 WRITE(6,388)PHIZ,SE,XLL,GAMMA,XL

```

SUBROUTINE LSQENP      74/175    OPT=1      FTN 4.7+485

```

239 GO TO 243
248 IF (IFSS2.EQ.0)GO TO 242
    WRITE (6,379)PHIZ,SE,XL
242 GO TO 243
243 WRITE (6,385)PHIZ,SE,XL
244 GO TO 310
244 PHIL=PHI
C*#
    DO 247 J=1,K
    IF (ABS(DB(J)/(ABS(B(J)) + TAU)).GE.E)GO TO 251
    CONTINUE
247 WRITE (6,399)
    IBS=4
    GO TO 371
251 IF (IWS4.EQ.0)GO TO 257
    IF (IWS4.EQ.1)GO TO 255
    IWS4=IWS4-1
    GO TO 257
255 WRITE (6,400)
    GO TO 371
257 XKDB = 1.
    IF (PHIL.GT.PHIZ)GO TO 281
259 XLS=XL
    DO 262 J=1,K
    BA(J)=B(J)
262 B(J)=BS(J)
    IF (XL.GT.:00000001)GO TO 268
264 DO 266 J=1,K
    B(J)=BA(J)
266 BS(J)=B(J)
    GO TO 82
268 XL=XL/10.
    IBK1=2
    GO TO 310
271 PHL4=PHI
C*#
    WE NOW HAVE PHI(LAMBDA/10)
273 IF (PHL4.GT.PHIZ)GOTO 276
274 DO 274 J=1,K
    BS(J)=B(J)
276 GO TO 82
    XL=XLS
    DO 279 J=1,K

```

```

279 BS(J)=BA(J)
280 B(J)=BA(J)
281 GO TO 82
282 IBK1=4
283 XLS=XL
284 XL=XL/10.
285 DO 285 J=1,K
286 B(J)=BS(J)
287 GO TO 310
288 IF (PHI.LE.PHIZ)GO TO 296
289 XL=XLS
290 IBK1=3
291 XL=XL*10.
292 DO 292 J=1,K
293 B(J)=BS(J)
294 GO TO 310
295 PHI4=PHI
296 WE NOW HAVE PHI(10*LAMBDA)
297 GO TO 299
298 IF (PHIT4.GT.PHIZ)GO TO 299
299 DO 297 J=1,K
300 BS(J)=B(J)
301 GO TO 82
302 IF (GAMMA.GE.GAMCR)GO TO 290
303 XKDB=XKDB/2.
304 DO 303 J=1,K
305 IF (ABS(DB(J))/(ABS(B(J))+TAU)).GE.E)GO TO 291
306 CONTINUE
307 DO 305 J=1,K
308 B(J)=BS(J)
309 WRITE (6,410)
310 CONTINUE
311 IBS=4
312 GO TO 371
313 .....SET UP FOR MATRIX INVERSION
314 CONTINUE
315 DO 312 I=1,K
316 A(I,I)=A(I,I)+XL
317 GET INVERSE OF A AND SOLVE FOR DB (J)S
318 IBKM=1
319 .....
320 .....

```

```

SUBROUTINE LSQENP      74/175  OPT=1      FTN 4.7+485

C**
C**
314 CALL GJR(A,K,ZETA,MSING)
C**
C**
316 GO TO(316,38),MSING
      IF (IBKM .EQ. 1) GO TO 321
      IBKS=2
      CALL CONLIM(IBKS,IBO,Y,X,B,IB)
      GO TO(82,314,23,359,43),IBO
      END OF MATRIX INVERSION, SOLVE FOR DB(J)

C**
321 DO 325 I=1,K
      DB(I)=0.
      DO 324 J=1,K
        DB(I)=A(I,J)*G(J)+DB(I)
        DB(I)=XKDB*DB(I)
        XLL=0.
        DTG = 0.
        DO 334 J=1,K
          XLL=XLL+DB(J)
          DTG = DTG + DB(J)*G(J)
          DTG = DTG + G(J)**2
          IF (SA(J) .GT. 0.0) GO TO 333
          IFORMAT(6,332),J,SA(J)
          FOR MAT(5X,J=*,I5,5X*SA(J) = *,E15.6)
332 GO TO INUE 335
333 CONTINUE
335 DB(J)=DB(J)/SA(J)
334 CONTINUE
      B(J)=B(J)+DB(J)
      CONTINUE
      KIP=K-IP
      IF (KIP .EQ. 1) GO TO 350
      CGAM=DTG/SQRT(XLL*GTG)
      JGAM=1
      IF (CGAM .GT. 0) GO TO 342
      CGAM = ABS(CGAM)
      JGAM = 2
340 CGAM = 57.2957795*(1.5707288+CGAM*(-0.2121144+CGAM*(0.074261
342 1 -CGAM*0.187293))) + SQRT(ABS(1.-CGAM))
      GO TO(351,344),JGAM
344 GAMMA = 180.-GAMMA

```







```

381 FORMAT (13X,4H PHI 10X,7H LAMBDA 6X,7H GAMMA 6X,7H LENGTH /
5X,1E18.8,2E13.3)
382 FORMAT (1X,1E9.2,1X,1H+ 99X,1H+ )
383 FORMAT (1X,5X,1E9.2,1X,1H+ 99X,1H+ )
1 E10.3,5X,1E9.2,1X,1H+ 99X,1H+ )
1 E10.3,5X,1E9.2,1X,1H+ 99X,1H+ )
384 FORMAT (1X,5X,1E9.2,1X,1H+ 99X,1H+ )
385 FORMAT (1X,5X,1E9.2,1X,1H+ 99X,1H+ )
386 FORMAT (1X,5X,1E9.2,1X,1H+ 99X,1H+ )
387 FORMAT (1X,5X,1E9.2,1X,1H+ 99X,1H+ )
388 FORMAT (1X,5X,1E9.2,1X,1H+ 99X,1H+ )
389 FORMAT (1X,5X,1E9.2,1X,1H+ 99X,1H+ )
390 FORMAT (1X,5X,1E9.2,1X,1H+ 99X,1H+ )
391 FORMAT (1X,5X,1E9.2,1X,1H+ 99X,1H+ )
392 FORMAT (1X,5X,1E9.2,1X,1H+ 99X,1H+ )
393 FORMAT (1X,5X,1E9.2,1X,1H+ 99X,1H+ )
394 FORMAT (1X,5X,1E9.2,1X,1H+ 99X,1H+ )
395 FORMAT (1X,5X,1E9.2,1X,1H+ 99X,1H+ )
396 FORMAT (1X,5X,1E9.2,1X,1H+ 99X,1H+ )
397 FORMAT (1X,5X,1E9.2,1X,1H+ 99X,1H+ )
398 FORMAT (1X,5X,1E9.2,1X,1H+ 99X,1H+ )
399 FORMAT (1X,5X,1E9.2,1X,1H+ 99X,1H+ )
400 FORMAT (1X,5X,1E9.2,1X,1H+ 99X,1H+ )
401 FORMAT (1X,5X,1E9.2,1X,1H+ 99X,1H+ )
402 FORMAT (1X,5X,1E9.2,1X,1H+ 99X,1H+ )
403 FORMAT (1X,5X,1E9.2,1X,1H+ 99X,1H+ )
404 FORMAT (1X,5X,1E9.2,1X,1H+ 99X,1H+ )
405 FORMAT (1X,5X,1E9.2,1X,1H+ 99X,1H+ )
406 FORMAT (1X,5X,1E9.2,1X,1H+ 99X,1H+ )
407 FORMAT (1X,5X,1E9.2,1X,1H+ 99X,1H+ )
408 FORMAT (1X,5X,1E9.2,1X,1H+ 99X,1H+ )
409 FORMAT (1X,5X,1E9.2,1X,1H+ 99X,1H+ )
410 FORMAT (1X,5X,1E9.2,1X,1H+ 99X,1H+ )
411 FORMAT (1X,5X,1E9.2,1X,1H+ 99X,1H+ )
412 FORMAT (1X,5X,1E9.2,1X,1H+ 99X,1H+ )

```

SUBROUTINE LSQENP      74/175    OPT=1

FTN 4.7+485

END

SUBROUTINE GJR

74/175 OPT=1

FTN 4.7+485

```

C**GAUSS-JORDAN-RUTISHAUSER MATRIX INVERSION WITH DOUBLE PIVOTING.
DIMENSION A(50,1),B(50),C(50),P(50),Q(50)
INTEGER P,Q
MSING=1
DO 39 K=1,N
  DETERMINATION OF THE PIVOT ELEMENT
  PIVOT=0.
  DO 13 I=K,N
    DO 13 J=K,N
      IF (ABS(A(I,J))-ABS(PIVOT))13,13,10
10  PIVOT=A(I,J)
  P(K)=I
  Q(K)=J
13  CONTINUE
  IF (ABS(PIVOT)-EPS)56,56,15
  EXCHANGE OF THE PIVOTAL ROW WITH THE KTH ROW
15  IF (P(K)-K)16,21,16
16  DO 20 J=1,N
    L=P(K)
    Z=A(L,J)
    A(L,J)=A(K,J)
    A(K,J)=Z
20  EXCHANGE OF THE PIVOTAL COLUMN WITH THE KTH COLUMN
21  IF (Q(K)-K)22,27,22
22  DO 26 I=1,N
    L=Q(K)
    Z=A(I,L)
    A(I,L)=A(I,K)
    A(I,K)=Z
26  A(I,K)=Z
27  CONTINUE
  JORDAN STEP
DO 36 J=1,N
  IF (J-K)33,30,33
30  B(J)=1./PIVOT
  C(J)=1.
  GO TO 35
33  B(J)=-A(K,J)/PIVOT
  C(J)=A(J,K)
35  A(K,J)=0.
36  A(J,K)=0.
DO 39 I=1,N

```

SUBROUTINE GJR

74/175 OPT=1

FTN 4.7+485

```

C**
39  DO 39 J=1,N
    A(I,J)=A(I,J)+C(I)*B(J)
REORDERING THE MATRIX
DO 54 M=1,N
K=N-M+1
IF(P(K)-K) 43,48,43
43  DO 47 I=1,N
    L=P(K)
    Z=A(I,L)
    A(I,L)=A(I,K)
47  A(I,K)=Z
48  IF(Q(K)-K) 49,54,49
49  DO 53 J=1,N
    L=Q(K)
    Z=A(L,J)
    A(L,J)=A(K,J)
53  A(K,J)=Z
54  A(K,J)=Z
55  CONTINUE
56  WRITE(6,57) P(K),Q(K),PIVOT
57  FORMAT(16H0SINGULAR MATRIX3H I=I3,3H J=I3,7H PIVOT=E16.8/)
    RETURN
    FORMING=2
    RETURN
    END

```

SUBROUTINE CONLIM 74/175 OPT=1

FTN 4.7+485

```

C** SUBROUTINE CONLIM(IBKS,IBD,Y,X,B,IB)
C** REVISED TO REARRANGE LABELED COMMON PARAM TO AGREE WITH WRITE-UP
C**
C**.....THIS IS THE CONFIDENCE LIMIT CALCULATION
C** DIMENSION BS(50),DB(50),BA(50),G(50),W(51),SA(50),P(50),A(50,51)
C** DIMENSION X(500,1),Y(1),B(1),IB(1)
C** COMMON /INT/ N7,K7,M7,IP7
C** COMMON /PLOT/ IFF,YMIN,YMAX
C** COMMON /PARAM/FF,T,E,TAU,XL,GAMCR,DEL,ZETA,IPA
C** COMMON /AFCLSQ/
1 BS,DB,BA,G,W,SA,P,A, J,IBKM,KEND,IFSS3, IFSS2,IBOUT,
1 IBKA,IBK2, J,IBKM,KEND,IFSS3,
1 I,IBKP,IBKN,J1,KST,IWS6,JJ,SPL,W$1,DD,XK2,BL,PU,SE,OPL,SPU,PKN,PHID,XK3,
1 WS,PHI2,STE,XK1,BC,8U,PHI
1 PL,HJTD,OPU,PC,D,XK1,BC,8U,PHI
N=N7
K=K7
M=M7
IP=IP7
TO=INIBKS
IF (IBKS.EQ.4) GO TO 21
GO TO (15,17,18),IBKS
15 IBKA1=IBKA-1
17 GO TO (27,32),IBKA1
18 GO TO 43
IBK21=IBK2-1
J=INDEX
GO TO (158,27,125,134,144),IBK21
21 DO 22 J=1,K
22 B(J)=BS(J)
WRITE (6,201)N,K,IP,M,FF,T,E,TAU
IBKA=2
IBD=1
GO TO 204
27 IF (IFP.LE.0) GO TO 32
28 IBKA=3
IFP=0
IBD=1
GO TO 204
32 WS=N-K+IP

```

THIS WILL PRINT THE Y,YHAT,DELTA Y



```

SE=SQRT(PHI/WS)
PHIZ=PHI
IF (IFSS2.EQ.0) GO TO 38
WRITE (6,189) PHIZ, SE, XL
GO TO 39
38 WRITE (6,190) PHIZ, SE, XL
C** NOW WE HAVE MATRIX A
39 CONTINUE
40 IBKM=2
41 IBD=2
C** GO TO 204
C**
C** NOW WE HAVE C = A INVERSE
43 DO 45 J=1,K
44 IF (A(J,J).LT.0) GO TO 47
45 SA(J)=SQRT(A(J,J))
46 GO TO 48
47 IBOUT=1
48 KWRITE (6,194)
49 KST=KST+5
50 KEND=KST+4
51 IF (KEND.LT.K) GO TO 54
52 KEND=K
53 DO 55 I=1,K
54 WRITE (6,196) I, (A(I,J), J=KST, KEND)
55 IF (KEND.LT.K) GO TO 50
56 IF (IBOUT.EQ.0) GO TO 61
57 WRITE (6,203)
58 IBD=3
59 GO TO 204
60 DO 68 I=1,K
61 DO 68 J=1,K
62 WS=SA(I)*SA(J)
63 IF (WS.GT.0.) GO TO 67
64 A(I,J)=0.
65 GO TO 68
66 A(I,J)=A(I,J)/WS
67 CONTINUE
68 DO 70 J=1,K
69 A(J,J)=1.
70 WRITE (6,195)

```

SUBROUTINE CONLIM 74/175 OPT=1 FTN 4.7+485

```

73 KST=-9
   KST=KST+10
   KEND=KST+9
   IF (KEND.LT.K) GO TO 77
   KEND=K
77 DO 78 I=1,K
78 WRITE (6,202) I, (A(I,J), J=KST, KEND)
   IF (KEND.LT.K) GO TO 73
C** GET T*SE*SQRT(C(I,I))
   DO 81 J=1,K
81 SA(J)= SE*SA(J)
82 WRITE (6,197)
   WS=K-IP
   DO 98 J=1,K
   IF (IP.LE.0) GO TO 89
86 DO 88 I=1,IP
   IF (J.EQ.IB(I)) GO TO 97
88 CONTINUE
89 HJTD=SQRT(WS*FF)*SA(J)
   STE=SA(J)
   CPL=BS(J)-SA(J)*T
   OPU=BS(J)+SA(J)*T
   SPL=BS(J)-HJTD
   SPU=BS(J)+HJTD
   WRITE (6,200) J, STE, OPL, OPU, SPL, SPU
   GO TO 98
97 WRITE (6,191) J
98 CONTINUE
C**
   IF (IWS6.EQ.1) IBD=3
   IF (IWS6.EQ.1) GO TO 204
   WS=K-IP
   WS1=N-K+IP
   PKN=WS/WS1
   PC=PHIZ*(1.+FF*PKN)
   WRITE (6,198) PC
   IFSS3=1
   J=1
109 IBKP=1
112 DO 112 JJ=1,K
   B(JJ)=BS(JJ)

```

NONLINEAR CONFIDENCE LIMIT

SUBROUTINE CONLIM      74/175    OPT=1      FTN 4.7+485

```

114 IF (IP.LE.0)GO TO 117
116 DO 116 JJ=1,IP
117 IF (J.EQ.IB(JJ))GO TO 173
CONTINUE
119 DO=-1.
IBKN=1
O=DD
B(J)=BS(J)+O*SA(J)
IBK2=4
IBD=4
INDEX=J
GO TO 204
125 PHI1=PHI
IF (PHI1.GE.PC)GO TO 137
127 O=D+DC
IF (O/DD.GE.5.) GO TO 177
129 B(J)=BS(J)+O*SA(J)
IBK2=5
IBD=5
INDEX=J
GO TO 234
134 PHI1=PHI
IF (PHI1.LT.PC)GO TO 127
IF (PHI1.GE.PC)GO TO 146
137 O=D/2.
IF (O/DD.LE.0.01)GO TO 177
139 B(J)=BS(J)+O*SA(J)
IBK2=6
IBD=6
INDEX=J
GO TO 204
144 PHI1=PHI
IF (PHI1.GT.PC)GO TO 137
146 XX1=PHI1/(1.-O)+PHI1/(O*(D-1.))
XX2=-(PHI1*(1.+O)/O+D/(1.-O)*PHI1+PHI1/(O*(D-1.)))
XX3=PHI1-PC
BC=(SQRT(XK2*XK2-4.*XK1*XK3)-XK2)/(2.*XK1)
GO TO(151,153),IBKN
151 B(J)=BS(J)-SA(J)*BC
GO TO 154
153 B(J)=BS(J)+SA(J)*BC
154 IBK2=2

```

## SUBROUTINE CONLIM

74/175 OPT=1

FTN 4.7+485

```

158 IBD=4
159 INDEX=J
      GO TO 204
      GO TO (159,164),IBKN
      IBKN=2
      DO=1.
      BL=8(J)
      PL=PHI
      GO TO 119
      BU=8(J)
      PU=PHI
      GO TO (167,169,171,175),IBKP
167 WRITE (6,196) J, BL, PL, BU, PU
169 GO TO 185
      GO TO (167,193) J, BU, PU
171 WRITE (6,196) J, BL, PL
173 GO TO 185
      GO TO (167,191) J
175 GO TO 185
      GO TO (167,192) J
177 GO TO 185
      GO TO (178,180),IBKN
      DELETE LOWER PRINT
178 IBKP=2
      GO TO 158
      GO TO (181,183),IBKP
      DELETE UPPER PRINT
181 IBKP=3
      GO TO 158
      LOWER IS ALREADY DELETED, SO DELETE BOTH
183 IBKP=4
      GO TO 158
      J=J+1
      J1=J-1
      IF (J1.NE.K) GO TO 109
      DO 184 JJ=1,K
184 B(JJ)=BS(JJ)
      IBD=5
189 FORMAT (/13X,4H PHI 14X,4H S E
190 1 25H ESTIMATED PARTIALS USED / 5X,2E18.8, E13.3)
      FORMAT (/13X,4H PHI 14X,4H S E
      9X,7H LAMBDA 6X,
      9X,7H LAMBDA 6X,

```

```

SUBROUTINE CONLIM      74/175  OPT=1      FTN 4.7+485

      1 25H ANALYTIC PARTIALS USED /5X, 2E18.8, E13.3)
191  FORMAT(2X, I3, 20H PARTIALS USED /5X, 2E18.8, E13.3)
192  FORMAT(2X, I3, 12H PARAMETER NOT FOUND )
193  FORMAT(2X, I3, 16X, 2E18.8)
194  FORMAT(1H /13H PARAMETER INVERSE )
195  FORMAT(1H /13H PARAMETER CORRELATION MATRIX )
196  FORMAT(1H /13H PARAMETER STD 17X, 16H ONE - PARAMETER 21X,
197  14H UPPER 12X, 2H B 7X, 6H ERROR 12X, 6H LOWER 12X,
      1 6H UPPER 12X, 6H UPPER )
198  1  FORMAT(1H /1H /30H LOWER LIMITS / /
      1 16H PHI / 6H NONLINEAR CONFIDENCE LIMITS / /
199  1  FORMAT(1H /1H /30H LOWER LIMITS / /
      1 8X, 10H UPPER 18.8)
200  1  FORMAT(2X, I3, 5X, 5H K = I3, 5X, 5H M = I3, 5X,
201  1  5H IN = I3, 5X, 5H TAU = E10.3 / 6H FF = E10.3, 5H T = E10.3,
      1 5X, 5H E = E10.3, 5X, 7H TAU = E10.3 / 6H FF = E10.3, 5H T = E10.3,
202  1  FORMAT(3X, I5, 2X, 10F10.4)
203  1  FORMAT(27H0 NEGATIVE DIAGONAL ELEMENT )
204  RETURN
      END

```



FTN 4.7+485

SUBROUTINE PCODE 74/175 OPT=1

C

SUBROUTINE PCODE(P,X;B;F,I)  
DIMENSION P(50),B(50),X(500,3)  
RETURN  
END



FUNCTION PNORM 74/175 OPT=1

```

C
C
C
C
C
10
20
40
C
30

FUNCTION PNORM(X,EB,I,R,P)
DIMENSION EB(15)
PNORM=0.0
FRONT=(R*(P+1))**(-1/P)
SUM1=0.0
II=I-1
IF (II.EQ.0)10,20
PNORM=FRONT*(X**(1+1/P))
GO TO 30
CONTINUE
MINUS=-1
INT=-1
DO 40 J=1,II
INT=INT*MINUS
SUM1=SUM1+2*INT*(EB(J+1)**(P+1))
CONTINUE
INT1=INT*MINUS
PNORM=FRONT*((SUM1+INT1*(X**(1+P)))**(1/P))
CONTINUE
RETURN
END

```

C

```

10  FUNCTION TRY(X,X0,B)
11  DIMENSION B(10)
12  A=X0-B(3)
13  F1=(B(1)/2)*A*(1+ERF(A/(B(2)*SQRT(2.))))
14  +B(2)*SQRT(2./3.14159)*EXP(-(A*A)/(2*B(2)*B(2)))
15  IF(X.EQ.X0) 10,20
16  CONTINUE
17  TRY=F1
18  GO TO 30
19  CONTINUE
20  TRY=(X/X0)*F1
21  CONTINUE
22  TRY=TRY/(X+1.0)
23  RETURN
24  END

```

## LISTING OF INPUT PARAMETERS

NO. OF ITERATIONS ASKED= 30  
 NO. OF UNDETERMINED COEFFICIENTS= 4  
 NO. OF VARIABLES= 3  
 PARTIAL DERIVATIVE OPTION= 1  
 CONFIDENCE LIMIT OPTION= 1  
 PRINTED OUTPUT OPTION= -1

## INITIAL GUESSES OF COEFFICIENTS

0      .6500E+00   .3000E+00   .1600E+01   .1000E+02



```

PF = 185 .400E+01 4 T = IP = 200E+01 M E = 3 .500E-04 IFR = 0 TAU = GAMMA CRIT = .450E+02 .100E-01 DELTA = .100E-30
PARAMETERS .65000000E+00 .30000000E+00 .16000000E+01 .10000000E+02 .10000000E+02 ESTIMATED PARTIALS USED
      PHI SE .19127070E-01 0. LENGTH GAMMA LAMBDA .100E-01
.66583755E-01
PARAMETERS .64115401E+00 .54888406E+00 .14617086E+01 .10000000E+02 ESTIMATED PARTIALS USED
      PHI SE .11105466E-01 .510E+00 GAMMA .917E+01 LAMBDA .100E-01
.22446311E-01
PARAMETERS .63860429E+00 .46937845E+00 .14502052E+01 .10000000E+02 ESTIMATED PARTIALS USED
      PHI SE .10825879E-01 .558E-01 GAMMA .233E+02 LAMBDA .100E-01
.21329540E-01
PARAMETERS .63773482E+00 .46295457E+00 .14476739E+01 .10000000E+02 ESTIMATED PARTIALS USED
      PHI SE .10824289E-01 .337E-02 GAMMA .219E+02 LAMBDA .100E-01
.21324074E-01
PARAMETERS .63773484E+00 .46278430E+00 .14476837E+01 .10000000E+02 ESTIMATED PARTIALS USED
      PHI SE .10824288E-01 .801E-04 GAMMA .481E+02 LAMBDA .100E-02
.21324069E-01
PARAMETERS .63752423E+00 .46195687E+00 .14469847E+01 .10000000E+02 ESTIMATED PARTIALS USED
      PHI SE .10824254E-01 .145E-03 GAMMA .509E+02 LAMBDA .100E-02
.21323933E-01
PARAMETERS .63750391E+00 .46183273E+00 .14469150E+01 .10000000E+02 ESTIMATED PARTIALS USED
      PHI SE .10824253E-01 .197E-04 GAMMA .330E+02 LAMBDA .100E-02
.21323931E-01
EPSILON TEST

```













## A P P E N D I X F

## INTEGRATION OF ORIENTATION-FUNCTION INTEGRAL

The expression in Equation (25),

$$\begin{aligned}
 f_h &= \int_{-\infty}^{\|\epsilon\|} N(\epsilon_y) f_i(\epsilon_y) d\epsilon_y \\
 &= C \frac{\epsilon}{\|\epsilon\|} \cdot \frac{1}{S\sqrt{2\pi}} \int_{-\infty}^{\|\epsilon\|} e^{-\frac{(\epsilon_y - \bar{\epsilon})^2}{2S^2}} (\|\epsilon\| - \epsilon_y) d\epsilon_y
 \end{aligned}$$

may be divided into two integrals:

$$I_1 = C \frac{\epsilon}{\|\epsilon\|} \cdot \frac{1}{S\sqrt{2\pi}} \int_{-\infty}^{\|\epsilon\|} e^{-\frac{(\epsilon_y - \bar{\epsilon})^2}{2S^2}} \cdot \|\epsilon\| d\epsilon_y$$

and

$$I_2 = -C \frac{\epsilon}{\|\epsilon\|} \cdot \frac{1}{S\sqrt{2\pi}} \int_{-\infty}^{\|\epsilon\|} e^{-\frac{(\epsilon_y - \bar{\epsilon})^2}{2S^2}} \cdot \epsilon_y d\epsilon_y$$

letting

$$n = \frac{\epsilon_y - \bar{\epsilon}}{S\sqrt{2}} ; \quad dn = \frac{d\epsilon_y}{S\sqrt{2}}$$

and changing the limits of integration by noting than when  $\epsilon_y = \|\epsilon\|$ ,

$$n = \frac{\|\epsilon\| - \bar{\epsilon}}{S\sqrt{2}}, \text{ the two integrals become}$$

$$I_1 = C \frac{\epsilon}{\sqrt{\pi}} \int_{-\infty}^{\frac{\|\epsilon\| - \bar{\epsilon}}{S\sqrt{2}}} e^{-n^2} dn = \frac{C\epsilon}{2} \left[ 1 + \operatorname{erf} \left( \frac{\|\epsilon\| - \bar{\epsilon}}{S\sqrt{2}} \right) \right]$$

$$\begin{aligned} I_2 &= -C \frac{\epsilon}{\|\epsilon\|} \cdot \frac{1}{\sqrt{\pi}} \int_{-\infty}^{\frac{\|\epsilon\| - \bar{\epsilon}}{S\sqrt{2}}} e^{-n^2} (S\sqrt{2} n + \bar{\epsilon}) dn \\ &= \frac{C}{2} \frac{\epsilon}{\|\epsilon\|} \left[ -\epsilon \left[ 1 + \operatorname{erf} \left( \frac{\|\epsilon\| - \bar{\epsilon}}{S\sqrt{2}} \right) \right] + S\sqrt{\frac{2}{\pi}} e^{-\frac{-(\|\epsilon\| - \bar{\epsilon})^2}{2S^2}} \right] \end{aligned}$$

where erf is the error function. Collecting terms yields

$$f_h = I_1 + I_2$$

$$f_h = \frac{C}{2} \frac{\epsilon}{\|\epsilon\|} \left\{ (\|\epsilon\| - \bar{\epsilon}) \left[ 1 + \operatorname{erf} \left( \frac{\|\epsilon\| - \bar{\epsilon}}{S\sqrt{2}} \right) \right] + S\sqrt{\frac{2}{\pi}} \exp \left[ \frac{-(\|\epsilon\| - \bar{\epsilon})^2}{2S^2} \right] \right\}$$

## A P P E N D I X G

EXACT ANALYTICAL EXPRESSIONS FOR  $L_p$  NORM FOR CONSTANT STRAIN RATE HYSTERESIS TESTS

The analytical expressions for the  $L_p$  norm of the strain,  $\|e\|_p$ , defined as

$$\|e\|_p \equiv \left[ \int_0^t |e(\xi)|^p d\xi \right]^{1/p}$$

for the strain history shown in Figure 62 are as follows ( $R$  = strain rate)

Zone 1.  $0 < t < t_1$

$$e = Rt, \quad e_1 = Rt_1$$

$$\|e\|_p = [R(p+1)]^{-1/p} e^{\frac{p+1}{p}} = K_p e^{\frac{p+1}{p}}$$

Zone 2.  $t_1 < t < t_2$

$$\|e\|_p = K_p (2e_1^{p+1} - e^{p+1})^{1/p}$$

Zone 3.  $t_2 < t < t_3$

$$\|e\|_p = K_p (2e_1^{p+1} - 2e_2^{p+1} + e^{p+1})^{1/p}$$

Zone 4.  $t_3 < t < t_4$

$$\|e\|_p = K_p (2e_1^{p+1} - 2e_2^{p+1} + 2e_3^{p+1} - e^{p+1})^{1/p}$$

etc.

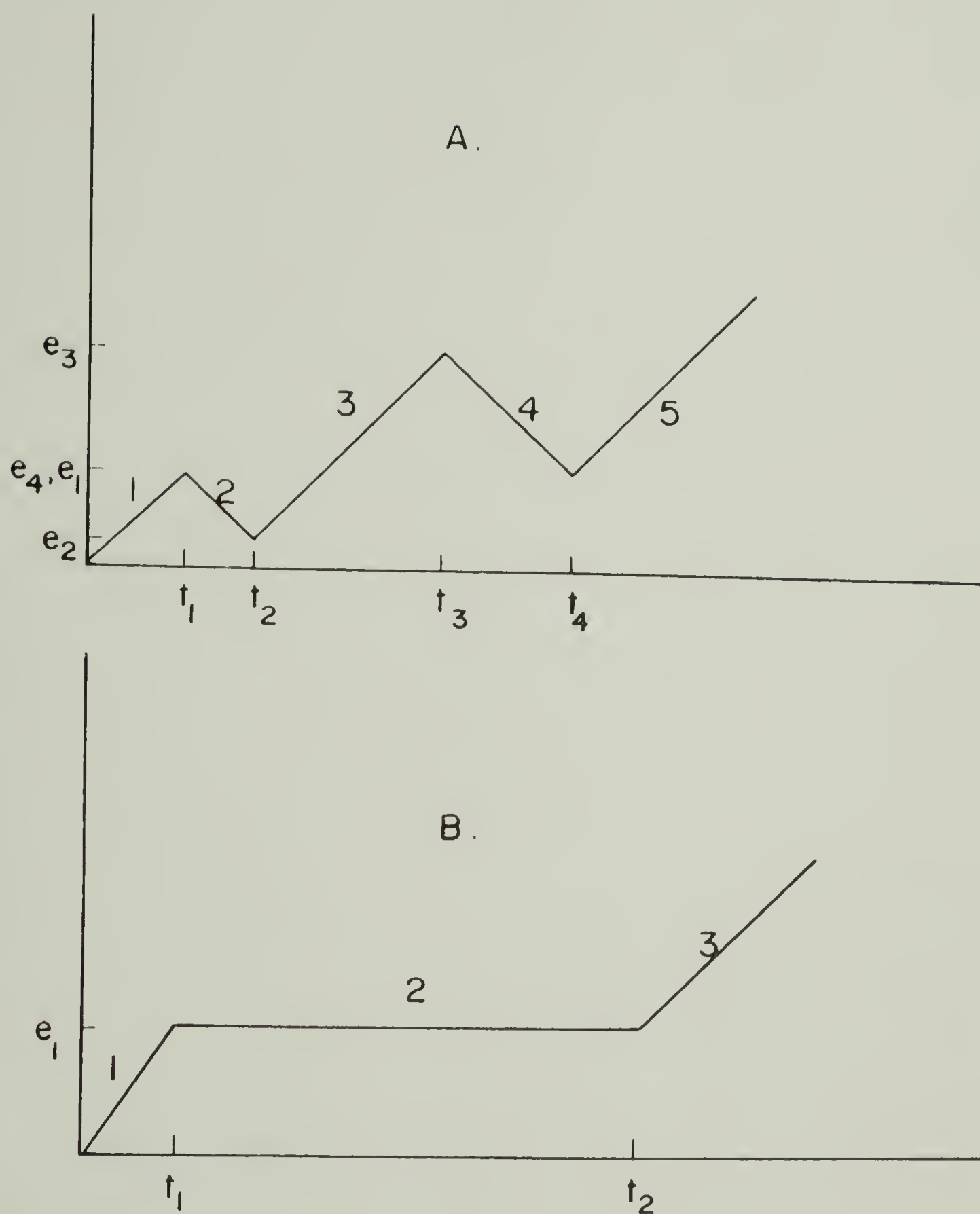


Figure 62. Strain histories used in Appendices G and I (A.) and Appendix H (B.).



## A P P E N D I X   H

### EXACT ANALYTICAL EXPRESSIONS FOR $L_p$ NORM FOR STRESS RELAXATION EXPERIMENT

The analytical expressions for the  $L_p$  norm of the strain,  $\|e\|_p$ , defined as

$$\|e\|_p = \left[ \int_0^t |e(\xi)|^p d\xi \right]^{1/p}$$

for the strain history shown in Figure 62 are as follows ( $R$  = strain rate):

Zone 1.  $0 < t < t_1$

$$e = Rt$$

$$\|e\|_p = [R(p+1)]^{-1/p} e^{\frac{p+1}{p}} = K_p e^{\frac{p+1}{p}}$$

Zone 2.  $t_1 < t < t_2$

$$\|e\|_p = e_1 \left[ t - \frac{t_1 p}{p+1} \right]^{1/p}$$

Zone 3.  $t_2 < t < t_3$

$$\|e\|_p = R \left[ t_1^p (t_2 - t_1) + \left( \frac{t + t_1 - t_2}{p+1} \right)^{p+1} \right]^{1/p}$$

# A P P E N D I X I

## EXACT ANALYTICAL EXPRESSIONS FOR FADING MEMORY VISCOELASTIC INTEGRAL FOR CONSTANT STRAIN RATE HYSTERESIS TESTS

The analytical expressions for the fading memory integral

$$S = \int_0^t (t-\tau)^n \dot{e}(\tau) d\tau = R \int_0^t (t-\tau)^n d\tau, \quad -1 < n < 0$$

for a constant strain rate history ( $\dot{e}(\tau) = R$ ) shown in Figure 62, are as follows:

Zone 1.  $0 < t < t_1$

$$S = \frac{R^{-n}}{n+1} e^{n+1} = K_n e^{n+1}$$

Zone 2.  $t_1 < t < t_2$

$$S = K_n [(2e_1 - e)^{n+1} - 2(e_1 - e)^{n+1}]$$

Zone 3.  $t_2 < t < t_3$

$$S = K_n [(e + 2e_1 - 2e_2)^{n+1} - 2(e + e_1 - 2e_2)^{n+1} + 2(e - e_2)^{n+1}]$$

Zone 4.  $t_3 < t < t_4$

$$S = K_n [ (-e + 2e_1 - 2e_2 + 2e_3)^{n+1} - 2(-e + e_1 - 2e_2 + 2e_3)^{n+1} \\ + 2(-e - e_2 + 2e_3)^{n+1} - 2(-e + e_3)^{n+1} ]$$

etc.



